NONDISCLOSURE STATEMENT

This dissertation contains confidential and proprietary information and is for the purpose of evaluation within the dissertation committee

Please do not disclose the contents of this dissertation to anyone outside the dissertation committee before October 1, 2016

DESIGN AND SYNTHESIS OF PROSTATE SPECIFIC ANTIGEN-ACTIVATED PRODRUGS

by

HERVE ALOYSIUS

A Dissertation submitted to the

Graduate School-New Brunswick

Rutgers, The State University of New Jersey

in partial fulfillment of the requirements

for the degree of

Doctor of Philosophy

Graduate Program in Medicinal Chemistry

written under the direction of

Professor Longqin Hu

and approved by

_____

_____

_____

_____

New Brunswick, New Jersey

October, 2014

ABSTRACT OF THE DISSERTATION

DESIGN AND SYNTHESIS OF PROSTATE SPECIFIC ANTIGEN-ACTIVATED PRODRUGS

HERVE ALOYSIUS

Dissertation Director: Professor Longqin Hu

The feasibility of targeted delivery of cytotoxic agents to prostate cancer cells via selective activation of peptide-linked prodrugs by prostate-specific antigen (PSA) has been previously demonstrated. PSA is a chymotryspin-like serine protease that uniquely cleaves after Gln. Using cleavage maps for its natural substrates, semenogelins I and II, the highly specific PSA substrate glutaryl-Hyp-Ala-Ser-Chg-Gln was discovered, and subsequently coupled to various cytotoxic agents as a promoiety to synthesize prodrugs with enhanced selectivity for prostate cancer cells. In order to obtain PSA peptide substrates with improved specificity and plasma stability from the known substrate sequence glutaryl-Hyp-Ala-Ser-Chg-Gln, we systematically replaced the *N*-terminal segment with D-retro-inverso-peptides and incorporated 7-amino-4-methylcoumarin (7-AMC) after Gln for convenient fluorometric determination and ranking of the PSA substrate activity. Based on PSA cleavage rate and resistance to hydrolysis in plasma, GABA←mGly-Ala-Ser-Chg-Gln and glutaryl-Ser-Ala-Ser-Chg-Gln were identified as optimal promoieties and coupled to doxorubicin or phosphoramide mustard as PSA-cleavable prodrugs, using various linkers. The doxorubicin conjugates demonstrated comparable PSA cleavage rates, equal or improved cytotoxic profiles in PSA-producing

tumor cells compared to the prodrug L-377,202 (glutaryl-Ser-Ala-Ser-Chg-Gln-Ser-Leu-Dox). We found that human neprilysin rapidly cleaved L-377,202 through its Ser-Leu linker and may be responsible for prodrug instability in blood and normal tissues. Thus, in addition to enhancing prodrug selectivity against non-PSA-secreting prostate cancer cell lines, stability in normal tissues was improved. Our results indicated that enhanced tumor specificity of peptide prodrugs targeted for activation by PSA in prostate cancer tumors was achievable with peptide sequence and linker modifications.

ACKNOWLEDGEMENTS

I am grateful to my advisor Dr. Longqin Hu for his mentorship, patience and always seeing the best in me.

I greatly appreciate the constructive feedback of my research committee members, Dr. Longqin Hu, Dr. Edmond LaVoie, Dr. Joseph Rice and Dr. Kaushik Mitra.

I would like to thank the Merck Drug Metabolism management staff for supporting my decision to pursue graduate studies in Medicinal Chemistry; special thanks to Dr. Kaushik Mitra and Dr. Sanjeev Kumar for their guidance and advice, Dr. Richard Tschirret-Guth for stimulating my personal and scientific growth, Dr. Lucinda Cohen for being supportive as well as a great source of inspiration, and Dr. Kathleen Cox for her contanst encouragements to keep the focus.

I couldn’t have overcome the challenges of graduate school if it weren’t for the support, training and help of my dear friends and colleagues at Rutgers and Merck; special thanks to Daigo Inoyama, Yu Chen, Xinghua Wu, Dr. Magesh Sadagopan, Dr. Lin Chen, Dhulfiqar Abed, Haifa Albanyan, Dr. Huijuan Jin, Dr. Cody Kelley, Gifty Blankson, Hye Yeon Sagong, Dr. Laurie Joseph, Dr. Zoltan Szekely, Zhe Feng, Zahid Hussain, Dr. Zhoupeng Zhang, Randy Miller and Dr. Amjad Ali.

I'm forever thankful and indebted to my loving parents, Richard Aloysius and Therese Essovi for planting the seeds of tenacity and courage in my mind at an early age.

I'm blessed with the special friendship of Raj and Nirmala Muralitharan, Harry Kokinos, Mark Kirshteyn and Sam Kirhsteyn who constatntly encourage me to press forward.

Many thanks to my brothers and sisters for their incessant prayers.

Thank you, Lord, for always walking with me.

TABLE OF CONTENTS

LIST OF FIGURES

LIST OF TABLES

LIST OF SCHEMES

ABBREVIATIONS

Ac Acetyl

ABC ATP-binding cassette

ACN Acetonitrile

ADEPT Antibody-directed enzyme prodrug therapy

12ADT 12-Aminododecanoyl-thapsigargin

Ala Alanine

AFC 7-Amino-4-(trifluoromethyl)-coumarin

AMC 7-Amino-4-methyl-coumarin

Arg Arginine

Asp Asparagine

AZD 7-azido-4-methylcoumarin

Bn Benzyl

Boc *t*-Butoxycarbonyl

Bu Butyl

Cbz Benzoxycarbonyl

Chg Cyclohexylglycine

CP Cyclophosphoramide

CPM Counts per min

CYP Cytochrome P-450

Cys Cysteine

DBU 1,8-diazabicycloundec-7-ene

DCM Dichloromethane

DEA Diethylamine

DIEA Diisopropylethylamine

DMAP 4-Dimethylaminopyridine

DMF *N*, *N* - Dimethylformamide

DMSO Dimethyl sulfoxide

Dox Doxorubicin

EDA Ethylenediamine

EtOAc Ethyl acetate

FBS Fetal bovine serum

FCC Flash column chromatography

FGF fibroblast growth factors

Fm 9-Fluorenylmethyl

Fmoc 9-Fluorenylmethoxycarbonyl

FUDR 5-Fluoro-2´-deoxyuridine

GABA γ-Aminobutyric acid

GDEPT Gene-directed enzyme prodrug therapy

Gln Glutamine

HBTU 2-(1H-benzotriazole-1-yl)-1,1,3,3-tetramethyluronium

His Histidine

HOBt 1-Hydroxybenzotriazole

HOSu *N*-Hydroxysuccinimide

HRPC Hormone-refractory prostate cancer

Hyp *trans*-4-Hydroxyproline

IGFBP Insulin-like growth factor binding protein

Ile Isoleucine

IP Intraperitoneal

IPCF Isopropyl chloroformate

IS Internal standard

IV Intravenous

LC-MS Liquid chromatography-mass spectrometry

Leu Leucine

Lys Lysine

MeOH Methanol

MSNT 1-(Mesitylene-2-sulfonyl)-3-nitro-1H-1,2,4-triazole

MTD Maximum tolerated dose

MTX Methotrexate

MTT 3-(4,5-Dimethylthiazol-2-yl)-2,5-diphenyltetrazolium bromide

Mu Morpholinylcarbonyl

NAD(P)H Nicotinamide adenine dinucleotide (phosphate), reduced form

NaSeH Sodium hydrogen selenide

NMP *N*-Methylpyrolidone

NO Nitric oxide

NTR Nitroreductase

PABA *para*-Aminobenzyl alcohol

PGA Penicillin G amidase

P-gp P-glycoprotein 1

Phe Phenylalanine

PSA Prostate-specific antigen

Ser Serine

SERCA Sarcoplasmic/endoplasmic reticulum Ca^{2+}-dependent ATPase

SRM Selected-reaction monitoring

TFA Trifluoroacetyl

THF Tetrahydrofuran

Thr Threonine

TLC Thin-layer chromatography

Trp Tryptophan

Trt Trityl

Tyr Tyrosine

Val Valine

VEGF Vascular endothelial growth factor

CHAPTER ONE

INTRODUCTION

Prostate cancer is the most common cancer and the second leading cause of morbidity and death among American males next to lung cancer. According to the American Cancer Society, there will be around 233,000 newly diagnosed cases of prostate cancer and about 29,480 estimated deaths from prostate cancer in 2014.[1, 2] From 2006 to 2010, over 65% of diagnosed cases ranged between 55 and 74 years of age with an average incidence rate of 152 per 100,000 men.[3] There is an age-dependent increase in benign hyperplasia incidence in 80% of men older than 80 years of age, which does not necessarily lead to prostate cancer. Unlike benign hyperplasia, prostate cancer originates from an intraepithelial neoplasia of the prostate, a multifocal lesion characterized by dysplasia of the prostate lumen and erosion of the basal cell layer. Moreover, metastatic prostate cancer preferentially progresses to bone tissues where lesions are formed.[4, 5] Factors involved in the initiation and progression of prostate cancer include modulation of tumor suppressor genes, transcription factors, oncogenes, and activation of the androgen receptor (AR).[6] Localized tumors are typically treated by prostatectomy and/or radiation therapy; however, continuous androgen deprivation therapy (ADT), usually coupled with the use of AR antagonists, remains the standard treatment for advanced prostate cancer. ADT may initially reduce tumor growth and metastasis rates (typical disease regression of 24-36 months), but is rarely curative since tumors become refractory to therapy within one to two years due to exaggerated androgen receptor reactivation and disruption of signaling pathways that regulate cell proliferation.[7] Resistance or relapse to androgen

therapy leads to hormone-refractory prostate cancer (HRPC) with the propensity to progress through osteoblastic metastases. AR reactivation is mediated by the intratumoral conversion of dehydroepiandrosterone and androstenedione by the cytochrome P450 enzymes CYP11A1 and CYP17A1 into testosterone and dihydrotestosterone, ligands which further activate the receptor. The anti-androgen abiraterone, for example, was effective against bone metastases in advanced prostate cancer patients who were previously on docetaxel therapy. However, due to CYP17A1 induction upon abiraterone treatment and increasing intratumoral *de novo* androgen synthesis from cholesterol, a new resistance/relapse mechanism developed, which compromised therapeutic effectiveness.[8-10] Resistance and relapse to ADT are common complications of prostate cancer progression and may be triggered by other factors such as AR up-regulation, functionalization of AR mutations, androgen activation by growth factors and cytokines, and up-regulation of AKT, MAPK, EGFR and PI3K cellular signaling pathways.[11-14] Due to the development of HRPC to ADT and the challenging regimens associated with androgen antagonist administration, adjunct or alternative treatment options have been explored.

I. Prostate Cancer Treatment

A. Androgen Antagonists and Biosynthesis Inhibitors

Several anti-androgens have been developed as antagonists of androgen binding and/or inhibitors of androgen biosynthesis to improve androgen activity modulation in HRPC patients. The first-generation non-steroidal anti-androgens, flutamide, nilutamide, and bicalutamide showed modest survival benefits when used in combination with

prostatectomy in advanced prostate cancer patients.[15-17] Following a 200 mg dose of bicalutamide to patients with advanced prostate cancer, prostate-specific antigen (PSA, a serological marker for prostate cancer) levels were significantly reduced by 50-80%.[18] A recent phase II study of bicalutamide reported clinical improvements in 47% patients when combined with sorafenib.[19] Likewise, the improved AR antagonist, enzalutamide (MDV-3100) exhibited anti-tumor activity and a reduction in PSA levels, as well as mitigation of osteoblastic metastases. Although enzalutamide was well tolerated in most patients, three subjects experienced seizures at a doses of 360, 480 and 600 mg per day.[20] In a multinational randomized phase III study involving 1,199 HRPC patients on docetaxel, daily oral administration of enzalutamide (160 mg) demonstrated significant clinical benefits with a 37% reduction in mortality rate. In the study, the median overall survival (OS) was increased by approximately 6 months in patients receiving enzalutamide compared to placebo. The drug was well tolerated with minor adverse effects, namely diarrhea, fatigue, hot flushes and seizures (0.6% of subjects).[21] In 2012, enzalutamide was approved by the Food and Drug Adminstration (FDA) for patients with HRPC on docetaxel chemotherapy. As mentioned earlier, the CYP17A1 inhibitor, abiraterone acetate represents a class of anti-androgens that inhibit *de novo* androgen biosynthesis thereby slowing the progression of bone metastases in advanced prostate cancer. Abiraterone demonstrated a greater than 50% reduction PSA levels in patients on docetaxel chemotherapy in two separate phase II studies with adverse effects including edema and hypertension; the observed edema was effectively mitigated with prednisone co-administration.[22-25] In a phase III study, abiraterone (1000 mg) and prednisone (5 mg) co-administration demonstrated a 26% reduction in PSA levels, improved survival and a

35% reduction in mortality risk in HRPC patients that were previously treated with docetaxel. Fatigue was the primary adverse effect reported during the study although elevated mineralocorticoid levels due to CYP17 inhibition, abnormal liver function and cardiac abnormalities were also observed.[9] The FDA approved abiraterone acetate in 2011 for patients with HRPC on prior docetaxel therapy.[26] The antifungal ketoconazole, a broad cytochrome P450 inhibitor, is also used as an androgen biosynthesis inhibitor in HRPC patients.[27] Following co-administration of ketoconazole, dutasteride (5α-reductase inhibitor) and hydrocortisone, reduction of serum PSA levels was observed in 56% of patients.[28] Less robust clinical benefits were demonstrated in similar studies involving smaller patient populations with reports of gastrointestinal-related toxicities.[29, 30] More serious adverse effects such as rhabdomyolysis and drug-drug interactions were also observed raising concerns about the utility of ketoconazole as a co-administration agent in future studies.

B. Immunotherapy

Eliciting tumor-specific immune responses as a therapeutic approach is supported by growing preclinical evidence and characterization of various tumor-specific antigens. Tumor cells secrete a variety of growth factors capable of activating the receptor activator of nuclear factor (NF)-kB ligand (RANKL) through bone stromal cell induction. RANKL in turn causes destructive bone desorption by promoting osteoclast formation. Denosumab is a humanized monoclonal antibody that targets RANKL in its regulation of osteoclast formation. In a comparative phase III study against zometa (zoledronic acid), denosumab showed improved skeletal-related event prevention response by 3.6 months in

HRPC patients receiving 4 mg of zometa intravenously or 120 mg denosumab subcutaneously; no differences in time to disease progression were observed, and hypocalcemia was a prevalent side-effect of denosumab administration.[31] Nevertheless, the pox viral vaccine PROSTVAC® demonstrated improved OS in HRPC patients during a randomized phase II study. PROSTVAC® is an optimized heterologous vaccine consisting of recombinant vaccinia and fowlpox viruses, vectors for PSA encoding DNA and the co-stimulatory protein triad CD54-CD58-CD80. PROSTVAC® was designed to induce tumor-associated-antigen-specific cytotoxic T lymphocyte activity and anti-tumor responses.[32]

Alternative immunotherapeutic approaches of HRPC include targeting the process of angiogenesis in growing tumors to slow the progression of prostate cancer, stemming from the key inductive roles of tumor-derived growth factors such as the vascular endothelial growth factor (VEGF) and fibroblast growth factors (FGF).[33, 34] The humanized monoclonal antibody bevacizumab is anti-proliferative VEGF inhibitor that was advanced in phase II trials. Bevacizumab (15 mg/kg every 21 days) administration to patients on docetaxel (75 mg/m^2) caused a greater than 50% reduction in PSA levels and improved OS. Various serious adverse effects were reported including neutropenia, thrombosis and myocardial infarction.[35] Endothelin antagonists represent another class of biologic used for the treatment of HRPC due to the central roles of endothelin-1 and the endothelin A receptor in tumor cell proliferation and overexpression in prostate cancer tumors.[36] In a phase III study with advanced prostate cancer patients, the endothelin

antagonist zibotentan did not improve OS significantly following a 10 mg daily dose. Observed adverse effects included headaches, congestive heart failure and edema.[37]

C. Radiopharmaceuticals

The general strategy for targeted delivery of radiation to sites osteoblastic metastases is based on the preferential retention of certain radiopharmaceuticals in areas of osteogenesis and metastases compared to normal bone. While Strontium-89 and samarium-153 are FDA-approved beta-emitting agents for mitigating bone metastases, they failed to demonstrate consistent efficacy, and the their clinical use is limited by myelosuppression.[38-40] Nevertheless, in a study involving patients on doxorubicin chemotherapy, strontium-89 administration reduced pain associated with metastases and improved OS.[41]

D. Chemotherapy

Chemotherapy has also been carried out in conjunction with ADT to slow relapse or resistance in HRPC patients. Docetaxel (Taxotere) is an anti-mitotic agent approved by the FDA for the treatment of breast, ovarian and prostate cancer. Co-administration of docetaxel with prednisone remains the treatment standard for HRPC. A combination of ADT and docetaxel administration improved OS by 4.7 months in a phase II clinical study conducted in patients with HRPC patients.[42] Similarly, co-administration of prednisone with docetaxel (30 mg/m^2 weekly) or the DNA-intercalating anthraquinone mixanthrone (12 mg/m^2) showed that docetaxel elicited greater pain reduction and improved OS when compared to mixanthrone. Side-effects associated with docetaxel and

mixanthrone administration included neurotoxcity, fatigue, hematologic and cardiac toxicities.[43, 44] Because of its reduced adverse effects compared to its analog cisplatin, the clinical use of carboplatin in cancer patients as a chemotherapeutic agent is also common. Carboplatin is a platinum-based antineoplastic drug mainly used for the treatment of lung and ovarian cancer. Single administration and combination of carboplatin with taxanes were both effective at reducing PSA levels and improving OS in advanced prostate cancer patients.[45]

Several years of biochemical research have shed light on the significant challenges of implementing ADT. Significant clinical development efforts have been made over the past years, but the lack of adequate imaging tools for tracking bone metastases, a complication of HRPC, makes it difficult to effectively assess drug efficacy. Currently, there is a need to develop effective non-hormonal therapeutic approaches for the treatment of HRPC. Chemotherapeutics such as docetaxel, mitoxantrone, doxorubicin demonstrated clinical benefits singly or in conjunction with ADT; however, their use is limited by systemic toxicity stemming from non-discriminatory drug exposure to normal tissue.[46-48] Moreover, prolonged chemotherapy commonly results in multidrug resistance due to adaptive enhancement of DNA repair mechanisms, glutathione *S*-transferase induction and up-regulation of efflux pumps.[49-51] Enhanced tumor-selectivity can be achieved through targeted prodrug delivery strategies that are currently being investigated and evaluated at various stages of preclinical and clinical development.

II. Targeted Prodrug Approaches

A. Antibody-directed Enzyme Prodrug Therapy

One anticancer prodrug strategy, termed antibody-directed enzyme prodrug therapy (ADEPT), targets the tumor antigens for selective delivery of enzymes to cancer cells using enzyme-antibody conjugates. ADEPT involves initial administration of an enzyme-antibody conjugate which is allowed adequate time to bind to tumor antigens. Once the enzyme-antibody conjugate clears from systemic circulation, a prodrug designed to be selectively activated in the tumor extracellular space by the antibody-linked enzyme is administered (Fig. 1).

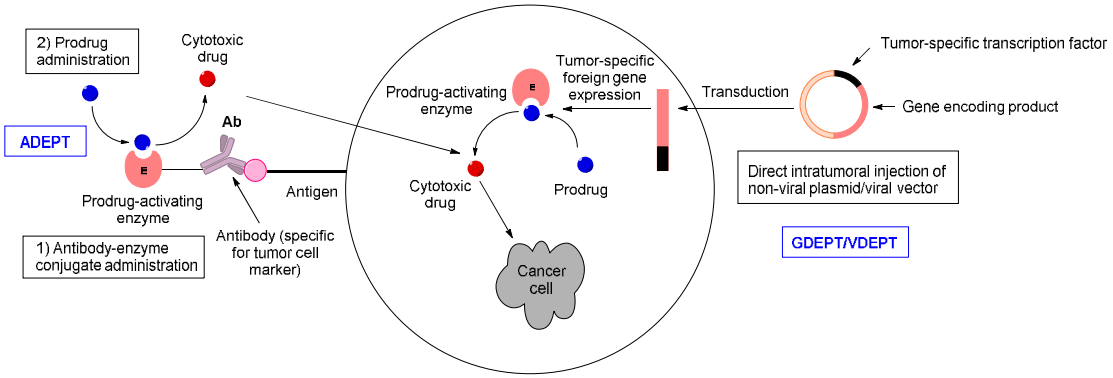

Figure 1. An Outline of Antibody-directed Enzyme Prodrug Therapy (ADEPT) and gene-directed Enzyme Prodrug Therapy (GDEPT)[52]

The enzymes used in ADEPT include penicillin V/G amidase,[53-55] carboxypeptidase A/G2,[56, 57] β-glucuronidase,[58] alkaline phosphatase,[59] β-lactamase[60] and nitroreductase.[61] Since the ADEPT strategy has been extensively reviewed for many types of cancers[62, 63] and limited applications in prostate cancer treatment were found, only a few illustrative examples will be discussed here.

To evaluate its utility for ADEPT, a water-soluble glutamate prodrug of the non-steroidal estrogen diethylstilbestrol (**2**) was designed for specific activation by carboxypeptidase G2 (Fig. 2). Diethylstilbestrol (**1**) is used for the treatment of prostate cancer but causes osteoporosis upon prolonged administration.[64-66] A glutamate diethylstilbestrol prodrug (**2**) was synthesized by incorporating a carbamate linker between diethylstilbestrol and glutamic acid via an isocyanate intermediate of bis-*t*-butyl-glutamate ester.[56] The prodrug was selectively cleaved (greater than 80% in 30 min) by carboxypeptidase G2 to release diethylstilbestrol. Although no follow-up studies of the glutamate diethylstilbestrol prodrug in prostate cancer cell lines have been reported, these preliminary results indicated that the ADEPT strategy could potentially be used for prostate tumor-specific delivery of diethylstilbestrol.

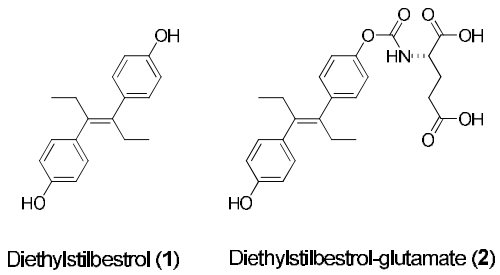

Figure 2. Chemical Sructures of Diethylstilbestrol and its Glutamate Prodrug.

Because the prodrug in ADEPT is activated in the extracellular space of tumor cells, the released cytotoxic agent must be capable of permeating across the cell membrane and reaching its intracellular target to exert its activity. Furthermore, the scarcity of tumor-selective antigens and the possibility of triggering adverse immune responses generally

limit the applicability of the ADEPT strategy.[67, 68] To circumvent the issues of using mouse-derived monoclonal antibodies, a single chain fragment variable of the anti-γ-seminoprotein antibody (anti-γ-Sm-scFv) was conjugated with human carboxypeptidase-A (hCPA) and used to activate the methotrexate (MTX) prodrugs MTX-α-Phe and MTX-α-Arg *in vitro* and *in vivo*.[57] The anti-γ-Sm-scFv-hPCA fusion protein was expected to be less immunogenic and more stable than a monoclonal antibody *in vivo*. The fusion protein efficiently distributed into tumors in BALB/c nude mice bearing PC-3m human prostate cancer xenografts, which was confirmed by ^{125}I-labeling of the fusion protein coupled with Emission Computer Tomography. There was no toxicity associated with fusion protein injections. Both MTX-α-Phe and MTX-α-Arg prodrugs caused anti-γ-Sm-scFv-hPCA-specific cytotoxic responses (comparable to MTX) in LNCaP and PC-3m cell lines with approximately a 1000-fold selectivity. Tumor growth inhibition was robust and nearly 100% in the 5 ADEPT-treated mice. Improved survival from 31 to 91 days was also noted in the ADEPT group.[57]

B. Gene-directed Enzyme Prodrug Therapy

The limitations of ADEPT are somewhat mitigated in the gene-directed enzyme prodrug therapy (GDEPT) approach. GDEPT involves the specific delivery of genes that encode prodrug-activating enzymes to cancer cells through nonviral plasmid transfection or viral transduction. Gene-delivery agents such as peptides, cationic lipids and viral vectors (using retroviruses and adenoviruses) are all used in GDEPT. When a gene encoding for the prodrug-activating enzyme is introduced to tumors by a viral vector, GDEPT is also referred to as virus-directed enzyme prodrug therapy (VDEPT).[69-73] Effective destruction

of cancer cells with GDEPT depends on many factors including the targeted delivery of genes to tumor cells, the tumor-specific expression of prodrug-activating enzyme, prodrug transport through tumor cell membrane, prodrug activation, and formation of toxic metabolites. Complete gene targeting are difficult to achieve using current vectors for gene delivery; a "bystander effect" is often required where the activated prodrug species can permeate across cellular membranes and kill neighboring tumor cells that are not expressing the prodrug-activating enzyme. The ability of the activated prodrug species to induce a significant bystander effect is a crucial determinant of the success of GDEPT. The literature contains excellent reviews on GDEPT and its various applications.[74, 75] Expression of *E. coli* nitroreductase (NTR) in tumor cells through retroviral transduction was initially used for the selective activation of prodrugs in tumor cells, and one of the first NTR-activated prodrugs used in GDEPT is the alkylating agent 5-aziridinyl-2,4-dinitro-benzamide, CB1954 (**3**).[76] Besides its ability to alkylate DNA through its aziridinyl functionality, CB1954 can be metabolized by NTR to two hydroxylamine metabolites one of which is further activated with acetyl-CoA to yield a reactive intermediate ultimately leading to DNA-crosslinking by CB1954 (Fig. 3).[77]

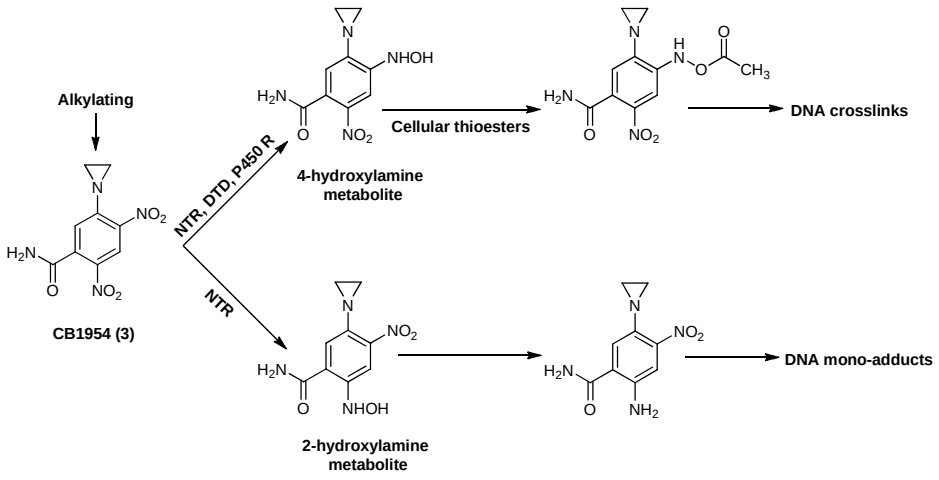

Figure 3. Metabolic Activation of CB1954 by NTR.[78]

NTR expression was achieved with both retrovirus and adenovirus vectors to sensitize human tumor cells to CB 1954.[76, 79, 80] Treatment of nude mice with CB1954 reduced human tumor cell xenografts expressing NTR, increased median survival and reduced tumor growth.[81, 82] Furthermore, distribution of activated CB1954 between tumor cells was found to compensate for suboptimal NTR delivery through the bystander effect.[81-83] In a phase I/II clinical trial conducted with CB1954 using the NTR-encoding adenovirus vector CTL02 in localized prostate cancer patients, NTR incorporation into tumors (monitored by staining) was demonstrated. Up to a 50% decrease in PSA levels was reported in patients that received intraprostatic injections of CTL02 followed by intravenous infusion of CB1954 at 24 mg/m^2.[84]

Other prostate cancer prodrugs delivered by GDEPT include fludarabine phosphate (fludara, **4**), designed to be converted to its cytotoxic metabolite 2-fluoroadenine by *E. coli* purine nucleoside phosphorylase (Fig. 4); 2-fluoroadenine exerts its apoptotic activity by inhibiting DNA, RNA and protein synthesis.[85] Using a hybrid prostate-specific promoter derived from the prostate-specific membrane antigen (PMSA), a purine nucleoside phosphorylase reporter gene was delivered via a recombinant ovine atadenovirus vector (OAdV623, 10^{10} particles) to androgen-sensitive LNCaP-LN3 and androgen-insensitive PC-3 human prostate cancer xenografts in nude mice. This was followed by daily intraperitoneal administration of fludarabine phosphate at 75 mg/m^2/day for 5 days. Purine nucleoside phosphorylase was effectively expressed in xenografts *in vivo* for a minimal period of 6 days. Following its administration, tumor-

specific activation of fludarabine phosphate was achieved with a greater than 50% inhibition in tumor growth for both LNCaP-LN3 and PC-3 cell lines.[85] In immunocompetent C57BL/6 mice bearing androgen-independent RM1 xenografts, similar findings were reported with a single intraprostatic injection of the recombinant ovine atadenovirus vector OAdV220 (10^{10} particles) followed by daily intraperitoneal administration of fludarabine phosphate at 600 mg/m^2/day. Prostate volume was decreased by approximately 50% and apoptosis-activating CD90$^+$ cell infiltration into tumors was detected by immunostaining.[86] Similar approaches using the PSA promoter for enhanced prostate-specific delivery of cytosine deaminase or thymidine kinase as prodrug-activating enzyme have also been reported.[87, 88]

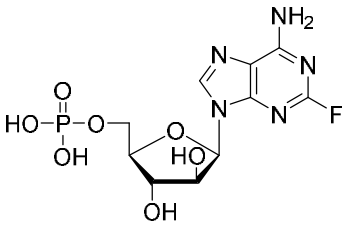

Fludara (**4**)

Figure 4. Chemical Structure of Fludarabine Phosphate (Fludara, **4**).

In addition, a combination of purine nucleoside phosphorylase-mediated GDEPT with docetaxel treatment was also explored in HRPC human PC-3 and murine RM1 cell lines. Cells were infected with an adenoviral vector containing the purine nucleoside phosphorylase gene and then treated with varying concentrations of docetaxel (0.1 -100 nM) and/or fludarabine phosphate (1 μg/mL). Evaluation of cell viability revealed significant synergistic cytotoxic effects in both PC-3 and RM1 cell lines *in vitro*. Co-administration of fludarabine phosphate (50 mg/m^2/d, i.p. for 5 days) and docetaxel (3

doses of 10 mg/kg, every 6 days) following a subcutaneous injection of adenoviral vector containing the purine nucleoside phosphorylase gene to BALB/c nude mice led to significant tumor weight reduction, no toxicity and enhanced immune cell infiltration.[89] A phase I dose escalation study was initiated in Australia in 2008 (publication of results pending) to evaluate the safety and tolerability of the PNP-expressing ovine atadenovirus vector FP253 administered in combination with fludarabine phosphate. Six cohorts (3 HRPC patients each) received single escalating doses of FP253 from $1x10^9$ to $3.2\ x10^{11}$ particles, followed by five intravenous doses of fludarabine at 20 mg/m^2 administered at 24 h intervals.[90]

A double GDEPT approach was reported for simultaneous expression of the yeast FCY1 and the thymidine kinase of herpes simplex virus (HSV-TK) genes in LNCaP and PC-3 prostate cancer cells through a pIRES plasmid driven by PSMA promoter for the activation of two prodrugs, 5-fluorocytosine (**5**) and ganciclovir (**6**) (Fig. 5).[91] The FCY1 gene is the yeast equivalent of cytosine deaminase (CD) that can activate 5-fluorocytosine (**5**) to 5-fluorouracil, an antimetabolite capable of interfering with both DNA and RNA synthesis leading to cell death. The HSV-TK gene activates ganciclovir (**6**) to phosphorylated ganciclovir that gets incorporated into DNA causing death of the dividing cancer cells. The combination was shown to be much more effective than either single GDEPT. Tumor transfection followed by treatment with ganciclovir (0.01-100 μg/mL) and 5-fluorocytosine (10-160 μg/mL) resulted in additive growth inhibition in LNCaP and PC-3 cell lines (roughly 70 and 60%, respectively). In this study, the most robust tumor growth inhibition (95%) and decreased metastasis were observed in the

castrated nude mice bearing transfected LNCaP xenografts following prodrug co-administration.[91]

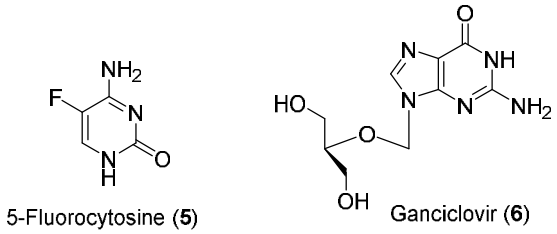

Figure 5. Chemical Structures of 5-Fluorocytosine and Ganciclovir.

The efficacy of ProstAtak™ towards the prevention of the relapse of localized prostate cancer is currently being investigated in a double-blind, randomized, Phase III trial in newly diagnosed prostate cancer patients receiving radiation therapy with and without ADT.[92] ProstAtak™ is a gene-mediated cytotoxic immunotherapy (GMCI™) product containing a HSV-TK-expressing adenoviral vector. When administered with an anti-herpetic prodrug (ganciclovir or valaciclovir) and radiation therapy, ProstAtak™ triggers synergistic tumor-specific cytotoxicity through prodrug activation, antigen presenting cell activation and anti-tumor T-cell stimulation thereby preventing metastasis and recurrence. HSV-TK gene product, which is not produced by mammalian cells, efficiently phosphorylates ganciclovir or aciclovir (the hydrolyzed metabolite of valaciclovir) that is incorporated into newly synthesized DNA causing chain termination and cell death. The safety and tolerability of ProstAtak™ were demonstrated via intraprostatic viral injections in patients with clinically localized prostate cancer but high risk for recurrence; 43% of the patients treated responded with a mean decrease in PSA

of 44% and tumor-specific effect mediated by systemic and local immune response was observed in phase I/II clinical trials.[93, 94] In a phase II trial, ProstAtak™ in combination with radiation resulted in immune stimulation with evidence of prolonged T cell activation and a greater than 3-fold decrease in recurrences.[95]

While GDEPT was effective in preclinical and clinical studies, the inability to achieve complete gene transduction of tumor cells *in vivo* remains a significant challenge. To mitigate potential immunogenicity issues associated with non-human enzymes, several attempts to design humanized enzyme immnoconjugates with improved toxicological and pharmacokinetic profiles are under investigations.[96, 97] Nevertheless, as mentioned earlier, several GDEPT agents advanced to clinical trials demonstrated adequate safety, tolerability, and in some cases, good efficacy when used in combination with existing prostate cancer therapies. Furthermore, some of the caveats of enzyme-antibody conjugates or delivery of foreign enzymes as prodrug activating-enzymes to prostate cancer cells can be overcome by directly targeting endogenous enzymes that are specifically expressed in the tumor microenvironment for prodrug activation.[98] The prostate-specific membrane antigen (PSMA) and the prostate-specific antigen (PSA) have been targeted as viable tumor-specific prodrug-converting proteases for improving the chemoselectivity as discussed in the following section.

C. PSMA-mediated Activation of Prodrugs

1. Prostate-specific Membrane Antigen (PSMA)

PSMA is a type II membrane-bound glycoprotein that is selectively expressed in epithelial cells of the prostate. It is overexpressed in metastatic prostate tumors although present in detectable levels in the brain and brush border cells of the small intestine.[99, 100] PSMA is a glutamate carboxypeptidase that cleaves terminal γ-linked residues from poly-γ-glutamated dietary folates thereby promoting their uptake into epithelial cells.[101, 102] It possesses both pteroyl poly-γ-glutamyl carboxypeptidase and *N*-acetylated α-linked acidic dipeptidase activities. The overexpression of PSMA in prostate carcinomas has been explored for tumor-specific delivery and activation of prodrugs designed to be activated by PSMA's proteolytic action as described below.

2. Prodrugs Designed for PSMA Activation

a. H-3Glu2, a Polypeptide Prodrug of Amoebapore for PSMA Activation

A PSMA-cleavable prodrug of the H3 domain of the pore-forming cytolytic polypeptide amoebapore (isolated from *Entamoeba histolytica*) was designed for selective activation in PSMA-positive LNCaP cells.[103] While a promoter region of the PSMA gene was previously targeted to induce the expression of cytosine deaminase thereby sensitizing C4-2 cell lines (a subline of LNCaP cells) to 5-fluorocytosine,[104] this was the first report of a prodrug designed to be activated by the proteolytic action of PSMA. Of the four α-

helical domains contained within the cytolytic amoebapore, H3 was identified to possess high pore-forming activity *in vitro*.[105] The amoebapore prodrug, $H3Glu_2$ (Gly-Phe-Ile-Ala-Thr-Leu-Cys-Thr-Lys-Val-Leu-Asp-Phe-Gly-Ile-Asp-Lys-Leu-Ile-Gln-Leu-Ile-Glu-Asp-Lys(γGlu-γGlu)-NH_2), consisted of the H3 domain coupled through its ε-amino group of its C-terminal Lys to two γ-linked glutamate residues. Modification of the ε-amino group of the C-terminal Lys rendered the helical domain inactive so that $H3Glu_2$ could be selectively activated in PMSA-expressing prostate cancer cells. As anticipated, H-$3Glu_2$ was non-cytotoxic in non-PSMA-containing PC-3 cell lines but induced cytotoxic activity in PSMA-expressing LNCaP cells (40% lysis at 50 μM). The cytolytic effects observed in LNCaP cells were abolished by the addition of a carboxypeptidase inhibitor 4,4'-phosphonicobis (butane-1,3- dicarboxylic acid). Furthermore, transfection of PC-3 cells with a PSMA plasmid led to effective prodrug activation and subsequent cytolytic activity (~20% lysis at 50 μM). Administration of $H3Glu_2$ to nude mice (200 μg, twice a week for 7 weeks) bearing human LNCaP prostate tumor xenografts led to up to a 100% reduction in tumor size and PSA levels (5 out 12 mice). Following a 30 mg/kg dose, the prodrug was non-toxic and distributed into prostate tumors with steady state concentrations up to 6 hours.[106]

b. PSMA-cleavable MTX-Peptide Conjugates

In order to develop substrates with improved specificity, a series of methotrexate (MTX) peptide conjugates were screened for PSMA hydrolysis, serum stability and cytotoxicity in PSMA- and non-PSMA-producing cell lines.[107] Since poly-γ-glutamated MTX was a

known substrate of PSMA, MTX was conveniently used as a cytotoxic agent for substrate screening. Due to its low response in advanced prostate cancer patients and its propensity to resistance,[108] MTX may not be a preferred agent to be incorporated into prodrugs for prostate cancer. The MTX conjugates were generated by coupling the carboxyl group of the *N*-(2,4-diamino-6-pteridinylmethyl)-*N*-methyl-4-aminobenzoate (APA) moiety of MTX to the amino terminus of various small peptides primarily containing acidic amino acids as represented by the conjugate APA-Asp-γGlu-γGlu-Asp-Glu (**7**) (Fig. 6).

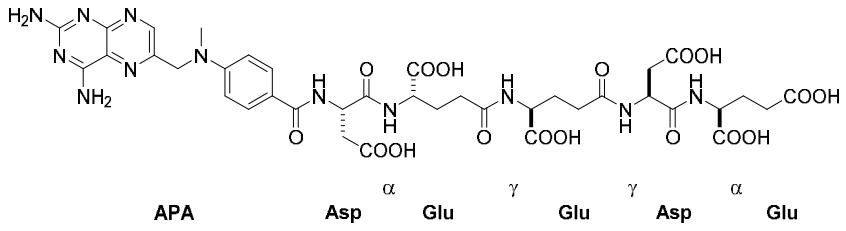

Figure 6. Chemical Structure of a Representative PSMA-cleavable Methotrexate Conjugate (APA-Asp-γGlu-γGlu-Asp-Glu).

The highest PSMA hydrolysis rates were observed for conjugates containing all γ-linked glutamate residues with the fastest being nearly complete hydrolysis within 24 h for APA-γGlu-γGlu-γGlu-γGlu-Glu. However, the all γ-linked glutamate conjugates were also less stable to non-specific hydrolysis in plasma. Thus, the APA-γGlu-γGlu-γGlu-γGlu-Glu conjugate did cause maximal growth inhibition of 100% in PSMA-producing TSU cell lines but also exhibited significant growth inhibition of ~40% in non-PSMA-producing TSU cells at 0.1 μM for 72 h. It would be necessary to use conjugates containing both α and γ-linked amino acids like that shown in conjugate **7** to achieve the desired plasma stability and selective PSMA-mediated hydrolytic activation.[107]

c. PSMA-activated Thapsigargin Prodrug

Numerous cell-based and animal studies identified the sarcoplasmic and endoplasmic reticulum Ca^{2+}-dependent ATPase (SERCA) inhibitor thapsigargin (**8**), isolated from *Thapsia garganica*, as a potential chemotherapeutic agent.[109-111] The most recent example of a PSMA-targeted prodrug activated by proteolysis involves the engineering of G-202 (12ADTβAsp-γGlu-γGlu-γGlu–Glu, **9**), which consists of the PSMA-specific substrate, Asp-γGlu-γGlu-γGlu–Glu, coupled to the thapsigargin derivative 8-*O*-(12-aminododecanoyl)-8-*O*-debutanoyl thapsigargin (12ADT).[112] G-202 was designed to be activated by the poly-γ-glutamyl carboxypeptidase and *N*-acetylated α-linked acidic dipeptidase activities of PMSA, and incorporates the optimized peptide sequence γGlu-γGlu-γGlu–Glu from the previously mentioned substrate optimization studies with MTX conjugates (Fig. 7). Upon PSMA cleavage, G-202 releases the cytotoxic conjugate 12ADTβAsp, which exhibits IC_{50} values of 40 and 72 nM in PSMA-expressing LNCaP and PSMA-negative TSU cells, respectively. G-202 was effective at inhibiting clonal survival in LNCaP cells with IC_{50} of 191 nM, and demonstrated a 57-fold selectivity over PSMA-negative TSU cells. PSMA-mediated growth inhibition of LNCaP cells by G-202 was further confirmed with co-incubations with the PSMA inhibitor 2-(phosphonomethyl)-pentanedioic acid; the inhibitor suppressed the concentration-dependent growth inhibitory effect of G-202 up to a prodrug concentration of 500 nM. Following an acute intravenous dose of 67 mg/kg to BALB/c mice, G-202 was cleared with a half-life of 4.9 h, and less than 1% of the administered dose converted to the active metabolite 12ADTβAsp. In mice receiving 56 mg/kg/day intravenous doses for up to

three days, ~50% tumor regression was observed *in vivo* against human prostate cancer xenografts.[112]

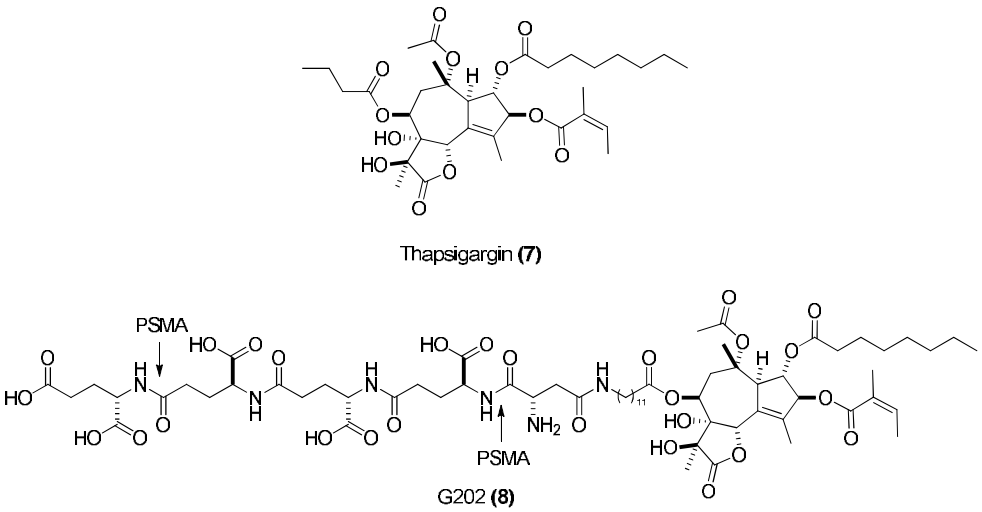

Figure 7. Chemical Structures of Thapsigargin and G-202.

While the feasibility of PSMA-targeted prodrugs has been extensively demonstrated in cell culture systems and rodent models, it is not clear whether it is an applicable strategy in humans *in vivo* as significant levels of PSMA were also detected in extra-prostatic tissues including normal human brain, small intestine and salivary gland tissues.[99, 100, 113-115] There are ongoing clinical trials to investigate the safety and efficacy of G-202 in patients with recurrent or progressive glioblastoma[116], and hepatocellular carcinoma receiving orafenib therapy.[117] In a previous phase I dose escalation study in 28 patients with advanced solid tumors that received intravenous infusions of G-202 at dose levels ranging from 1.2 to 88 mg/m^2, common adverse effects included fatigue (39% of patients), nausea (36% of patients), rash (29% of patients) and vomiting. G-202 exhibited biphasic pharmocokinetics (half-lives of 1.7 and 18.1 h) with an apparent volume of

distribution of 4059 mL/m^2 at steady state (low tissue distribution) and a systemic clearance of 181 mL/h/m^2. The established MTD was 66.8 mg/m^2.[118] A follow-up phase II trial was scheduled in 2012 to further evaluate the safety and efficacy of G-202 in HRPC patients, but it was withdrawn prior to enrollment while two other phase II clinical studies of G-202 against hepatocellular carcinoma and recurrent or progressive glioblastoma are still ongoing.[119]

D. PSA-mediated Activation of Prodrugs

1. Prostate-specific Antigen (PSA)

Human PSA is a 33-kDa kallikrein-related serine protease with chymotrypsin-like activity that is secreted in the ductal acinar epithelium of the prostate gland as a semen liquefaction enzyme. Serum PSA levels are routinely screened as a serological marker for prostate cancer. Hyperplasia-induced disruption of the epithelium causes PSA to leak into the interstitial space of tumor cells and ultimately diffuse into the systemic circulation.[120, 121] However, low systemic concentrations of the antigen are also detectable in healthy males.[122-124] Reports of high levels of PSA in both androgen-dependent and -independent prostate cancer patients, especially bone and soft tissue tumors, suggest that the protease could be involved in disease progression. PSA may play a significant role in prostate cancer growth, invasion and metastasis through several mechanisms including the proteolytic activation of cytokines involved in inflammation and growth stimulation such as the insulin-like growth factor binding proteins-3 (IGFBP-3) to generate IGF-1.[125] While there is a controversy around the involvement of IGFBP-3 and IGF-1 in prostate cancer progression, the proliferative and anti-apoptotic properties of IGF-1 were clearly

demonstrated in prostate epithelial cells.[126, 127] PSA has also been associated with the proteolytic activation of parathyroid hormone-related protein (PTHrP), which ultimately regulates osteoclastic factor RANKL release.[128-130] In addition to its interaction with cytokines, PSA was shown to cleave the gel-forming proteins semenogelins I and II in human semen. Mapping of PSA cleavage sites revealed scissile bonds after Leu and Tyr, but more surprisingly after Gln since approximately 40% of the peptide fragments mapped comprised Gln.[131, 132] The crystal structure of PSA in complex with the monoclonal antibody 8G8F5 and the fluorogenic semenogelin I-derived substrate Mu-Lys-Gly-Ile-Ser-Ser-Gln-Tyr-AFC was first reported by Ménez and colleagues (Fig. 8).[133]

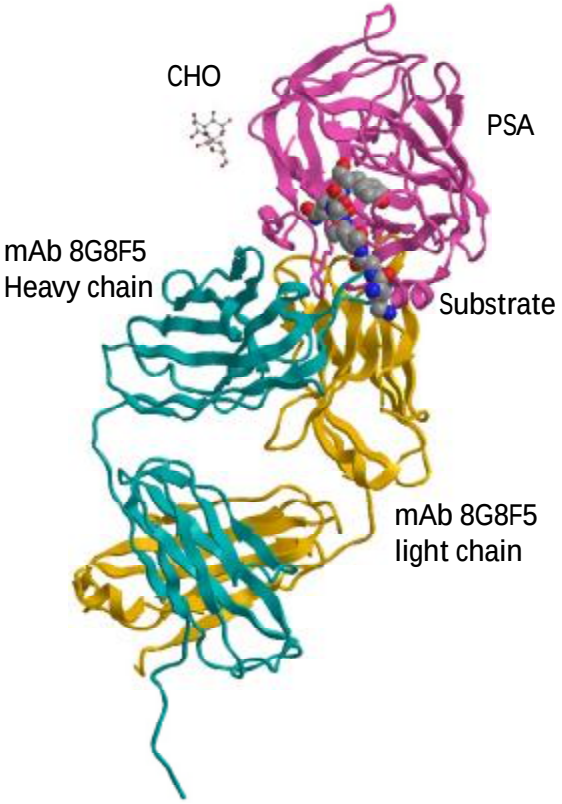

Figure 8. Ternary Fab′8G8F5-PSA-Mu-KGISSQY-AFC Complex[133]

The monoclonal antibody 8G8F5 was shown to enhance the activity of seminal PSA through specific binding to an epitope overlapping with the kallikrein loop,[133, 134] and the ternary antibody-PSA-substrate complex was trapped and crystallized as the acyl intermediate covalently linked to the catalytic serine upon inhibition by zinc ions at physiological pH.[133]

The unique proteolytic properties and activity profile of PSA in the tumor microenvironment make it an attractive target for tumor-specific activation of peptide conjugates of potent chemotherapeutic agents as prodrugs for the treatment of prostate cancer. In the prostate, 80-90% of extracellular PSA is enzymatically active with concentrations ranging from 1.6 to 2.1 μM whereas intracellular PSA is inactive due to zinc inhibition.[135] Inhibition by α1-antichymotrypsin and α2-macroglobulin in the serum further limits the proteolytic activity of PSA to the tumor microenvironment.[136, 137] Thus, the unique ability of PSA to cleave after Gln and restriction of its proteolytic activity in the local environment of prostate tumors can be effectively leveraged through prodrugs designed to be activated by PSA. By coupling PSA-cleavable peptides to anticancer agents, targeted prodrugs can be designed to be selectively activated by the proteolytic action of PSA in prostate tumors. Based on the cleavage map for its natural substrates, semenogelins I and II, several short peptides were engineered as pro-moieties to be rapidly cleaved by PSA (Table 1)[138, 139] and significant discovery efforts have been invested in designing such targeted prodrugs over the past decade.[139-141] Initial PSA substrates designed based on a septapeptide sequence near the PSA cleavage site were coupled to 7-amino-4-methylcoumarin (AMC) for convenient fluorescence detection

following scissile bond hydrolysis. Substrates with improved K_m and k_{cat} values were developed and those with Tyr at P1 exhibited the fastest PSA cleavage rates.[138] However, these substrates with Tyr at P1 were also cleaved by elastase and chymotrypsin 10-20 times faster than by PSA. Improved PSA specificity was achieved with Gln at P1 with a compromise in cleavage rate. Substrate evaluation in various sera led the final peptide conjugate His-Ser-Ser-Lys-Leu-Gln-AMC (K_m = 470 μM, k_{cat}/K_m = 23 M^{-1} s^{-1}) which was further assayed for PSA activity in tissues and incorporated into PSA-cleavable prodrugs.[141, 142] In addition to the studies using AMC-conjugates, independent PSA substrate optimization efforts[139] showed striking similarities in peptide substrate sequences which were later substantiated by PSA X-ray studies[133] (Table 1).

Table 1. Preferred Amino Acids Substitutions for Maintaining PSA Specificity.

Position	Preferred amino acid[a]	Properties from X-ray structure studies[133]
P1'	Ser	Ser residue effectively forms a H-bond with -OH of Ser[217]
P1	**Gln**, Tyr, Phe, Asn	Critical H-bonding interactions between Tyr(-OH) / Gln(-NH_2) and Gln[503] (O^{ε}) are required
P2	Chg, Tyr, **Leu**	Hydrophobic residue is required for backbone interactions with Gly[216], Ser[217] and Glu[218]
P3	Ser, **Lys**	H-donor/acceptor is involved in H-bonding interaction with Gln[174]
P4	Ala, **Ser**	Small hydrophobic residue is involved in van der Waals interactions with kallikrein loop
P5	[b]**Pro, Ser**	Side-chains of Pro and Ser are optimal for interactions with Gln[170]-Val[171]-His[172]-Pro[173]
P6	His	His is involved in H-bonding with Gln[170]

[(a)] most preferred amino acids are indicated in bold. [(b)] Restricted conformer of Ser

Semenogelin cleavage map construction was coupled with systematic amino acid substitution flanking scissile bonds to generate a series of peptides which were

subsequently coupled to doxorubicin through their C-terminal carboxyl group to afford various conjugates. The peptide conjugates were evaluated for PSA cleavage rate and cytotoxic response in PSA-producing LNCaP and non-PSA-producing DuPro prostate cancer cell lines. The results showed highly conserved motifs for the region between P1 and P4.

The first reported PSA-activated prodrug, glutaryl-Hyp-Ala-Ser-Chg-Gln-Ser-Leu-Dox (L-377,202) containing the optimized PSA substrate sequence, was found to have a half-life of 30 min for PSA cleavage. It exhibited a high selectivity towards PSA-producing LNCaP cells with EC_{50} values of 5 and >100 μM in LNCaP and DuPro cell lines, respectively. The optimal conjugate was also efficacious in nude mice causing a 95% decrease in serum PSA levels and 87% reduction of tumor weight.[139] Similarly, PSA-targeted prodrugs of paclitaxel,[143] thapsigargin,[142, 144] diazeniumdiolate,[145] protoxin,[146] 5-fluoro-2′-deoxyuridine,[147] nitrogen mustard,[148-151] doxorubicin,[139, 140] and vinblastine[152, 153] were designed and evaluated in PSA-producing prostate tumor cell lines as well as *in vivo* in mouse models as discussed in the following sections. Among the PSA-activated prodrugs developed over the past two decades, the doxorubicin conjugate glutaryl-Hyp-Ala-Ser-Chg-Gln-Ser-Leu-dox (L-377,202) was advanced to clinical trials to demonstrate proof-of-concept.[154, 155] In its phase I clinical trial, the doxorubicin conjugate was well tolerated and was shown to be metabolized to the cytotoxic Leu-doxorubicin and doxorubicin. At 225 and 315 mg/m^2 doses, two of the five patients completing three or more cycles of therapy had >75% decrease in PSA and one had a stabilized PSA, indicating the presence of therapeutic effect of the prodrug in human prostate cancer.[154]

2. *Prodrugs Designed for PSA Activation*

a. *Prodrugs of Paclitaxel*

Paclitaxel (**9**) is an antitumor taxane effective against a broad spectrum of malignancies including advanced prostate cancer.[156-158] However, the clinical use of paclitaxel as a chemotherapeutic agent is limited by its lack of selectivity resulting in numerous adverse effects, namely mucositis, neutropenia and neurotoxicity.[159, 160] To improve the selectivity and aqueous solubility of paclitaxel, PSA-activated prodrugs **10-13** consisting of the peptides His-Ser-Ser-Lys-Leu-Gln or Ser-Ser-Lys-Tyr-Gln coupled to paclitaxel via either a para-aminobenzyl alcohol (PABA) or ethylene diamine (EDA) linker were designed and synthesized (Fig. 9).[143] Overall, PSA cleavage rate was significantly improved with linker insertion, but the PABA-linked prodrugs exhibited poor serum stability due to their readily hydrolyzable carbonate bond. Premature nonspecific hydrolysis was mitigated with the introduction of an EDA linker and the resulting prodrugs were cytotoxic against the PSA-producing CWR22Rv1 prostate cancer cells. The best paclitaxel prodrug (**13**) was effective in the CWR22Rv1 cancer cell line with an IC_{50} of 1 μM (paclitaxel IC_{50} < 1 nM) and a 3- to 5-fold selectivity against the non-PSA-producing cancer lines DU145 and TSU. Solubility of the prodrug was also improved by up to 90-fold. While paclitaxel prodrug **13** was effective in PSA-producing prostate cancer cell lines, it was 1000-fold less potent than paclitaxel; the lower potency of prodrug **13** could be explained by a slow chemical release of paclitaxel from the linker following PSA cleavage.[143]

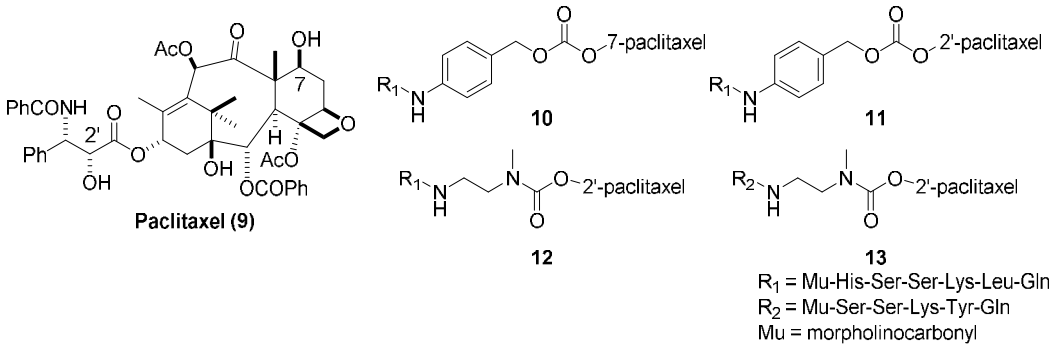

Figure 9. PSA-activated Paclitaxel Prodrugs.

b. Prodrugs of Thapsigargin

Due to the inherent ability of thapsigargin (**7**) to induce apoptotic responses against both proliferative and quiescent G_0 cells,[111] its anticipated lack of selectivity toward prostate tumor cells could potentially be circumvented through the use of a prodrug like **14** consisting of the PSA peptide substrate His-Ser-Ser-Lys-Leu-Gln coupled to 8-*O*-(12-[L-leucylamino]dodecanoyl)-8-*O*-debutanoylthapsigargin (L12ADT) (Fig. 10).[142] Previous attempts to couple toxins directly to Gln afforded prodrugs that were inefficiently cleaved by PSA. However, introduction of a Leu linker between the peptide sequence and the toxin led to conjugates with improved PSA cleavage rate.[141, 161] Since the thapsigargin analog 12ADT was found to be as potent as thapsigargin,[144, 162] it was coupled to His-Ser-Ser-Lys-Leu-Gln via a Leu linker and evaluated. The resulting prodrug **14** demonstrated good stability towards nonspecific hydrolysis in plasma and produced effective cytotoxic response in PSA-secreting LNCaP human prostate tumor cell line with an IC_{50} of 74 nM.[142] Following an acute intravenous dose of 7 mg/kg to BALB/c mice, prodrug **14** was cleared from plasma with a half-life of 2.8 h with less than 0.5% circulating free L12ADT. Tumor growth inhibition was observed in LNCaP xenograft mouse model

receiving 7 mg/kg daily intravenous infusions of the prodrug for 28 days with no obvious toxicity issues. As expected, a similar regimen in mice bearing non-PSA-producing human SN12C renal cell carcinoma xenografts did not show tumor growth inhibition.[142]

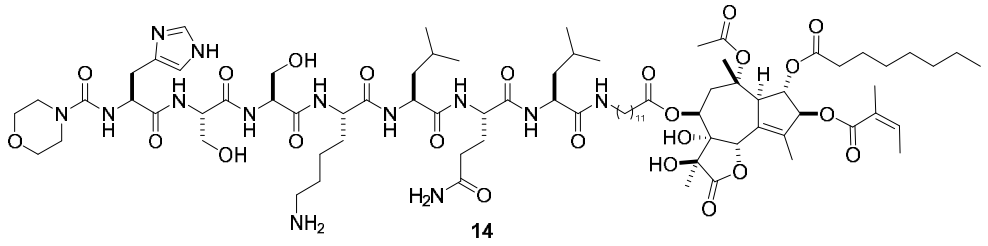

Figure 10. PSA-activated Thapsigargin Prodrug **14**.

c. Prodrugs of Nitric Oxide (NO)

In addition to its implication in various vasoactive processes and neurotransmission, nitric oxide (NO) has been identified as an effective anti-tumor agent. Produced by macrophages, natural killer T-cells, endothelial and Kupffer cells, NO can kill a broad spectrum of tumors by altering protein function and causing DNA damage. Reaction of NO with oxygen radical species generates reactive intermediates capable of nitrosating protein and DNA.[163-167] Diazeniumdiolates, which provide a convenient controlled release source of NO,[168, 169] were coupled to various PSA substrates derived from substrate phage display and iterative optimization studies[170] to generate prodrugs for selective PSA activation in tumor cells (Fig. 11).[145] While other highly specific PSA substrates were reported, the peptide sequences Ser-Ser-Tyr/Phe-Tyr were initially selected due to synthetic feasibility since they could readily be coupled to diazeniumdiolates via *O*-alkylation. The smaller size of diazeniumdiolates allows for

direct coupling to the peptide sequences through a short acetal linker due to the minimal steric hindrance to PSA catalysis; a similar approach was used and demonstrated for small molecular weight cytotoxins such as phosphoramide mustard.[151, 171] The prodrugs were designed to produce a diazeniumdiolate intermediate as an NO donor following PSA cleavage that undergoes spontaneous chemical release of NO (quantifiable using an electrochemical NO meter) through a self-immolative acetal linker. Evaluation in the presence of purified PSA and α-chymotrypsin revealed that the synthesized prodrugs **15-17** were activated by both PSA and α-chymotrypsin. The use of a PSA-selective peptide substrate sequence could confer specificity to the prodrugs towards PSA-mediated cleavage.[145]

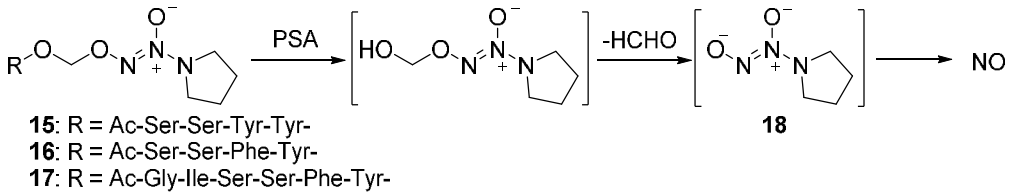

Figure 11. PSA Activation of Diazeniumdiolate Prodrugs **15-17**.

d. PSA-activated Protoxin

Proaerolysin is a 53 KDa protein produced by the Gram-negative aquatic bacterium *Aeromonas hydrophila*. It contains a C-terminal inhibitory domain and, upon proteolytic cleavage of the inhibitory domain by membrane-bound furins, generates aerolysin, a pore-forming protein that induces apoptosis.[172, 173] A PSA-activated protoxin (PRX302) was designed and synthesized via site-directed mutagenesis of the furin recognition site

of proaerolysin, Lys-Val-Arg-Arg-Ala-Arg, to the PSA substrate His-Ser-Ser-Lys-Leu-Gln.[146, 174] Incubation of PRX302 with furin, PSA and select proteases indicated that the protoxin was completely resistant to proteolytic activation by furin or thrombin, but somewhat susceptible to trypsin and chymotrypsin activation. PSA inhibitors present in serum and androgen were used to demonstrate the specificity of PRX302 activation in prostate cancer cells. Untreated PSA-producing LNCaP cells were significantly more sensitive to PRX302 (IC_{50} of 25 pM) compared to PSA-null PC-3 cell lines (IC_{50} of 1130 pM) with greater than 40-fold selectivity, and the sensitivity of LNCaP cells to PRX302 correlated with PSA levels produced. Insignificant sensitivity of most normal human cells (except for renal epithelial cells) to PRX302 was also observed.[174] Evaluation of PRX302 in LNCaP, PC-3, CWR22H, and DU145 prostate cancer cell lines and the bladder cancer cell line TSU indicated that PRX302 caused tumor-specific cytotoxicity in PSA-producing LNCaP cell lines at picomolar concentrations. Compared to native proaerolysin, PRX302 was 27-fold less toxic to non-PSA-producing TSU cells, and selectively toxic to PSA-producing LNCaP cells. Direct intratumoral injections of 5 and 10 μg of PRX302 resulted in complete tumor reduction in 10 out of 26 mice bearing LNCaP or CWR22H xenografts, but not in non-PSA-producing bladder cancer xenografts. The PRX302 exhibited prostate-specific damage in cynomolgus monkeys, but did not adversely affect any other organs. PRX302 showed promising safety and efficacy in preliminary Phase I and Phase II studies conducted in a small population of 33 benign prostatic hyperplasia patients. Greater than 60% of patients treated with PRX302 at doses ranging from 0.034 to 0.9 μg/prostate by transperineal injection demonstrated more than 30% improvement in their International Prostate Symptom Score (IPSS), significant

enhancement in Quality of Life (QoL) Score and decreased prostate volume. No severe adverse effects related to PRX302 treatment were reported except for mild and transient genitourinary tract toxicities.[175] A follow-up Phase IIa clinical trial was conducted in 18 patients with locally recurrent prostate cancer that previously received primary radiation therapy treatment to determine an optimal dosing volume (at a fixed concentration of 3 μg/mL) for PRX302. There was a dose-dependent improvement (15-54%) in IPSS, and significant QoL enhancement (up to 67% at 12 months post-treatment) in patients dosed at volumes greater than 1 mL, and PRX302 was safe and well-tolerated at all dosing volumes examined.[176] Significant improvements in IPSS (roughly 60%) were observed in a double-blinded placebo controlled Phase II study of PRX302 (TRIUMPH) in patients with moderate to severe benign prostate hyperplasia. The study was conducted to further evaluate the efficacy of PRX302 against placebo at the optimal dose volume established in the aforementioned phase IIa study in subjects treated at a dose volume equivalent to 20% of total prostate volume by ultrasound-assisted intravenous injection.[177] In addition, the safety and efficacy of a single transrectal intraprostatic administration of PRX302 is further being investigated for lower urinary tract symptoms secondary to benign prostatic hyperplasia.[178]

e. Prodrug of 5-Fluoro-2′-deoxyuridine (FDUR)

A PSA-activated prodrug of the anticancer agent 5-fluoro-2′-deoxyuridine (FDUR, **19**) was designed and synthesized by coupling the PSA substrate His-Ser-Ser-Lys-Leu-Gln FDUR via a self-immolative diamino acid linker (Fig. 12).[147] FDUR is an antimetabolite that exerts its activity through the inhibition of thymidylate synthetase thereby preventing

DNA synthesis.[179] Incubation of the FDUR prodrug (**20**) in LNCaP cells at a concentration of 50 μM resulted in a 75% FDUR release in 120 h via PSA-mediated hydrolysis. The prodrug was also effective against PSA-producing LNCaP cells with an IC_{50} of 117 nM, with a ~60-fold selectivity over non-PSA-producing TSU cells (IC_{50} = 7200 nM).

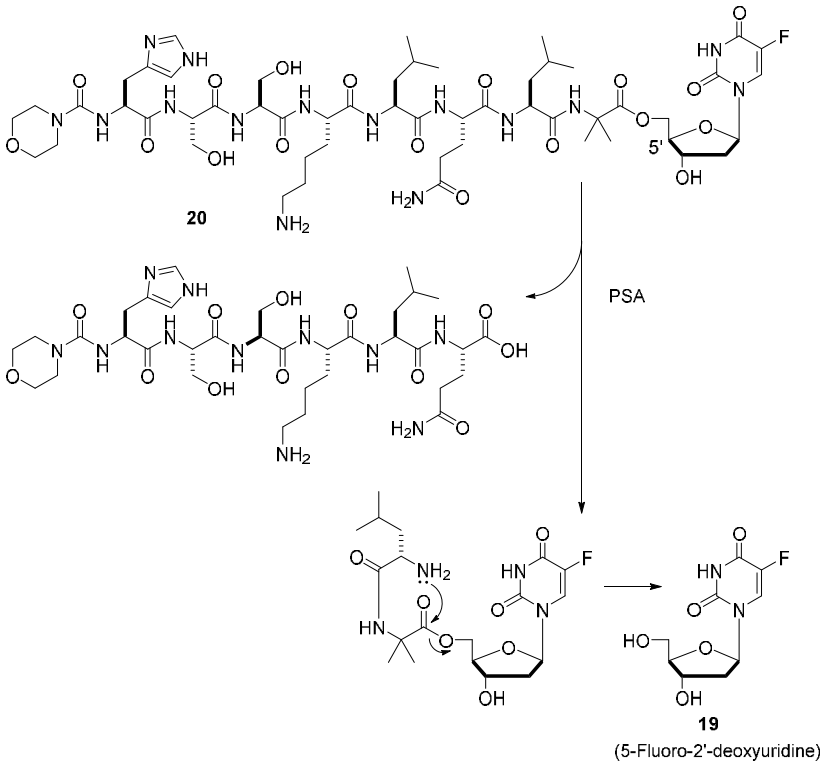

Figure 12. PSA Activation of FDUR Prodrug **20**.

f. Prodrugs of Nitrogen Mustard

Nitrogen mustard prodrugs have been extensively investigated in GDEPT approaches following the example of CB1954. The novel 4-nitrobenzyl phosphoramide mustard prodrug LH7 (**21**) with improved efficacy in SKOV3 ovarian cells expressing *E. coli*

NTR and a toxicity profile comparable to that of CB1954 was developed (Fig. 13).[180] The cytotoxic agent released upon activation of prodrug **21** by NTR is phosphoramide mustard, an active metabolite of the DNA-alkylating agent cyclophosphamide.

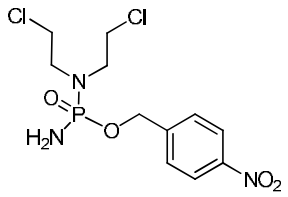

LH7 (**21**)

Figure 13. Chemical Structure of LH7 (**21**).

In combination with other anticancer agents, cyclophosphamide is used for the treatment of lymphomas and certain types of leukemia.[181] Independent of its inherent DNA alkylating properties, the toxicity of cyclophosphamide is primarily mediated by cytochrome P450 2B6 oxidation to active 4-hydroxycyclophosphamide which is ultimately converted to toxic metabolites acrolein (associated with hemorrhagic cystitis) and phosphoramide mustard.[182] In general, cyclophosphamide administration is associated with moderate clinical side-effects including vomiting, diarrhea and bone marrow suppression. However, more serious side-effects such as bloody urine, mouth sores and joint pain have been observed.[183] Due to its ability to spontaneously decompose to phosphoramide mustard under physiological conditions, 4-aminocyclophosphamide (4-NH_2-CPA) was used as a prodrug moiety. The feasibility of designing 4-NH_2-CPA peptide conjugates was first evaluated as model prodrugs for activation by proteases and *cis*-(*2R, 4R*)-4-NH_2-CPA (**22**) found to be required stereochemically for proteolytic activation.[149] Subsequent synthesis and evaluation of various 4-NH_2-CPA tetrapeptide

conjugates **22** showed that PSA cleavage was stereoselective and that the *cis*-(*2R, 4R*)-isomer was activated by PSA with a half-life of 12 min (Fig. 14). Release of 4-NH_2-CPA followed by its rapid degradation to phosphoramide mustard was confirmed by LC/MS analysis.[148]

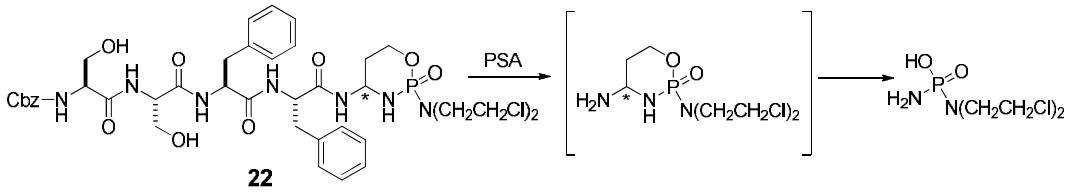

Figure 14. PSA Activation of 4-NH_2-CPA Peptide Conjugates **22**.

Similar studies with peptide conjugates of various lengths demonstrated that the peptide conjugate glutaryl-Hyp-Ala-Ser-Chg-Gln-NH-CPA (**25**) exhibited the shortest half-life of 55 min following PSA cleavage after glutamine to release 4-NH_2-CPA (Fig. 15). Likewise, the peptide conjugates succinyl-His-Ser-Ser-Lys-Leu-Gln-NH-CPA (**23**) and succinyl-Ser-Lys-Leu-Gln-NH-CPA (**24**) were cleaved by PSA with half-lives of 6.5 and 12 h, respectively.[171]

Based on previous observations that fluorinated prodrugs designed for NTR activation in GDEPT exhibited improved bystander effect, cytotoxicity and selectivity, a series of PSA-activated phosphoramide mustard prodrugs were designed.[151] Various fluorinated aminobenzyl alcohol linkers were incorporated between the highly specific PSA substrate, Hyp-Ala-Ser-Chg-Gln, and phosphoramide mustard to promote rapid drug release following PSA cleavage (Fig. 16).

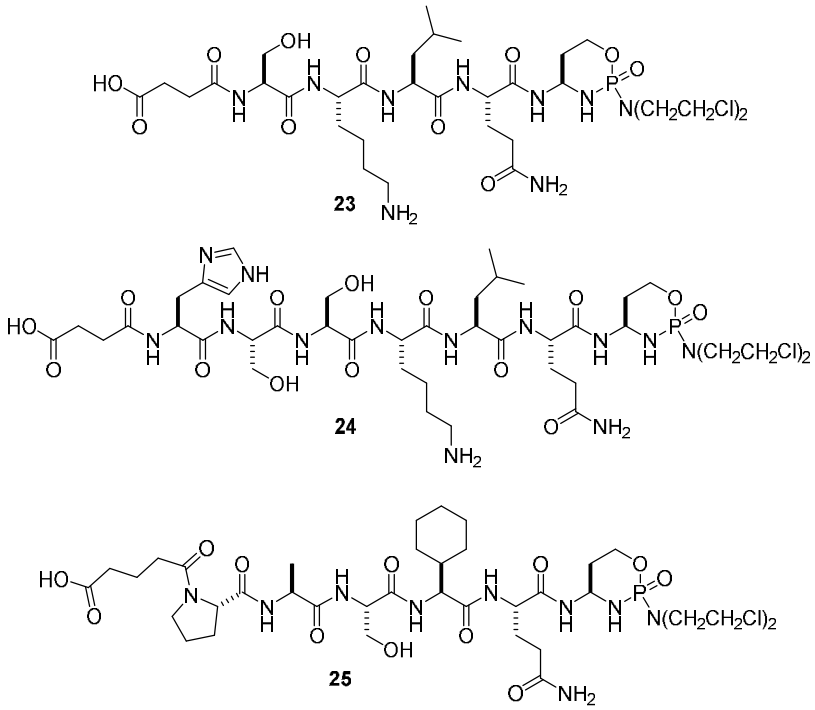

Figure 15. Chemical Structures of 4-NH_2-CPA Peptide Conjugates **23-25**.

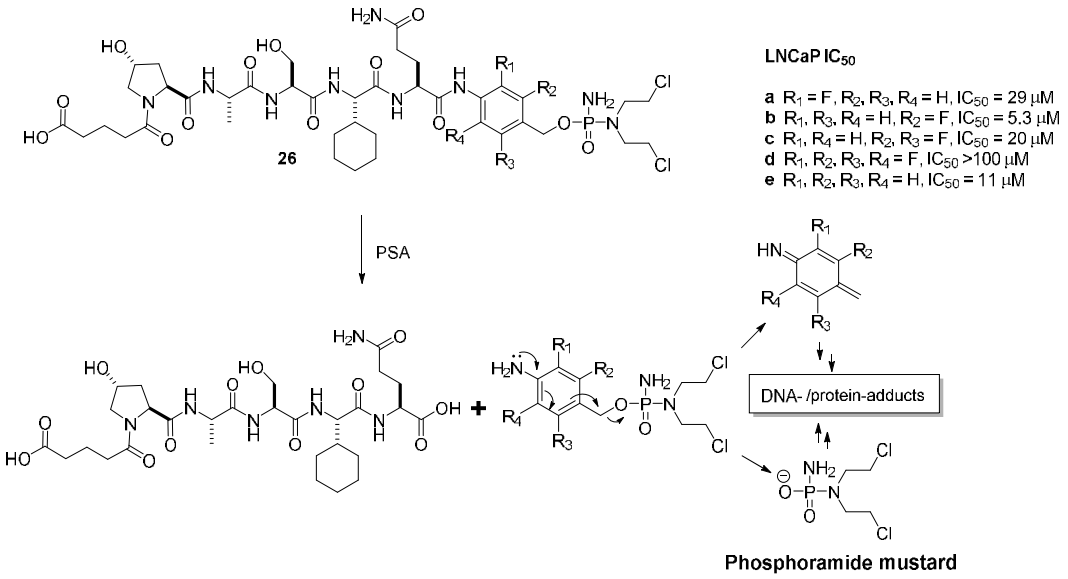

Figure 16. PSA Activation of Phosphoramide Mustard Conjugates **26**.

The most effective linker was 2-fluoro-4-aminobenzyl which was used to couple the PSA peptide substrate Hyp-Ala-Ser-Chg-Gln to phosphoramide mustard. The resulting prodrug LH202 (**26b**) was cleaved by PSA with a half-life of 0.95 h and demonstrated a 19-fold selectivity against PSA-producing LNCaP prostate cancer cell line with an IC_{50} of 5.3 μM.[151] The synthetic challenge of coupling peptide sequences to phosphoramide mustard was overcome by first coupling Gln to the aminobenzyl phosphoramide mustard ester using a selenocarboxylate/azide amidation strategy.[184, 185]

g. Prodrugs of Doxorubicin

Doxorubicin is a highly potent cytotoxic and anticancer agent effective against a wide spectrum of solid tumors. It is an active agent against metastatic breast cancer next to taxanes, and a second-line therapy for the treatment of various cancers.[186, 187] It belongs to the first series of anthracyclines introduced in the early 1960s. Although effective as a chemotherapeutic agent, its clinical use is limited by dose-dependent systemic toxicity.[187] A commonly reported and severe adverse effect associated with doxorubicin administration is cardiomyopathy, possibly through its interference with iron metabolism.[188] Based on the cleavage sequences of PSA's natural substrates, semenogelins I and II, the highly specific PSA substrate glutaryl-Hyp-Ala-Ser-Chg-Gln was developed and coupled to the aminoglycoside of doxorubicin via a Ser-Leu linker (Fig. 17). Glutaryl-Hyp-Ala-Ser-Chg-Gln-Ser-Leu-Dox (**27**) was effective against PSA-producing LNCaP cells (IC_{50} of 5 μM), albeit less cytotoxic than doxorubicin (IC_{50} of 0.5-1.6 μM) in various PSA-negative cancer cell lines with IC_{50} values greater than 100 μM. Moreover, prodrug **27** reduced serum PSA levels by 97%, and caused an 87%

inhibition of tumor growth in nude mice at a dose of 21.5 μmol/kg; it was 15 times more effective at reducing mouse tumor weight than doxorubicin when both compounds were dosed at their MTDs. [140]

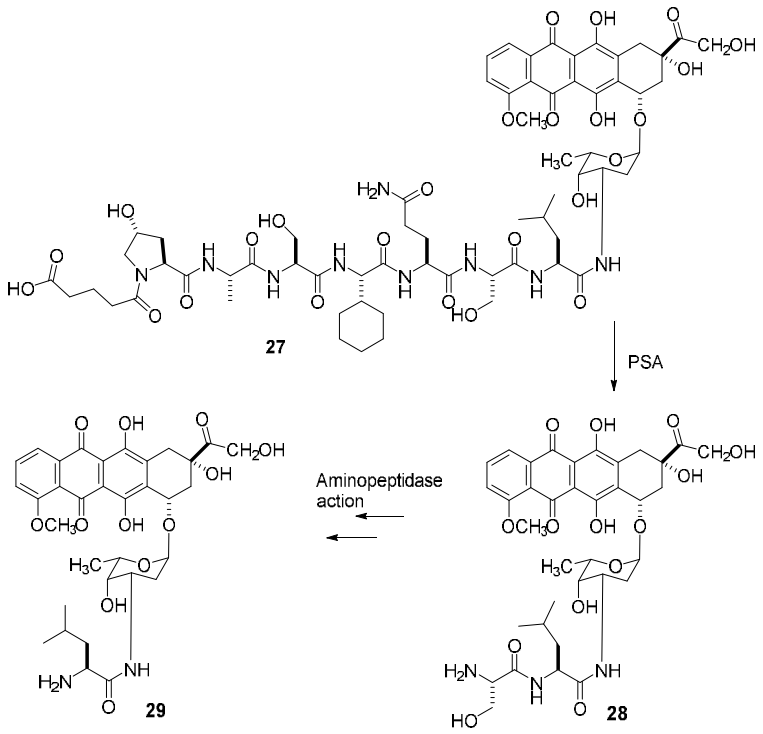

Figure 17. PSA Activation of Doxorubicin Prodrug **27**.

Based on its favorable preclinical profile, prodrug **27** was evaluated in phase I clinical trials.[189] Following intravenous administration of prodrug **27** to 19 patients with advanced hormone-refractory prostate cancer at escalating doses (up to 315 mg/m^2), there was greater than 75% decrease in serum PSA levels. Although prodrug **27** was well tolerated, circulating levels of the active metabolites Leu-doxorubicin (AUC = 4.3 μM·h, C_{max} = 5 μM) and doxorubicin (AUC = 1.2 μM·h, C_{max} = 0.12 μM) were detected at the

efficacious dose of 225 mg/m^2.[189, 190] Dose-limiting neutropenia was also observed in 1 out of 6 patients at this dose.[189]

h. Prodrugs of Vinblastine

Vinblastine is a vinca alkaloid with antimicrotubule properties derived from *Catharanthus roseus*. It is effective against a broad spectrum of cancers, namely Hodgkin's lymphoma, breast, lung, and testicular cancers. However, its therapeutic use is typically associated with dose-dependent toxicities such as neutropenia, hair loss, gastrointestinal disturbances, hypertension and depression.[191] A prodrug consisting of the octapeptide Ac-Hyp-Ser-Ser-Chg-Gln-Ser-Pro coupled to the 4-hydroxyl group of vinblastine was designed to be activated by PSA for the treatment of prostate cancer (Fig. 18).[152] The vinblastine prodrug **30** was cleaved by PSA after Gln with a half-life of 12 min. Prodrug administration to nude mice bearing LNCaP prostate cancer xenografts led to a 99% reduction in circulating PSA levels and 85% decrease in tumor weight at the MTD of 15.3 μmol/kg.[153] No significant changes in PSA levels or tumor weight were observed for the putative hydrolysis metabolite *des*-acetyl vinblastine (**32**) released by spontaneous diketopiperazine formation from a dipeptidyl intermediate (Fig. 18). Compared to the doxorubicin prodrug L-377,202 which was approximately 10-fold less toxic than doxorubicin, the vinblastine conjugate was greater than 80-fold less toxic than *des*-acetyl-vinblastine in LNCaP tumor-bearing nude mice.[153]

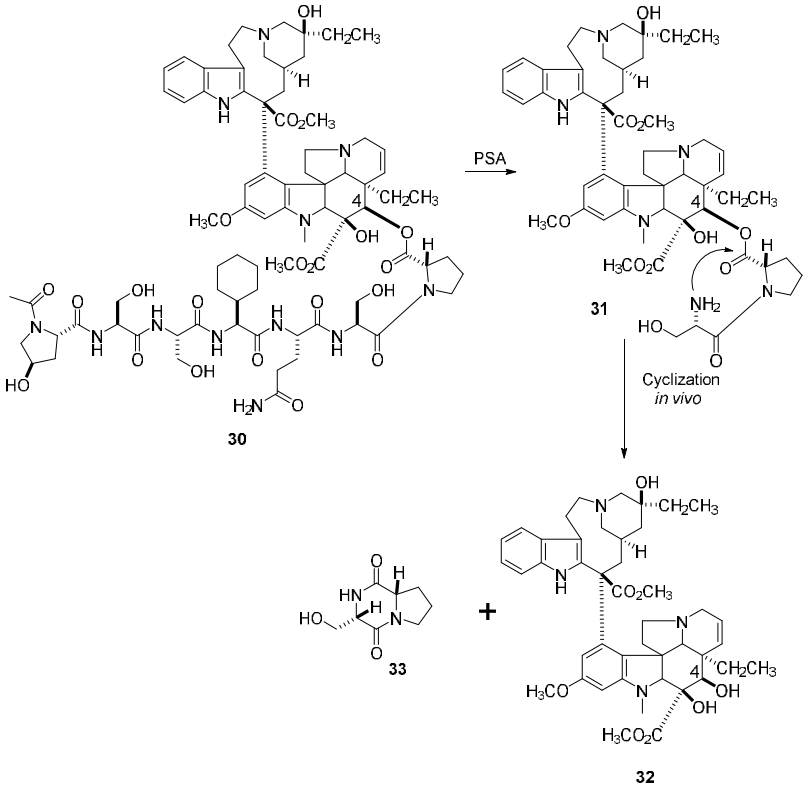

Figure 18. PSA activation of Vinblastine Prodrug **30**.

E. Summary

Although chemotherapeutics have demonstrated significant benefits in combination with ADT in the treatment of HRPC, their clinical utility is often limited by dose-dependent toxicity stemming from non-discriminatory drug exposure to normal tissue. In order to improve the selectivity of anti-cancer agents towards tumor cells, several targeted prodrug strategies are being developed. This review highlighted several ADEPT and GDEPT approaches that have been specifically used to target prostate cancer as well as the use of endogenous enzymes PSA and PSMA for the targeted activation of prodrugs in HRPC.

In ADEPT, a foreign enzyme is targeted to a cell surface antigen through the systematic administration of an antibody-enzyme conjugate before dosing with the prodrug. This is a multistep process and there are many challenges including, but not limited to, i) the selection of an surface antigen that is unique to prostate cancer cells, ii) the use of a monoclonal antibody that has high affinity to the targeted antigen, iii) the selection of an enzyme that has optimal activity at a pH close to the tumor extracellular environment, iv) the delivery of macromolecular antibody-enzyme conjugate to ensure its reach to and accumulation at the targeted prostate tumor sites, and v) the selection of a prodrug that after activation can permeate across cell membranes and kill both dividing and non-dividing tumor cells. The interval between the administrations of antibody-enzyme conjugate and the prodrug needs to be optimized for ADEPT to work effectively; antibody-enzyme conjugate must accumulate around tumors and cleared systematically before the administration of the prodrug to avoid systematic toxicity.

GDEPT avoids the problems associated with the poor tumor penetration of macromolecular antibody-enzyme conjugates by targeted expression of a gene-encoding enzyme in prostate cancer cells driven by a prostate-specific or a prostate cancer-specific element like the PSA or PSMA promoter. However, there are other issues, risks, and difficulties associated with the selective delivery and expression of the gene used in the GDEPT. As in ADEPT where the delivery of large conjugates is restricted, the retroviral delivery systems used in GDEPT only target the dividing tumor cells; Like ADEPT where it is not possible to deliver the conjugate to every tumor cell, the expression of a foreign enzyme encoding gene in GDEPT is often heterogeneous. Thus, both ADEPT and

GDEPT require the use of prodrugs that upon activation can diffuse efficiently, permeate through cellular membranes and kill neighboring prostate cancer cells that lack the activating enzyme via a bystander effect.

The reliance of ADEPT and GDEPT on the efficient delivery of a foreign enzyme as the prodrug-activating enzyme can be circumvented by utilizing endogenous tumor-specific proteases such as PSMA and PSA for tumor-specific prodrug activation. Effective prodrugs with excellent tumor-selectivity were designed for activation by PSMA and PSA, and several of them have been evaluated in both preclinical animal models and clinical trials.[155] Since the tissue distribution profiles of these prodrugs suggest an imminent challenge in both predicting and achieving adequate safety margins in humans due to cytotoxic drug or metabolite exposure to non-targeted tissues,[154, 190, 192] there is a persistent interest in optimizing the tumor selectivity of PSMA and PSA-activated prodrugs.

CHAPTER TWO

IMPROVING PSA SUBSTRATE SPECIFICITY

In our first series of experiments, we set out to further improve the PSA specificity of glutaryl-Hyp-Ala-Ser-Chg-Gln by introducing D-retro-inverso-peptide fragments in its sequence using urea and malonate linkages. Sequence optimization is streamlined with the choice of an appropriate fluorescent tag that can be readily coupled to a wide variety of peptides. The optimized sequences can then be coupled to cytotoxic drugs via appropriate linkers and evaluated. For our purpose, peptide conjugates of the fluorescent dye 7-AMC[138] were synthesized as convenient surrogates for developing peptide substrates with improved PSA specificity because enzyme-mediated cleavage of AMC-conjugates at the Gln-AMC bond results in quantifiable fluorescence increase.

I. PSA Substrate Optimization Strategy

Our general strategy for optimizing the sequence glutaryl-Hyp-Ala-Ser-Chg-Gln consisted of systematic D-amino acid substitution in P2-P5 using urea or malonate linkages to generate various AMC-peptide conjugates which were evaluated as PSA substrates (Fig. 19). Where urea or malonate linkage was used, peptides were synthesized by a combination of solid-phase and solution chemistry using an Fmoc strategy. The D-amino acid C-terminal ends of the peptide conjugates **35-43** were capped with γ-aminobutyric acid (GABA) in lieu of glutaryl, and Hyp was replaced by Ser.

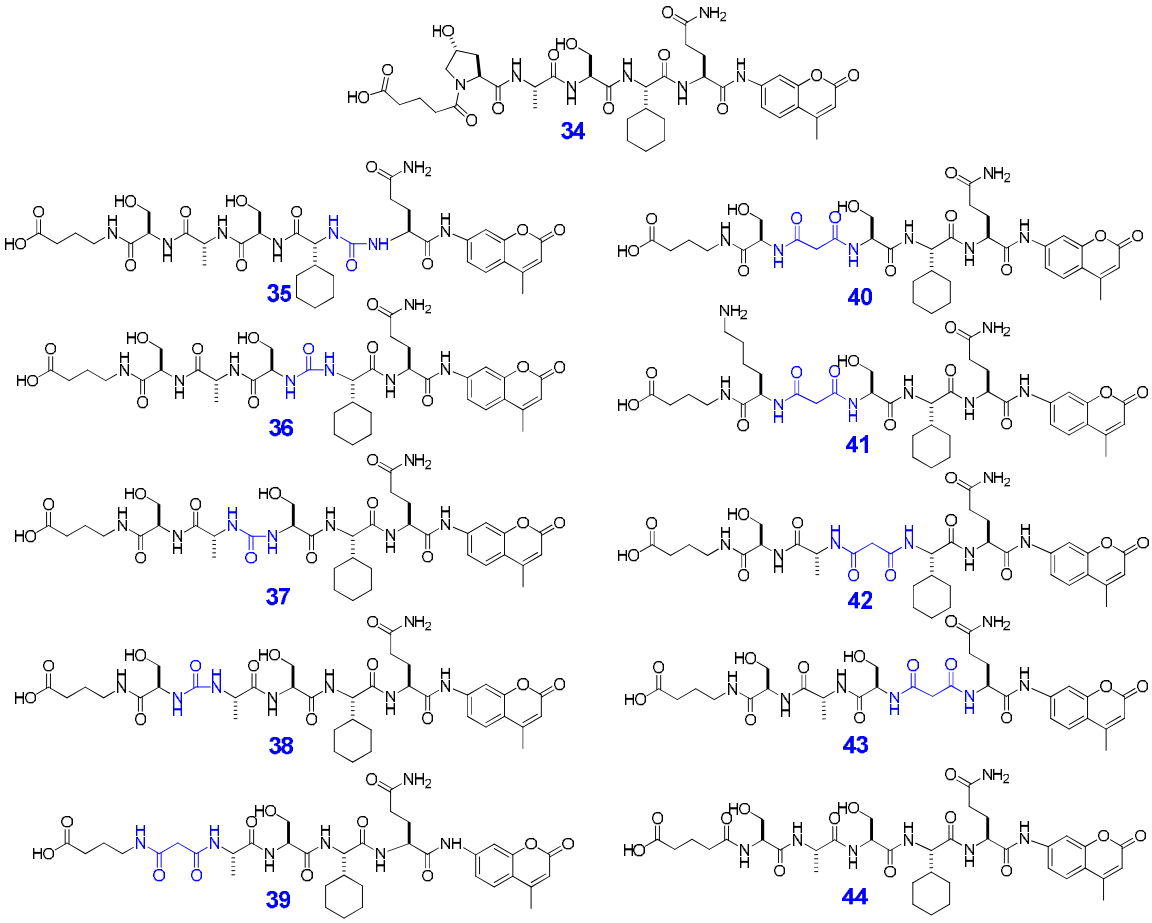

Figure 19. AMC-conjugates: **34**: Glutaryl-Hyp-Ala-Ser-Chg-Gln-AMC; **35**: GABA←D-Ser←*D*-Ala←*D*-Ser←*D*-Chg-ψ[NH-CO-NH]-Gln-AMC; **36**: GABA←*D*-Ser←*D*-Ala←*D*-Ser-ψ[NH-CO-NH]-Chg-Gln-AMC; **37**: GABA←*D*-Ser←*D*-Ala-ψ[NH-CO-NH]-Ser-Chg-Gln-AMC; **38**: GABA←*D*-Ser-ψ[NH-CO-NH]-Ala-Ser-Chg-Gln-AMC; **39**: GABA←mGly-Ala-Ser-Chg-Gln-AMC; **40**: GABA←*D*-Ser←mGly-Ser-Chg-Gln-AMC; **41**: GABA←*D*-Lys←mGly-Ser-Chg-Gln-AMC; **42**: GABA←*D*-Ser←*D*-Ala←mGly-Chg-Gln-AMC; **43**: GABA←*D*-Ser←*D*-Ala←*D*-Ser←mGly-Gln-AMC; **44**: Glutaryl-Ser-Ala-Ser-Chg-Gln-AMC

A. Optimization of Resin Loading Conditions

In order to synthesize urea- and malonate-containg peptide intermediates in acceptable purity and yield, it was necessary to couple GABA to Wang or 2-chloro-trityl chloride resin. However, efficient coupling of Fmoc-GABA to Wang resin using DIC, IPCF or

PyBOP in the presence of catalytic DMAP was difficult (Table 1). Under the conditions described in Table 1, Fmoc-GABA was pre-activated under nitrogen atmosphere for 30 min and added to the swollen Wang resin. After capping the resin with acetic anhydride in the presence of pyridine, loading levels could be determined by removing the Fmoc-protecting group with 20% piperidine at room temperature, and measuring the absorbance of the resulting fluorenyl-piperidine adduct solution at 290 nm (A_{290}). The maximum loading level achieved on Wang resin was 0.15 mmol Fmoc-GABA/g resin (Table 1).

Alternately, Fmoc-GABA (1.2 g, 3.6 mmol) was effectively coupled to 2-chloro-trityl chloride resin (1 g, 1.7 mmol) in 10 mL of anhydrous DCM/NMP (9:1) in the presence of 4 eq. DIEA at room temperature for 3 h. The 2-chloro-trityl chloride resin was capped with MeOH/DIEA (9:1) and loading levels determined as previously described. Since the highest loading levels were achieved on 2-chloro-trityl chloride resin in 3 h, conjugates **35-43** were synthesized using (2-chloro-trityl chloride resin)-*O*-GABA. While each D-retro-inverso peptide could also be generated starting from the C-terminus amino acid, synthesis from the common intermediate GABA-*O*-resin was most efficient. However, coulping of malonic acid to GABA-*O*-resin under various conditions was not as productive as anticipated. The inability to couple malonic acid to GABA-*O*-resin could be partly explained by the tendency of malonic acid to form a reactive, short-lived ketene in addition to acyl-ureas and mixed anhydride inetrmediates in the presence of activating/dehydrating agents such as EDC.[193]

Table 2. Fmoc-GABA Loading onto Wang or 2-Chloro-trityl Chloride Resin

Resin	Activation Conditions	Equivalents (relative to resin)	Loading level (mmol/g)
Wang	Fmoc-GABA/DIC	3/3	0.026
	Fmoc-GABA/DIC/DMAP	3/3/0.1	0.15
	Fmoc-GABA/IPCF/DIEA	3/3/3	0.0044
	Fmoc-GABA/PyBOP/DMAP	3/3/0.1	0.0065
	Fmoc-GABA/DIC/HOBt/DMAP	4/4/4/0.1	0.080
	Fmoc-GABA/HBTU/DIEA/DMAP	4/4/4/0.1	0.049
2-ClTrt	Fmoc-GABA/DIEA	2.2/4	0.48

Conditions: Fmoc-GABA was coupled to Wang resin in DCM/NMP (60:40) for 12 h or 2-chloro-trityl chloride resin in DCM/NMP (90:10) for 3h at room temperature. Pre-activation under nitrogen atmosphere was carried out for Wang resin coupling.

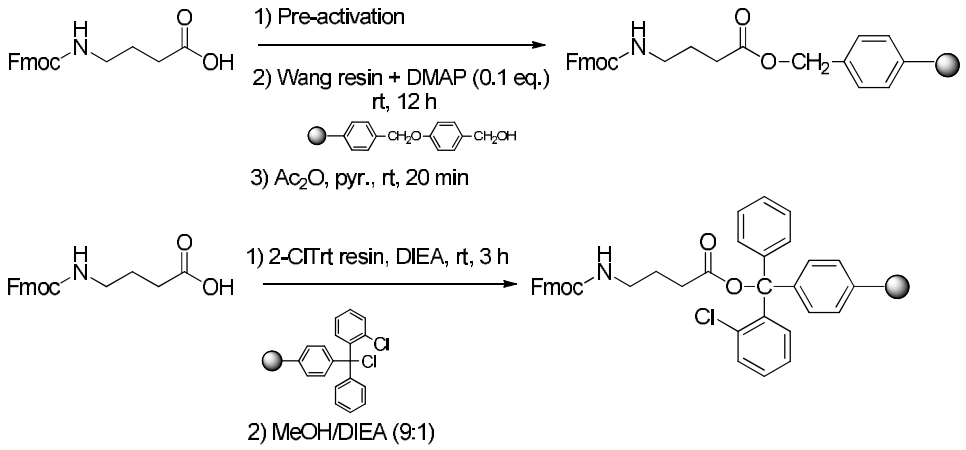

Scheme 1. Fmoc-GABA Loading onto Wang or 2-Chloro-trityl Chloride Resin

B. Synthesis of D-Retro-inverso AMC-Conjugates

Urea-containing peptides and AMC-conjugate **44** were synthesized by a combination of solid-phase and solution chemistry using an Fmoc strategy. All AMC-conjugates were prepared by directly coupling the appropriate peptide segments to Gln-AMC, which was obtained using our previously reported methodology for the convenient preparation of aminoacyl-AMC peptide conjugates (Scheme 2);[194] standard coupling methods using HBTU, IPCF, DCC, or PyBOP afforded low product yields (<10%). Boc-Gln-AMC was generated in excellent yield (84%) by the amidation of the selenocarboxyalte of Boc-Gln with 7-azido-4-methylcoumarin (AZD), followed by TFA-detprotection of the Boc-group at room temperature. Since TFA can be readily activated by HBTU in subsequent steps and coulple to Gln-AMC, residual TFA was removed using Amberlyst A-26.

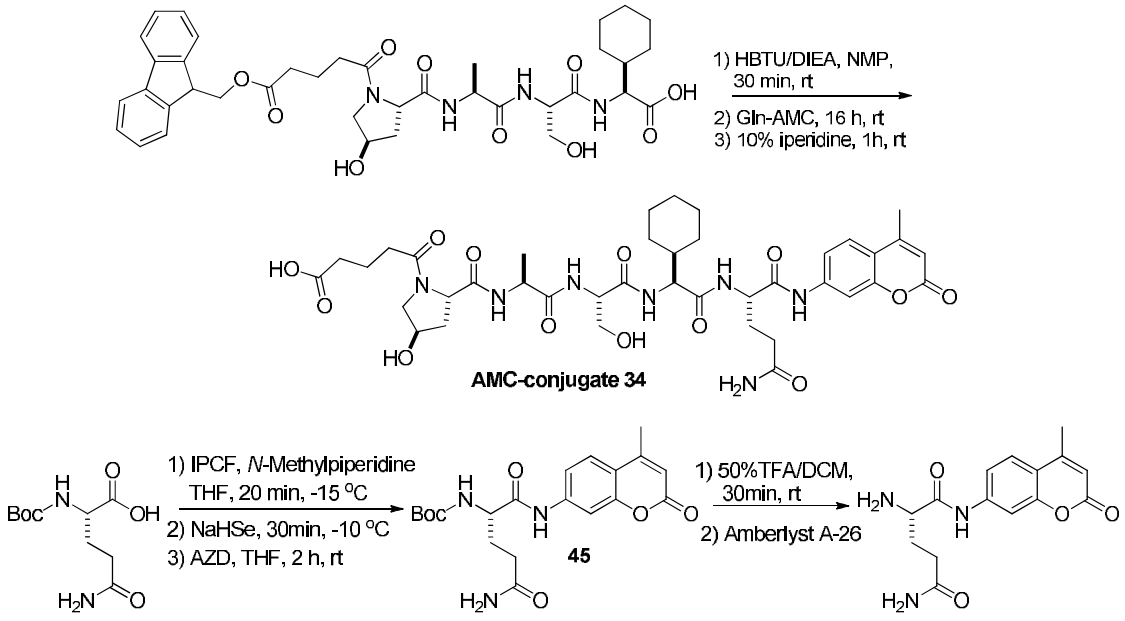

Scheme 2. Synthesis of AMC-conjugate **34**

Urea linkages (AMC-conjugates **35-38**) were inserted into the peptide sequence of XXX-Ala-Ser-Chg-Gln by first activating the amino end of the appropriate resin-bound peptide intermediate with carbonyldiimidazole (CDI) at room temperature, followed by coupling of the corresponding AMC-peptide conjugate (Scheme 3). Due to HPLC purification challenges encountered with the final peptide conjugates, the TFA-deprotection step was performed on the purified *t*-butyl-protected conjugates.

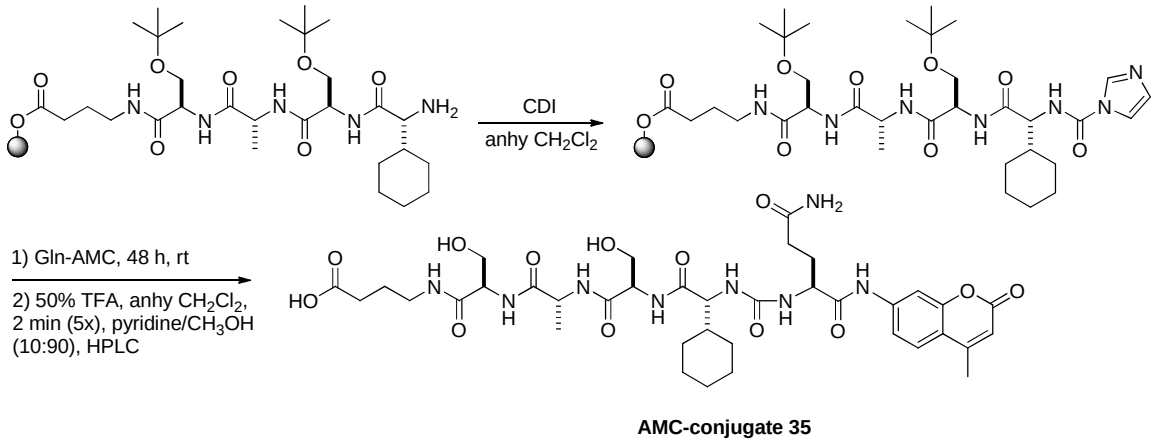

Scheme 3. Synthesis of AMC-conjugate **35**

As mentioned earlier, several solid-phase conditions were explored for introducing the malonate linkage featured in the sequences of conjugates **39-43** with no success. For example, attempts to couple the peptide, H-Ser(*t*Bu)-Chg-Gln-AMC to resin-GABA←*D*-Ser(tBu)-H via a malonate linkage to generate conjugate **40** were unsuccessful when malonic acid was first activated with HBTU or EDC, and reacted with resin-GABA←*D*-Ser(*t*Bu)-H. The lack of reactivity of activated malonic acid towards the amino group of resin-bound peptides was somewhat surprising since malonic acid could be effectively activated and trapped with benzylamine in solution. The acylation of sterically hindered alcohols through the ketene intermediate of malonic acid in the presence of dehydrating

agents was previously reported.[193] In our case, the OBt ester, acyl-urea or ketene intermediate generated from malonic acid was anticipated to react much more readily with amino groups compared to sterically hindered alcohols. However, since the ketene intermediate is reactive and short-lived, its coupling with the amino group on solid-phase may not be the major pathway. For example, the ketene could be trapped by EDC through a [4+2] cycloaddition mechanism similar to DCC.[193]

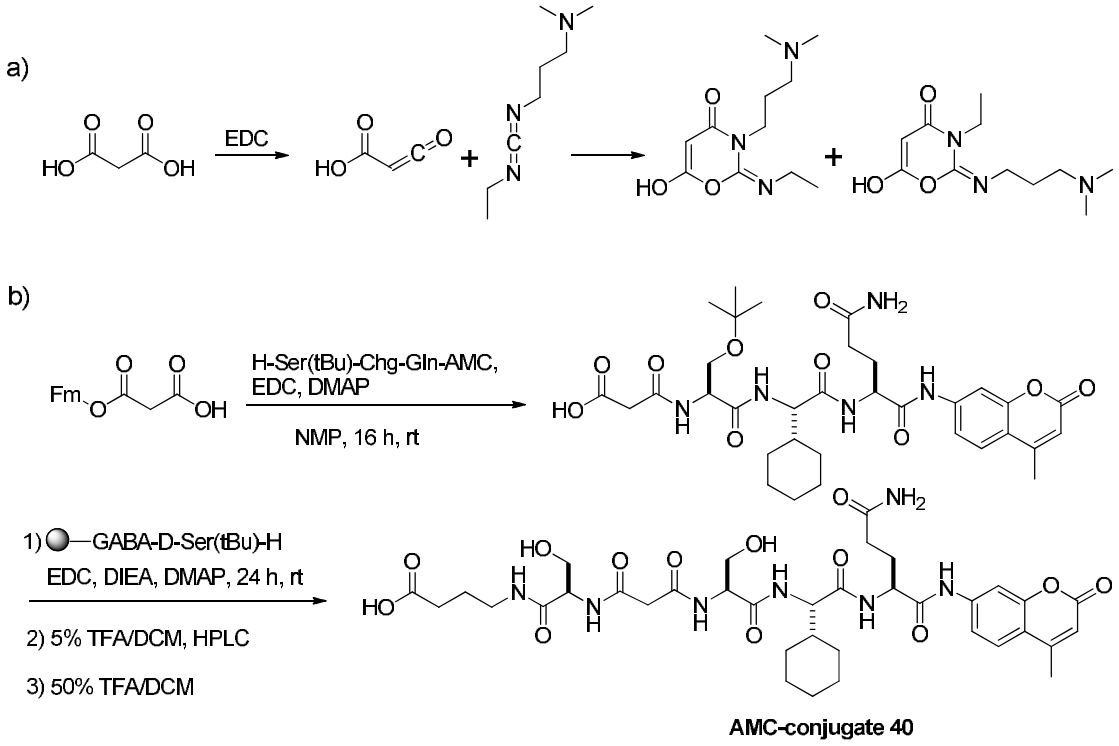

Scheme 4. Synthesis of AMC-conjugate **40**

Optimized conditions involved activation of the fluorenylmethyl malonate mono-ester with EDC in the presence of 2.5 eq. DMAP to afford the mono-amide which was spontaneously de-protected upon prolonged exposure to DMAP (Scheme 4). Interestingly, the malonate mono-amide effectively coupled to resin-GABA←*D*-

Ser(*t*Bu)-H, affording conjugate **40**; a similar approach was followed for preparing conjugates **39**, **41-43**. Ready access to AMC-conjugate **44** was possible by coupling H-Ala-Ser(ΨMe,Me pro)-Chg-Gln-AMC to Fmoc-Ser(*t*Bu)-OH, followed by DEA deprotection and final amino end capping with glutaric anhydride at room temperature (Scheme 5). The peptide intermediate H-Ala-Ser(ΨMe,Me pro)-Chg-Gln-AMC was generated from fragment condensation of H-Ala-Ser(ΨMe,Me pro), Fmoc-Chg-OH, and Gln-AMC. Finally, AMC-conjugate **34** was synthesized using standard solid-phase peptide synthesis procedures starting with Fmoc-Chg-OH pre-loaded onto Wang resin (loading level of 0.35 mmol/g resin). The final peptide was coupled to Gln-AMC using HBTU pre-activation.

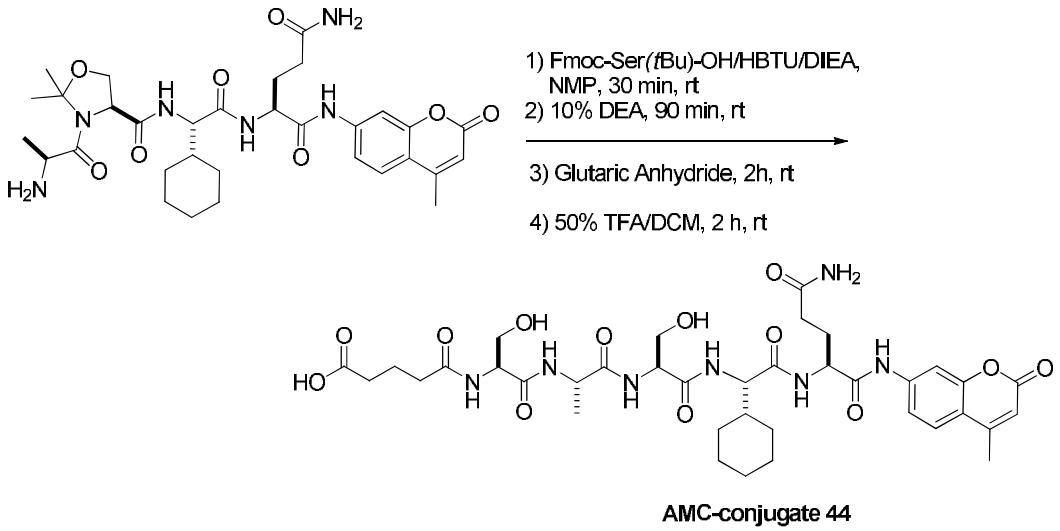

Scheme 5. Synthesis of AMC-conjugate **44**

II. Results and Discussion

The highly specific PSA substrate, glutaryl-Hyp-Ala-Ser-Chg-Gln, was coupled to doxorubicin via a Ser-Leu linker as a non-cytotoxic PSA-activated prodrug for the treatment of prostate cancer. However, the clinical development of glutaryl-Hyp-Ala-Ser-Chg-Gln-Ser-Leu-Dox (L-377,202) was discontinued possibly due to toxicity concerns stemming from significant systemic levels of the active metabolite Leu-Dox as well as free doxorubicin following L-377,202 administration in humans. Subsequent metabolism studies of L-377,202 suggested that *in vivo* non-PSA mediated hydrolysis may be responsible for the extra-prostatic release of doxorubicin.[139, 154, 192] In the present study, we set out to further optimize the peptide sequence glutaryl-Hyp-Ala-Ser-Chg-Gln to improve its PSA specificity. Thus, we synthesized a series of partial D-retro-inverso-peptide conjugates which were evaluated as PSA substrates. Sequence optimization was carried out using the convenient release of fluorescent 7-AMC from peptide conjugates following PSA cleavage of the Gln-AMC bond.

A. Evaluation of 7-AMC Conjugates as PSA Substrates

As shown in Table 3, AMC-conjugates **35-37** and **41-43** were poor substrates for PSA and did not generate any significant amount of 7-AMC. From the urea-containing AMC-conjugates synthesized, conjugate **38** exhibited modest substrate specificity for PSA with a 7-AMC formation rate of 92 pmol/min/100 nmol PSA. These results indicate that, although amino acid side-chain orientation was maintained with D-amino acid substitution (as compared to conjugate **34,** representative of the peptide sequence of L-377,202), introducing urea between P1 and P5 may have disrupted critical peptide

substrate binding interactions with PSA such as backbone H-bonding and side-chain interactions. In addition, introduction of the urea linkage may have decreased overall peptide chain flexibility, a property that promotes induced fit of the substrate in the active site of PSA. Our findings support previous optimization studies which suggested that further amino acid substitution in P1-P4 for the optimized sequence of conjugate **34** compromised substrate specificity for PSA.[192] We also explored the strategic insertion of malonate between D- and L-amino acids in the peptide sequence of conjugate **34**. Although P2-P5 substitution decreased PSA cleavage rate, it was gratifying to find that peptide conjugate **39** showed a significant improvement over conjugate **34** (representative sequence of L-377,202). Furthermore, AMC-conjugate **39** exhibited the second fastest cleavage rate of 225 pmol/min/100 nmol PSA. Introduction of urea linkages in the peptide sequence of AMC-conjugate **34** increased the peptide chain length by one carbon atom whereas malonate preserves the original sequence length. Moreover, the malonate linkage imparts less rotational restriction to the peptide chain overall compared to urea. The lower rotational conformation restriction is demonstrated with AMC-conjugate **39** as the malonate linkage is moved farther away from P1; only modest effects on PSA cleavage rate were observed with the corresponding urea-containing AMC-conjugate **38** (Fig. 20). The fastest cleavage rate of 351 pmol/min/100 nmol PSA was observed with AMC-conjugate **44**. It is possible that the bend and rigidity introduced by Hyp at P5 in conjugate **34** compromised optimal substrate binding. Moreover, for conjugate **44**, the hydroxyl of Ser may have contributed to additional stabilizing H-bonding interactions in the active site of PSA. Overall, we confirmed that PSA specificity was lost with modifications in P2-P5 as suggested by previous substrate optimization studies.

Additionally, we showed that PSA cleavage rate was maintained or improved by up to 2-fold with P5 substitutions.

Table 3. Hydrolysis of AMC-peptide Conjugates by Human PSA

AMC-conjugate	**7-AMC Fluorescence (counts/min)**	**PSA cleavage rate (pmol/min/100 nmol PSA)**
Glutaryl-Hyp-Ala-Ser-Chg-Gln-AMC (**34**)	156	171
GABA←*D*-Ser←*D*-Ala←*D*-Ser←*D*-Chg-ψ[NH-CO-NH]-Gln-AMC (**35**)	< 1	< 1
GABA←*D*-Ser←*D*-Ala←*D*-Ser-ψ[NH-CO-NH]-Chg-Gln-AMC (**36**)	< 1	< 1
GABA←*D*-Ser←*D*-Ala-ψ[NH-CO-NH]-Ser-Chg-Gln-AMC (**37**)	< 1	< 1
GABA←*D*-Ser-ψ[NH-CO-NH]-Ala-Ser-Chg-Gln-AMC (**38**)	84	92
GABA←mGly-Ala-Ser-Chg-Gln-AMC (**39**)	205	225
GABA←*D*-Ser←mGly-Ser-Chg-Gln-AMC (**40**)	37	41
GABA←*D*-Lys←mGly-Ser-Chg-Gln-AMC (**41**)	< 1	< 1
GABA←*D*-Ser←*D*-Ala←mGly-Chg-Gln-AMC (**42**)	< 1	< 1
GABA←*D*-Ser←*D*-Ala←*D*-Ser←mGly-Gln-AMC (**43**)	< 1	< 1
Glutaryl-Ser-Ala-Ser-Chg-Gln-AMC (**44**)	320	351

Conditions: Each peptide conjugate (1 μM) was subject to human PSA (100 nM) in 50 mM Tris buffer, pH 8 containing 2 mM $CaCl_2$ and 0.1% Tween 20 in triplicate. Fluorescence was measured using a 335/460 (ex/em) filter over a period of 3 h. PSA cleavage rates were computed by taking the slopes of the linear portions of fluorescence counts-time curves (see Fig. 20) and using a standard curve generated with known amounts of 7-AMC.

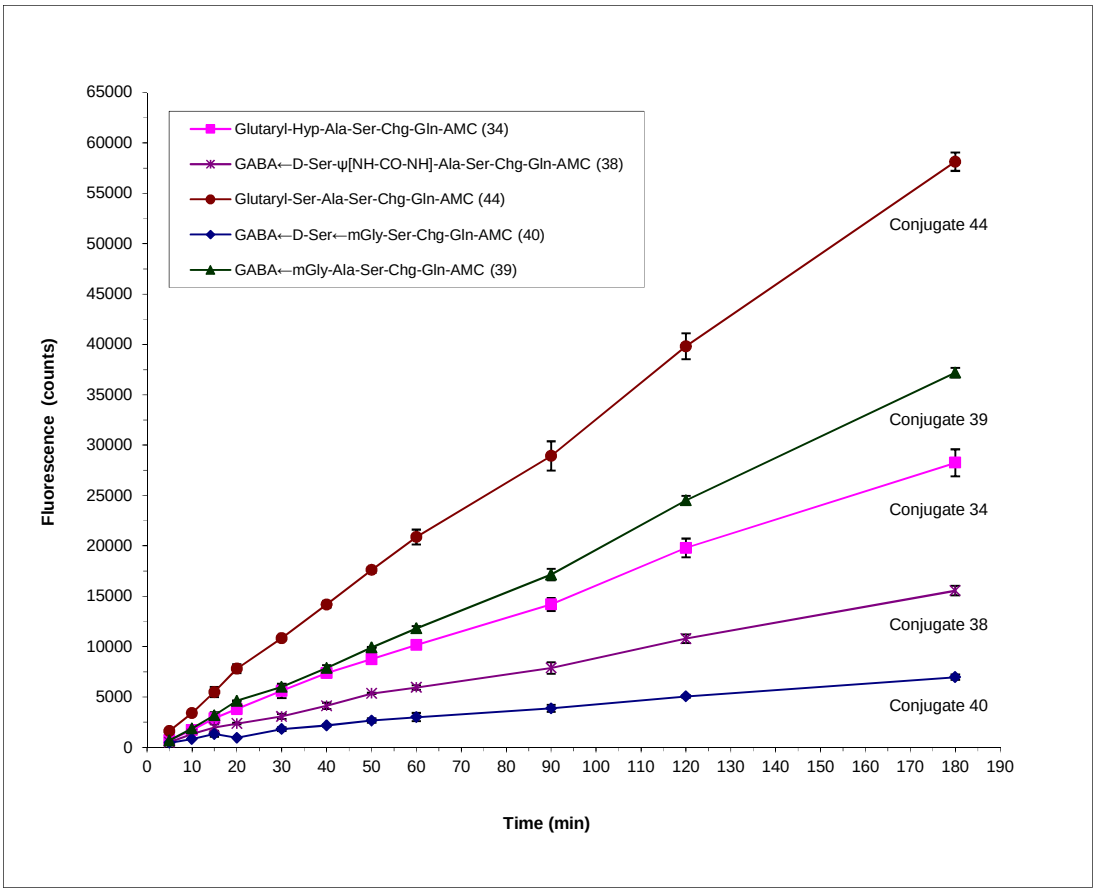

Figure 20. Hydrolysis of AMC-peptide Conjugates by Human PSA

B. Stability of 7-AMC Conjugates in Mouse and Human Plasma

To further assess the PSA specificity of the peptide sequences generated, we measured conjugate stability in mouse and human plasma (Table 4, Fig. 21). The selected peptide conjugates were examined in mouse plasma because prodrugs generated from the peptide substrate with the highest PSA specificity could further be evaluated in nu/nu mouse PK/PD studies. Peptide conjugates with PSA cleavage rates greater than 1 pmol/min/100 nmol PSA were incubated with mouse or human plasma for 24 h and 7-AMC formation monitored by fluorescence. Although 7-AMC formation was insignificant during the first 3 h post-incubation, Gln-AMC hydrolysis increased to detectable levels (up to 10 nM) at

24 h, suggesting that non-PSA mediated hydrolysis did occur. The apparent delay in 7-AMC formation observed in Fig. 4 is due to the fact that non-specific endopeptidase cleavage must first occur at scissile bonds other than the Gln-AMC before hydrolysis of the Gln-AMC bond via subsequent aminopeptidase action. Furthermore, all peptide conjugates exhibited greater non-PSA-mediated hydrolysis in mouse plasma than in human plasma (Fig. 21 and 22) suggesting the involvement of multiple proteases or isoforms of the same protease in peptide hydrolysis.

Table 4. Non-PSA-mediated Hydrolysis of AMC-peptide Conjugates in Mouse and Human Plasma at 24 h

AMC-conjugate	**7-AMC generated in mouse plasma (nM)**	**7-AMC generated in human plasma (nM)**
Glutaryl-Hyp-Ala-Ser-Chg-Gln-AMC (**34**)	9.7	1.1
GABA←D-Ser-ψ[NH-CO-NH]-Ala-Ser-Chg-Gln-AMC (**38**)	0	1.1
GABA←mGly-Ala-Ser-Chg-Gln-AMC (**39**)	4.7	1.4
GABA←D-Ser←mGly-Ser-Chg-Gln-AMC (**40**)	8.1	0.98
Glutaryl-Ser-Ala-Ser-Chg-Gln-AMC (**44**)	2.4	0.82

Conditions: Each peptide conjugate (1 μM) was incubated in mouse or human plasma. Fluorescence was measured using a 335/460 (ex/em) filter over a period of 24 h (see Fig. 21).

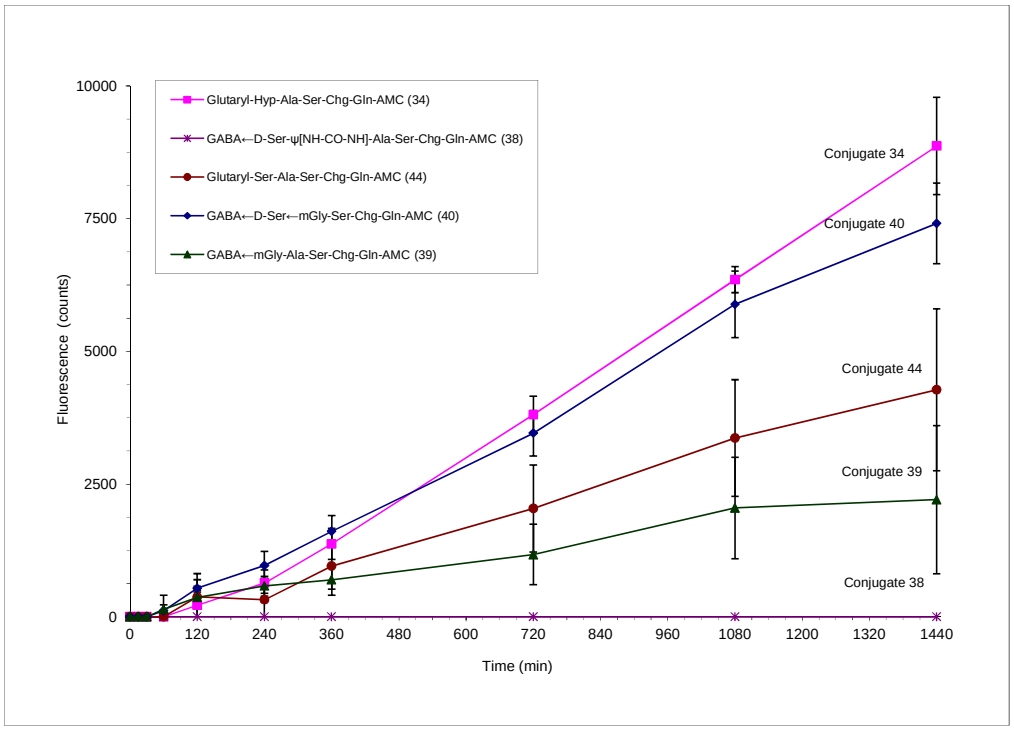

Figure 21. Stability of AMC-peptide Conjugates in Mouse Plasma

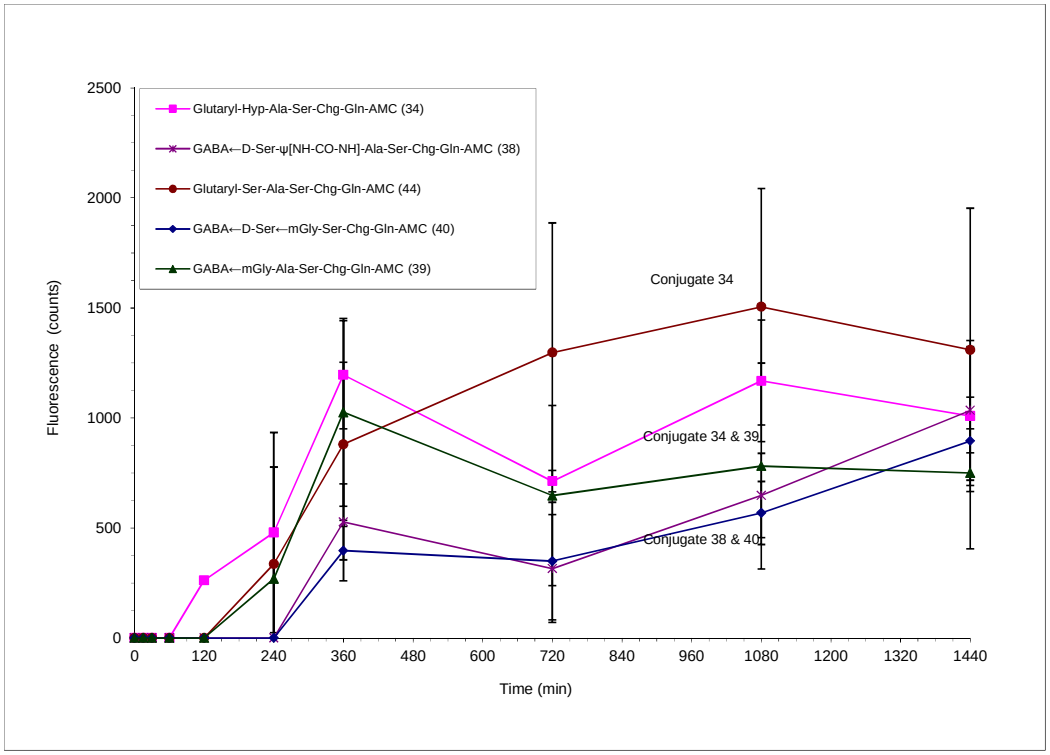

Figure 22. Stability of AMC-peptide Conjugates in Human Plasma

Conjugates **38** and **39** were most stable in mouse plasma indicating that urea and malonate substitutions in P4-P5 effectively mitigated non-PSA-mediated hydrolysis, possibly due to an unknown protease with scissile bond between P4 and P5. P5 substitution appears to mitigate cleavage by this protease, the major contributor to non-PSA hydrolysis for conjugates **34**, **40** and **44** in mouse plasma. Although conjugate **38** was completely stable in mouse plasma over 24 h, it did exhibit minor instability in human plasma. Moreover, non-PSA-mediated hydrolysis appears to be comparable for all conjugates in human plasma (Fig. 22). Nevertheless, differences in hydrolysis rate for conjugates **38** and **39** in mouse plasma suggest that at least two additional proteases with different cleavage maps may be responsible for the residual hydrolysis observed for conjugate **38** in human plasma and conjugate **39** in both matrices. The protease(s) responsible for the non-specific hydrolysis of the sequences examined herein and their PSA specificity were investigated by coupling the optimized sequence GABA←mGly-Ala-Ser-Chg-Gln to select cytotoxic agents. Noteworthy, the extent of hydrolysis of conjugate **39** in mouse plasma (2.42 nM eq. 7-AMC at 24 h) was lower compared to conjugate **34** (9.74 nM eq. AMC at 24 h), further suggesting that modifications in P5 (but not exclusively) also improved peptide stability.

III. Summary

In summary, we carried out D-amino acid substitutions between P1 and P4 using urea and malonic acid linkages in order to improve the specificity of the PSA substrate, glutaryl-Hyp-Ala-Ser-Chg-Gln. Our results suggest that modifications between P1 and P4 adversely affect PSA specificity while substitutions in P5 improved PSA cleavage rate

and resistance to non-PSA-mediated hydrolysis. To assess the utility of the optimized sequences for peptide prodrug design, the PSA specificity of the optimized sequences coupled to cytotoxic agents as prodrugs were further investigated.

CHAPTER THREE

SYNTHESIS AND EVALUATION OF PSA-ACTIVATED PRODRUGS

In our continuing efforts to design prodrugs with enhanced tumor selectivity, we designed and synthesized a series of peptides as PSA substrates with improved cleavage rates and resistance to non-specific hydrolysis in mouse and human plasma compared to the known sequence glutaryl-Ser-Ala-Ser-Chg-Gln. Evaluation of various D-retro-inverso-7-AMC-peptide surrogates revealed that the optimal sequences for rapid PSA cleavage were glutaryl-Ser-Ala-Ser-Chg-Gln and GABA←mGly-Ala-Ser-Chg-Gln-AMC whereas GABA←D-Ser-Ψ[NH-CO-NH]-Ala-Ser-Chg-Gln-AMC and GABA←mGly-Ala-Ser-Chg-Gln-AMC were more resistant to non-specific hydrolysis in plasma when compared to the known substrate glutaryl-Hyp-Ala-Ser-Chg-Gln. The latter peptide substrate was previously incorporated into the doxorubicin prodrug glutaryl-Hyp-Ala-Ser-Chg-Gln-Ser-Leu-Dox, a clinical prodrug activated by PSA.

I. Prodrug Design and Activation Mechanisms

A. Design Principle

In order to further evaluate the utility of our newly designed sequences as promoieties with improved stability to non-PSA-mediated metabolism, we conjugated glutaryl-Ser-Ala-Ser-Chg-Gln and GABA←mGly-Ala-Ser-Chg-Gln with doxorubicin or phoshoramide mustard. The necessity of incorporating a linker between the cytotoxic drug and the PSA peptide substrate has previously been demonstrated.[133, 139, 140, 149, 192] Initially, peptides were either coupled to the aminoglycoside of doxorubicin via a Ser-

Leu linker or phosphoramide mustard using a 4-aminoarylmethyl alcohol linker as previously reported (Scheme 6).[139, 149]

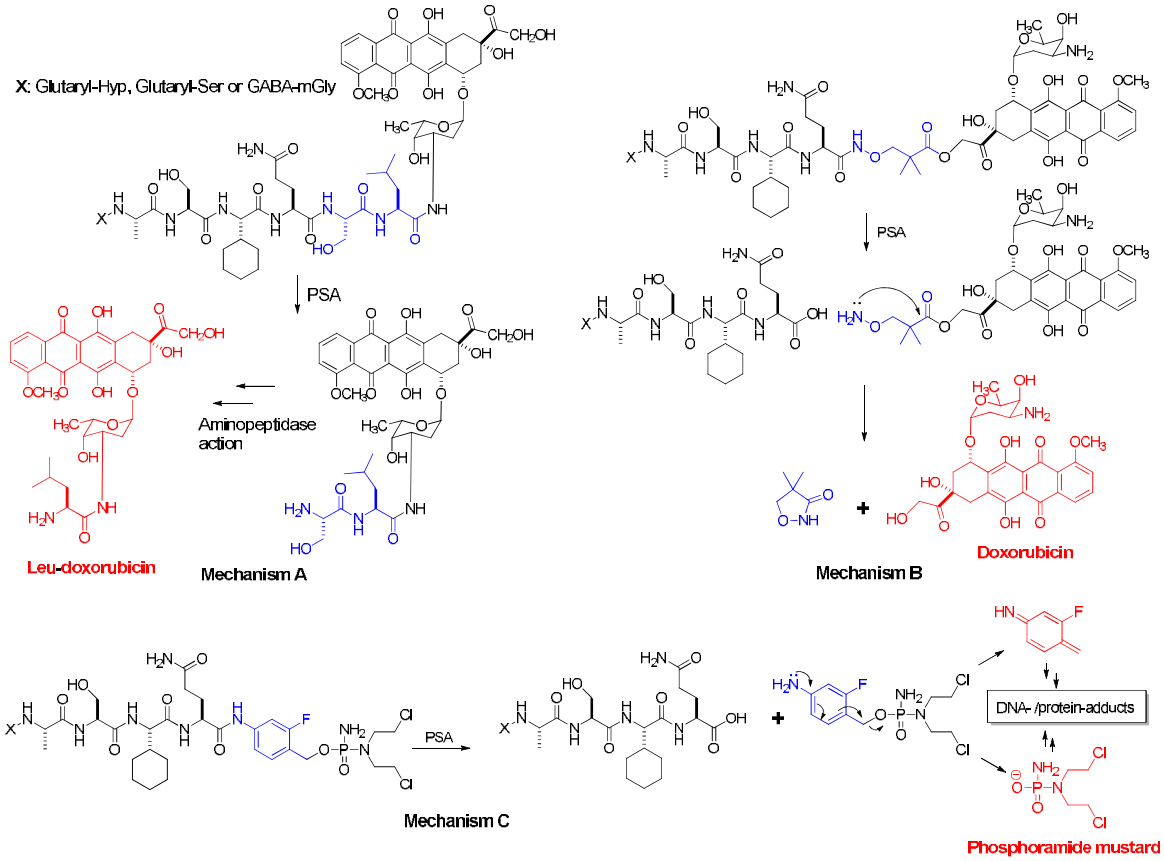

Scheme 6. Proposed Activation Mechanisms of Doxorubicin and Phosphoramide Mustard Prodrugs by PSA

However, metabolism studies in blood and cultured hepatocytes indicated that the Ser-Leu linker was succeptible to hydrolysis by human neprilysin (see section IV). As an alternative to Ser-Leu for the doxorubicin conjugates, a 3-aminoxypropionate linker may mitigate this non-PSA-mediated metabolism. The 3-aminoxypropionate linker could be coupled to the C-14 α-hydroxyl of doxorubicin as previously demonstrated with FUDR.[195] Furthermore, insertion of a 3-aminoxypropionate linker is anticipated to result

in doxorubicin being released into prostate cancer cells leading to enhanced tumor-specific cytotoxic effects because the active metabolite Leu-doxorubicin was found to be 10-fold less toxic than doxorubicin in LNCaP tumor cell lines, and was not completely converted to doxorubicin *in vivo*.[139, 192] Phosphoramide mustard was selected as a candidate for peptide conjugation due to its cytotoxic activity against both cycling and non-cycling cells.[196] Moreover, the feasibility of coupling the cyclophosphamide metabolite, 4-NH_2-CPA, to various peptides as model prodrugs has been previously explored and demonstrated.[149] Using a similar strategy, the attachment of phosphoramide mustard to various peptide sequences can be achieved with ease, to overcome the synthetic challenges of coupling peptides to the amino-glycoside or C-14 α-hydroxyl of doxorubicin. Optimization of the 4-aminoarylmethyl alcohol linker in our laboratories indicated that the 2-fluoro analog promoted the fastest release of phoshporamide mustard.[151] We also anticipated that, coupling of optimized PSA peptide substrates to phosphoramide mustard and doxorubicin via 4-aminoarylmethyl alcohol and 3-aminoxypropionate linkers, respectively, could afford peptide conjugates with improved resistance to non-PSA-mediated hydrolysis in murine and human blood and/or cultured hepatocytes, fast cleavage rates, and enhanced tumor selectivity in PSA-producing LNCaP versus non-PSA-secreting DU145 cells.

B. Synthetic Strategy

All prodrugs were synthesized by first coupling Gln to the appropriate linkers for ready attachment to various peptide sequences (Scheme 7).

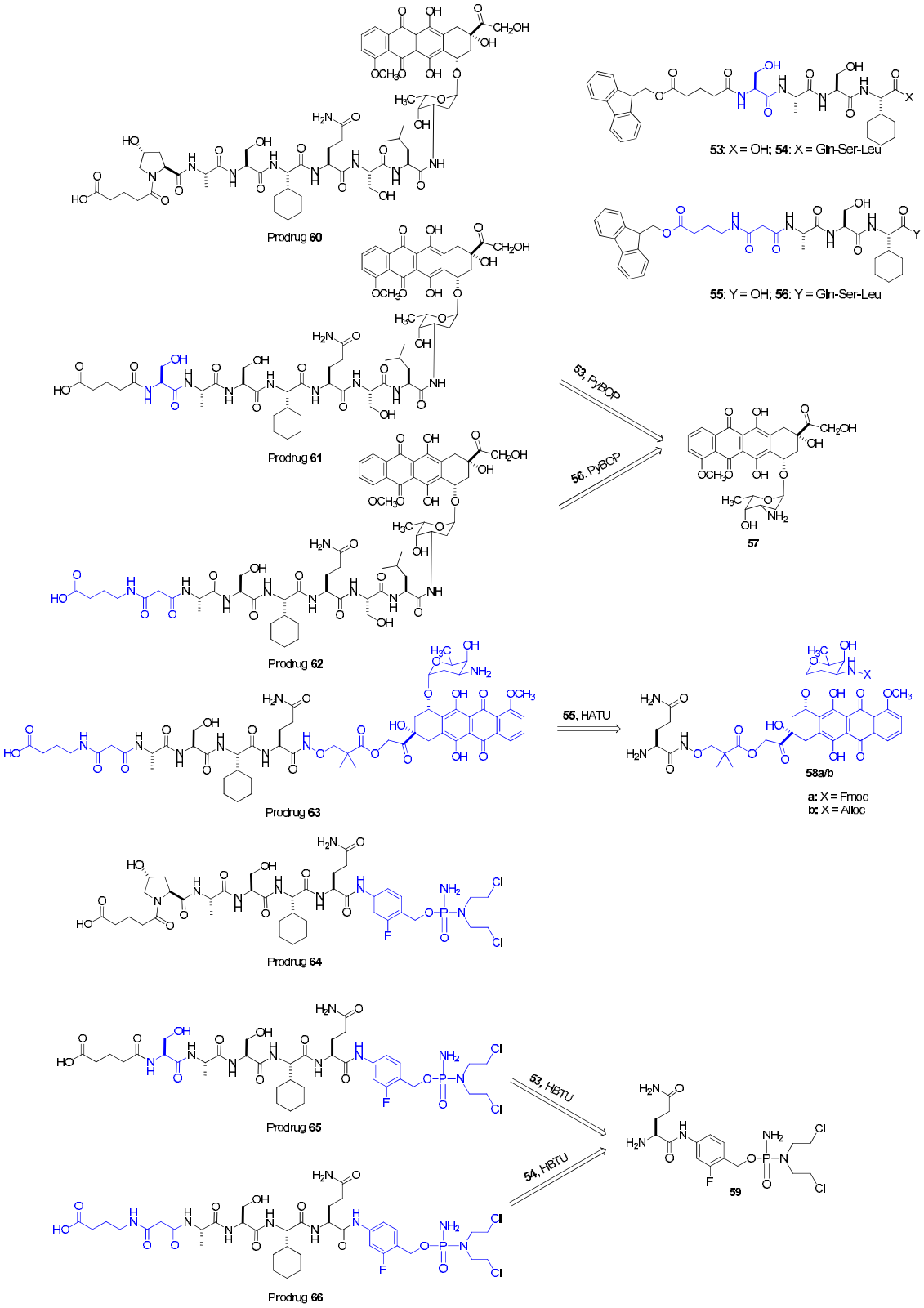

Scheme 7. Prodrug Synthetic strategy

Preparation of Fm-GABA←mGly-Ala-Ser-Chg and Fm-GABA←mGly-Ala-Ser-Chg-Gln-Ser could not be achieved following standard automated peptide synthesis methods because coupling of Fm-GABA←mGly to Ala-Ser-Chg-*O*-resin failed when EDC, HBTU or PyBOP were used to activate the acid. Furthermore, premature removal of the Fm-protecting group was observed under conditions featuring greater than 1 eq. of DMAP. Instead, Fm-GABA←mGly-OSu was prepared and coupled to H-Ala-Ser-Chg-Gln-Ser or Ala-Ser-Chg in solution. Additionally, Fm-GABA←mGly-Ala-Ser-Chg could be readily generated by coupling the Fm-GABA←mGly-OSu ester to H-Ala-Ser-Chg-*O*-resin at room temperature in 48 h. All other peptides were synthesized using standard solid phase procedures, and coupled to 2-fluoro-4-glutaminylaminobenzyl phosphoramide mustard and aminoglycoside of doxorubicin using HBTU and PyBOP coupling procedues, respectively, or the C-14 α-hydroxyl of doxorubicin via a 3-aminoxypropionate linker as shown in Scheme 7.

The 3-aminoxypropionate linker of prodrug **63** was obtained using our previously reported procedure with modifications.[195] Ready access to the protected linker **68** was achieved in a single step starting from either methyl or benzyl 3-hydroxy-2,2-dimethylpropanoate in greater than 50% yield. Using methyl 3-hydroxy-2,2-dimethylpropanoate as a starting point, removal of the phthalimido group with anhydrous hydrazine afforded the methyl ester of the 3-aminoxypropionate linker **69** which was subsequently coupled to Alloc-Gln(Trt)-OH via its OSu ester (Scheme 8). Trityl-protection of the Gln side-chain amide was introduced in earlier steps for convenient UV detection during the FCC purification of compound **73**.

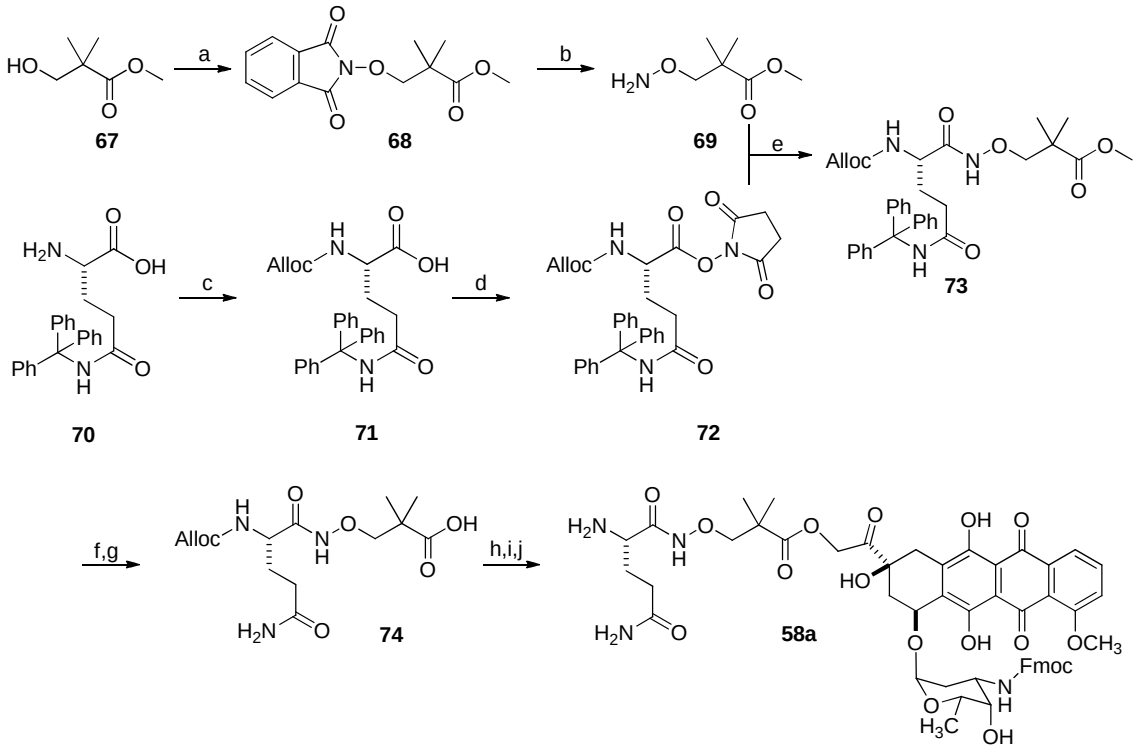

Scheme 8. Synthesis of the Aminoxypropionate-doxorubicin Conjugate **58a**. Reagents and conditions: (a) PhtOH, Ph_3P, DIAD, THF, 0 ºC to rt, 24 h; (b) H_2NNH_2, Et_2O, rt, 2 h; (c) allyl chloroformate, 10%K_2CO_3/MeCN (1:2), rt, 10 min; (d) EDC, HOSu, MeCN, rt, 2 h; (e) rt, 24 h; (f) 0.1 NaOH/THF, rt, 24 h; (g) 95% TFA/DCM, 0 ºC, 5 min; (h) 14-bromodaunorubicin, $NaHCO_3$ (1 eq.), 3Å mol. sieves, acetone, rt, 72 h; (i) Fmoc-OSu, $NaHCO_3$, MeCN, rt, 1 h; (j) tetrakis(triphenylphosphine)palladium(0)/dimedone, THF, rt, 1 h.

Due to the poor stability of doxorubicin under acidic deprotection and hydrogenation conditions, an orthogonal protection strategy involving an acid- and base-stable protecting group for either the α-amino or C-4 amino group of Gln or doxorubicin, respectively, was necessary. While TFA-protection was stable to organic base for up of 24 h, this approach was not pursued because of the anticipated hydrolysis of the doxorubicin-14-*O*-ester during subsequent (typically 24- to 48-h) deprotection steps with 10% K_2CO_3. Additionally, the removal of a TFA-protecting group from the C-4 amino

grroup of doxorubicin with Acylase I was found to proceed in low yield (< 10% deprotection in 100 mM $KHPO_4$ buffer, pH 7.4, in 24 h). Thus, a Fmoc/Alloc orthogonal protection strategy was used so that the Alloc group could be removed with tetrakis(triphenylphosphine)palladium(0) in the presence of the allyl scavenger dimedone, and Fmoc deprotected with a non-nucleophilic base such as 1,8-diazabicycloundec-7-ene (DBU). Various conditions for the preparation of Alloc-Gln(Trt)-OH starting from H-Gln(Trt)-OH were explored. To cirmcunvent the poor solubility of H-Gln(Trt)-OH in most solvents, a 2-phase reaction system (10% K_2CO_3 and acetonitrile) followed by slow allylchloroformate addition afforded Alloc-Gln(Trt)-OH in excellent yield (95%) and purity. Coupling of compound **69** to Alloc-Gln(Trt)-OH using EDC was unproductive, and yields greater than 40% could not be achieved with Alloc-Gln(Trt)-OSu and 2,2-dimethyl-3-aminoxypropionic acid or methyl 2,2-dimethyl-3-aminoxypropionate. We suspected that the poor conversion yield originated from the instability of the OSu ester over a period of 24 h, and carried out a one-pot procedure in the presence of excess EDC; this improved the yield to 86%.

Much effort was dedicated to optimizing the challenging synthesis of doxorubicin-14-*O*-esters. A few specific doxorubicin-14-*O*-esters were prepared by chemoenzymatic methods using *C. Antarctica lipase* (type B);[197, 198] however, the conventional approach for synthesizing doxorubicin-14-*O*-esters involves a nucleophilic displacement-type esterification of 14-bromodaunorubicin (**76**) under basic conditions. To access 14-bromodaunorubicin, C-14 bromination was efficiently carried out through ketalization of the carbonyl group at C-13 (Scheme 9).[199-201]

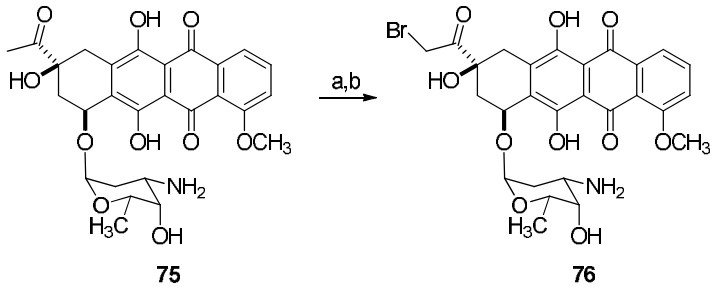

Scheme 9. Synthesis of 14-bromodaunorubicin **76**. Reagents and conditions: (a) $HC(MeO)_3$, Dioxane/MeOH (2;1), rt, 20 min; (b) $Br_2/CHCl_3$, rt, 40 min.

Noteworthy, our previous attempts to esterify Fmoc-Dox via Mitsunobu and Appel reactions failed. Adaptation of a previously reported methodology for *N*-Fmoc-doxorubicin-14-*O*-hemiglutarate[202] involving coupling of the mixed anhydride with Fmox-Dox in the presence of TEA at room temperature in 48 h did not produce the desired ester either. We also performed CDI and EDCC/DMAP coupling with little success; increasing the equivalents of CDI or DMAP led to premature removal of the Fmoc-protecting group. Moreover, ester **58a** could not be generated using EDC and catalytic 4-pyrrolopyridine or using 1-(mesitylene-2-sulfonyl)-3-nitro-1H-1,2,4-triazole (MSNT) as an activating agent, and Fm-GABA←mGly-Ala-Ser-Chg-Gln-NH-O-CH_2-$C(Me)_2COOH$ was unreactive towards 14-bromodaunorubicin under neutral conditions. Nevertheless, preliminary studies with hydroxypivalic acid (**77**) indicated that its doxorubicin-14-*O*-ester (**78**) could be readily synthesized from sodium hydroxypivalate and 14-bromodaunorubicin at 50 °C in dry acetone (Scheme 10) as previously reported for various doxorubicin-14-*O*-esters generated from aspartic acid derivatives and fatty acids.[199-201] Under those conditions, significant aglycone formation also occurred due to *in situ* generation of HBr. In addition, hydrolysis of 14-bromodaunorubicin to doxorubicin (~10%) was observed leading to a further reduction of the reaction yield to

less than 50%. In our hands, reaction conditions were optimized to afford nearly quantitative conversion to the hydroxypivalate doxorubicin-14-*O*-ester by increasing the solvent volume and adding 3 Å molecular sieves to the reaction mixture to trap HBr.[203]

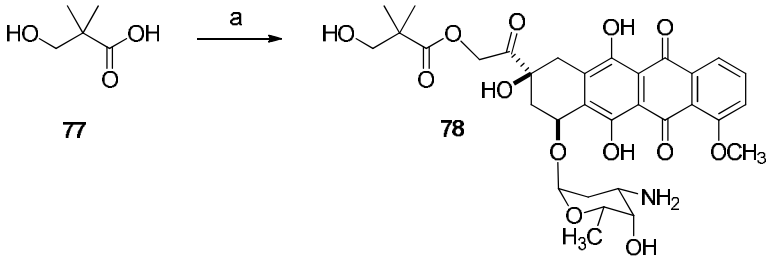

Scheme 10. Synthesis of Hydroxypivalate Doxorubicin-14-*O*-ester **77**. Reagents and conditions: (a) **76**, $NaHCO_3$ (1 eq.), 3Å mol. sieves, acetone, 50 °C, 1 h.

Convenient access to doxorubicin-14-*O*-esters **58a** and **58b** was thus possible through coupling of compound **74** or **82** to 14-bromodaunorubicin (**76**) at room tempertaure for 48 h, followed by Alloc- or Fmoc-protection, respectively (Schemes 8 and 11). The conversion yield of the bromo-substitution steps affording esters 58**a** and 58**b** was improved to up 80% when a minimum of 5 equivalents of the acid was used; nevertheless, longer reaction times led to significant hydrolysis of the esters to doxorubicin (greater than 20%) and overall yields greater than 40% could not be achieved for the protected esters. Additionally, FCC purification of the protected esters was difficult due to their poor solubility. Nonetheless, the deprotected ester **58b** could be purified and isolated by HPLC in sufficient quantities for the next step.

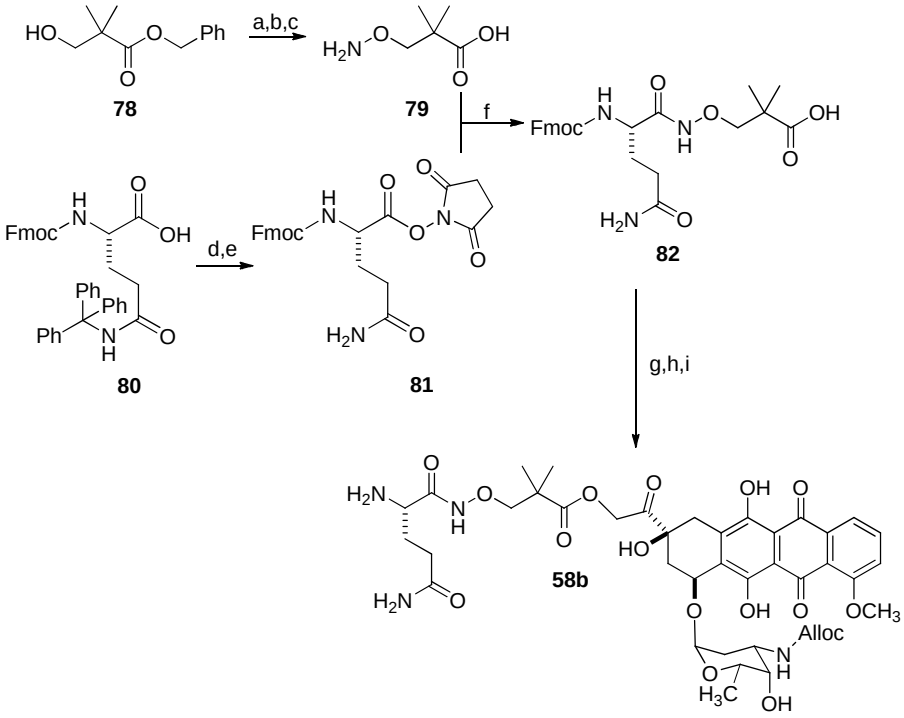

Scheme 11. Synthesis of the Aminoxypropionate-doxorubicin Conjugate **58b**. Reagents and conditions: (a) PhtOH, Ph_3P, DIAD, THF, 0 ºC to rt, 24 h; (b) H_2/ Pd-C, MeOH, rt, 5 h; (c) H_2NNH_2, Et_2O, rt, 2 h; (d) EDC, HOSu, MeCN, rt, 2 h; (e) 95% TFA/MeCN, rt, 5 min; (f) rt, 24 h; (g) **76**, $NaHCO_3$ (1 eq.), 3Å mol. sieves, acetone, rt, 72 h; (h) Alloc-OSu, $NaHCO_3$, MeCN, rt, 1 h; (i) 1%DBU, DMF, rt, 10 min.

Following modified procedures from our laboratories, phosphoramide mustard prodrugs were synthesized as shown in Scheme 9. To prepare the linker, 2-fluoro-4-aminobenzyl alcohol was readily accessed through $NaBH_4$ reduction of the OBt ester, followed by Pd-catalyzed hydrogenation in excellent yield (Scheme 9, 85%, 2 steps). Conversion of 2-fluoro-4-aminobenzyl alcohol to the azido-intermediate followed by selenocarboxylate azide amidation afforded 2-fluoro-4-glutaminylaminobenzyl phosphoramide mustard.[194] With the Gln-linker intermediates on-hand, prodrugs **61**-**66** were synthesized according to Scheme 7.

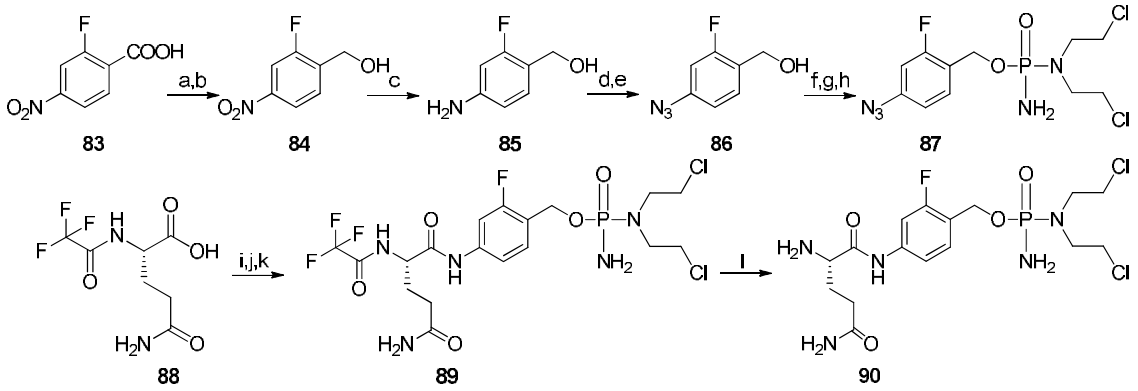

Scheme 12. Synthesis of 2-Fluoro-4-glutaminylaminobenzyl Phosphoramide Mustard (**90**). Reagents and conditions: (a) HOBt/EDC, THF, rt, 1 h; (b) $NaBH_4$, THF, rt, 2 h; (c) H_2/ Pd-C, MeOH, rt, 5 h; (d) $NaNO_2$, rt, 30 min; (e) NaN_3, 10% HCl, rt, 1 h; (f) BuLi, THF, rt, 20 min; (g) $Cl_2PON(CH_2CH_2Cl)_2$; (h) liquid NH_3, -78 ºC, 10 min; (i) IPCF, *N*-methtylpiperidine, THF, -20 to -10 ºC, 20 min; (j) LiAlHSe, THF, -15 ºC, 30 min; (k) azide **87**, rt, 20 h; (l) K_2CO_3 , MeCN/H_2O (3:1), rt, 48 h.

II. Evaluation of Peptidylaminoarylmethyl Phosphoramide Mustard and Doxorubicin Prodrugs in PSA- and non-PSA-producing Cells

A. Prodrug Stability in Tris Buffer

The stability of phosphoramide mustard and doxorubicin peptide conjugates in 50 mM Tris buffer, pH 8 was studied over a period of 48 h. Prodrug disappearance was monitored by LC-MS/MS analysis using selected-reaction monitoring (SRM). As shown in Fig. 23, most prodrugs were ~ 80% stable in Tris buffer, pH 8 over a period of 24 hours except for prodrugs **65** and **66** (60 and 70% remaining in 24 h, respectively). LC-MS analysis of the buffer incubates revealed that one of the major degradants of doxorubicin conjugates **60**, **61** and **62** was a putative Tris-adduct (confirmed by accurate mass) probably originating from the condensation of trisaminomethane with trace amounts of the terminal aldehyde (tautomerized α-hydroxyketone) of doxorubicin. Another late-eluting degradant with retention time of 17.5 min was detected but could not

be identified based on mass spectral data. Phosphoramide mustard conjugates slowly converted to their corresponding 2-fluoro-4-peptidylaminobenzyl alcohol conjugate through hydrolysis. Slow peptide conjugate dedgradation was insignificant over 8 hours and did not affect our enzyme assay result interpretation. In future paragraphs, we will show that the instability of doxorubicin conjugates in biological matrices proceeds through mechanisms affecting their peptide promoiety, which are distinct from the slow degradation observed in buffer. It was difficult to reach similar conlusions for phosphoramide mustard conjugates since the degradation processes described above appear to be similar and accelerated in biological matrices and *in vivo* (from mouse PK data not shown).

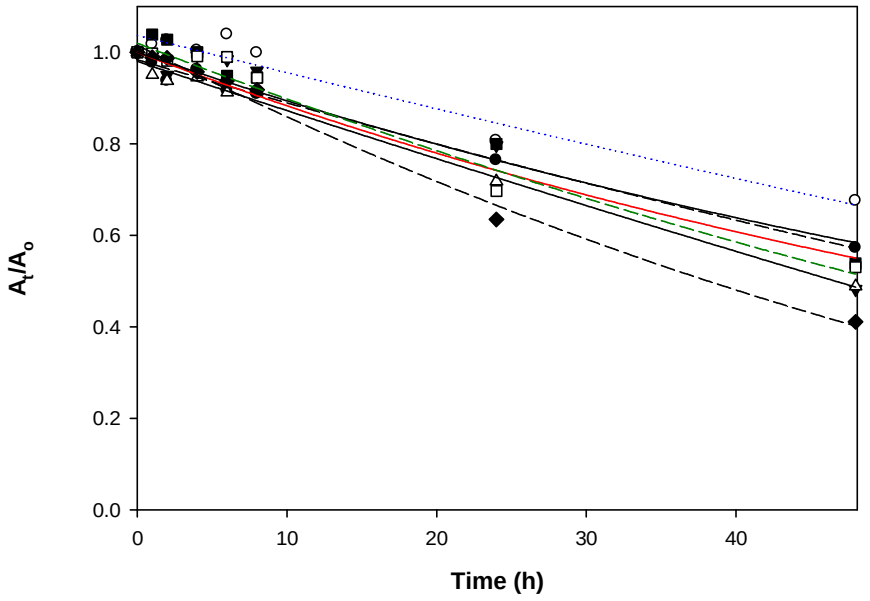

Figure 23. Stability of Doxorubicin and Phosphoramide Mustard Prodrugs in Tris Buffer. Each conjugate (100 µM) was incubated in 50 mM Tris/HCl buffer, pH 8.0 containing 10 mM $CaCl_2$ and 0.1% TWEEN-20 at 37 °C. L-377202 (--●--), 61 (···○···), 62 (–▼–), 63 (–▽–), 64 (–■–), 65 (--□--), 66 (¯®¯).

B. PSA Cleavage Rate and Half-life Determination

To determine PSA cleavage rates, doxorubicin and phosphosramide mustard prodrugs were incubated with human PSA over a period of 3 h. As previously described, substrate disappearance was monitored by LC-MS/MS analysis using SRM. The percentage of prodrug remaining at any given time point could be computed by taking the ratio of its peak area response and that of the the 0-h time point. Overall, the doxorubicin conjugates exhibited the fastest cleavage rates with comparable profiles (Fig. 24).

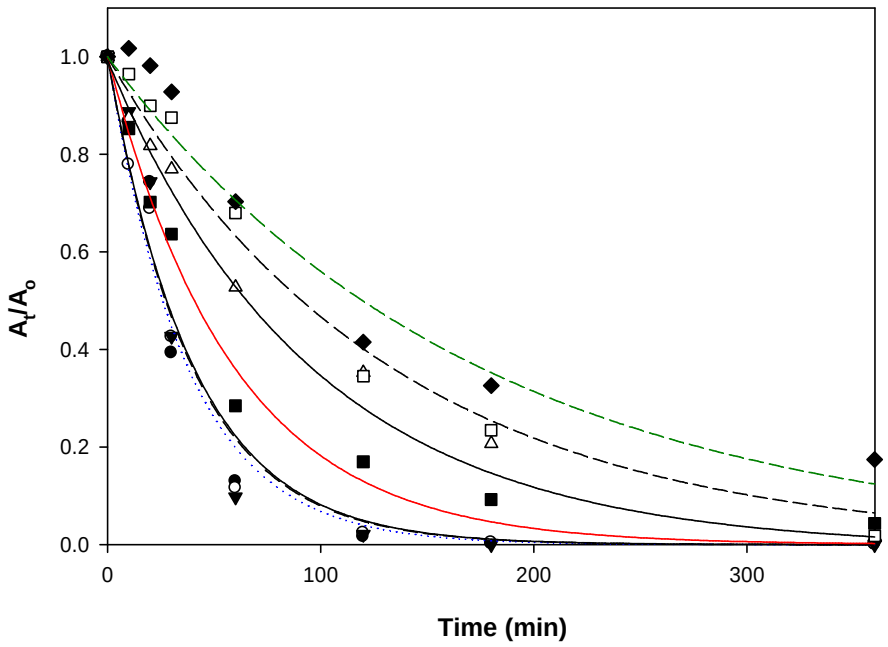

Figure 24. Disappearance of Doxorubicin and Phosphoramide Mustard Prodrugs during PSA Hydrolysis. Each conjugate (1 µM) was incubated with PSA (1 mM) in 50 mM Tris/HCl buffer, pH 8.0 containing 10 mM CaCl2 and 0.1% TWEEN-20 at 37 °C.
L-377202 (--●--), 61 (···○···), 62 (−▼−), 63 (− ▽−), 64 (-■-), 65 (--□--), 66 (¯®¯).

Differences in PSA cleavage rates observed for AMC-conjugates were not reproduced with the corresponding prodrugs probably due to experimental conditions (lowerr

substrate enzyme ratio of 1:1 for prodrugs versus 10:1 for conjugates) and potential PSA inhibition mechanisms (see future paragraphs). Our original substrate optimization studies suggested that glutaryl-Ser-Ala-Ser-Chg-Gln-AMC and GABA←mGly-Ala-Ser-Chg-Gln-AMC were cleaved by PSA 1.3- and 2-fold faster than glutaryl-Hyp-Ala-Ser-Chg-Gln-AMC, respectively. Although modifications were carried out across the entire sequence of glutaryl-Hyp-Ala-Ser-Chg-Gln, only P5 substitutions led to notable increases (up-to a 2-fold) in PSA cleavages rate for the AMC-conjugates. Because the most effective amino acid substitutions were distant from the PSA scissile bond, we hypothesized that only susbtrate Km was improved for the AMC-conjugates developed. However, as shown in Table 5, modifications in P1' and P2' negatively affected PSA cleavage rate as suggested by the longer half-life (67 min) of the doxorubicin prodrug **63** compared to prodrugs **60**-**62** (half-life values of 22-23 min). A full characterization of the Michaelis-Menten kinetic curves for prodrugs **60**-**66** could help further explain the results summarized in Fig. 20 and 24. Nevertheless, for our purpose, the doxorubicin conjugates were cleaved at sufficiently fast rates, and some comparable to that of L-377,202. Of the phosphoramide mustard conjugates synthesized, prodrugs **65** and **66** were unexpectedly no better than our previously designed prodrug **64** as suggested by their longer half-lives (greater than 60 min). These results were surpising since we anticipated no effects of peptide conjugation with phosphormaide mustard on PSA cleavage due the small size of phosphoramide mustard compared to doxorubicin.

Table 5. Hydrolysis of Doxorubicin and Phosphoramide Mustard Prodrugs by Human PSA

Prodrug	**% of prodrug at 60 min**	**$t_{1/2}$ (min)**
Glutaryl-Hyp-Ala-Ser-Chg-Gln-Ser-Leu-Dox (**60**)	13	23
Glutaryl-Ser-Ala-Ser-Chg-Gln-Ser-Leu-Dox (**61**)	12	22
GABA←mGly-Ala-Ser-Chg-Gln-Ser-Leu-Dox (**62**)	9.8	22
GABA←mGly-Ala-Ser-Chg-Gln-NH-O-CH_2-C$(Me)_2$C(O)-14-*O*-Dox (**63**)	53	67
Glutaryl-Hyp-Ala-Ser-Chg-Gln-NH-2-F-Bz-phosphoramide mustard (**64**)	28	35
Glutaryl-Ser-Ala-Ser-Chg-Gln-NH-2-F-Bz-phosphoramide mustard (**65**)	68	80
GABA←mGly-Ala-Ser-Chg-Gln-NH-2-F-Bz-phosphoramide mustard (**66**)	70	107

Conditions: Each peptide conjugate (1 μM) was incubated with human PSA (1 μM) in 50 mM Tris/HCl buffer, pH 8, for 360 min, and the % of prodrug determined using LC-MS/MS (SRM).

We previously demonstrated and herein confirmed that prodrug **64** is cleaved by PSA with a half-life of 35 min compared to 22-67 min for the doxorubicin conjugates (Table 5). A plausible explanation for these results is that conjugation of glutaryl-Ser-Ala-Ser-Chg-Gln and GABA←mGly-Ala-Ser-Chg-Gln with phosphoramide mustard may have afforded poorer substrates for PSA. However, because the half-life appeared to increase for our improved peptide substrate glutaryl-Ser-Ala-Ser-Chg-Gln and GABA←mGly-Ala-Ser-Chg-Gln, a more likely explanation is that PSA was inhibited by activated

phosphoramide mustard or electrophilic quinonimine methides released from the phosphoramide mustard moiety. Thus, the faster the release of the aforementioned PSA inactivators the slower the PSA cleavage rate due to time-dependent inhibition of the enzyme. It may be beneficial to explore combinations of our improved PSA peptide substrates with previously synthesized phosphoramide mustard analogs[151] from our laboratories to reach the optimal balance between PSA peptide cleavage rate and phosphoramide mustard or electrophilic quinonimine methides release although our initial strategy was to conjugate the 2-fluoro analog.

C. Prodrug Cytotoxicity in DU145 and LNCaP Cell Lines

To assess cytotoxicity and tumor selectivity, all prodrugs were incubated in cultured cell lines secreting (LNCaP) or lacking (DU145) PSA for a period of 72 h. Doxorubicin was included in the study as a positive control, and cell viability determined at the end of the incubation period using the MTT assay. We anticipated that peptide prodrugs would be activated extracellularly in LNCaP, but not DU145 cells, by the proteolytic action of PSA releasing cytotoxic agents that would ultimately lead to cell death. Various studies suggested that doxorubicin exerts its apoptotic action in tumor cells via selective binding to nuclear DNA with subsequent free radical-mediated DNA damage promoted by its metabolic activation. However, in non-tumor cells, its primary cytotoxic mechanism involves the generation of free-radical intermediates in subcellular compartments.[204] Consequently, after being activated in the microenvironment of prostate cancer tumor cells, transport of Leu-Dox or doxorubicin across the cell membrane would be necessary to induce cell death in LNCaP cells. Meanwhile, drug sensitivity, and more importantly,

chemoresistance to doxorubicin have been associated with ATP-binding cassette (ABC) transporters such as P-glycoprotein 1 (P-gp) and ABCB5.[205-207] As mentioned earlier, proof-of-concept was first demonstrated for L-377,202 in humans, and both Leu-Dox and doxorubicin are believed to contribute to its cytotoxic effect elicited in tumor cells *in vitro* and *in vivo*. Currently, there is no clear understanding of the transport mechanisms involved in shuttling Leu-Dox and doxorubicin across tumor cell membranes, and it's difficult to predict the contribution of each cytotoxin to overall prodrug effect. In addition, it is not known whether doxorubicin (and possibly Leu-Dox) efflux out of tumor cells leads to any significant circulating drug and metabolite levels although non-PSA-mediated metabolism is suspected to be the main perpetrator.[192] In our cell culture studies, conjugate **62** was the most cytotoxic prodrug against PSA-secreting LNCaP cells with excellent selectivity against non-PSA-producing DU145 cells (Fig. 25, Table 6). Since PSA cleavage rates among most doxorubicin conjugates **60**-**62** were similar (Fig. 24, Table 5) alternate unknown mechanisms must have contributed to differences in prodrug selectivity in LNCaP and DU145 tumor cell lines. While tumor cell lines generally possess lower metabolic capability compared to cultured hepatocytes, prodrug stability can not be ruled out as a possibility. We previously demonstrated that GABA←mGly-Ala-Ser-Chg-Gln was a more specific PSA substrate compared to glutaryl-Ser-Ala-Ser-Chg-Gln and glutaryl-Hyp-Ala-Ser-Chg-Gln based on the PSA cleavage rate and plasma stability of their AMC-conjugates and the results in Fig. 25 appear to suggest similar trends although the various mechanisms involved in prodrug cytotoxicity are difficult to tease out. Despite it lower PSA cleavage rate compared to doxorubicin conjugates **60**-**62**, prodrug **63** exhibited a cytotoxicity profile comparable to

that of prodrugs **60**. As mentioned earllier, the cytotoxin released by prodrug **63** is free doxorubicin rather than Leu-doxorubicin. Because doxorubicin was shown to be 10 times more potent than Leu-doxorubicin at killing tumor cells,[139, 192] its slower release from prodrug **63** was as effective as the relatively faster release of leu-doxorubicin from prodrug **60** (Fig. 26). Moreover, unlike prodrug **60**, prodrug **63** does not rely on the hydrolytic action of additional aminopeptidases to generate the final cytotoxin. The PSA-mediated proteolytic activation mechanism of phosphoramide mustard prodrugs follows a similar path as the doxorubicin conjugates.

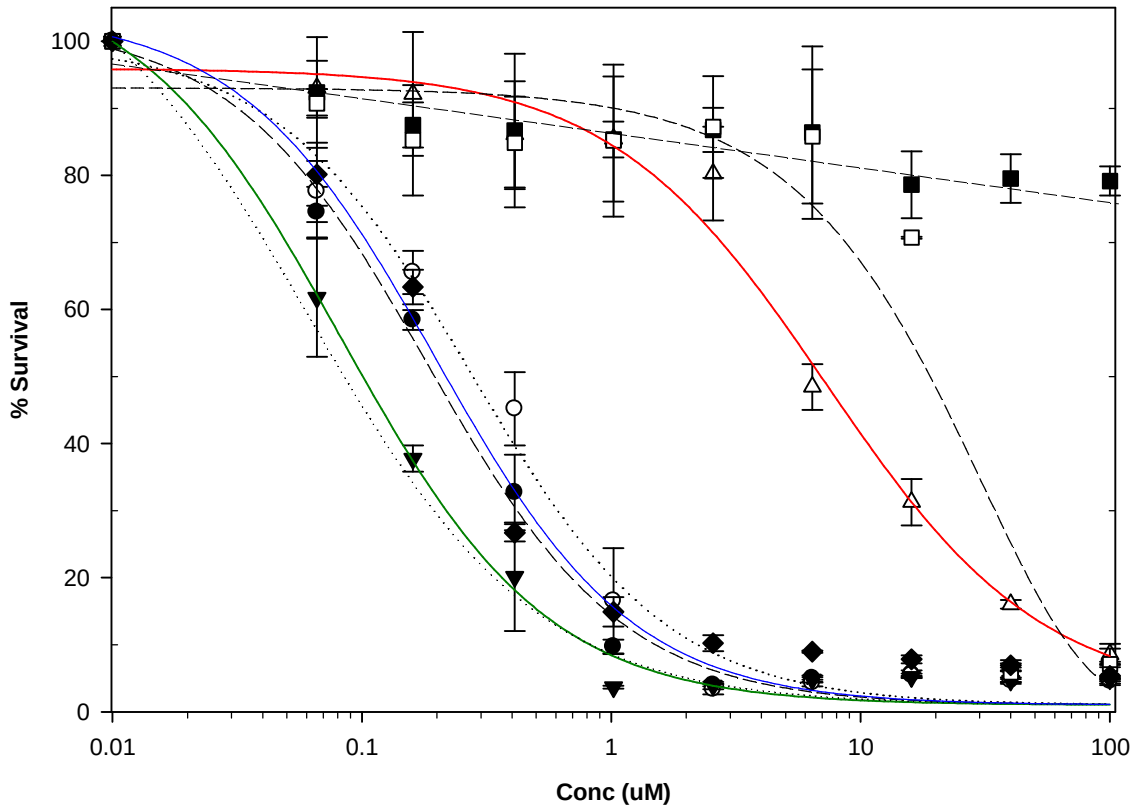

Figure 25. Cytotoxicity of Doxorubicin and Phophoramide Mustard Prodrugs in LNCaP Cells. Doxorubicin (⋯●⋯), L-377202 (--●--), 61 (⋯○⋯), 62 (–▼–), 63 (–®–), 64 (– ∆ –), 65 (--■--), 66 (--□--).

Table 6. Prodrug Cytotoxicity in PSA-producing LNCaP Cell Lines

Prodrug	**LNCaP IC_{50} (mM)**	**Selectivity[a] against DU145**
Dox	<0.07	1
Glutaryl-Hyp-Ala-Ser-Chg-Gln-Ser-Leu-Dox (**60**)	0.18	560
Glutaryl-Ser-Ala-Ser-Chg-Gln-Ser-Leu-Dox (**61**)	0.27	370
GABA←mGly-Ala-Ser-Chg-Gln-Ser-Leu-Dox (**62**)	0.082	1220
GABA←mGly-Ala-Ser-Chg-Gln-NH-O-CH_2-C(Me)$_2$C(O)-14-*O*-Dox (**63**)	0.19	560
Glutaryl-Hyp-Ala-Ser-Chg-Gln-NH-2-F-Bz-phosphoramide mustard (**64**)	7.3	14
Glutaryl-Ser-Ala-Ser-Chg-Gln-NH-2-F-Bz-phosphoramide mustard (**65**)	>100	>100
GABA←mGly-Ala-Ser-Chg-Gln-NH-2-F-Bz-phosphoramide mustard (**66**)	30	1

Conditions: PSA-producing LNCaP and non-PSA-producing DU145 cell lines were treated with doxorubicin or prodrugs **60-66** at concentrations ranging from 0.07 to 100 μM for 72 h and cell viability determined using the MTT assay. [a] Selectivity-fold expressed as the ratio of the LNCaP and DU145 (data not shown) IC_{50} values.

Phosphoramide mustard, the DNA-alkylating metabolite of cyclophosphamide, is expected to be released into the extracellulr space of tumor cells upon PSA activation of prodrugs **64-66.** Cyclophosphamide alkylates N-7 of guanine, thereby inhibiting DNA replication. Inactive cyclophosphamide and related prodrugs are believed to be actively

transported into cells and activated intracellularly.[183] In our case, the first activation steps occurs extracellularly releasing phoshoramide mustard which is expected to be transported through mechanisms similar to that of cyclophosphamide.

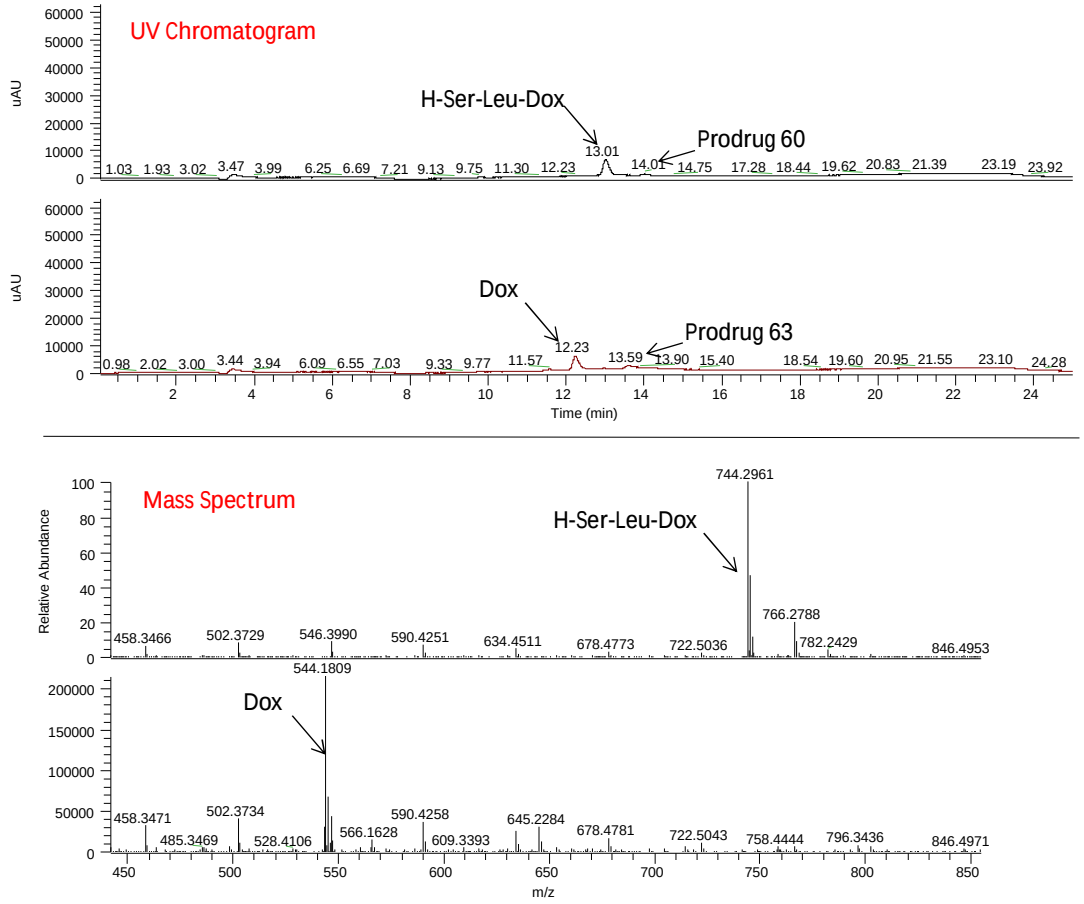

Figure 26. PSA-mediated Hydrolysis of Prodrugs **60** and **63.** Conditions: Each peptide conjugate (1 μM) was incubated with human PSA (1 μM) in 50 mM Tris/HCl buffer, pH 8, for 4 h. Samples were precipitated with 1 volume of ACN, centrifuged and analyzed by LC-MS-UV.

A caveat of the phosphoramide mustard conjugates is their slow activation by PSA as previously discussed. Nevertheless, once phosphoramide mustard enter the intracellular space through active transport, increased hydrolysis by phosphoramidases which are

typically induced in tumors should increase its effectiveness. Consistent with our results in Fig. 25, prodrug **64** showed cytotoxic response in LNCaP with and IC_{50} of 7.3 μM and a 14-fold selectivity against DU145. Prodrug **66** was equally cytotoxic against both cell lines (DU145 data not shown) whereas prodrug **65** was inactive. These results can be explained by the lack of robust PSA activation of prodrugs **65** and **66** as depicted in Fig. 25. The cytotoxicity observed with prodrug **66** in both LNCaP and DU145 cell lines is unlikely to be mediated by PSA and may be due slow spontaneous prodrug hydrolysis and concomitant phosphoramide release as suggested by its marginally lower stability in buffer as compared to prodrugs **64** and **65** (Fig. 23).

III. Stability of Peptidylaminoarylmethyl Phosphoramide Mustard and Doxorubicin Prodrugs in Human and Mouse Blood and Cultured Hepatocytes

Initial studies to evaluate the tumor specificity of prodrugs **60-62** and **64-66** were conducted in biological matrices lacking active PSA. Prodrugs were incubated in heparinized human or mouse blood at 100 μM over a period of 24 h and the fraction of prodrug remaining at various time points determined by LC-MS/MS using SRM as previously described. Blood samples were treated with sodium heparin since EDTA is known to inhibit the activity of various metalloproteases through chelation of divalent ions such as Zn^{2+}. As shown in Table 7 and Fig. 27, prodrugs were quickly degraded in human blood to approximately 20 μM in less than 10 h except for prodrugs **62**.

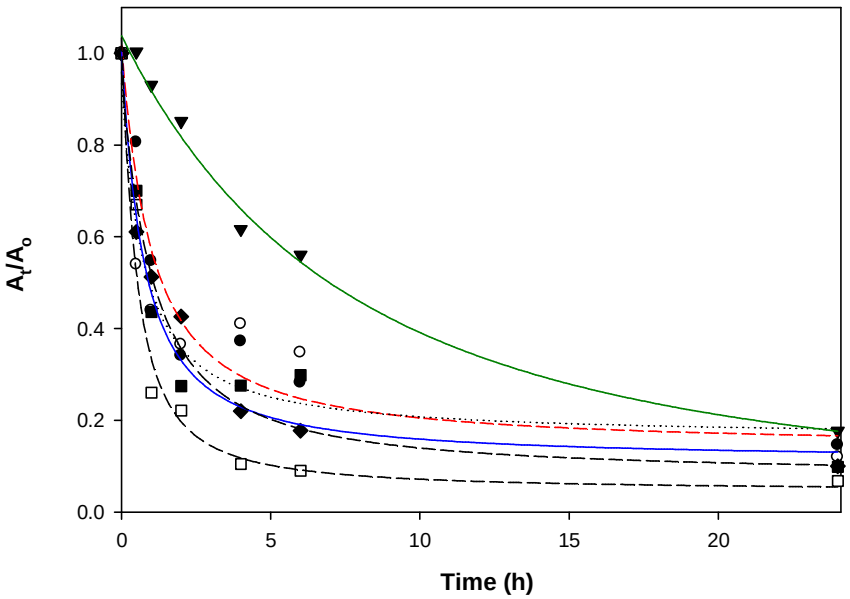

Figure 27. Stability of Doxorubicin and Phosphoramide Mustard Prodrugs in Human Blood. Each conjugate (100 µM) was incubated in human blood at 37 °C over a period of 24 h. L-377202 (--●--), 61 (···○···), 62 (–▼–), 64 (-■-), 65 (--□--), 66 (¯®¯).

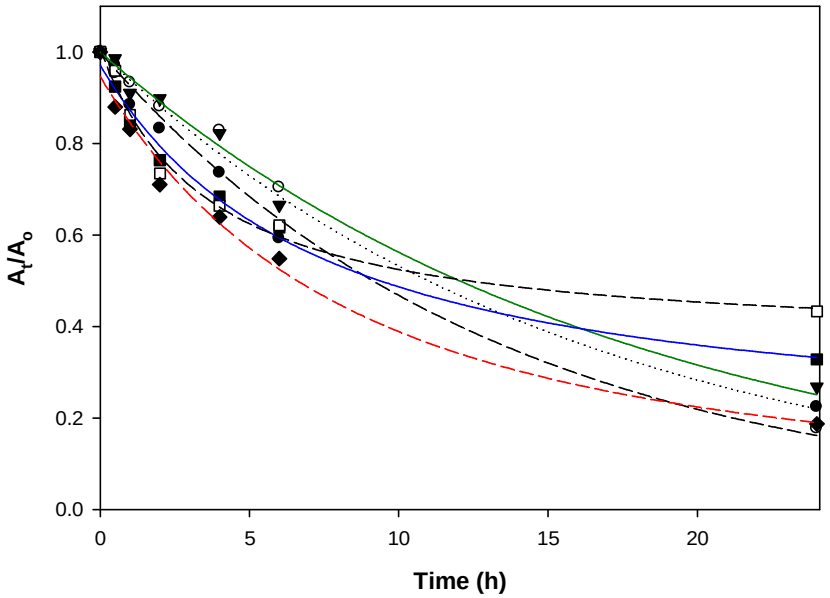

Figure 28. Stability of Doxorubicin and Phosphoramide Mustard Prodrugs in Mouse Blood. Each conjugate (100 µM) was incubated in mouse blood at 37 °C over a period of 24 h. L-377202 (--●--), 61 (···○···), 62 (–▼–), 64 (-■-), 65 (--□--), 66 (¯®¯).

Table 7. Non-PSA-mediated Prodrug Hydrolysis in Mouse and Human Blood

Prodrug	**$t_{1/2}$ (h)**	
	Human	**Mouse**
Glutaryl-Hyp-Ala-Ser-Chg-Gln-Ser-Leu-Dox (**60**)	1.4	9.1
Glutaryl-Ser-Ala-Ser-Chg-Gln-Ser-Leu-Dox (**61**)	0.91	11
GABA←mGly-Ala-Ser-Chg-Gln-Ser-Leu-Dox (**62**)	7.0	12
Glutaryl-Hyp-Ala-Ser-Chg-Gln-NH-2-F-Bz-phosphoramide mustard (**64**)	0.91	9.4
Glutaryl-Ser-Ala-Ser-Chg-Gln-NH-2-F-Bz-phosphoramide mustard (**65**)	0.54	12
GABA←mGly-Ala-Ser-Chg-Gln-NH-2-F-Bz-phosphoramide mustard (**66**)	1.1	6.5

Conditions: Each peptide conjugate (100 μM) was incubated in human or mouse blood for 24 h, and the % of prodrug determined using LC-MS/MS (SRM).

Similar experiments in heparinized mouse blood indicated that overall 50% of most prodrugs remained after 8 h except for prodrug **66** (Fig. 28). The most stable prodrugs were **62** in human blood, and **62** and **65** in mouse blood based on half-life determinations (Table 7). In agreement with our previous plasma stability studies conducted with AMC-conjugates, prodrug **62** exhibited enhanced stability in human blood, probably due to the P5 modifications carried out in their peptide sequences. Other prodrugs were quickly hydrolyzed in human blood by proteases other than PSA although somewhat stable in mouse blood with half-life values ranging from 7 to 11 h. As previously observed with AMC-conjugates, blood stability results suggest that one or more endopeptidase (s) may be cleaving the peptide promoieties of the prodrugs; LC-MS identification of the peptide

fragments released from each prodrug in blood overtime should help determine critical metabolic soft spots for prodrug stability. The half-life value for prodrugs **62** was found to be 7 h in human blood, and greater than 12 h in mouse blood. However, the corresponding phosphoramide prodrug **66** showed poor stability in both human and mouse blood for unclear reasons. We also found that prodrug **66** was the least stable in Tris buffer suggesting that a combination of spontaneous chemical degradation and enzymatic hydrolysis may be have contributed to its instability in blood.

To further evaluate their specificity to PSA (and tumor selectivity), the stability of prodrugs **60-62** and **64-66** in cultured hepatocytes was determined by LC-MS/MS analysis. Our preliminary attempts to assess prodrug stability in select biological matrices indicated that, contrary to published PK and metabolism results, L-377,202 was stable in hepatic microsomes, cytosolic, and S9 suspensions (data not shown). Since the metabolic capacity of the the aforementioned matrices do not extend over 2 h, we set out to further investigate prodrug stability in sytems with extended metabolic activity lasting behond 24 h, and cultured hepatocytes were a reasonable choice. Depending on experimental conditions, cultured hepatocytes can remain metabolic active for at least 48 h. Similar to blood stability results, all prodrugs demonstrated good stability in cultured mouse hepatocytes, but not human (Fig. 29 and 30). Compared to blood, half-life values were extended to a minimum of 10 h for all prodrugs although significant differences in half-life and stability were observed in human hepatocytes (Table 8).

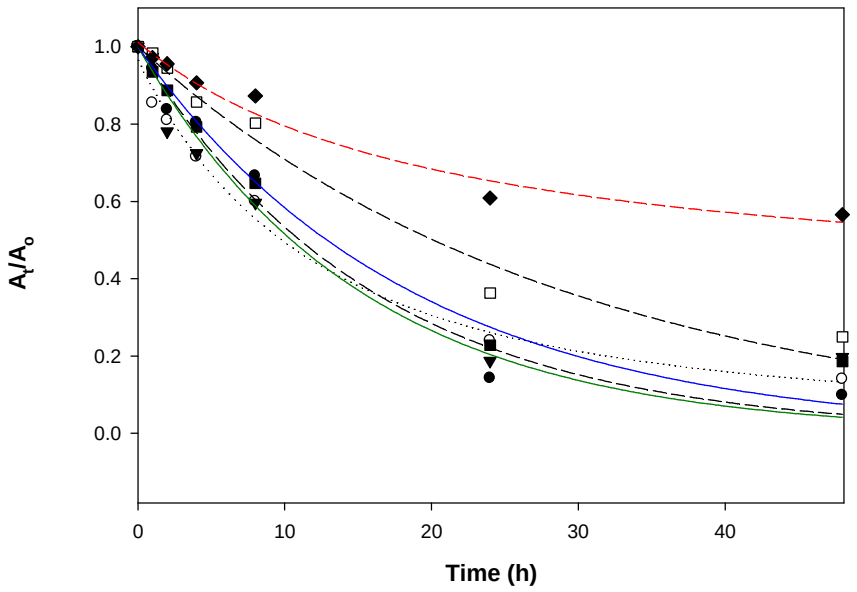

Figure 29. Stability of Doxorubicin and Phosphoramide Mustard Prodrugs in Plated Human Hepatocytes. Each conjugate (100 µM) was incubated in plated human hepatocytes at 37 °C over a period of 48 h. L-377202 (--●--), 61 (···○···), 62 (–▼–), 64 (– ■ –), 65 (--□--), 66 (¯®¯).

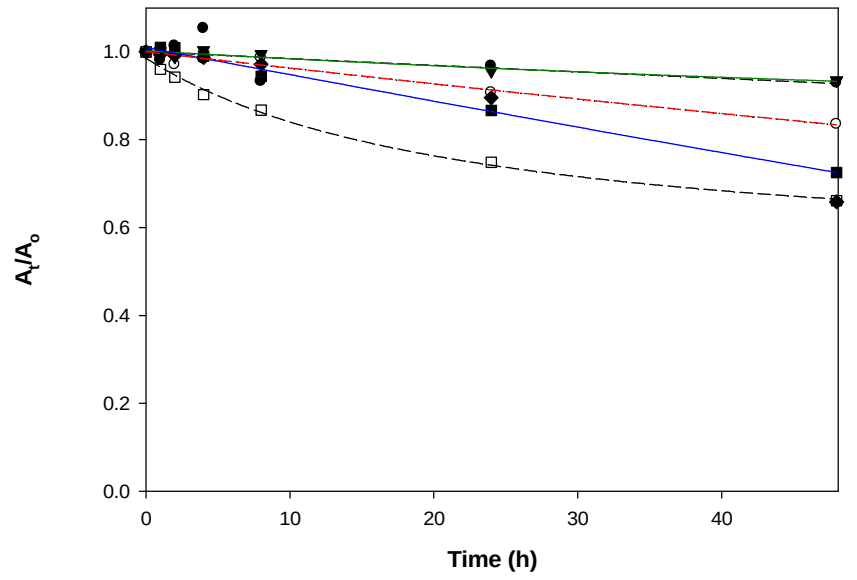

Figure 30. Stability of Doxorubicin and Phosphoramide Mustard Prodrugs in Plated Mouse Hepatocytes. Each conjugate (100 µM) was incubated in plated Mouse hepatocytes at 37 °C over a period of 48 h. L-377202 (--●--), 61 (···○···), 62 (–▼–), 64 (– ■ –), 65 (--□--), 66 (¯®¯).

Table 8. Non-PSA-mediated Prodrug Hydrolysis in Mouse and Human Hepatocytes

Prodrug	**$t_{1/2}$ (h)**	
	Human	**Mouse**
Glutaryl-Hyp-Ala-Ser-Chg-Gln-Ser-Leu-Dox (**60**)	11	>48
Glutaryl-Ser-Ala-Ser-Chg-Gln-Ser-Leu-Dox (**61**)	9.6	>48
GABA←mGly-Ala-Ser-Chg-Gln-Ser-Leu-Dox (**62**)	11	>48
Glutaryl-Hyp-Ala-Ser-Chg-Gln-NH-2-F-Bz-phosphoramide mustard (**64**)	13	>48
Glutaryl-Ser-Ala-Ser-Chg-Gln-NH-2-F-Bz-phosphoramide mustard (**65**)	20	>48
GABA←mGly-Ala-Ser-Chg-Gln-NH-2-F-Bz-phosphoramide mustard (**66**)	>48	>48

Conditions: Each peptide conjugate (100 μM) was incubated in cultured human or mouse hepatocytes for 48 h, and the % of prodrug determined using LC-MS/MS.

Overall, the improved prodrug stability in cultured hepatocytes compared to blood can be attributed to several possible mechanisms. Key differences in metabolic properties between blood include protease levels (blood > hepatocytes) and transport mechanisms; in hepatocytes, peptide conjugates must first permeate cell membranes through passive diffusion and/or active transport before being exposed to intracellular proteases. Peptide transporter 1 (PepT 1) is known to be involved in the transport of oligopeptides and peptidomimetics. As shown in Table 8, the differences in half-life values for the doxorubicin were somewhat attenuated in hepatocytes. In human cell cultures, phosphoramide mustard demonstrated improved stability compared to doxorubicin conjugates. It is possible that the proteases/esterases which hydrolyze the phosphoramide

mustard prodrugs in blood were not present in cultured hepatocytes at significant levels. In addition, it is not known whether all prodrugs were transported into hepatocytes with similar efficiency (although this is an unlikely scenario). Finally, all podrugs were stable in cultured mouse hepatocytes with half-life values exceeding 48 h, mirroring trends for mouse blood stability results.

In summary, we designed peptide conjugates as prodrugs targeted for PSA activation in tumor cells. Newly designed doxorubicin conjugates were cleaved by PSA at similar rates and elicited equal or improved cytotoxic profiles and tumor selectivity in prostate cancer cell lines; no additional improvements from our previously introduced phosphoramide mustard **64** could be achieved through peptide modifications. To further evaluate prodrug tumor selectivity, we conducted blood and hepatocyte stability studies. Blood and hepatocyte stability results confirmed that P5 substitutions in the peptide promoiety of L-377,202 somewhat improved prodrug resistance to non-PSA-mediated metabolism. The improvements were more apparent in human matrices as indicated by significant differences in prodrug half-life values between the known prodrug **60** and the newly synthesized prodrug **62**. Our results suggested that phosphoramide mustard prodrugs are metabolized through pathways distinct from the doxorubicin conjugates. Mouse matrices were included in all experiments because improved prodrugs could be further evaluated in mouse PK/PD studies (current prostate cancer efficacy model is the nu nu mouse). To further understand the mechanisms underlying prodrug instability in blood and hepatocytes, analysis of blood and hepatocyte metabolic profiles by LC-MS with accurate mass determination was performed.

IV. Mechanisms of Non-PSA-mediated Prodrug Metabolism

The rationale for performing time-course studies of prodrug metabolism is based on the premise that non-PSA-mediated metabolism is carried out out by other endopeptidases that target the peptidic portions of the prodrugs. As illustrated in Fig. 31, soft hydrolytic spots for non-PSA endopeptidases include the peptide promoiety for all prodrugs and the di-peptide linker for the doxorubicin conjugates. Despite the anticipated resistance of their aminobenzyl alcohol linker to endopeptidase action, phoshphoramide mustard prodrugs may be susceptible to hydrolysis by phopsphoamidases which are typically elevated in tumors. Once prodrugs are hydrolyzed by endopeptidases other than PSA, they become more vulnerable to degradation by aminopeptidases and carboxypeptidases.

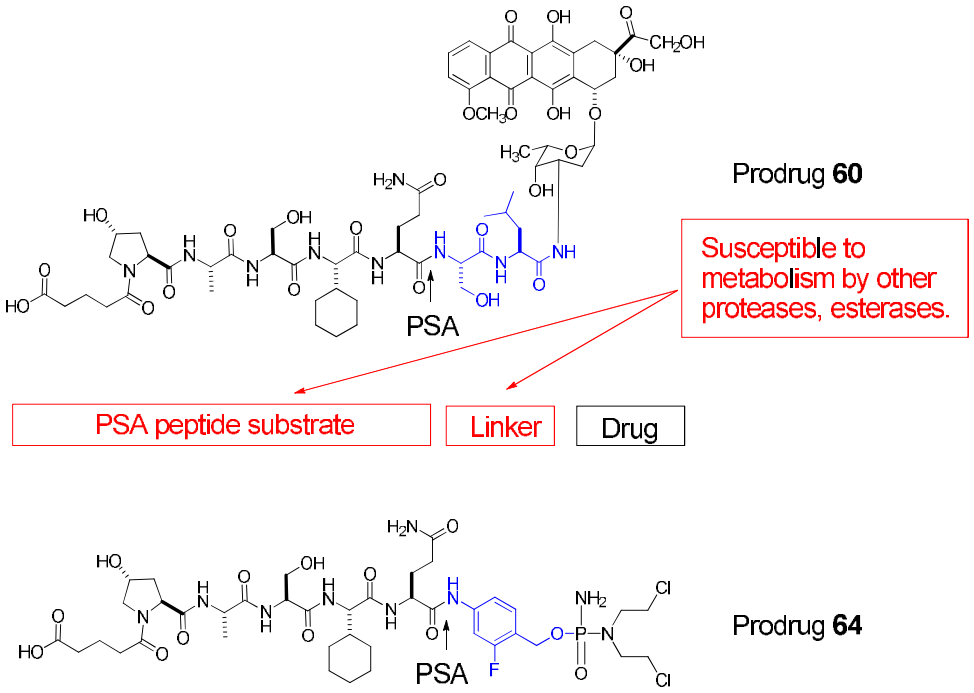

Figure 31. Non-PSA-mediated Hydrolytic Mechanisms of Peptide Prodrugs

In order to identify the early steps in non-PSA-mediated peptide hydrolysis, prodrugs were incubated in blood and cultured hepatocytes, and prodrug-related fragments resolved and characterized by LC-MS with accurate mass determination. In addition, we leveraged the unique UV-VIS spectrum of doxorubicin to identify peptide fragments. Doxorubicin and its peptide conjugates showed a maximal aborbance at 484 nm and could therefore be readily detected in a complex matrix such as blood. Phosphosphoramide mustard conjugates were mainly identified by accurate mass resolution using their extracted ion chromatogram (XIC) due to significant matrix interferences from biological matrices.

Following a 1-h incubation of doxorubicin prodrugs in human blood and hepatocytes, a key fragment, **M1** with measured accurate mass 657.2657 was detected in all blood and and cultured hepatocytes samples (Fig. 32 and 33, Table 9). M1 was unambiguously identified to be Leu-Dox suggesting that the first step in prodrug hydrolysis was cleavage of the Ser-Leu linker. Prolonged prodrug exposure to blood (24 h) and hepatocyte cultures (48 h) led to increased levels of **M1**, which was slowly converted to doxorubicin (Fig. 34 and 35) (accurate mass: 544.1815). While additional minor metabolites could be detected by accurate mass spectral analysis (Table 9), blood and hepatocyte metabolic profiles clearly indicated that **M1** or Leu-Dox was the earliest and major metabolite originating from the hydrolysis of prodrugs **60**-**62**.

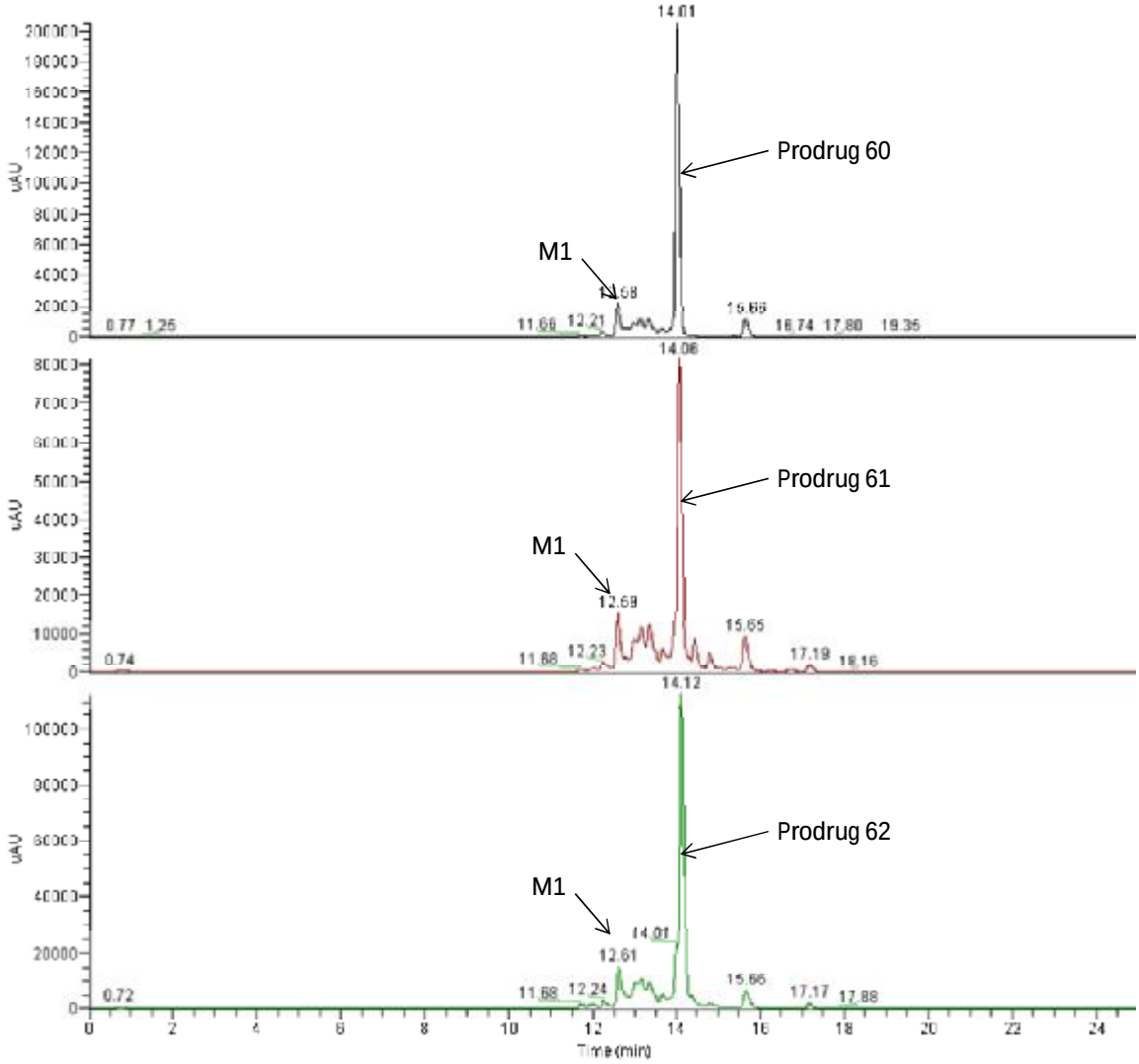

Figure 32. Metabolic Profiles of Prodrugs **60-62** in Human Blood at 1 h

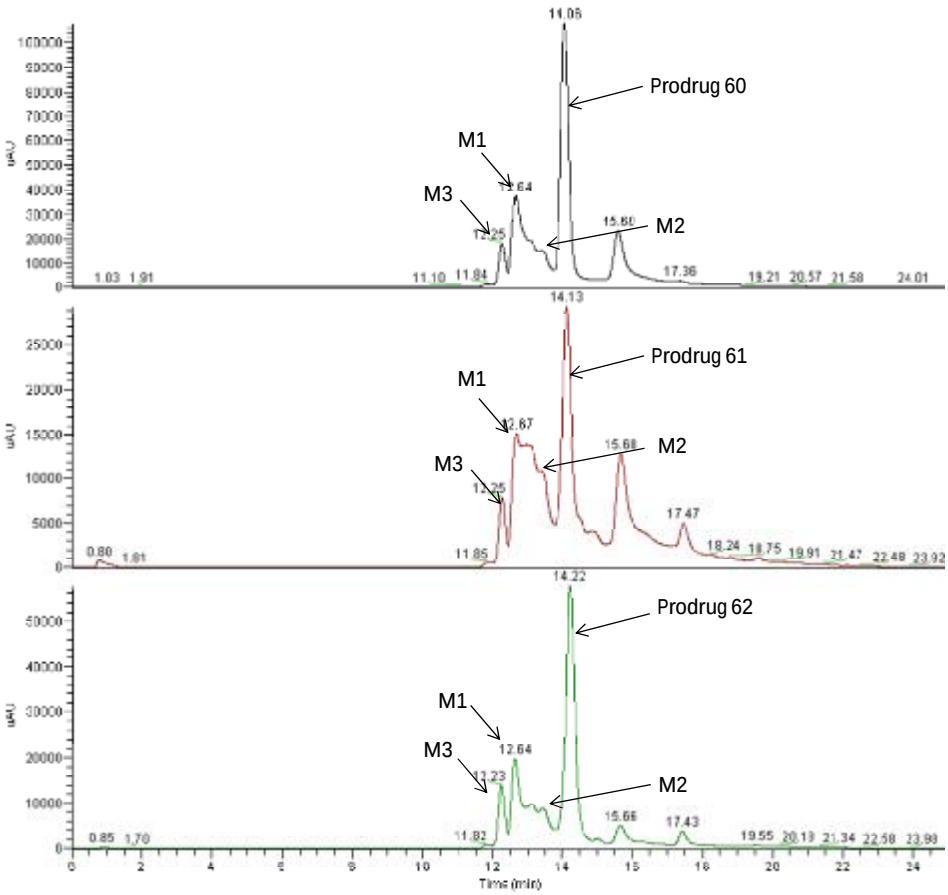

Figure 33. Metabolic Profiles of Prodrugs **60-62** in Human Blood at 8 h

Table 9. Metabolites of Doxorubicin Prodrugs **60-62**

Metabolite (theoretical mass)	**M1 (657.2659)**	**M2 (1011.4563)**	**M3 (544.1819)**
(Base peak, retention time)	**[a]Measured mass of base peak, retention time (amu, min)**		
60 (1396.6071, 14.1)	657.2657, 12.5	1011.4570, 13.5	544.1815, 12.2
61 (1370.5920, 14.2)	657.2657, 12.5	1011.4570, 13.5	544.1815, 12.2
62 (1340.5817, 14.2)	657.2657, 12.5	1011.4570, 13.5	544.1815, 12.2

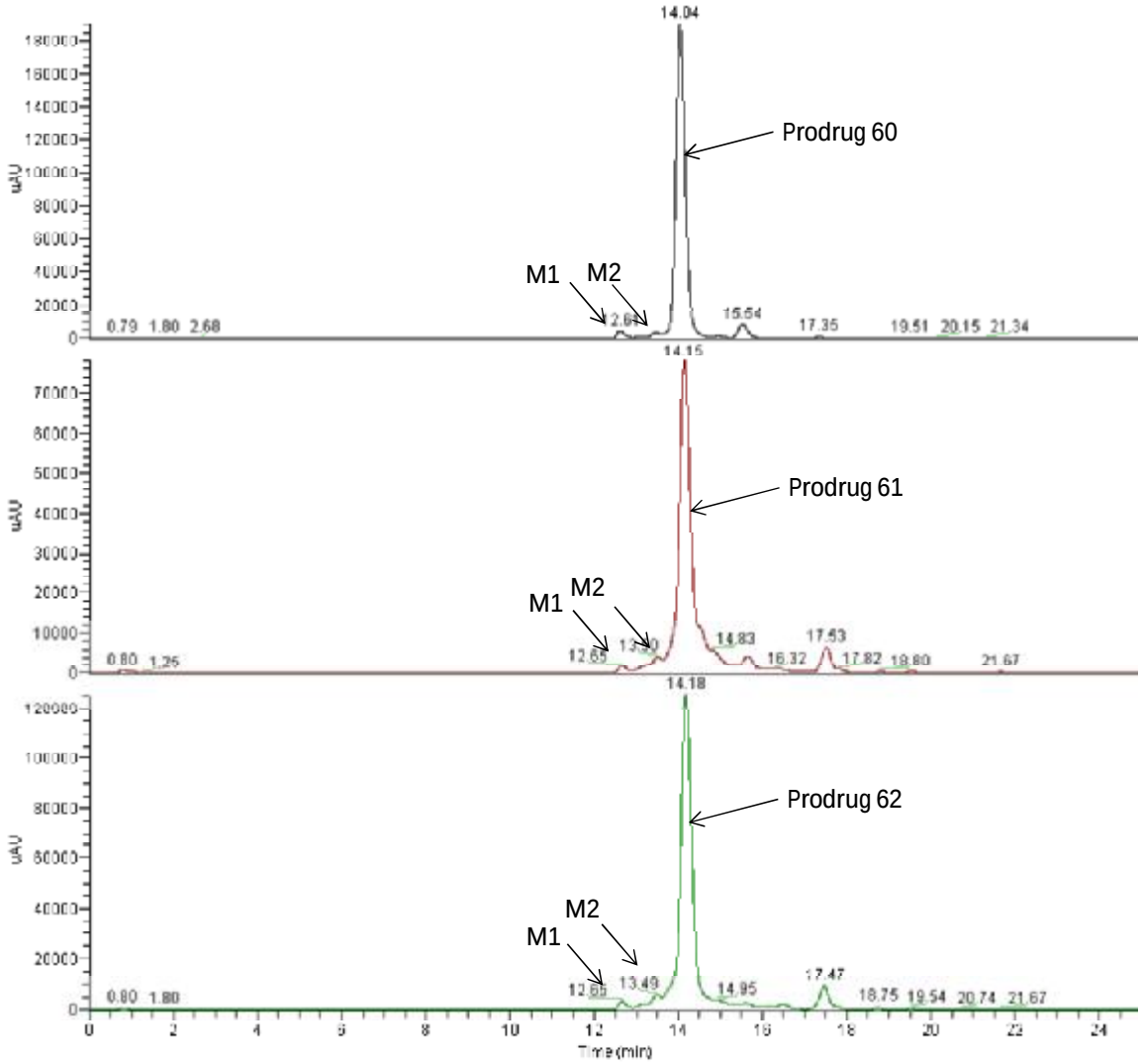

Figure 34. Metabolic Profiles of Prodrugs **60-62** in Cultured Human Hepatocytes at 1 h

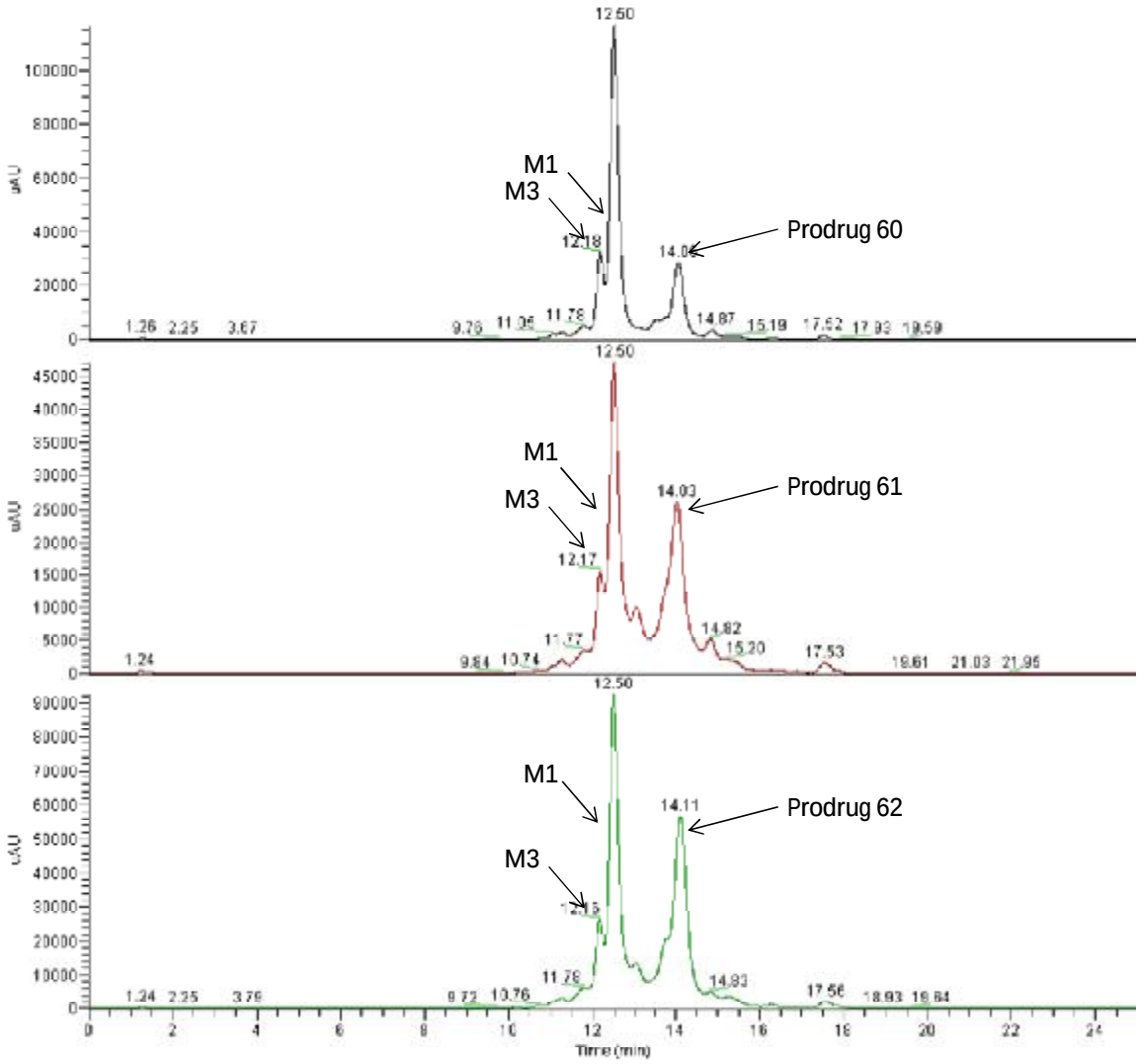

Figure 35. Metabolic Profiles of Prodrugs **60-62** in Cultured Human Hepatocytes at 48 h

Similar metabolic profiles were obtained in mouse blood and hepatocytes; however, as suggested by earlier stability studies, lower levels of **M1** were produced in mouse blood (Fig. 36 and 37) and hepatocytes (Fig. 38 and 39). Since there were differences in sample processing procedures between the stability and metabolic profiling samples, parent prodrug and metabolite recovery may not be comparable. Nevertheless, the general trends

in our stability and metabolic profiling results indicated that human and mouse blood and hepatocytes produced structurally similar metabolites.

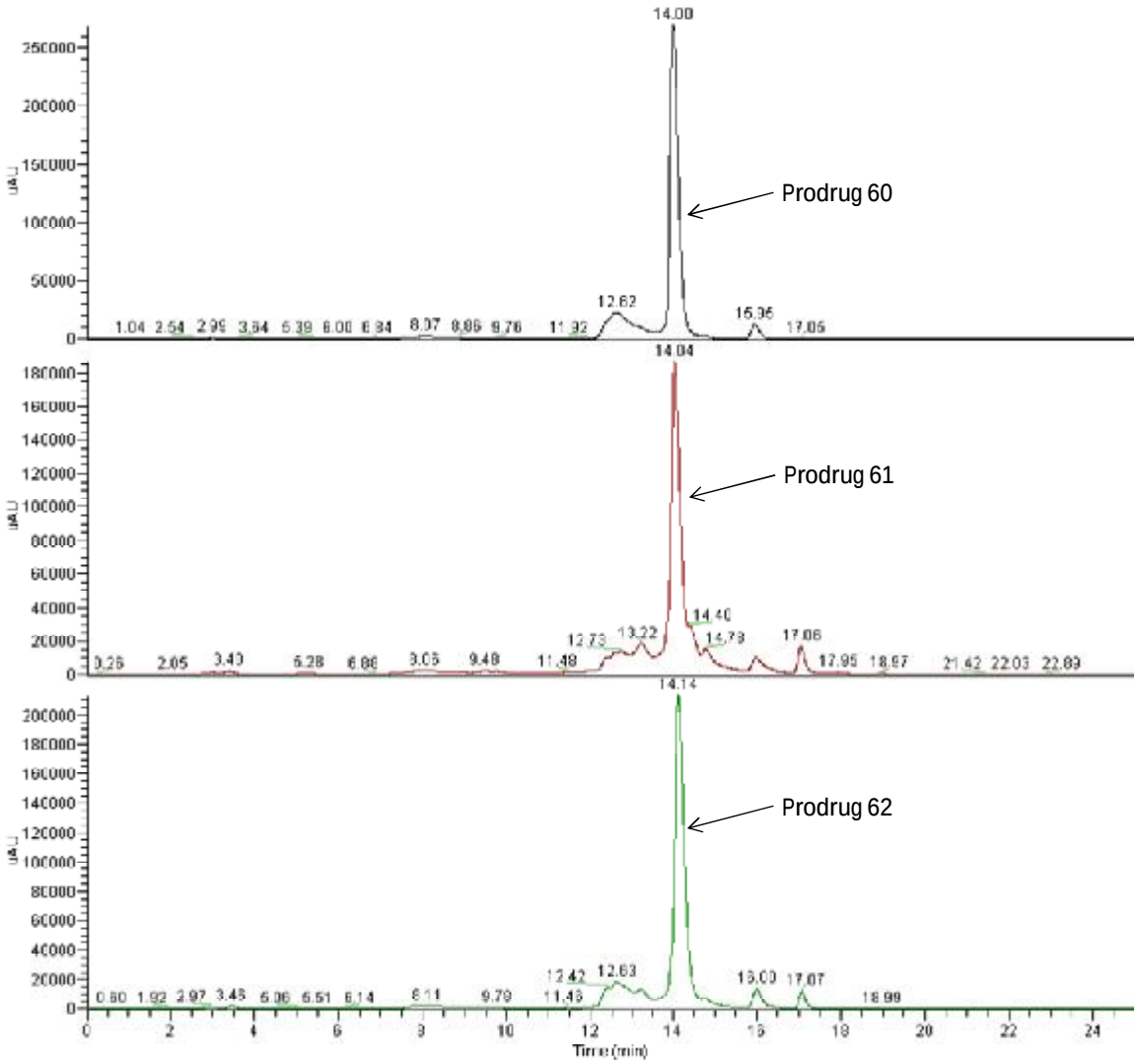

Figure 36. Metabolic Profiles of Prodrugs **60-62** in Mouse Blood at 1 h

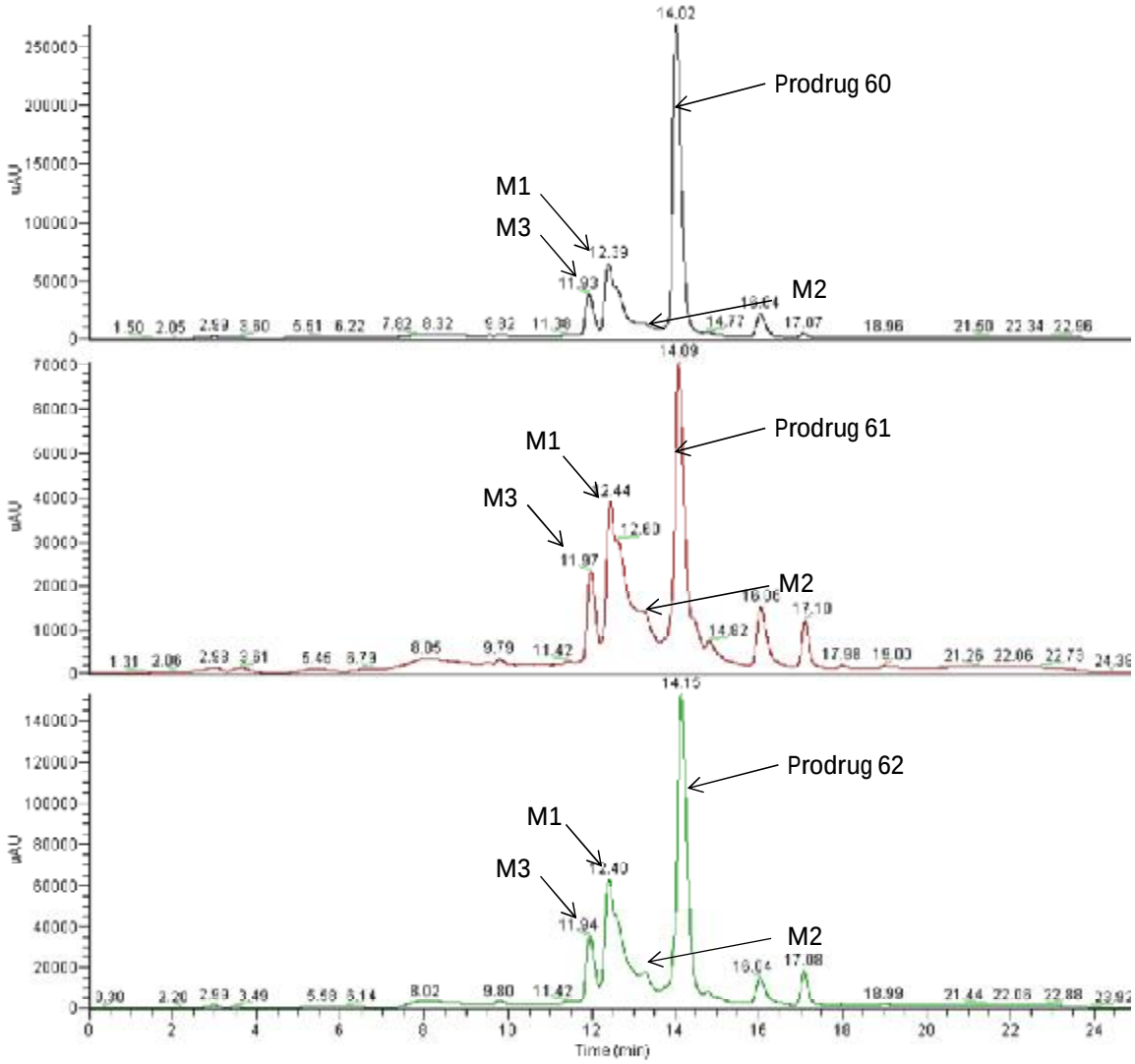

Figure 37. Metabolic Profiles of Prodrugs **60-62** in Mouse Blood at 8 h

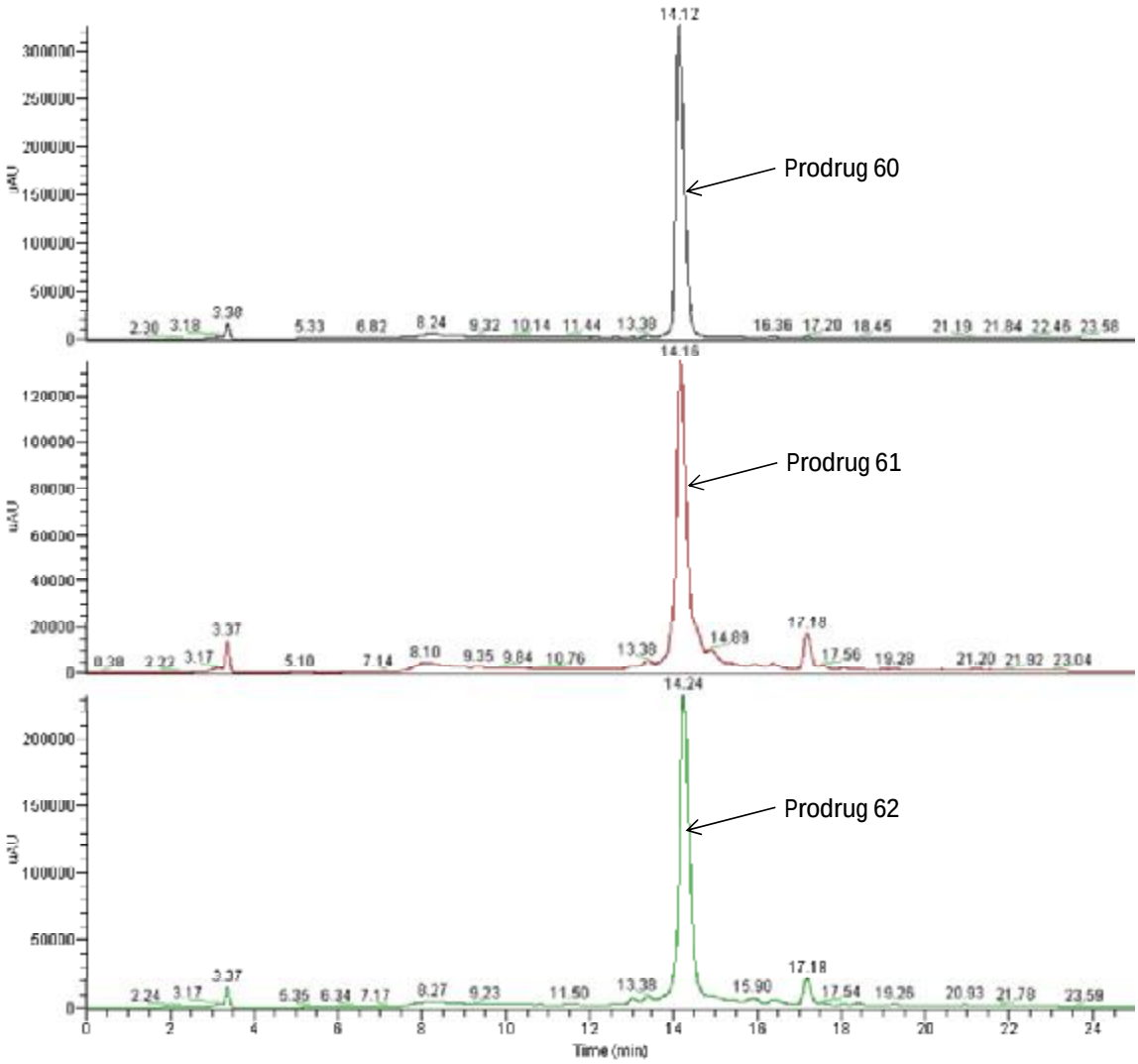

Figure 38. Metabolic Profiles of Prodrugs **60-62** in Cultured Mouse Hepatocytes at 1 h

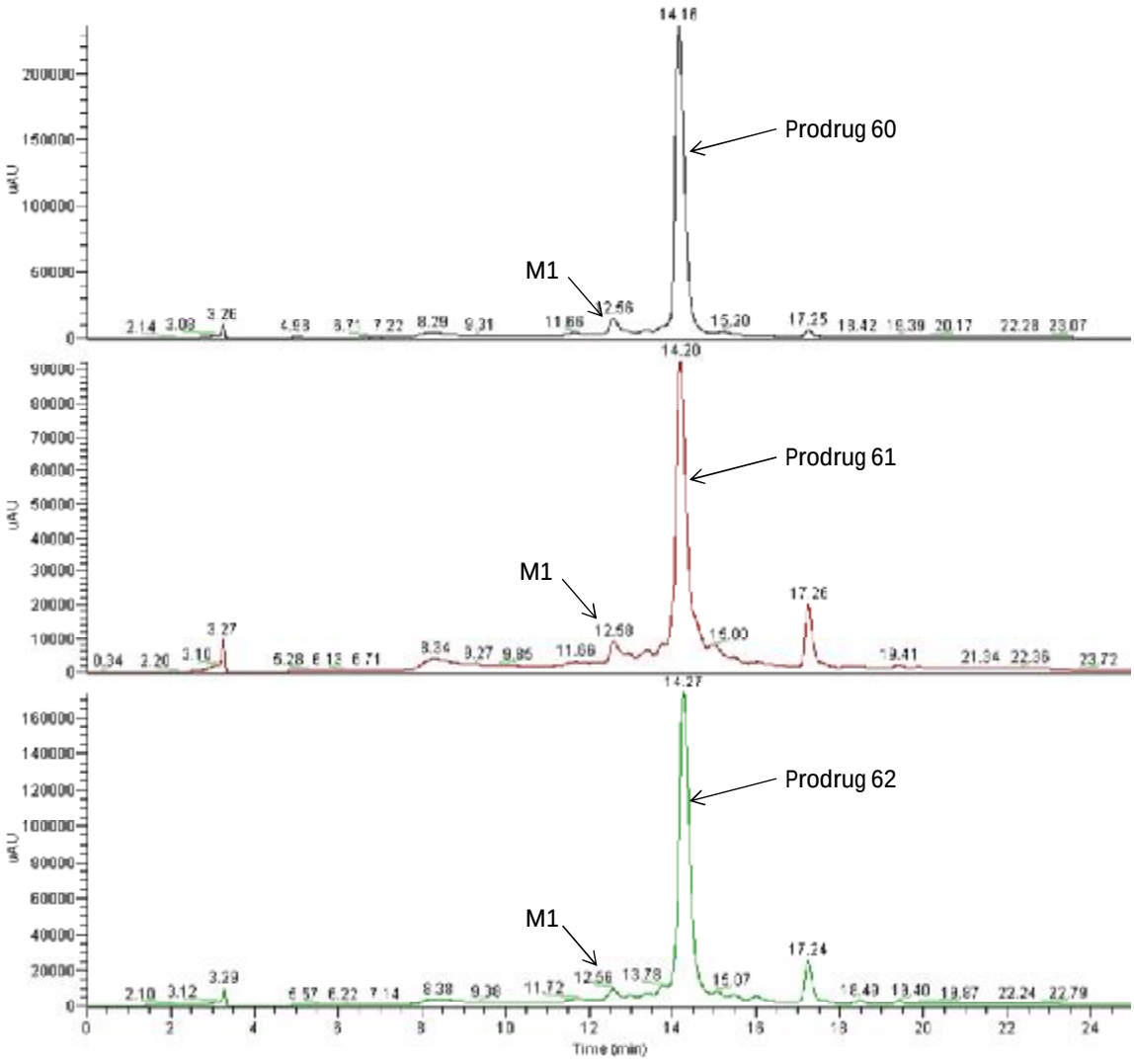

Figure 39. Metabolic Profiles of Prodrugs **60-62** in Cultured Mouse Hepatocytes at 48 h

Incubation of phosphoramide mustard prodrugs in human blood and hepatocyte cultures revealed the earliest degradants to be **M4a**, **M4b** and **M4c**, also observed in Tris buffer incubations after 48 h (~30% formed) as previously discussed. Consequently, we concluded that **M4a**, **M4b** and **M4c** were not due to blood or hepatocyte enzymatic activity. It is possible however that the spontaneous chemical degradation observed in

Tris buffer was accelerated in cultured human and mouse hepatocytes thereby generating **M4a**, **M4b** and **M4c**, which could be further converted to metabolites **M5a**, **M5b** and **M5c** by enzymatic intervention as indicated by the results in Table 10 and Fig. 40-45; blood sample analysis was not possible due to matrix interferences. Thus, the major metabolic liability of phosphoramide mustard appeared to be intimately linked to their spontaneous degradation to the corresponding 2-fluoro-4-peptidylaminobenzyl alcohol conjugates which were futher acted upon by phosphoramidases.

Table 10. Metabolites of Phosphoramide Mustard Prodrugs

Metabolite (theoretical mass)	**M4a (873.3559)**	**M4b (847.3403)**	**M4c (817.3297)**	**M5a (794.3736)**	**M5b (768.3580)**	**M5c (738.3474)**
(Base peak, retention time)	**Measured mass of base peak, retention time (amu, min)**					
64 (996.3577, 14.1)	873.3553, 12.1	-	-	794.3732, 12.9	-	-
65 (970.3417, 14.1)	-	847.3407, 12.2	-	-	768.3569, 12.9	-
66 (940.3311, 14.2)	-	-	817.3303, 11.5	-	-	738.3478, 12.5

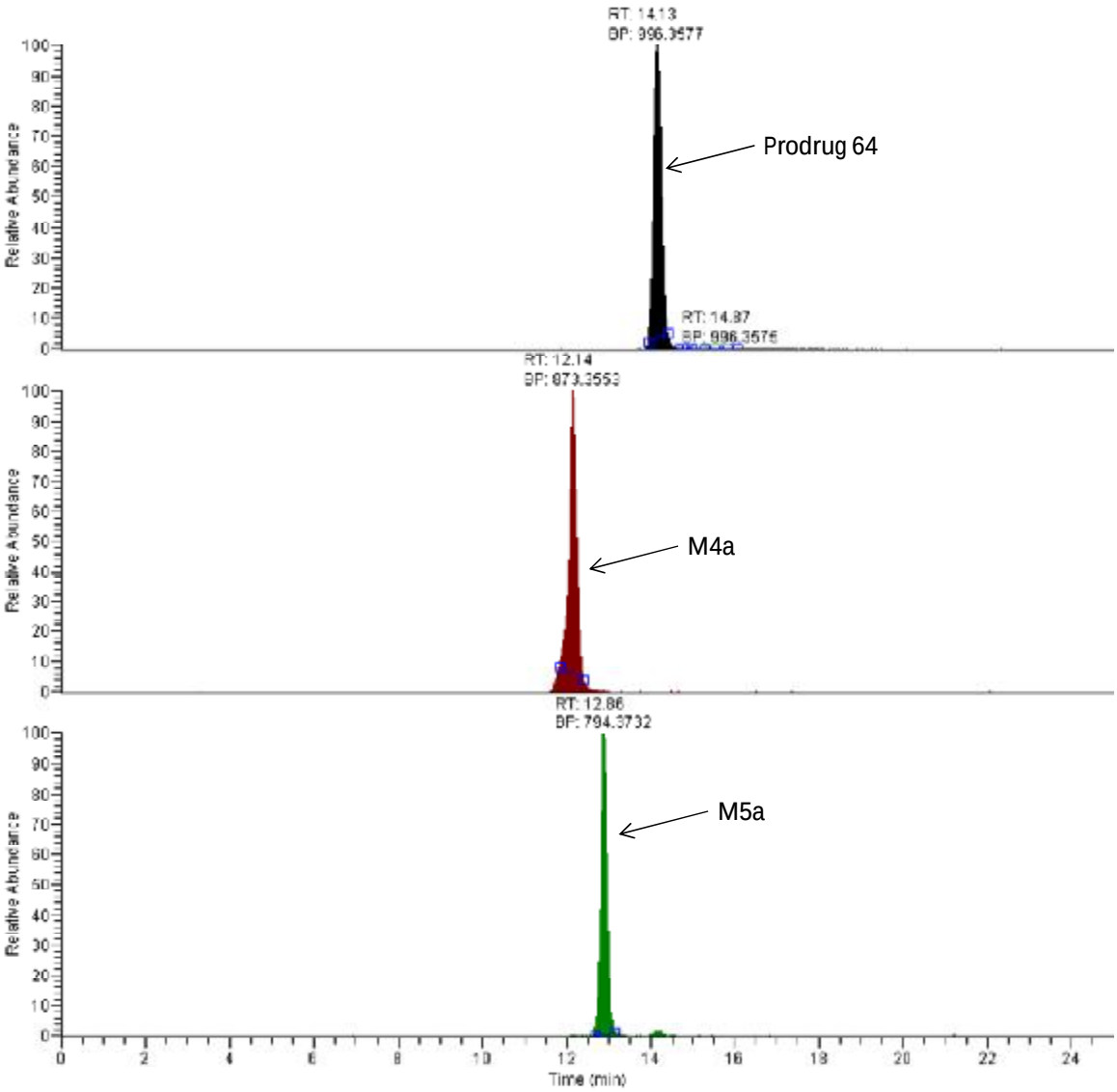

Figure 40. Metabolic Profile (XIC) of Prodrug **64** in Cultured Human Hepatocytes at 1 h

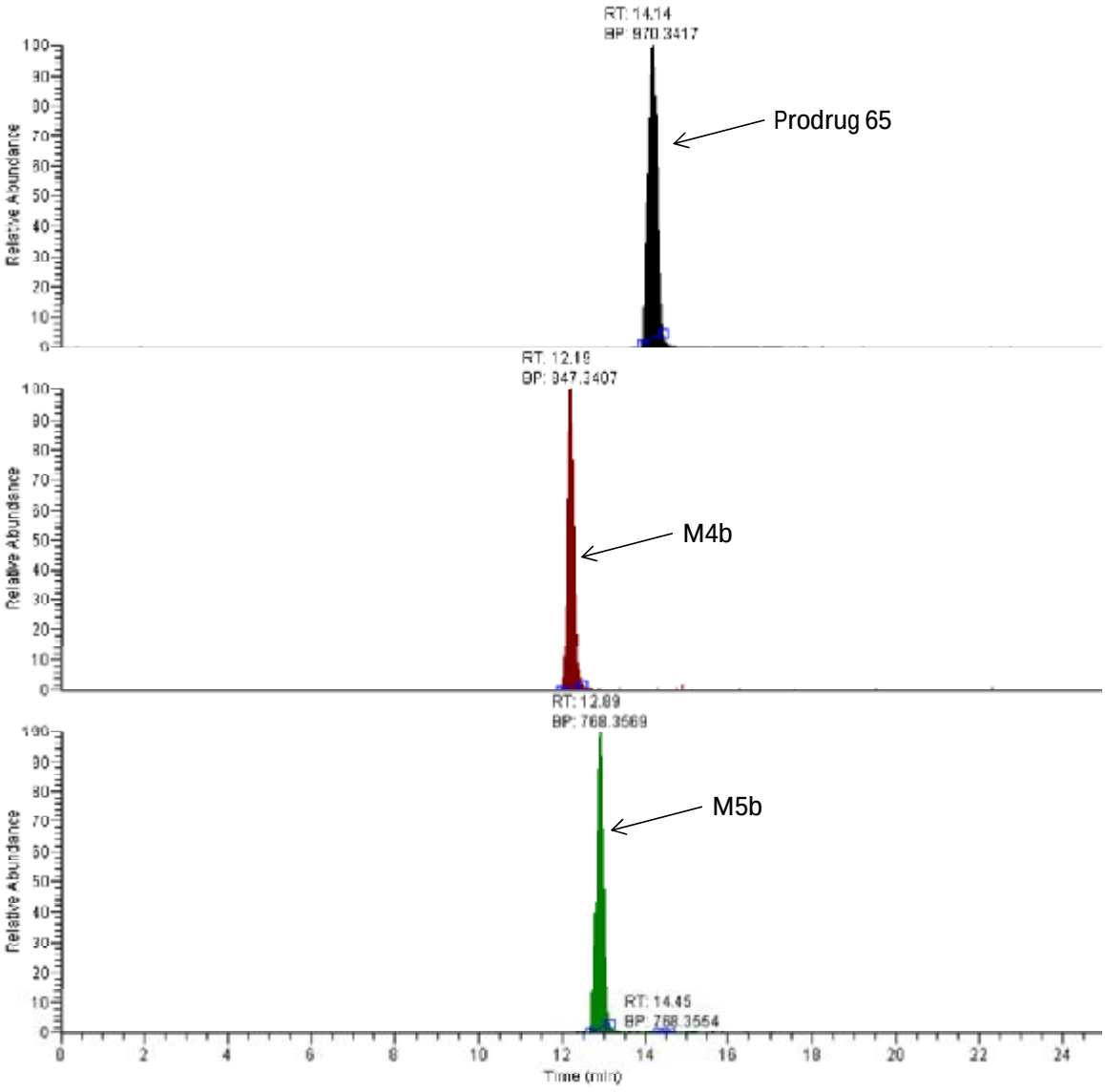

Figure 41. Metabolic Profile (XIC) of Prodrug **65** in Cultured Human Hepatocytes at 1 h

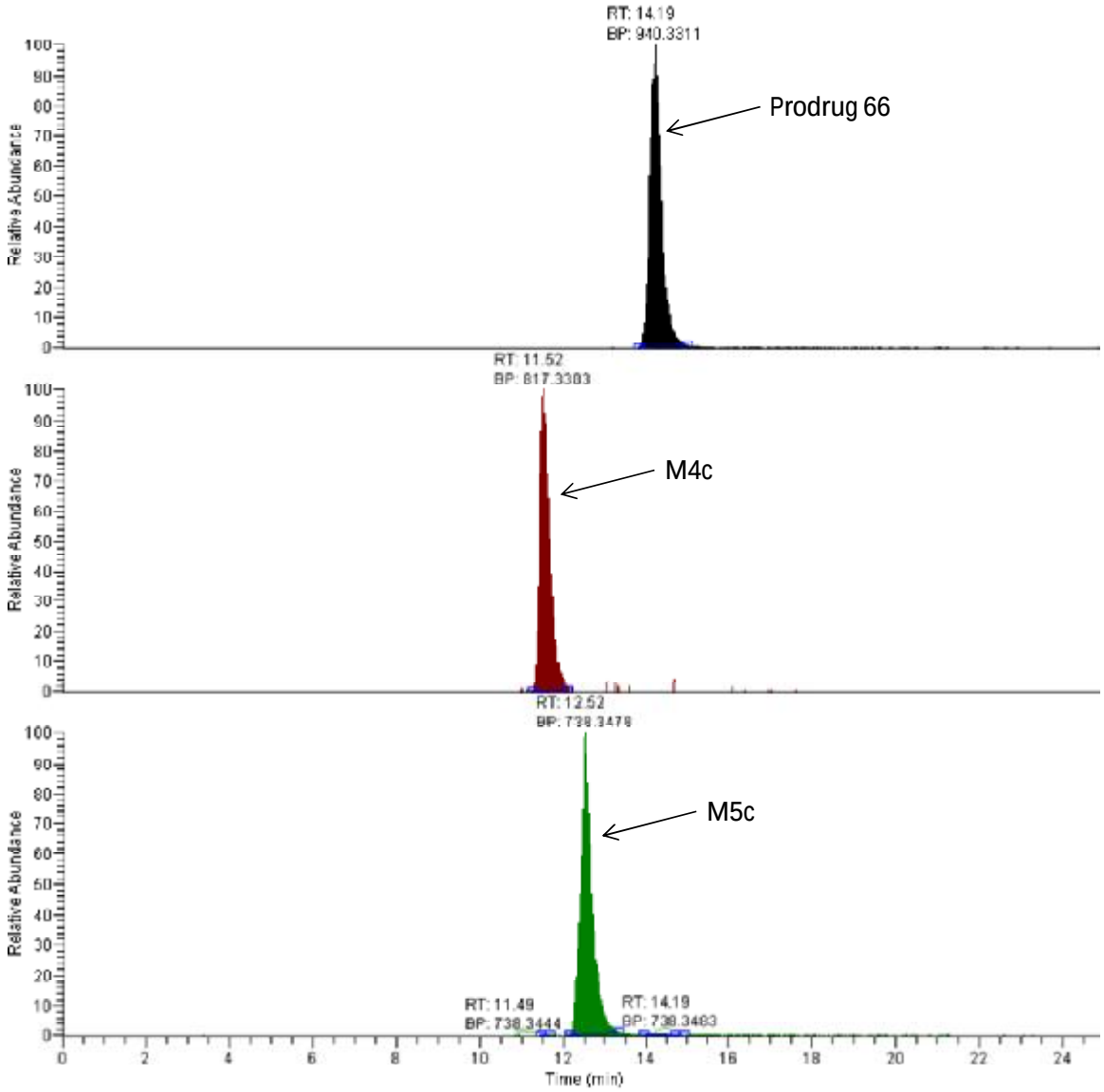

Figure 42. Metabolic Profile (XIC) of Prodrug **66** in Cultured Human Hepatocytes at 1 h

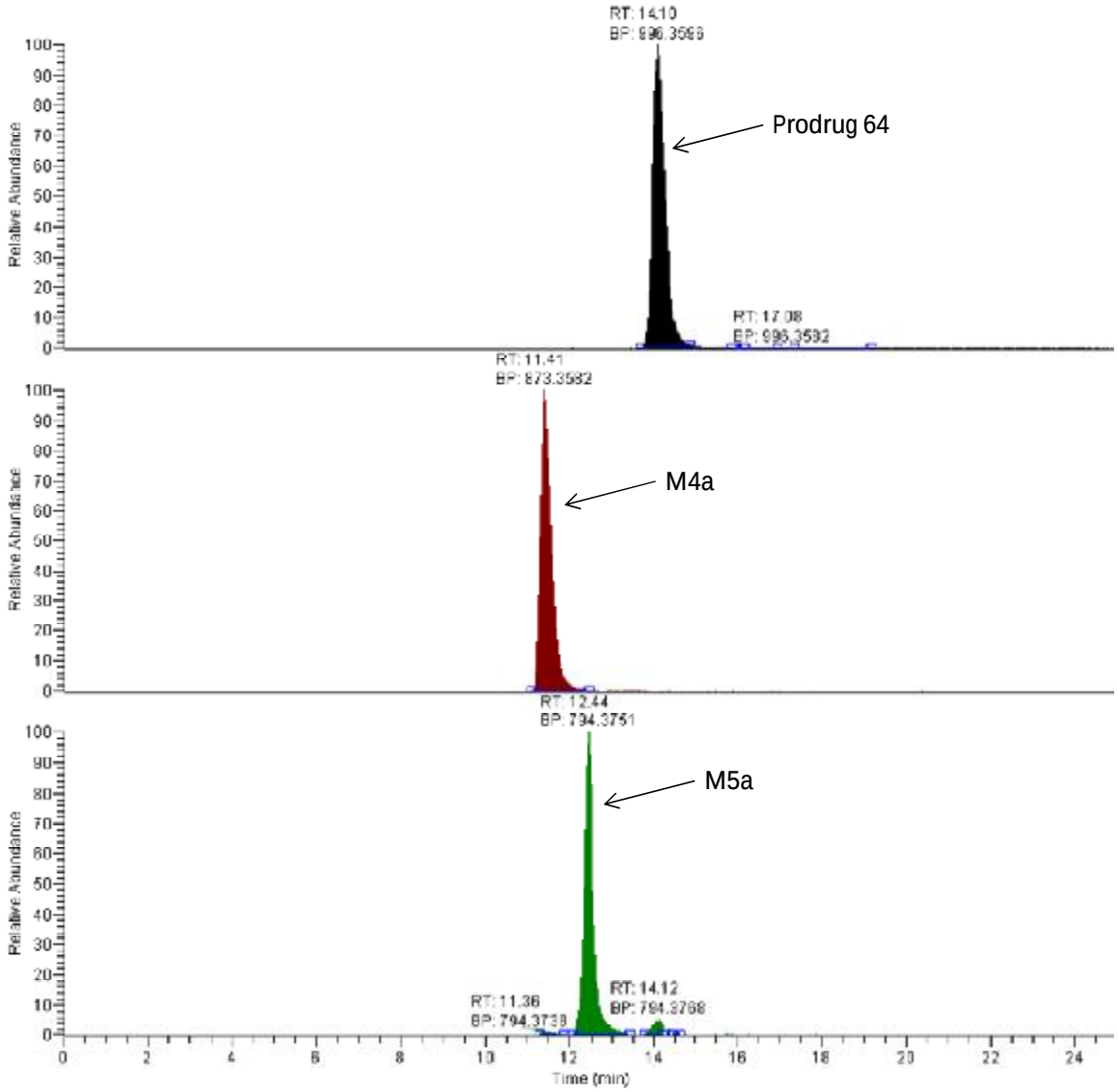

Figure 43. Metabolic Profile (XIC) of Prodrug **64** in Cultured Mouse Hepatocytes at 1 h

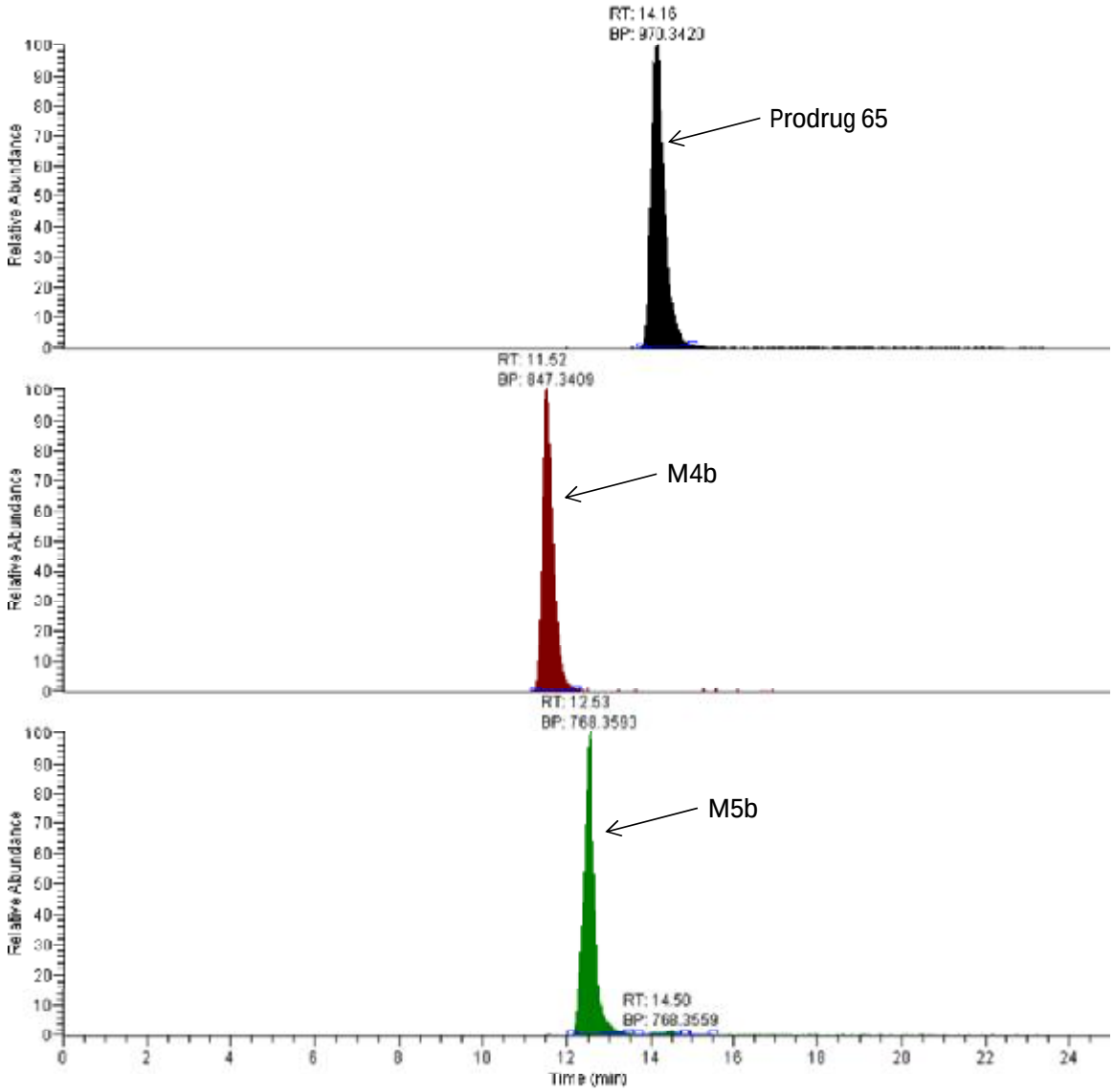

Figure 44. Metabolic Profile (XIC) of Prodrug **65** in Cultured Mouse Hepatocytes at 1 h

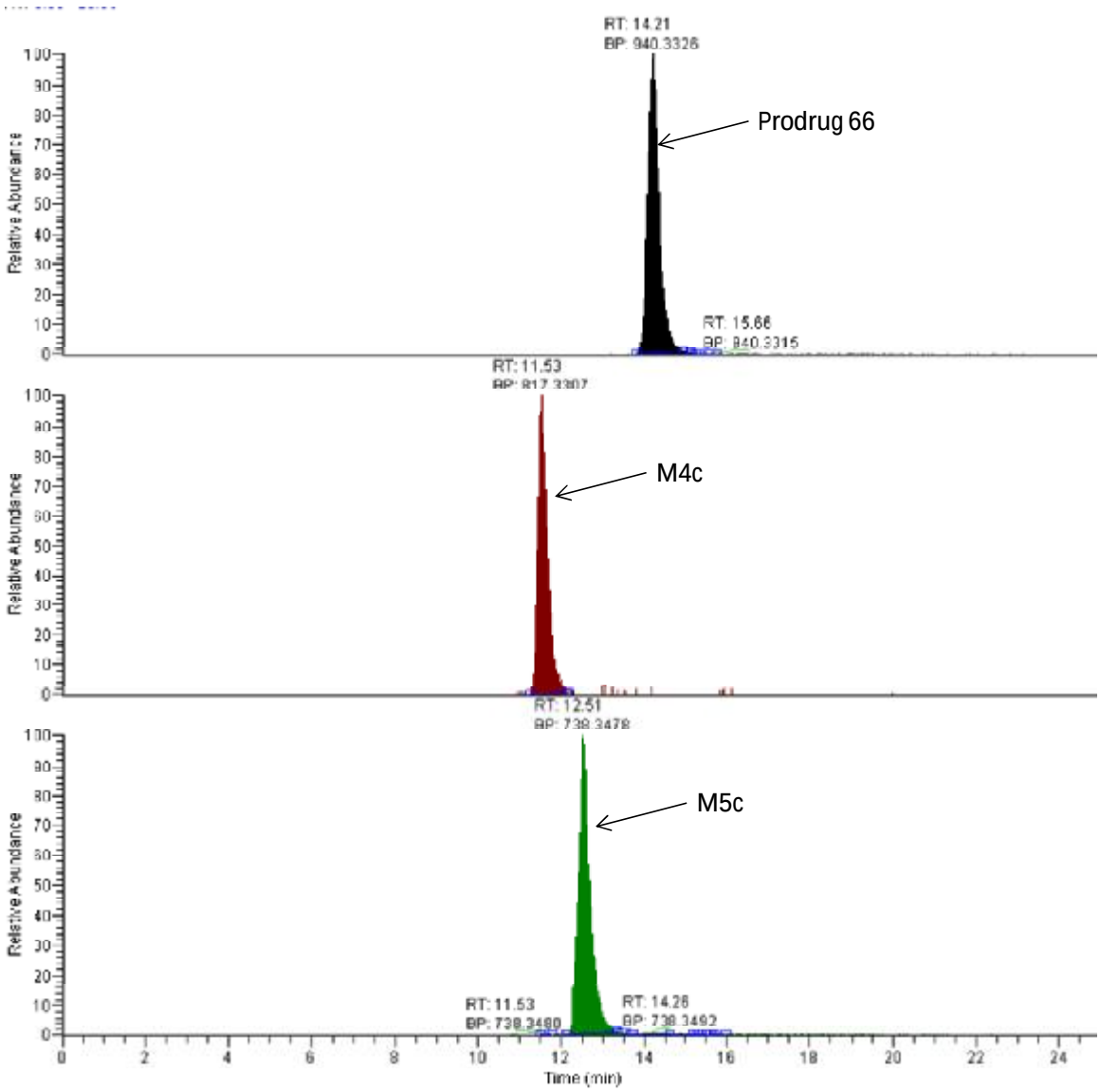

Figure 45. Metabolic Profile (XIC) of Prodrug **66** in Cultured Mouse Hepatocytes at 1 h

In retrospect, the unexpectedly low cytotoxic responses of prodrugs **65** and **66** could not be explained by their spontaneous chemical degradation to metabolites **M4a**, **M4b** and **M4c** since prodrug **64** was effective against LNCaP cells within the same assay. In fact, because phosphoramidase levels are generally increased in the cytosol and subcellular

membranes of tumor cells, it would be reasonable to anticipate enhanced released of nitrogen mustard from prodrugs **64-66** once transported into cells.

V. Identification of Protease(s) Responsible for Doxorubicin Prodrug Instability

The metabolites generated in blood and hepatocyte profiling studies (Fig. 35 and 37) together with the current knowledge on protease cleavage maps indicated that the protease involved in the hydrolysis of the Ser-Leu linker of prodrugs **60-62** would share the same substrate specificity as thermolysin (EC 3.4.24.27), a zinc metalloprotease produced by the genus *Bacillus thermoproteolyticus*. Because chymotrypsin hydrolysis has largely been mitigated in the sequence of prodrug **60** by replacing Phe with Chg,[139] it was quickly eliminated as a possibility.

A. Doxorubicin Prodrug Metabolism by Thermolysin

Thus, we set out to study the time-dependent metabolism of prodrug **60** by thermolysin. Incubation of prodrug **60** (100 μM) with purified thermoylsin (300 μg/ml) indeed generated significant levels of metabolite **M1** within 20 min (Fig. 46) suggesting that thermolysin hydolyzed the Ser-Leu of prodrug **60** as observed in blood and hepatocyte profiling studies. Prolonged exposure to thermolysin led to complete conversion of prodrugs **60** to metabolite **M1** within 60 min (Fig. 45).

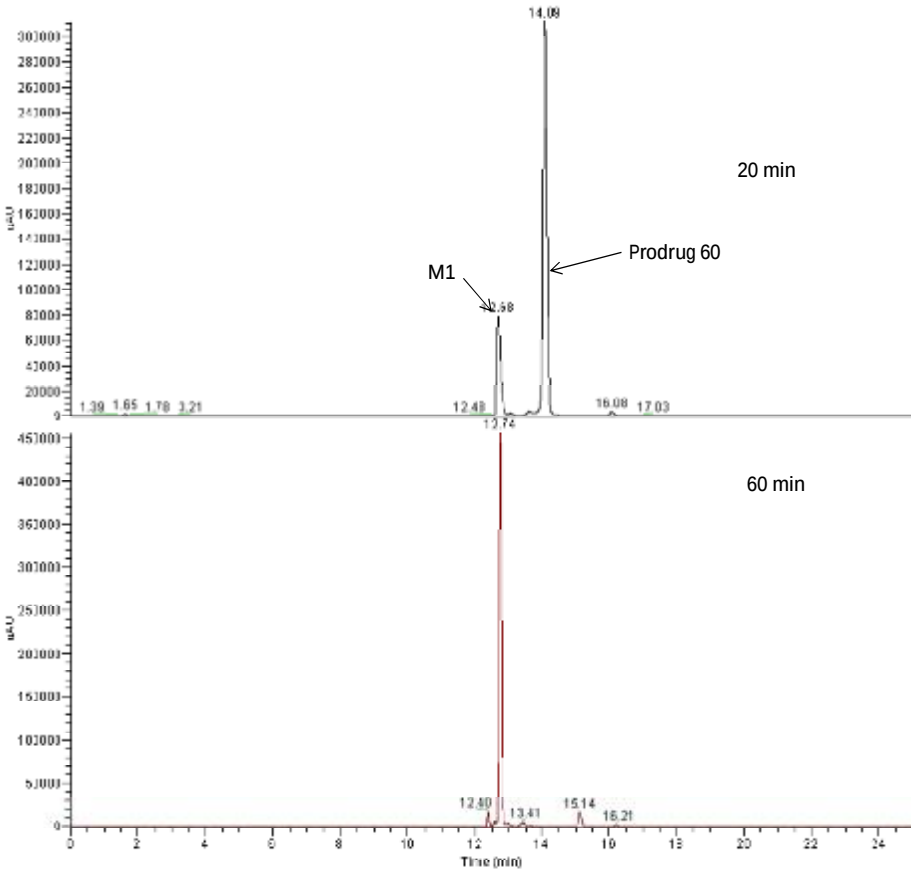

Figure 46. Time-dependent Hydrolysis of Prodrugs **60** by Thermolysin

A literature search on mammalian proteases with susbtrate specificity similar to that of thermolysin indicated that the membrane surface zinc metalloprotease neprylsin (EC 3.4.24.11) may be involved in the hydrolysis of prodrugs **60**-**62**. Using various substrates and inhibitors, several studies have shown that thermolysin and neprylisin, despite their weak homology, share similar C-terminal fragments and substrate specificity (Fig. 47).[208-212] Neprilysin also known as CD10 or common acute lymphoblastic leukemia antigen (CALLA) is used a clinical marker for several hemataologic disorders including angioimmunoblastic T cell lymphoma, hairy cell leukemia and Burkitt lymphoma.

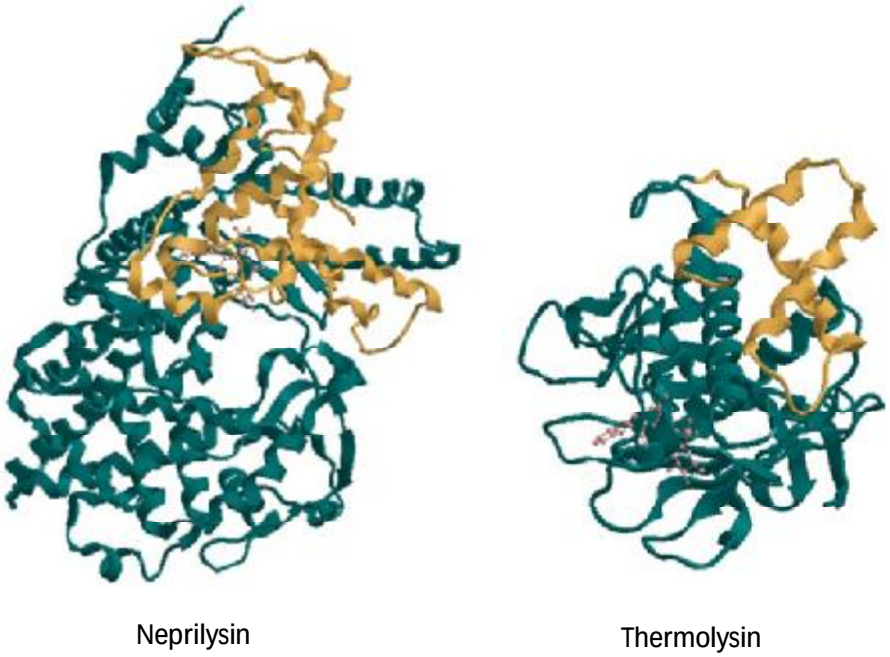

Figure 47. Crystal Structures of Neprilysin and Thermolysin Complexes With the Inhibitor Phosphoramidon (purple color).[212-214] The thermolysin-like C-terminal catalytic domain (brown color) of neprilysin is compared to thermolysin.

As part of its physiological function in modulating hypertensive effects, it converts big endothelin-1 (big ET-1) by proteolysis.[208, 209] Neprilysin also hydrolyzes various small endogenous peptides such as the β-amyloid peptide implicated in the initiation and progression of Alzheimer's disease. The involvement of neprilysin in the regulation of signaling peptides as enkephalins, endothelin, substance P and atrial natriuretic factor has also been demonstrated by designing speficic inhibitors that inactivates its function.[213, 215] The highest concentrations of neprilysin are found on the apical (luminal) membrane of kidney and lung cell, but the enzyme may also be induced in certain types of tumors.[216, 217]

B. Doxorubicin Prodrug Metabolism by Neprilysin

To determine whether prodrugs **60-63** are substrates for neprilysin, incubations with purified human neprilysin (50 μg/mL) were carried out. As shown in Fig. 48, prodrugs **60-62** were converted to significant levels of Leu-Dox (**M1**) and trace amounts of **M2** in 30 min. Prolonged incubation led to increased levels of **M1** and modest formation of **M2**, suggesting that the major hydrolytic step was cleavage of the Ser-Leu linker (Fig. 49). While we did not evaluate the possible conversion of **M2** to **M1**, this scenario was unlikekly since the intervention of additional proteases was required. Moreover, **M1** or **M2** was not detected in 4- and 48-h buffer incubations further confirming the formation of **M1** and **M2** was catalyzed by human neprilysin. These results were in agreement with our findings from blood and cultured hepatocytes which indicated that the key metabolytic step in the degradation of prodrugs **60-62** was the hydrolysis of their shared Ser-Leu linker. The lack of robust hydrolysis in mouse samples may be explained by substrate specificity differences between mouse and human neprilysin although the topography of neprilysin in non-lymphoid organs such as liver and lungs were found to be strikingly similar between mouse and humans.[218] The instability of prodrugs **60-62** could not be effectively predicted with their corresponding AMC-conjugates (Fig. 21 and 22) which were more effectively hydrolyzed in mouse rather than human plasma. Nevertheless, such preliminary experiments guided our choice of optimal PSA substrates to be further developed as promoieties. The exclusive localization of neprilysin on the luminal membrane[217] of hepatocytes may help further explain the slower formation of **M1** in cultured hepatocytes compared to blood since the prodrug must first be transported into cells before being cleaved by neprilysin. This implies potential cytotoxicity of **M1** to

hepatocytes; however, as discussed earlier, little is known about mechanisms involved with the active transport of doxorubicin (**M3**) and **M1**.

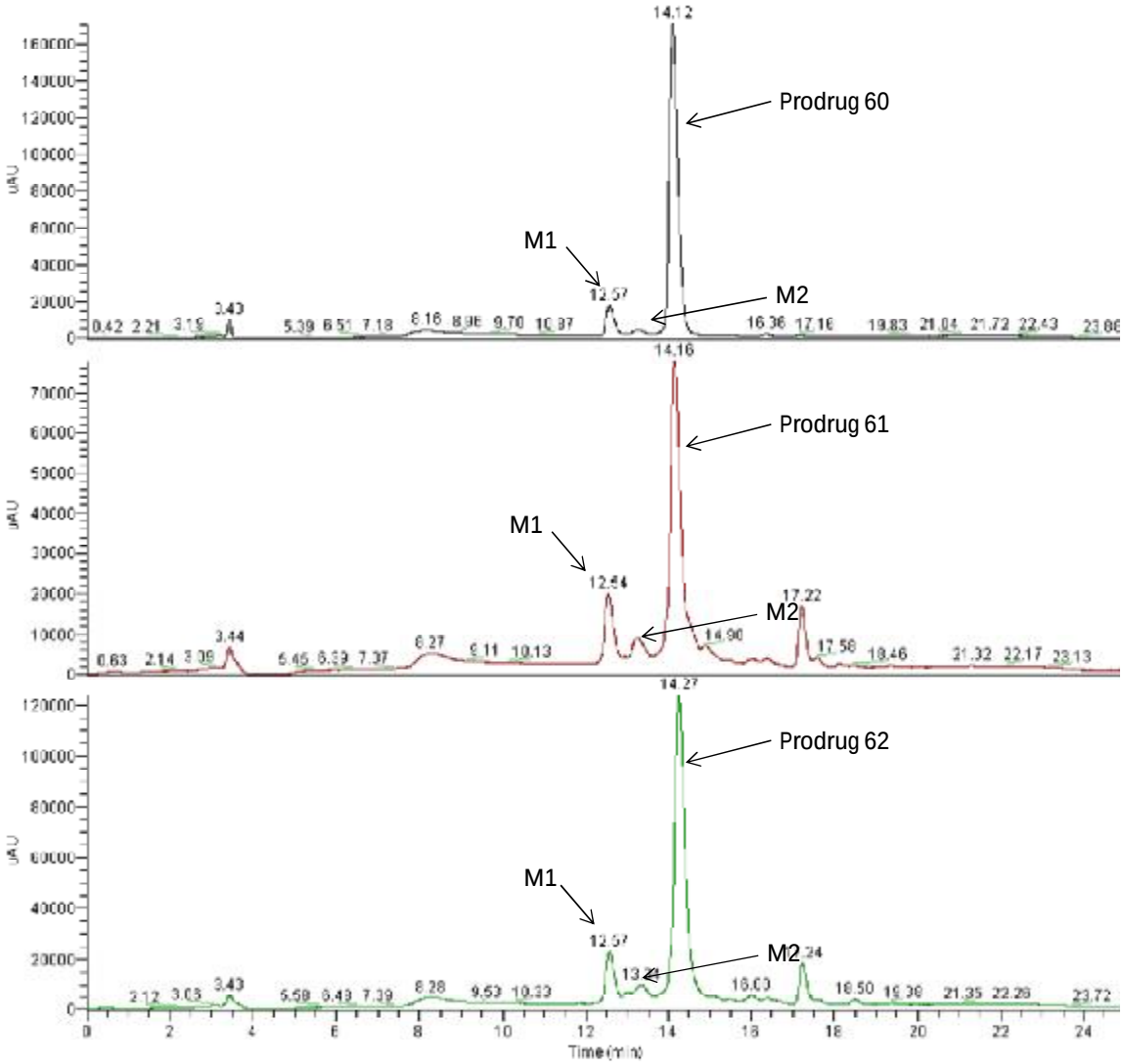

Figure 48. Hydrolysis of Prodrugs **60-62** by Neprilysin in 30 min

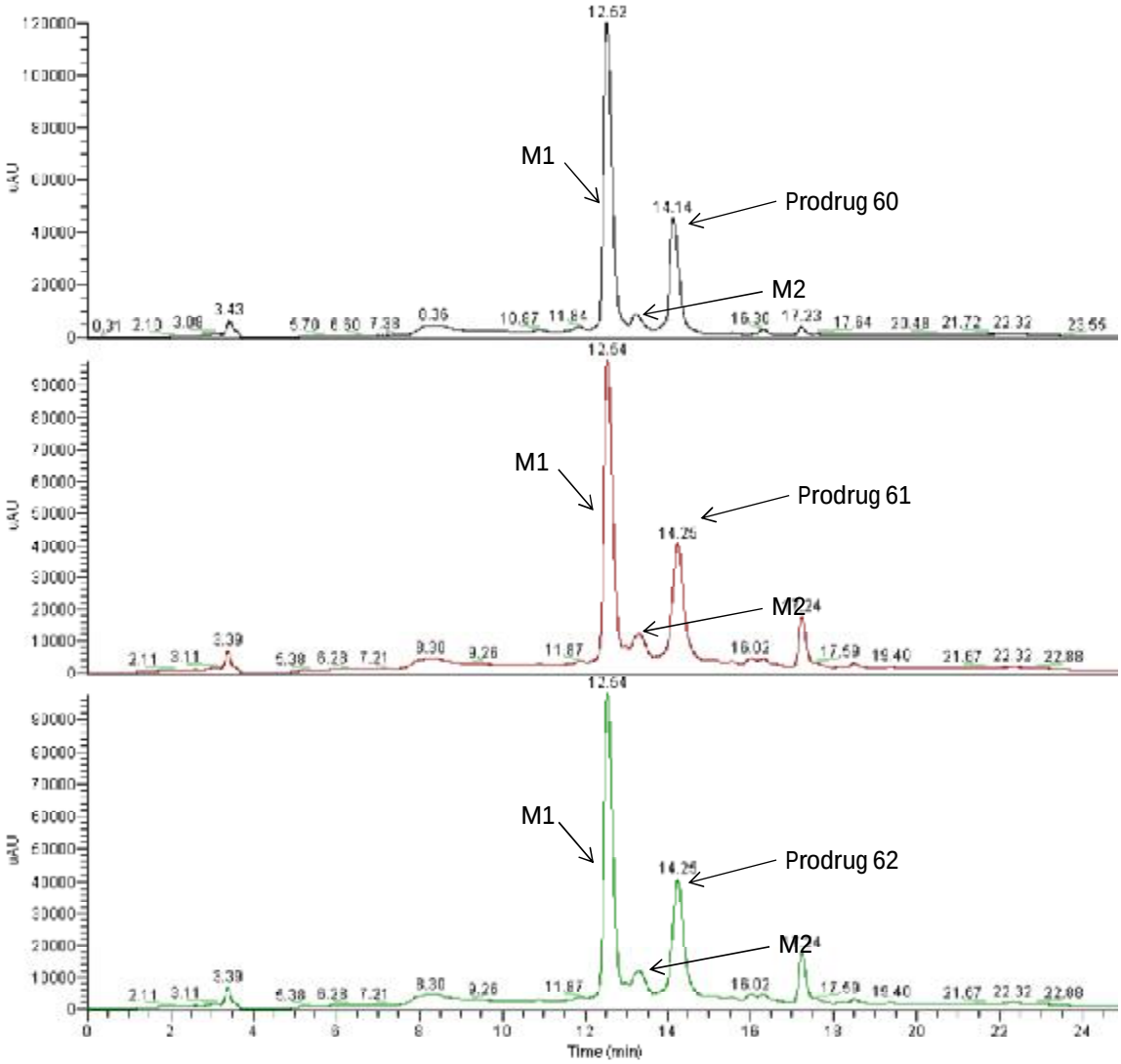

Figure 49. Hydrolysis of Prodrugs **60-62** by Neprilysin in 4 h

As expected, prodrug **63** effectively resisted proteolytic cleavage by human neprilysin over a 4-h incubation period thereby suggesting that the insertion of a 3-aminoxypropionate linker between the peptide promoiety and doxorubicin may have improved the stability of prodrug **63** to non-PSA metabolism despite the insignificant conversion of prodrug **63** (less than 10%) to doxorubicin in Tris buffer (Fig. 50). In order

to further evaluate the tumor specificity of prodrug **63** and its stability in normal or non-PSA-producing tissues, metabolism and stability studies in blood and cultured hepatocytes could be conducted. Fig. 51 summarizes the metabolism of doxorubicin (**60-63**) and phosphoramide (**64-66**).

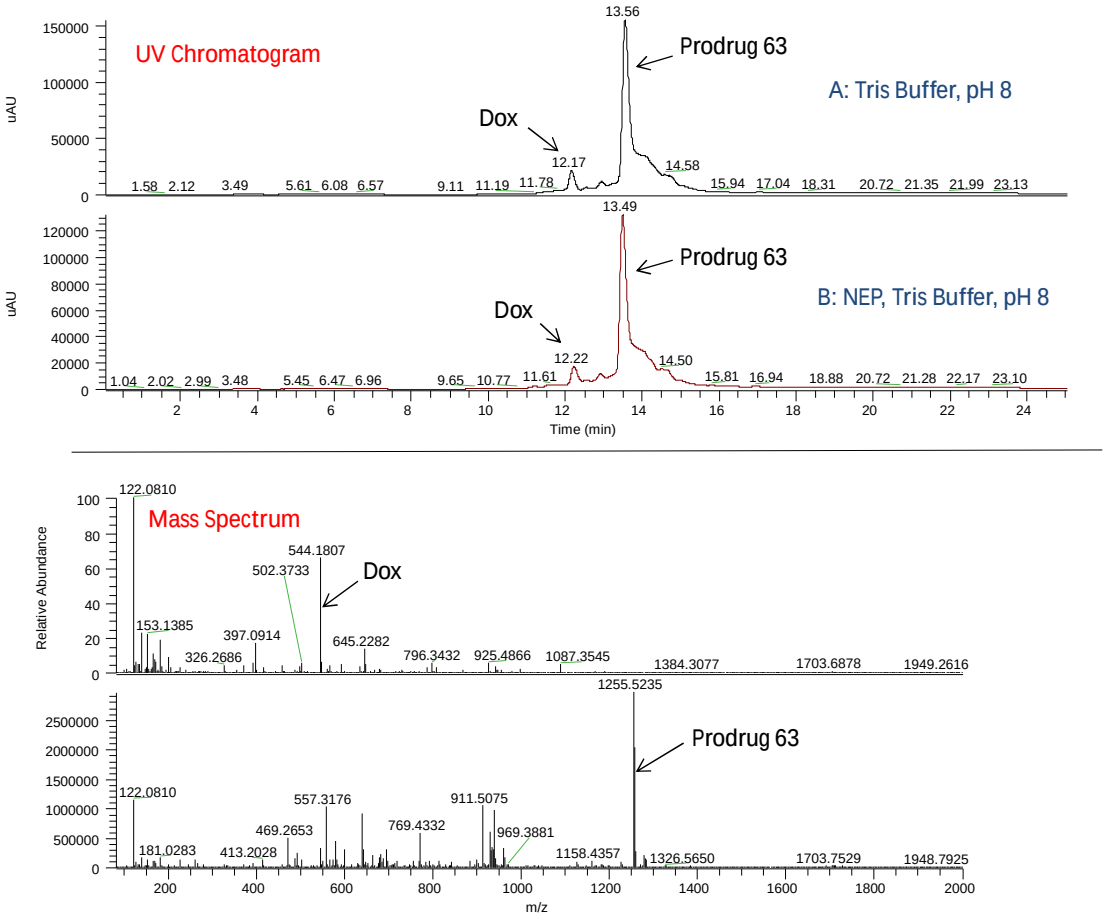

Figure 50. Stability of Prodrug **63** to Proteolysis by Neprilysin. Conditions: Prodrug **63** (1 μM) was incubated in 50 mM Tris buffer, pH 8 (**A**) or with human Neprilysin (NEP, 50 μm/mL) in 50 mM Tris/HCl buffer, pH 8 (**B**), for 4 h. Samples were precipitated with 1 volume of ACN, centrifuged and analyzed by LC-MS.

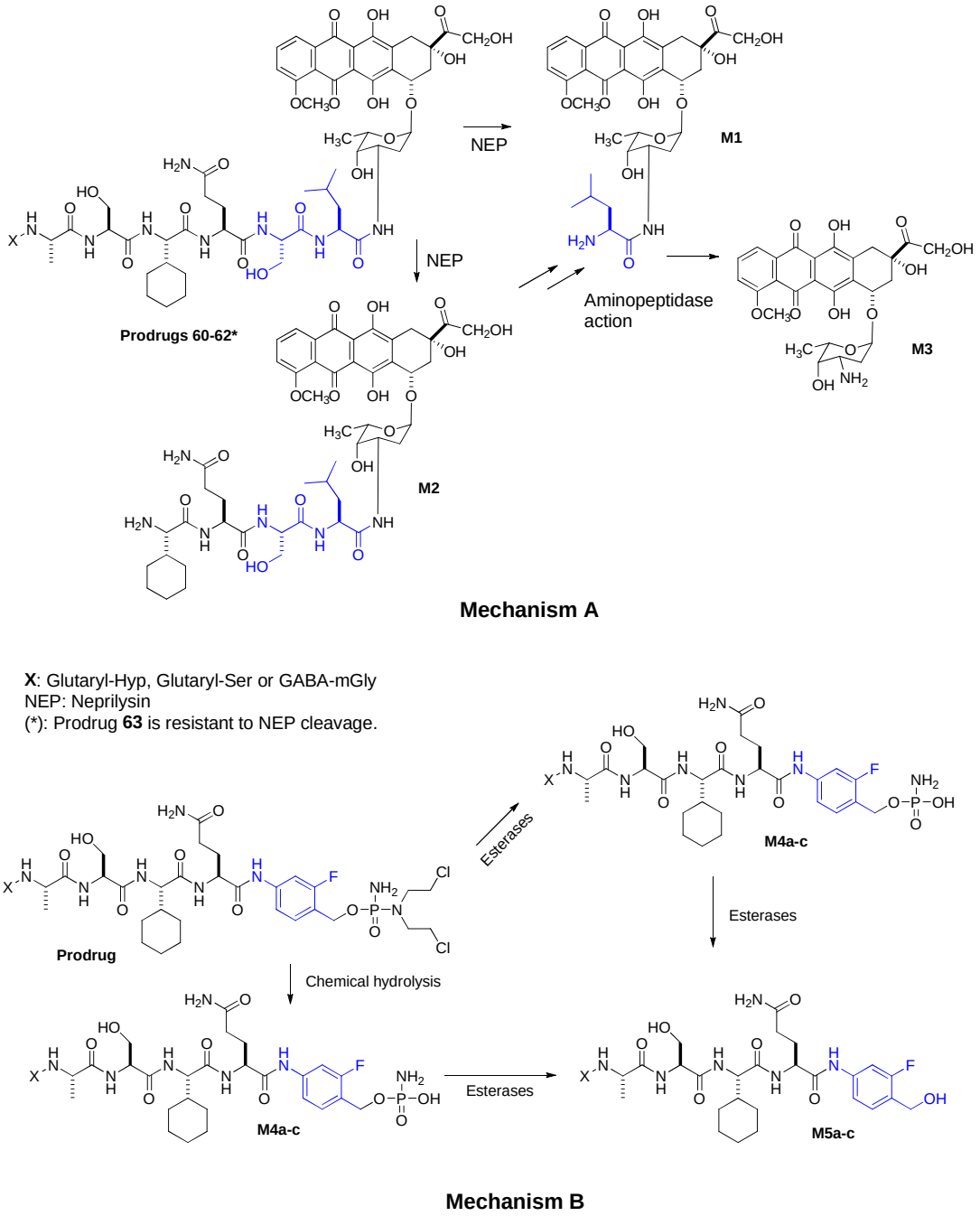

Figure 51. Non-PSA-mediated Metabolism of Doxorubicin and Phosphoramide Mustard Prodrugs in Blood and Cultured Hepatocytes

VI. Summary

In order to improve the PSA specificity and the stability of the prostate cancer prodrug L-377,202 in normal non-PSA producing tissues, we modified its peptide sequence, glutaryl-Hyp-Ala-Ser-Chg-Gln, towards the design and synthesis of various phosphoramide mustard and doxorubicin prodrugs. Systematic substitution of the *N*-terminal segment of glutaryl-Hyp-Ala-Ser-Chg-Gln with D-retro-inverso-peptides led to GABA←mGly-Ala-Ser-Chg-Gln and glutaryl-Ser-Ala-Ser-Chg-Gln as optimal promoieties which were subsequently coupled to phosphoramide mustard and doxorubicin using 2-fluoro-4-aminobenzyl and Ser-Leu linkers, respectively. L-377,202 or glutaryl-Hyp-Ala-Ser-Chg-Gln-Ser-Leu (**60**), glutaryl-Ser-Ala-Ser-Chg-Gln-Ser-Leu-Dox (**61**) and GABA←mGly-Ala-Ser-Chg-Gln-Ser-Leu-Dox (**62**) were rapidly cleaved by PSA with comprable half-life values (< 23 min) followed by glutaryl-Hyp-Ala-Ser-Chg-Gln-NH-2-F-Bz-phosphoramide mustard (**64**, 35 min) and glutaryl-Ser-Ala-Ser-Chg-Gln-NH-2-F-Bz-phosphoramide mustard (**65**, 80 min). The *in vitro* antiproliferative activity profiles of the newly synthesized doxorubicin prodrugs compared to that of L-377,202 with a slight improvement in cytoxicity for prodrug **62**. To further evaluate the tumor selectivity of the synthesized phosphoramide mustard and doxorubcin prodrugs, their stability and metabolism were investigated in human and murine blood and cultured hepatocytes. Time-dependent metabolism data revealed that the stability of phosphoramide mustard prodrugs was likely compromised by a combination of chemical degradation and phosphoramidase-mediated hydrolysis. Similar to L-377,202, prodrugs **61** and **62** were found to undergo rapid hydrolysis of their shared Ser-Leu linker region, which compromised their stability significantly. Using cleavage maps of known

proteases, we anticipated that human neprilysin, a thermolysin-like protease, may be responsible for the hydrolysis of prodrugs **60-62.** As expected, time-dependent metabolism studies confirmed that purified human neprilysin robustly hydrolyzed prodrugs **60-62** between Ser and Leu within the linker region. This metabolic liability was effectively mitigated by replacing Ser-Leu with a self-immolative 3-aminoxypropionate linker coupled to doxorubicin through its C-14 alpha-hydroxyl group, affording GABA←mGly-Ala-Ser-Chg-Gln-NH-O-CH_2-C(Me)$_2$C(O)-14-*O*-Dox (**63**). While the PSA cleavage rate of prodrug **63** was somewhat slower than that of L-377,202, its ability to release free doxorubicin contributed to a cytotoxic profile comparable to that of its congener. Additional stability, metabolism and mouse PK studies will be conducted to further evaluate prodrug **63** as a PSA-activated prostate cancer prodrug.

CHAPTER FOUR

EXPERIMENTAL SECTION

General Methods

All chemicals and protected amino acids were purchased from Sigma-Aldrich (St. Louis, MO), Chem-Impex (Wood Dale, IL) or AAPPTEC (Louisville, KY). Solvents were either ACS reagent or HPLC grade and used without further purification. Prodrug **60** (L-377202, glutaryl-Ser-Ala-Ser-Chg-Gln-Ser-Leu-Dox) was supplied by Merck Sharpe & Dohme (Rahway, NJ). Prodrug **64** (LH202, glutaryl-Hyp-Ala-Ser-Chg-Gln-NH-2-F-Bz-phosphoramide mustard) was previously synthesized in our laboratories.[151] Purified PSA (99%, 1.37 mg protein/ml) was purchased from Fitzgerald (North Acton, MA). Thermolysin from *Geobacillus stearothermophilus* (100 units/mg, E1%/280) and recombinant human neprilysin (>95% pure) were supplied by Sigma-Aldrich. Cryopreserved human (lot EBP) and mouse (lot Mc559) hepatocytes were supplied by Celsis (Chicago, IL). HEPES buffer, Cryopreserved Hepatocyte Recovery Media (CHRM), Cryopreserved Hepatocyte Plating Media (CHPM) and all cell medium additives were purchased from Invitrogen (Life Technologies, Grand Island, NY). Cell maintenance buffer was prepared by supplementing 500 mL of William's E medium with 5 mL Penn-Strep Glutamine (100x), 5 μL Dexamethasone (10 mM in DMSO), 5 mL Insulin-Transferrin-Selenium and 7.5 mL 1 M HEPES pH 7.4. For cytotoxicity cell-based assays, cell growth medium was prepared by adding L-glutamine (2 mM), fetal bovine serum (10%), penicillin G (100 units/mL) and streptomycin sulfate (100 units/mL) to phenol red-containing RPMI 1640. Reactions were monitored by TLC and/or on an LC-MS system consisting of PE 200 Series autosampler and pumps (Perkin Elmer, Waltham,

MA) coupled to an LCQ ion trap mass spectrometer (Thermo Scientific, Waltham, MA). Flash column chromatography (FCC) was performed on a Teledyne ISCO CombiFlash Companion Automated Flash Chromatographic System (Teledyne Technologies, Thousand Oaks, CA) with pre-packed silica gel columns. Unless otherwise specified, HPLC purification of peptides and intermediates was carried out from H_2O/ACN containing 0.1% TFA. All ^{1}H and ^{13}C NMR spectra were recorded on a 400 MHz Bruker spectrometer at ambient temperature and calibrated using residual un-deuterated solvents as the internal reference. Accurate mass values of final peptide conjugates were determined by direct inlet infusion of 10 μg/mL solutions using a LTQ Orbitrap XL or Velos (Thermo Scientific, Waltham, MA). Metabolite identification was performed using an LTQ-Orbitrap mass spectrometer (Thermo Fisher, Waltham, MA) equipped with an electrospray source operated in positive ionization mode interfaced with Shimadzu LC-20ADXR pumps, a SIL-20ACXR autosampler and SPD-M20A diode array (Shimadzu, Columbia, MD). Chromatographic separation was achieved with a 2.1x100 mm, 1.7μm BEH C18 column (Waters Corporation, Huntingdon Valley, PA) using a water (A)/ACN (B) mobile phase system containing 0.1% formic acid (v/v) and UV detection at 254 and 484 nm. The gradient was performed at a total flow rate of 200 μL/min as follows, 2% B from 0 to 3 min, 2 to 95% B from 3 to 15 min, 95% B from 15 to 20 min, 95 to 2% B from 20 to 20.1 min, 2% B from 20.1 to 25 min. Prodrugs were quantified using LC-MS/MS on a Transcend LX2 system (Thermo Fisher, Waltham, MA) coupled to an API 4000 (AB Sciex, Framingham, MA). As shown in Table 11, both SRM transitions for sodium adduct and base peak from each prodrug were used for LC-MS/MS

quantification. Results were consistent with either transition although only data generated with the sodium adduct SRM transitions are shown.

Table 11. SRM Transitions Used for Prodrug Quantification by LC-MS/MS

	Transition 1[a]		**Transition 2**[b]	
Prodrug	**Q1**	**Q3**	**Q1**	**Q3**
60	1418.6	1022.7	982.6	228.1
61	1392.7	996.7	956.5	342.1
62	1362.7	966.6	926.5	312.3
63	-	-	1255.5	451.0
64	996.6	776.4	776.4	124.1
65	970.5	750.5	750.3	124.1
66	940.5	720.4	720.3	124.1

SRM transitions used to quantify prodrug-sodium adducts[a] or base peaks[b].

I. AMC-conjugate Synthesis

Synthesis of 7-Azido-4-methylcoumarin (7-AZD)

7-azido-4-methylcoumarin (yellow solid) was prepared as in 79 % yield (234 mg) starting from 7-amino-4-methyl coumarin (257 mg) as previously described.[194]

7-Azido-4-methylcoumarin (7-AZD, 46). ^{1}H NMR (DMSO-d6, 400 MHz): δ 7.83 (d, 1H, J = 8.5 Hz), 7.2 (m, 1H), 7.18 (d, 1H, J = 2.1 Hz), 6.39 (s, 1H), 2.47 (s, 3H); ^{13}C NMR (DMSO-d6, 100 MHz): δ 159.5, 154.0, 152.9, 143.3, 126.9, 116.7, 115.5, 113.2, 106.8, 18.0, MS (ESI+): m/z (intensity), 201.9 ([M+H]+, 100%).

Synthesis of 7-(N^a-*t*-butyloxycarbonyl-*L*-glutaminyl)amino-4-methylcoumarin (Boc-Gln-AMC, 45).

Boc-Gln-AMC was synthesized using a one-pot amidation procedure between Boc-Gln selenocarboxylate and 7-AZD as previously described.[194] Briefly, a fresh solution of NaHSe (2.0 mmol eq.) was obtained by reacting $NaBH_4$ and an isopropanolic suspension of Se as previously described.[219] In parallel, the mixed anhydride of Boc-Gln-OH was prepared by adding a 1.0 M solution of IPCF in toluene (2.0 mL, 2.0 mmol) to a solution of Boc-Gln-OH (2.0 mmol) and N-methylpiperidine (244 µL, 2.0 mmol) in 20 mL of anhydrous THF at -15 °C under nitrogen and allowing the mixture to stir for 20 min at -15 °C. The selenocarboxylate was generated in situ by adding the freshly prepared NaHSe reagent above to the mixed anhydride via cannula over a period of 5 min, and stirring the reaction mixture for an additional 30 min below -10 °C under nitrogen atmosphere. A solution of 7-AZD (1.62 mmol) in 2 mL of anhydrous THF was cannulated into the selenocarboxylate solution, and the reaction carried out at room temperature under nitrogen for 2 h. Organic solvents were removed, the residue suspended in 15 mL of a saturated sodium bicarbonate solution and extracted with 45 mL (3x) of ethyl acetate. The organic extracts were combined, washed sequentially with water and brine, and dried over anhydrous sodium sulfate. After filtering out sodium sulfate, the crude mixture was dry-loaded onto silica gel and purified by FCC (CH_2Cl_2/MeOH). The product (142 mg) was obtained as a light-yellow solid in 84% yield and confirmed by mass spectrometry and NMR.

7-(N^a-*t*-butyloxycarbonyl-*L*-glutaminyl)amino-4-methylcoumarin (Boc-Gln-AMC, 45). ^{1}H NMR (CD_3OD, 400 MHz): δ 7.70 (d, 1H, J = 2.0 Hz), 7.60 (d, 1H, J = 8.7 Hz),

7.39 (d, 1H, J = 8.2 Hz), 6.13 (s, 1H), 4.12 (s, 1H), 2.35 (s, 3H), 2.28 (t, 2H, J = 7.5 Hz), 2.02 (m, 1H), 1.87 (m, 1H), 1.36 (s, 9H); ^{13}C NMR ($CDCl_3$, 400 MHz): δ 177.8, 173.4, 163.2, 157.9, 155.4, 155.2, 149.9, 143.4, 126.7, 117.3, 117.2, 113.7, 108.1, 81.0, 56.5, 32.5, 29.1, 28.8, 18.5; MS (ESI+): m/z (intensity), 403.7 ([M+H]+, 12%), 706.7 ([2M+H-Boc]+, 100%); MS (ESI-): m/z (intensity), 402.1681 ([M-H]-, 100%), 448.1739 ([M-H+FA]-, 15%), 516.1613 ([M-H+TFA]-, 18%), 805.3436 ([2M-H]-, 26%).

Synthesis of Glutaryl-Hyp-Ala-Ser-Chg-Gln-AMC (AMC-conjugate 34)

The solid-phase synthesis of Fm-glutaryl-Hyp-Ala-Ser-Chg-OH was carried out using standard solid phase peptide synthesis procedures. Loading of Fmoc-Chg-OH on 1 g of Wang resin (0.35 mmol/g resin) yielded 148 mg of peptide which was used without further purification. In order to couple Gln-AMC to the peptide, Boc-Gln-AMC (60 mg, 0.15 mmol) was de-protected with 1 mL of TFA/DCM/H_20 (50:45:5) in 30 min at room temperature. Solvents were removed under a gentle stream of nitrogen, the residue reconstituted in 400 μL of methanol and treated with Amberlyst A-26 (0.5 g, 0.4 mmol) to remove residual TFA. After filtering out Amberlyst A-26, methanol was removed and the light yellow residue re-suspended in 500 μL of NMP ready for the next step. Gln-AMC (17 mg, 0.042 mmol) was coupled to Fm-glutaryl-Hyp-Ala-Ser-Chg-OH (9.6 mg, 0.013 mmol) in 600 μL of NMP using HBTU (10 mg, 0.027 mmol) pre-activation of the peptide for 30 min in the presence of 1 eq. diethylisopropylamine (DIEA) at room temperature, followed by the addition of Gln-AMC. The reaction was allowed to proceed for 16 h at room temperature, after which 10% piperidine de-protection was carried out followed by HPLC purification. The final peptide was obtained in 52% yield (5.9 mg) and was greater than 98% pure by LC-UV analysis. Glutaryl-Hyp-Ala-Ser-Chg-Gln-

AMC; HRMS (ESI+): *m/z* calc'd for $C_{39}H_{54}N_7O_{13:}$ $[M+H]^+$ = 828.3780, found: 828.3806. ([M+H]+, 100%).

Synthesis of *N*^{g}-(9-fluorenyloxycarbonyl)-aminobutyric Acid (Fmoc-GABA, 47)

To a solution of GABA (2.00 g, 19.4 mmol, in 14 mL 10% $NaHCO_3$), Fmoc-OSu (4 g, 11.7 mmol, in 40 mL ACN) was added drop-wise over a period of 2 h at room temperature. The mixture was allowed to stir at room temperature for an additional hour. ACN was removed under reduced pressure and the aqueous layer acidified to pH 1 with 10% HCl. The precipitate was washed with two 20 mL portions of water, 20 mL ethyl acetate and dried under reduced pressure. Fmoc-GABA was obtained as a white solid in 73% yield (2.8 g).

***N*^{g}-(9-fluorenyloxycarbonyl)-aminobutyric Acid (Fmoc-GABA, 47)**. ^{1}H NMR (DMSO-d6, 400 MHz): δ 7.89 (d, 2H, J = 7.4 Hz), 7.44 (d, 2H, J = 7.2 Hz), 7.42 (t, 2H, J = 7.5 Hz), 7.35 (s, 1H), 7.33 (t, 2H, J = 7.0 Hz), 4.30 (d, 2H, J = 7 Hz), 4.21 (t, 1H, J = 6.7 Hz), 3.01 (q, 2H, J = 5.6 Hz), 2.20 (t, 2H, J = 7.3 Hz), 1.63 (q, 2H, J = 7.1 Hz); ^{13}C NMR (DMSO-d6, 100 MHz): δ 142.6, 139.4, 137.4, 128.9, 127.2, 124.2, 121.3, 120.0, 109.6, 77.5, 61.8, 51.1, 31.6; MS (ESI+): m/z (intensity), 325.8 ([M+H]+, 100%).

Loading of Fmoc-GABA on 2-chloro-trityl Chloride Resin

Fmoc-GABA (1.2 g, 3.6 mmol) was loaded onto 2-chloro-trityl chloride resin (1 g, 1.7 mmol) in 10 mL of anhydrous DCM/NMP (9:1) in the presence of 4 eq. DIEA at room temperature for 3 h. The loading levels were determined to be 0.48 mmol/g resin by Fmoc-deprotection with 20% piperidine and UV analysis (A290). The unreacted 2-chloro-trityl chloride on the resin was end-capped with 2 mL of methanol/DIEA (9:1) in

10 mL of anhydrous DCM under nitrogen for 60 min at room temperature, and the resin was ready for further coupling after 20% piperidine de-protection.

Synthesis of GABA←D-Ser←D-Ala←D-Ser←D-Chg-ψ[NH-CO-NH]-Gln-AMC (AMC-conjugate 35)

Following standard automated peptide synthesis procedures, GABA←D-Ser(tBu)←D-Ala←D-Ser(tBu)←D-Chg-H was generated on 2-chloro-trityl chloride resin (1.8 g, 0.48 mmol/g resin) starting with GABA-resin. Resin-bound GABA was obtained by loading Fmoc-GABA on 2-chloro-trityl chloride resin as previously described. Resin-GABA←D-Ser(tBu)←D-Ala←D-Ser(tBu)←D-Chg-H (53 mg, 0.026 mmol) was activated with carbonyldiimidazole (CDI, 22 mg, 0.14 mmol) in 200 μL of anhydrous DCM for 3 h at room temperature to generate the carbonyl-imidazole intermediate (Scheme 1). After washing the resin with three 1-mL portions of anhydrous DCM, coupling to H-Gln-AMC (43 mg, 0.14 mmol) was carried out in 600 μL DCM/NMP (60:40) for 48 h at room temperature. The protected peptide was cleaved off the resin with 5% TFA/DCM. After HPLC purification, treatment with 50% TFA/DCM at room temperature for 2 h afforded the final peptide in 6% yield (1.5 mg, 95% pure by LC-UV analysis). GABA←D-Ser←D-Ala←D-Ser←D-Chg-ψ[NH-CO-NH]-Gln-AMC; HRMS (ESI+): *m/z* calc'd for $C_{37}H_{53}N_8O_{13}$: $[M+H]^+$= 817.3732, found: 817.3753.

Synthesis of H-Chg-Gln-AMC (48)

Fmoc-Chg-OH (104 mg, 0.27 mmol) was pre-activated with HBTU (107 mg, 0.28 mmol) in the presence of 5 eq. DIEA in 200 μL NMP for 1 h, and then coupled to H-Gln-AMC (72 mg, 0.24 mmol) at room temperature for 2 h under nitrogen atmosphere. The crude mixture was suspended in 10 mL of saturated $NaHCO_3$ and extracted with 30 mL of

DCM three times. The organic layer was dry-loaded on silica and purified by FCC. The protected peptide intermediate (134 mg) was deprotected with 0.5 M TBAF, and purified by HPLC to generate the desired peptide (m/z = 443.1) in 57% yield (60 mg).

Synthesis of GABA←D-Ser←D-Ala←D-Ser -y[NH-CO-NH]-Chg-Gln-AMC (AMC-conjugate 36)

The amino-end of resin-GABA←D-Ser(tBu)←D-Ala←D-Ser(tBu)-H (69 mg, 0.034 mmol) was pre-activated with CDI (27 mg, 0.17 mmol) in 200 μl of anhydrous DCM at room temperature for 3 h and, after three 1-mL DCM washes, coupled to H-Chg-Gln-AMC in 600 μL DCM/NMP (60:40) for 48 h at room temperature. The protected peptide was cleaved off the resin with 5% TFA/DCM. After HPLC purification, treatment with 50% TFA/DCM at room temperature for 2 h afforded the final peptide in 10% yield (2.1 mg, >99% pure by LC-UV analysis). GABA←D-Ser←D-Ala←D-Ser -ψ[NH-CO-NH]-Chg-Gln-AMC; HRMS (ESI+): *m/z* calc'd for $C_{37}H_{53}N_8O_{13}$: $[M+H]^+$= 817.3732, found: 817.3766.

Synthesis of H-Ser(*t*Bu)-Chg-Gln-AMC (49)

Fmoc-Ser(*t*Bu)-OH (116 mg, 0.30 mmol) was pre-activated with HBTU (120 mg, 0.32 mmol) in the presence of 5 eq. DIEA in 400 μL NMP for 30 min, and then coupled to H-Chg-Gln-AMC (119 mg, 0.27 mmol) at room temperature for 10 h under nitrogen atmosphere. The crude mixture was suspended in 10 mL of saturated $NaHCO_3$ and extracted with 30 mL of DCM three times. The organic layer was dry-loaded onto silica gel and purified by FCC. The protected peptide intermediate (53 mg) was de-protected with 0.5 M TBAF, and purified by HPLC to generate the desired peptide (m/z = 586.0 in 28% yield (21 mg).

Synthesis of GABA←D-Ser←D-Ala-ψ[NH-CO-NH]-Ser-Chg-Gln-AMC (AMC-conjugate 37)

Conjugate 4 was prepared by activating the amino-end of resin-GABA←D-Ser(*t*Bu)←D-Ala-H (50 mg, 0.025 mmol) with CDI (23 mg, 0.14 mmol) in 200 μL of anhydrous DCM at room temperature for 3 h and, after three 1-mL DCM washes, coupled to H-Ser(*t*Bu)-Chg-Gln-AMC in 600 μL DCM/NMP (60:40) for 24 h at room temperature. The protected peptide was cleaved off the resin with 5% TFA/DCM. After HPLC purification, treatment with 50% TFA/DCM at room temperature for 2 h afforded the final peptide in 7.8% yield (1.6 mg, >99% pure by LC-UV analysis). GABA←D-Ser←D-Ala-ψ[NH-CO-NH]-Ser-Chg-Gln-AMC; HRMS (ESI+): *m/z* calc'd for $C_{37}H_{53}N_8O_{13}$: $[M+H]^+$= 817.3732, found: 817.3754.

Synthesis of H-Ala-Ser(ΨMe,Me pro)-Chg-Gln-AMC (50)

Fmoc-Ala-Ser(ΨMe,Me pro)-OH (136 mg, 0.31) was pre-activated with HBTU (105 mg, 0.27 mmol) in the presence of 5 eq. DIEA in 400 μL NMP for 30 min, and then coupled to H-Chg-Gln-AMC (97 mg, 0.22 mmol) at room temperature for 3 h under nitrogen atmosphere. One-pot Fmoc-de-protection was carried out with 10% DEA and NMP removed with repeated hexane washes (5-mL portions, at least 10 times). The crude mixture was dissolved in 1 mL of 50% ACN/water and purified by FCC. The final peptide (m/z = 641.1) was obtained in 66% yield (93 mg) and greater than 98% pure by LC-UV analysis.

Synthesis of GABA←D-Ser-ψ[NH-CO-NH]-Ala-Ser-Chg-Gln-AMC (AMC-conjugate 38)

Conjugate 5 was prepared by activating the amino-end of resin-GABA←D-Ser(*t*Bu)-H (54 mg, 0.025 mmol) with CDI (20 mg, 0.12 mmol) in 200 μL of anhydrous DCM at room temperature for 3 h and, after three 1 mL-DCM washes, coupled to H-Ala-Ser(ΨMe,Me pro)-Chg-Gln-AMC (50 mg, 0.078 mmol) in 600 μL DCM/NMP (60:40) for 24 h at room temperature. The protected peptide was cleaved off the resin with 5% TFA/DCM. After HPLC purification, treatment with 50% TFA/DCM at room temperature for 2 h afforded the final peptide in 7.8% yield (2.6 mg, >98% pure by LC-UV analysis). GABA←D-Ser-ψ[NH-CO-NH]-Ala-Ser-Chg-Gln-AMC; HRMS (ESI+): *m/z* calc'd for $C_{37}H_{53}N_8O_{13}$: $[M+H]^+$= 817.3732, found: 817.3754.

Synthesis of 3-(fluorenylmethoxy)-3-oxopropanoic acid (51)

Malonic acid (283 mg, 2.7 mmol) and fluorenyl methanol (213 mg, 1.1 mmol) were dissolved in 2 mL of ACN at room temperature under nitrogen atmosphere. EDC (531 mg, 2.8 mmol) was added and the mixture stirred at room temperature for 30 min under nitrogen atmosphere. After removing ACN under reduced pressure, the residue was re-dissolved in 50 mL of DCM and extracted with two 20-mL portions of saturated $NaHCO_3$. The aqueous layers were combined, acidified to pH 1 and extracted with 35 mL of DCM three times. The organic layers were combined, washed with water, brine and dried over sodium sulfate. DCM was removed under reduced pressure and the product recovered as an off-white solid in 57% yield (176 mg, >99% pure by LC-UV analysis).

3-(Fluorenylmethoxy)-3-oxopropanoic acid (51), ^{1}H NMR ($CDCl_3$, 400 MHz): δ 7.80 (d, 2H, J = 7.4 Hz), 7.61 (d, 2H, J = 6.8 Hz), 7.44 (t, 2H, J = 8.0 Hz), 7.35 (t, 2H, J = 8.3 Hz), 4.52 (d, 2H, J = 7.2 Hz), 4.27 (t, 1H, J = 7.2 Hz), 3.55 (s, 2H); ^{13}C NMR ($CDCl_3$, 100 MHz): δ 167.9, 166.8, 143.5, 140.7, 127.7, 127.1, 125.2, 120.1, 66.4, 46.3, 41.6.

Synthesis of HO-mGly-Ala-Ser(ΨMe,Me pro)-Chg-Gln-AMC (52)

To a solution of 3-(fluorenylmethoxy)-3-oxopropanoic acid (14 mg, 0.050 mmol), H-Ala-Ser(ΨMe,Me pro)-Chg-Gln-AMC (20 mg, 0.031 mmol) and EDC (13 mg, 0.068 mmol) prepared in 400 μL of NMP in the presence of 5 eq. DIEA was added DMAP (9 mg, 0.07 mmol), and the reaction was carried out for 16 h at room temperature under nitrogen atmosphere. The reaction mixture was washed with 2 mL of hexane (five times) to remove NMP, reconstituted in 1 mL of 50% ACN/water and purified by HPLC. The final peptide (m/z = 641.1) was obtained in 62% yield (14 mg) and was greater than 98% pure by LC-UV analysis.

Synthesis of GABA←mGly-Ala-Ser-Chg-Gln-AMC (AMC-conjugate 39)

HO-mGly-Ala-Ser(ΨMe,Me pro)-Chg-Gln-AMC (12 mg, 0.017 mmol) was activated with EDC (9 mg, 0.05 mmol)/DMAP (6 mg, 0.05 mmol) in the presence of DIEA (5 eq.) in 400 μL of NMP, and coupled to GABA-resin (20 mg, 0.0094 mmol) for 48 h at room temperature. The protected peptide was cleaved off the resin with 5% TFA/DCM. After HPLC purification, treatment with 50% TFA/DCM at room temperature for 2 h afforded the final peptide in 32% yield (2.5 mg, >98% pure by LC-UV analysis). GABA←mGly-Ala-Ser-Chg-Gln-AMC; HRMS (ESI+): *m/z* calc'd for $C_{36}H_{50}N_7O_{12}$: $[M+H]^+$= 772.3517, found: 772.3520.

Synthesis of GABA←D-Ser←mGly-Ser-Chg-Gln-AMC (AMC-conjugate 40)

To a solution of 3-(fluorenylmethoxy)-3-oxopropanoic acid (8.2 mg, 0.029 mmol), H-Ser-Chg-Gln-AMC (14 mg, 0.024 mmol) and EDC (12 mg, 0.063 mmol) prepared in 400 μL of NMP in the presence of DIEA (5 eq.) was added DMAP (7.6 mg, 0.063 mmol), and the reaction carried out at room temperature for 16 h under nitrogen atmosphere. The

reaction mixture was washed with 2 mL of hexane (five times), reconstituted in 400 μL NMP and used for the second coupling step without further purification. Additional portions of EDC (25 mg, 0.13 mol) and DMAP (12 mg, 0.098 mmol) were added to couple the peptide to resin-GABA←D-Ser(tBu)-H (20 mg, 0.01 mmol) at room temperature for 16 h in the presence of 5 eq. DIEA. The protected peptide was cleaved off the resin with 5% TFA/DCM. After HPLC purification, treatment with 50% TFA/DCM at room temperature for 2 h afforded the final peptide in 32% yield (2.3 mg, >98% pure by LC-UV analysis). GABA←D-Ser←mGly-Ser-Chg-Gln-AMC; HRMS (ESI+): *m/z* calc'd for $C_{36}H_{50}N_7O_{13}$: $[M+H]^+$= 788.3467, found: 788.3454.

Synthesis of GABA←D-Lys←mGly-Ser-Chg-Gln-AMC (AMC-conjugate 41)

To a solution of 3-(fluorenylmethoxy)-3-oxopropanoic acid (20 mg, 0.071 mmol), H-Ser-Chg-Gln-AMC (27 mg, 0.046 mmol) and EDC (22 mg, 0.12 mmol) prepared in 400 μL of NMP in the presence of 5 eq. DIEA was added DMAP (14 mg, 0.12 mmol), and the reaction was carried out at room temperature for 16 h under nitrogen atmosphere. The reaction mixture was washed with 2 mL of hexane (five times), reconstituted in 400 μL NMP and used for the second coupling step without further purification. Additional portions of EDC (44 mg, 0.23 mol) and DMAP (28 mg, 0.13 mmol) were added to couple the peptide to resin-GABA←D-Lys(Boc)-H (20 mg, 0.01 mmol) at room temperature for 24 h in the presence of 5 eq. DIEA. The protected peptide was cleaved off the resin with 5% TFA/DCM. After HPLC purification, treatment with 50% TFA/DCM at room temperature for 2 h afforded the final peptide in 11% yield (1.1 mg, >98% pure by LC-UV analysis). GABA←D-Lys←mGly-Ser-Chg-Gln-AMC; HRMS (ESI+): *m/z* calc'd for $C_{39}H_{57}N_8O_{12}$: $[M+H]^+$= 829.4096, found: 829.4092.

Synthesis of GABA←D-Ser←D-Ala←mGly-Chg-Gln-AMC (AMC-conjugate 42)

To a solution of 3-(fluorenylmethoxy)-3-oxopropanoic acid (16 mg, 0.057 mmol), H-Chg-Gln-AMC (21 mg, 0.047 mmol) and EDC (23 mg, 0.12 mmol) prepared in 400 μL of NMP in the presence of DIEA (5 eq.) was added DMAP (13 mg, 0.11 mmol), and the reaction was carried out at room temperature for 16 h under nitrogen atmosphere. The reaction mixture was washed with 2 mL of hexane (five times), reconstituted in 400 μL NMP and used for the second coupling step without further purification. Additional portions of EDC (45 mg, 0.24 mol) and DMAP (31 mg, 0.25 mmol) were added to couple the peptide to resin-GABA←D-Ser(tBu)←D-Ala-H (26 mg, 0.013 mmol) at room temperature for 24 h in the presence of 5 eq. DIEA. The protected peptide was cleaved off the resin with 5% TFA/DCM. After HPLC purification, treatment with 50% TFA/DCM at room temperature for 2 h afforded the final peptide in 20% yield (2.0 mg, >95% pure by LC-UV analysis). GABA←D-Ser←D-Ala←mGly-Chg-Gln-AMC; HRMS (ESI+): *m/z* calc'd for $C_{36}H_{50}N_8O_{12}$: $[M+H]^+$= 772.3517, found: 772.3536.

Synthesis of GABA←D-Ser←D-Ala←D-Ser←mGly-Gln-AMC (AMC-conjugate 43)

To a solution of 3-(fluorenylmethoxy)-3-oxopropanoic acid (25 mg, 0.089 mmol), H-Gln-AMC (21 mg, 0.047 mmol) and EDC (20 mg, 0.10 mmol) prepared in 400 μL of NMP in the presence of 5 eq. DIEA was added DMAP (11 mg, 0.90 mmol), and the reaction was carried out at room temperature for 16 h under nitrogen atmosphere. The reaction mixture was washed with 2 mL of hexane (five times), reconstituted in 400 μL NMP and used for the second coupling step without further purification. Additional portions of EDC (67 mg, 0.35 mol) and DMAP (8 mg, 0.07 mmol) were added to couple the peptide to resin- GABA←D-Ser(tBu)←D-Ala←D-Ser(tBu)-H (26 mg, 0.013 mmol)

at room temperature for 48 h in the presence of 5 eq. DIEA. The protected peptide was cleaved off the resin with 5% TFA/DCM. After HPLC purification, treatment with 50% TFA/DCM at room temperature for 2 h afforded the final peptide in 21% yield (1.5 mg, >99% pure by LC-UV analysis). GABA←D-Ser←D-Ala←D-Ser←mGly-Gln-AMC; HRMS (ESI+): *m/z* calc'd for $C_{31}H_{42}N_7O_{13}$: $[M+H]^+$= 720.2841, found: 720.2869.

Synthesis of Glutaryl-Ser-Ala-Ser-Chg-Gln-AMC (AMC-conjugate 44)

Fmoc-Ser(*t*Bu)-OH (8.8 mg, 0.023 mmol) was pre-activated with HBTU (7.7 mg, 0.020 mmol) in the presence of 5 eq. DIEA in 200 μL of NMP for 30 min at room temperature under nitrogen atmosphere and then coupled to H-Ala-Ser(ΨMe,Me pro)-Chg-Gln-AMC (9.6 mg, 0.15 mmol) for 2 h. Fmoc-de-protection was carried out without purification by adding 20 μL of DEA to the reaction mixture and allowing the reaction to proceed for 90 min at room temperature. The reaction mixture was washed with 2 mL of hexane (five times), dried under reduced pressure (to remove residual DEA) and reconstituted in 200 μL NMP. The reconstituted mixture was reacted with glutaric anhydride (5.1 mg, 0.045 mmol) for 2 h at room temperature under nitrogen atmosphere. Solvents were removed under reduced pressure and the protected peptide purified by HPLC. Treatment with 50% TFA/DCM at room temperature for 2 h afforded the final peptide in 37% yield (93.9 mg, >98% pure by LC-UV analysis). Glutaryl-Ser-Ala-Ser-Chg-Gln-AMC; HRMS (ESI+): *m/z* calc'd for $C_{37}H_{52}N_7O_{13}$: $[M+H]^+$= 802.3623, found: 802.3656.

II. Prodrug Synthesis

Synthesis of Prodrug 61 (Glutaryl-Ser-Ala-Ser-Chg-Gln-Ser-Leu-Dox)

Fm-glutaryl-Ser-Ala-Ser-Chg-Gln-Ser-Leu-OH was prepared using standard automated peptide synthesis procedures. Fm-glutaryl-Ser-Ala-Ser-Chg-Gln-Ser-Leu-OH (88 mg, 0.086 mmol) and doxorubicin (25 mg, 0.043 mmol) were dissolved in 2 mL anhydrous DMF in the presence of 2 eq. DIEA. PyBOP (54 mg, 0.10 mmol) was added, and the mixture stirred at room temperature under nitrogen atmosphere for 2 h. Same-pot removal of the fluorenylmethyl-protecting group was achieved with the addition of 200 μL of DEA (10%). Trituration from DMF with 20 mL of ACN and HPLC purification (10 mM ammonium acetate/ACN) afforded the final peptide conjugate in 34% yield (20 mg). Glutaryl-Ser-Ala-Ser-Chg-Gln-Ser-Leu-Dox; HRMS (ESI+): *m/z* calc'd for $C_{63}H_{88}N_9O_{25}$: $[M+H]^+$= 1370.5891, found: 1370.5920.

Synthesis of *N*^{g}-*t*-butyloxycarbonyl-aminobutyric Acid (Boc-GABA, 91)

GABA (1.0 g, 9.8 mmol) was dissolved in 24 mL of a 6% $NaHCO_3$ solution at 0 °C. A pre-cooled solution of Boc-anhydride (15 mmol in 10 mL dioxane) was added slowly and the mixture stirred at 0 °C for 1 h, then overnight at room temperature. After removing dioxane under reduced pressure, the aqueous mixture was acidified to pH 1 with 1 N sodium bisulfate and extracted with 50 mL ethyl acetate three times. The combined organic layer was washed with 10 mL water, brine and dried over sodium sulfate. Ethyl acetate was removed under reduced pressure and the product collected as a white solid in 84% yield (1.7 g).

***N*^{g}-*t*-Butyloxycarbonyl-aminobutyric acid (Boc-GABA, 91).** ^{1}H NMR ($CDCl_3$, 400 MHz): δ 3.21 (m, 2H), 2.42 (t, 2H, J = 7.2 Hz), 1.84 (q, 2H, J_1 = 7.0 Hz, J_2 = 6.4 Hz), 1.46 (s, 9H); ^{13}C NMR ($CDCl_3$, 100 MHz): δ 166.7, 141.3, 125.0, 120.1, 67.8, 46.6, 40.8,

MS (ESI+): m/z (intensity), 203.7 ([M+H]+, 45%), 406.8 ([2M+H]+, 74%), 306.8 ([2M+H-Boc]+, 100%).

Synthesis of fluorenylmethyl *N*^{g}-*t*-butyloxycarbonyl-aminobutyrate (Boc-GABA-Fm, 92)

Boc-GABA (1.0 g, 9.8 mmol) was pre-activated with CDI (1.6 g, 9.8 mmol) in 2 mL of anhydrous DCM at room temperature under nitrogen atmosphere for 1 h. Fluorenylmethanol (1.3 g, 6.5 mmol) was added and the reaction carried out at room temperature under nitrogen atmosphere for 4h. The mixture was diluted to 20 mL with DCM, washed sequentially with 20 mL 5% $NaHCO_3$, brine and dried over sodium sulfate. After removing DCM under reduced pressure, the product was collected as an off-white solid in 95% yield (1.2 g). Removal of the Boc-protecting group was carried out with 50% TFA/DCM at room temperature in 30 min. All solvents were removed under a gentle nitrogen stream; the crude product obtained after repeated 20-mL hexane washes (5X) was ready to be used for the next step.

Fluorenylmethyl *N*^{g}-*t*-butyloxycarbonyl-aminobutyrate (Boc-GABA-Fm, 92). ^{1}H NMR ($CDCl_3$, 400 MHz): δ 7.80 (d, 2H, J = 8.0 Hz), 7.61 (d, 2H, J = 7.4 Hz), 7.44 (t, 2H, J = 7.3 Hz), 7.35 (t, 2H, J = 7.9 Hz), 4.56 (s, 1H), 4.45 (d, 2H, J = 6.7 Hz), 4.24 (t, 1H, J = 7.3 Hz), 3.13 (m, 2H), 2.43 (t, 2H, J = 7.3 Hz), 1.81 (q, 2H, J = 6.8 Hz), 1.46 (s, 9H); ^{13}C NMR ($CDCl_3$, 100 MHz): δ 143.8, 141.3, 127.8, 127.1, 125.0, 120.0, 66.2, 46.9, 38.4, 31.5, 28.4, 25.3, MS (ESI+): m/z (intensity), 381.7 ([M+H]+, 10%), 282.0 ([M+H-Boc], 100%).

Synthesis of *t*-BuO-mGly (93)

Malonic acid (5.0 g, 48 mmol) and *t*-BuOH (1.8 mL, 19 mmol) were dissolved in 150 mL of ACN at room temperature under nitrogen. EDC (9.2 g, 48 mmol) was added and the reaction conducted at room temperature under nitrogen for 30 min. ACN was removed under reduced pressure and the residue dissolved in 200 mL of ether. The product was back-extracted with two 50-mL portions of saturated $NaHCO_3$, and the combined aqueous layer acidified to pH 2 with 1 N sodium bisulfate. Finally, the product was extracted with three 200-mL portions of DCM which were combined and washed with water, brine and dried over sodium sulfate. DCM was removed under reduced pressure and the product obtained as a white solid in 76% yield (2.3 g).

***t*-BuO-mGly (93).** ^{1}H NMR ($CDCl_3$, 400 MHz): δ 3.28 (s, 2H), 1.42 (s, 9H); ^{13}C NMR ($CDCl_3$, 100 MHz): δ 168.5, 162.1, 83.5, 39.7, 27.9, 27.8, 25.6.

Synthesis of *t*-BuO-mGly-OSu (94)

To a solution (7 mL, ACN) of *t*-BuO-mGly (2.3 g, 15 mmol) and HOSu (1.7 g, 15 mmol) was added EDC (3.1 g, 16 mmol), and the mixture stirred at room temperature under nitrogen atmosphere for 1 h. ACN was removed under reduced pressure and the residue dissolved in 200 mL of DCM. The organic layer was washed with 50 mL water (2x), brine and dried over sodium sulfate. DCM was removed under reduced pressure and the crude product collected as a white solid in 84% yield (3.1 g).

Synthesis of Fm-GABA←mGly (95)

A solution of *t*-BuO-mGly-OSu (1.8 g, 6.9 mmol) and GABA-Fm (2.0 g, 6.9 mmol) was prepared in 25 mL of anhydrous DCM in the presence of DIEA (1.2 mL, 6.9 mmol) and stirred at room temperature under nitrogen atmosphere for 1 h. The reaction mixture was diluted to 40 mL with DCM, washed with 10 mL water (2x), brine and dried over sodium

sulfate. DCM was removed under reduced pressure and the crude mixture purified by FCC to afford the final product in 64% yield (1.9 g). Removal of the *t*-butyl-protecting group was achieved with 50%TFA/DCM to afford 1.7 g of the free acid which was carried forward to the next step without further purification.

Synthesis of Fm-GABA←mGly-Ala-Ser-Chg-Gln-Ser-Leu-OH (96)

The Fm-GABA←mGly-OSu ester was freshly prepared and coupled to the amino end of H-Ala-Ser-Chg-Gln-Ser-Leu-OH. The peptide intermediate was obtained using standard automated peptide synthesis procedures. To prepare the OSu ester, Fm-GABA←mGly (320 mg, 0.87 mmol) and HOSu (100 mg, 0.87 mmol) were dissolved in 6 mL of ACN. EDC (420 mg, 2.2 mmol) was added and the mixture stirred at room temperature under nitrogen for 1 h. ACN was removed, the residue dissolved in 40 mL of DCM, washed with 10 mL water (3x), brine and dried over sodium sulfate. The crude OSu ester (220 mg, 0.48 mmol) was directly coupled (< 1 min) to H-Ala-Ser-Chg-Gln-Ser-Leu-OH (310 mg, 0.48 mmol) in the presence of 1 eq. DIEA in 1 mL ACN/NMP (1:2). Trituration with 30 mL of ice-cold ether afforded 310 mg of the crude peptide which was used for the next step without further purification.

Synthesis of prodrug 62 (GABA←mGly-Ala-Ser-Chg-Gln-Ser-Leu-Dox)

Fm-GABA←mGly-Ala-Ser-Chg-Gln-Ser-Leu-OH (96 mg, 0.096 mmol) and doxorubicin (28 mg, 0.048 mmol) were dissolved in the presence of 2 eq. DIEA in 2 mL anhydrous DMF. PyBOP (60 mg, 0.12 mmol) was added and the mixture stirred at room temperature under nitrogen atmosphere for 2 h. Same-pot removal of the fluorenylmethyl-protecting group was achieved with the addition of 200 μL of DEA (10%). Trituration from DMF with 20 mL of ACN and HPLC purification (10 mM

ammonium acetate/ACN) afforded the final peptide conjugate in 28% yield (18 mg). GABA←mGly-Ala-Ser-Chg-Gln-Ser-Leu-Dox; HRMS (ESI+): *m/z* calc'd for $C_{62}H_{86}N_9O_{24}$: $[M+H]^+$= 1340.5786, found: 1340.5817.

Synthesis of methyl 3-((1,3-dioxoisoindolin-2-yl)oxy)-2,2-dimethylpropanoate (68)

A solution of DIAD (2.8 mL, 15 mmol) prepared in 5 mL anhydrous THF) was slowly added to a stirred mixture of methyl 3-hydroxy-2,2-dimethylpropanoate (2.0 g, 15 mmol), triphenylphosphine (4.4 g, 17 mmol) and *N*-hydroxyphthalimide (2.7 g, 317 mmol) prepared in 80 mL anhydrous THF at 0 °C. After stirring the mixture at room temperature under a nitrogen atmosphere for 24 h, THF was removed under reduced pressure and the residue re-dissolved in 40 mL of ethyl acetate. The ethyl acetate mixture was washed with water (10 mL) three times, brine and dry-loaded onto a 80-g silica column. The final product was obtained in 57% yield (2.4 g) as a white solid after FCC purification from hexane/ethyl acetate.

Methyl 3-((1,3-dioxoisoindolin-2-yl)oxy)-2,2-dimethylpropanoate (68). ^{1}H NMR ($CDCl_3$, 400 MHz): δ 7.84 (m, 2H), 7.76 (s, 2H), 4.28 (s, 2H), 3.77 (s, 3H), 1.40 (s, 6H); ^{13}C NMR ($CDCl_3$, 100 MHz): δ 175.7, 163.1, 136.0, 134.4, 129.0, 123.4, 83.7, 52.2, 43.1, 22.2, MS (ESI+): m/z (intensity), 278.2 ([M+H]+, 100%).

Synthesis of methyl 3-(aminooxy)-2,2-dimethylpropanoate (69)

To a solution of methyl 3-((1,3-dioxoisoindolin-2-yl)oxy)-2,2-dimethylpropanoate (160 mg, 0.57 mmol) prepared in 10 mL of anhydrous diethyl ether was added 73 μL (2.3 mmol) of 98% anhydrous hydrazine, and the mixture stirred at room temperature under a nitrogen atmosphere for 2 h. The mixture was filtered and the filtrate concentrated to

generate 75 mg of crude methyl 3-(aminooxy)-2,2-dimethylpropanoate (white solid) which was used for the next step without further purification.

Synthesis of N^{α}-allyloxycarbonyl-N^{δ}-trityl-L-glutamine (Alloc-Gln(Trt)-OH, 71)

A solution of allylchloroformate prepared in 20 mL of ACN was slowly added to a stirred suspension of H-Gln(Trt)-OH (390 mg, 1.0 mmol) in 10 mL of 10% K_2CO_3 at room temperature over a period of 10 min. After stirring the mixture for an additional 10 min at room temperature, the organic layer was collected and ACN removed under reduced pressure. Toluene (10 mL, 3x) was added to the residue and the solvent removed under reduced to pressure to give Alloc-Gln(Trt)-OH as a white solid in 95% yield (450 mg).

N^{α}-Allyloxycarbonyl-N^{δ}-trityl-L-glutamine (Alloc-Gln(Trt)-OH, 71). ^{1}H NMR ($CDCl_3$, 400 MHz): δ 7.27 (m, 15H), 5.95 (m, 2H), 5.32 (ddd, 1H, J_1 = 9.2 Hz, J_2 = 1.6 Hz, J_3 = 0.72 Hz), 5.19 (ddd, 1H, J_1 = 5.1 Hz, J_2 = 1.5 Hz, J_3 = 0.59 Hz), 4.53 (d, 2H, J = 2.4 Hz), 4.06 (t, 1H, J = 6.5 Hz), 2.39 (t, 2H, J = 8.3 Hz), 2.00 (m, 2H); ^{13}C NMR ($CDCl_3$, 100 MHz): δ 178.6, 175.1, 157.7, 146.1, 134.5, 130.1, 128.7, 127.7, 117.5 71.8, 66.6, 57.2, 34.4, 30.9, MS (ESI+): m/z (intensity), 473.4 ([M+H]+, 100%).

Synthesis of Alloc-Gln(Trt)-OSu (72)

To a stirred solution (20 mL of ACN) of Alloc-Gln(Trt)-OH (150 mg, 0.32 mmol) and HOSu (44 mg, 0.38 mmol) was added EDC (240 mg, 1.3 mmol), and the mixture stirred at room temperature under nitrogen atmosphere for 2 h. ACN was removed under reduced pressure and the residue dissolved in 40 mL of DCM. The organic layer was washed with 10 mL water (2x), brine and dried over sodium sulfate. DCM was removed under reduced pressure and the crude ester collected as a white solid in quantitative yield (190 mg).

Synthesis of methyl (S)-2,2-dimethyl-6,9-dioxo-7-(3-oxo-3-(tritylamino)propyl)-4,10-dioxa-5,8-diazatridec-12-enoate (Alloc-Gln(Trt)-NH-O-CH_2-C(Me)$_2$COOMe, 73).

To a stirred solution (80 mL of ACN) of Alloc-Gln(Trt)-OH (489 mg, 1.0 mmol) and HOSu (253 mg, 2.2 mmol) was added EDC (768 mg, 4.0 mmol) and the mixture stirred at room temperature under nitrogen atmosphere for 2 h. In parallel, methyl 3-((1,3-dioxoisoindolin-2-yl)oxy)-2,2-dimethylpropanoate (834 mg, 3.0 mmol) was de-protected with anhydrous hydrazine (383 μL, 12.0 mmol) as previously described, the resulting crude solid dissolved in 8 mL of anhydrous DCM, and directly added to the Alloc-Gln(Trt)-OSu ester solution. The mixture was stirred at room temperature under nitrogen atmosphere for 24 h, ACN removed under reduced pressure and the DMF solution triturated with 10 volumes (80 mL) of ice-cold water. After centrifugation at 3000 RPM for 15 min, the white precipitate was collected and dry-loaded on a 24-g silica column and purified from DCM/ACN. The final product was obtained as a white solid in 86% yield (520 mg).

Methyl (S)-2,2-dimethyl-6,9-dioxo-7-(3-oxo-3-(tritylamino)propyl)-4,10-dioxa-5,8-diazatridec-12-enoate (73). ^{1}H NMR (CD_3OD, 400 MHz): δ 7.27 (m, 15H), 5.95 (m, 1H), 5.32 (ddd, 1H, J_1 = 9.1 Hz, J_2 = 1.6 Hz, J_3 = 0.73 Hz), 5.19 (ddd, 1H, J_1 = 5.1 Hz, J_2 = 1.5 Hz, J_3 = 0.60 Hz), 4.56 (d, 2H, J = 5.1 Hz), 3.93 (m, 3H), 3.69 (s, 3H), 2.45 (m, 2H), 1.91 (m, 2H); ^{13}C NMR (CD_3OD, 100 MHz): δ 177.9, 174.1, 171.1, 158.2, 146.0, 134.3, 130.0, 128.7, 127.8, 117.8, 83.4, 71.7, 66.7, 53.8, 52.6, 44.1, 33.7, 29.0, 22.7, MS (ESI+): m/z (intensity), 602.4 ([M+H]+, 100%).

Syntheses of (S)-7-(3-amino-3-oxopropyl)-2,2-dimethyl-6,9-dioxo-4,10-dioxa-5,8-diazatridec-12-enoic acid (Alloc-Gln-NH-O-CH_2-C(Me)$_2$COOH, 74) and its sodium salt.

To a THF solution (36 mL) of Alloc-Gln(Trt)-NH-O-CH_2-C(Me)$_2$COOMe (524 mg, 0.87 mmol) was added 4 mL of a 1 N NaOH solution, and the mixture stirred at room temperature for 24 h. Solvents were removed under reduced pressure, the residue redissolved in 40 mL of DCM and washed with 10 mL of H_2O three times and 10 mL of brine. After drying the organic layer on sodium sulfate, solvents were removed to a white solid. The residue was allowed to stir in 2 mL of 95% TFA/DCM at 0 °C for 5 min. Following trituration with 10 mL of ice-cold water, the mixture was lyophilized. The sodium salt of Alloc-Gln-NH-O-CH_2-C(Me)$_2$COOH was obtained by dissolving the lyophilisate in 5 mL of ACN followed by neutralization to pH 7 (slow addition of a $NaHCO_3$ (2 eq.) solution at 0 °C) and lyophilizing the mixture. The sodium salt was used for the next step without further workup.

Synthesis of (S)-2,2-dimethyl-6,9-dioxo-7-(3-oxo-3-(tritylamino)propyl)-4,10-dioxa-5,8-diazatridec-12-enoic acid (Alloc-Gln(Trt)-NH-O-CH_2-C(Me)$_2$COOH, 73a, Alternate Method).

A solution of Alloc-Gln(Trt)-OSu (190 mg, 0.34 mmol) and 2,2-dimethyl-3-aminoxypropionic acid (67 mg, 0.50 mmol) in 10 mL anhydrous DCM was stirred at room temperature under nitrogen for 24 h. The mixture was dry-loaded onto a 24-g silica column and purified from DCM/ACN to give Alloc-Gln(Trt)-NH-O-CH_2-C(Me)$_2$COOH as a white solid in 38% yield (62 mg, crude).

Synthesis of 14-bromodaunorubicin HCl (76).

Timethylorthoformate (100 μL) was added to a solution of daunomycin HCl (100 mg, 0.18 mmol) prepared in 6 mL of Dioxane/MeOH (2:1) and the mixture stirred at room temperature for 20 min. A $Br_2/CHCl_3$ (0.22 mmol in 370 μL) solution was added dropwise and the mixture stirred at room temperature for an additional 40 min. Precipitation with 100 mL of ice-cold ether, followed by an ether wash (100 mL) and filtration afforded a red solid. The final product was obtained in 89% yield (102 mg) by recrystallization from 5 mL acetone/ether (1:1).

14-Bromodaunorubicin HCl (76). ^{1}H NMR (DMSO-d6, 400 MHz) δ 13.92 (s, 1H), 13.13 (s, 1H), 7.81 (m, 2H), 7.75 (s, 2H), 7.56 (dd, 1H, J_1 = 2.1, J_2 = 8.2 Hz), 5.22 (m, 1H), 4.85 (m, 1H), 4.12 (q, 1H, J = 7.7 Hz), 3.90 (s, 5H), 3.52 (s, 1H), 3.31 (m, 1H), 3.06 (d, 1H, J = 19.1), 2.83 (d, 1H, J = 33.1 Hz), 2.43 (q, 2H, J = 2.0 Hz), 2.21 (d, 1H, J = 14.3), 1.89 (dd, 1H, J_1 = 3.9, J_2 = 12.7 Hz), 1.68 (d, 1H, J = 11.6 Hz)), 1.18 (d, 3H, J = 5.7 Hz); ^{13}C NMR (DMSO-d6, 100 MHz): δ 213.7, 205.6, 186.4, 186.3, 160.7, 156.0, 154.4, 154.3, 136.2, 135.1, 134.6, 133.8, 119.9, 119.7, 119.0, 110.7, 99.1, 96.5, 89.4, 75.4, 69.7, 66.1, 56.6, 54.0, 40.1, 39.7, 34.1, 18.5, 16.7, MS (ESI+): m/z (intensity), 606.3 ([M+H]+, 100%).

Synthesis of 2-((2S,4S)-4-(((2R,4S,5S,6S)-4-((((9H-fluoren-9-yl)methoxy)carbonyl)amino)-5-hydroxy-6-methyltetrahydro-2H-pyran-2-yl)oxy)-2,5,12-trihydroxy-7-methoxy-6,11-dioxo-1,2,3,4,6,11-hexahydrotetracen-2-yl)-2-oxoethyl (S)-7-(3-amino-3-oxopropyl)-2,2-dimethyl-6,9-dioxo-4,10-dioxa-5,8-diazatridec-12-enoate (Alloc-Gln-NH-O-CH_2-C(Me)$_2$C(O)-14-*O*-(Fmoc-Dox), 58a1)

Alloc-Gln-NH-O-CH_2-C(Me)$_2$COOH (297 mg, 0.86 mmol) was converted to its sodium salt as previously described, added to a 10-mL acetone solution of 14-daunorubicinicin

HCl (50 mg, 0.078 mmol) in the presence of 3Å molecular sieves, and the mixture stirred at room temperature for 48 h. After adding 10 mL of methanol, the mixture was centrifuged at 3000 rpm for 15 min. The supernatant was collected, dried *in vaccuo* and reconstituted in 1 mL of anhydrous ACN in the presence of DIEA (2 eq.). Protection the aminoglycoside was carried out with the addition of Fmoc-Osu (27 mg, 0.08 mmol) and stirring the mixture for 30 min at room tempertaure. Two-step FCC purification from DCM/ACN; DCM/(20%MeOH/DCM) afforded 31 mg of crude (36% yield, >90% pure) Fmoc-Dox-PAD-Gln-Alloc as a dark orange solid (m/z = 1093.3). Alloc-deprotection was performed with tetrakis(triphenylphosphine)palladium(0) (3 mg, 0.0028 mmol)/ dimedone (27 mg, 0.19 mmol) in 2 mL of anhydrous THF at room temperature for 2 h. After removing THF, the amine was redissolved in 1 mL of anydrous DMF and triturated with 20 mL of ice-cold ether. The pellet was collected after centrifugation at 3000 rpm, and the tituration step was repeated two additional times to remove residual catalyst. The crude orange solid was used for the next step without further purification.

2-((2S,4S)-4-(((2R,4S,5S,6S)-4-((((9H-fluoren-9-yl)methoxy)carbonyl)amino)-5-hydroxy-6-methyltetrahydro-2H-pyran-2-yl)oxy)-2,5,12-trihydroxy-7-methoxy-6,11-dioxo-1,2,3,4,6,11-hexahydrotetracen-2-yl)-2-oxoethyl (S)-7-(3-amino-3-oxopropyl)-2,2-dimethyl-6,9-dioxo-4,10-dioxa-5,8-diazatridec-12-enoate (58a1). ^{1}H NMR (DMSO-d6, 400 MHz): δ 11.31 (s, 2H), 7.73 (m, 2H), 7.63 (m, 2H), 7.40 (m, 2H), 7.32 (m, 2H), 6.76 (m, 1H), 5.64 (s, 1H), 5.22 (m, 3H), 4.96 (s, 1H), 4.52 (d, 2H, J = 5.7 Hz), 4.40 (m, 1H), 4.00 (s, 3H), 3.77 (s, 2H), 3.52 (m, 1H), 3.46 (m, 1H), 2.86 (d, 1H, J = 17.9 Hz), 2.09 (m, 8H), 1.27 (s, 6H), 1.11 (d, 3H, J = 2.8 Hz); ^{13}C NMR (DMSO-d6, 100 MHz): δ 210.2, 186.4 176.4, 173.4, 172.7, 167.7, 156.1, 155.8, 140.6, 133.5, 133.4,

127.5, 127.0, 125.2, 120.2, 117.1, 75.2, 65.7, 64.1, 56.5, 42.4, 41.9, 40.1, 39.9, 39.7, 38.9, 31.3, 25.2, 23.2, 22.2, 22.0, MS (ESI+): m/z (intensity), 1093.4 ([M+H]+, 100%).

Synthesis of benzyl 3-((1,3-dioxoisoindolin-2-yl)oxy)-2,2-dimethylpropanoate (78)

A solution of diisopropylazodicarboxylate (DIAD, 0.52 mL, 2.8 mmol) prepared in 2 mL anhydrous THF) was slowly added to a stirred mixture of benzyl 3-hydroxy-2,2-dimethylpropanoate (590 mg, 2.8 mmol), triphenylphosphine (820 mg, 3.1 mmol) and *N*-hydroxyphthalimide (510 mg, 3.1 mmol) prepared in 20 mL anhydrous THF at 0 °C. After stirring the mixture at room temperature under a nitrogen atmosphere for 24 h, THF was removed under reduced pressure and the residue re-dissolved in 40 mL of ethyl acetate. The ethyl acetate mixture was washed with water (10 mL) three times, brine and dry-loaded onto a 40-g silica column. The final product was obtained in 73% yield (730 mg) as a white solid after FCC purification (hexane/ethyl acetate).

Benzyl 3-((1,3-dioxoisoindolin-2-yl)oxy)-2,2-dimethylpropanoate (78). ^{1}H NMR ($CDCl_3$, 400 MHz): δ 7.84 (m, 2H), 7.76 (s, 2H), 7.39 (m, 5H), 5.19 (s, 2H), 4.32 (s, 2H), 1.42 (s, 6H); ^{13}C NMR (CDCl3, 100 MHz): δ 175.0, 163.1, 136.0, 134.4, 129.0, 128.5, 128.1, 123.5, 83.6, 66.7, 43.2, 22.2, MS (ESI+): m/z (intensity), 354.4 ([M+H]+, 100%).

Synthesis of 3-((1,3-dioxoisoindolin-2-yl)oxy)-2,2-dimethylpropanoic acid (78a)

Hydrogenation of benzyl 3-((1,3-dioxoisoindolin-2-yl)oxy)-2,2-dimethylpropanoate (570 mg, 1.6 mmol) was accomplished in the presence of 10% Pd-C in 20 mL de-aerated methanol at room temperature for 5 h. The mixture was filtered through a layer of celite and concentrated to a crude oil (345 mg, 82%), which was used for the next step without further purification.

Synthesis of 3-(aminooxy)-2,2-dimethylpropanoic acid (NH_2-O-CH_2-C(Me)$_2$COOH, 79)

To a solution of 3-((1,3-dioxoisoindolin-2-yl)oxy)-2,2-dimethylpropanoic acid (150 mg, 0.57 mmol) prepared in 10 mL of anhydrous diethyl ether was added 36 μL (1.1 mmol) of 98% anhydrous hydrazine, and the mixture stirred at room temperature under a nitrogen atmosphere for 2 h. The mixture was filtered and the filtrate concentrated to generate 78 mg of crude NH_2-O-CH_2-C(Me)$_2$COOH (white solid) which was used for the next step without further purification.

Synthesis of Fmoc-Gln-OSu (81)

To a stirred solution (20 mL of ACN) of Fmoc-Gln(Trt)-OH (611 mg, 1.0 mmol) and HOSu (150 mg, 1.3 mmol) was added EDC (290 mg, 1.5 mmol), and the mixture stirred at room temperature under nitrogen atmosphere for 2 h. ACN was removed under reduced pressure and the residue dissolved in 40 mL of DCM. The organic layer was washed with 10 mL water (2x), brine and dried over sodium sulfate. DCM was removed under reduced pressure, and the residue treated with 10 mL of 95%TFA at room temperature for 5 min. FCC purification (20% MeOH/DCM) afforded 471 mg of crude Fmoc-Gln-Osu (**81**) as a white solid.

Synthesis of (S)-5-(3-amino-3-oxopropyl)-1-(9H-fluoren-9-yl)-10,10-dimethyl-3,6-dioxo-2,8-dioxa-4,7-diazaundecan-11-oic acid (Fmoc-Gln-NH-O-CH_2-C(Me)$_2$COOH, 82).

Crude NH_2-O-CH_2-C(Me)$_2$COOH (450 mg, 3.3 mmol) and Fmoc-Gln-OSu (466 mg, 1.0 mmol) were dissolved in 5 mL of anhydrous DMF and the mixture stirred at room temperature under nitrogen atmosphere for 24 h. DMF was removed under reduced

pressure and the residue dry-loaded onto a 40 g silica column. FCC purification (DCM/ACN/(20%MeOH/DCM)) afforded Fmoc-Gln-NH-O-CH_2-C(Me)$_2$COOH as a white solid in 66% yield (321 mg).

(S)-5-(3-amino-3-oxopropyl)-1-(9H-fluoren-9-yl)-10,10-dimethyl-3,6-dioxo-2,8-dioxa-4,7-diazaundecan-11-oic acid (82). ^{1}H NMR (CD_3OD, 400 MHz): δ 7.81 (d, 2H, J = 7.61 Hz), 7.68 (d, 2H, J = 5.71 Hz), 7.40 (t, 2H, J = 6.66 Hz), 7.33 (t, 2H, J = 7.61 Hz), 4.39 (d, 2H, J = 3.76 Hz), 4.23 (t, 1H, J = 6.88 Hz), 3.94 (s, 2H), 2.29 (m, 2H), 2.06 (m, 2H), 1.26 (s, 6H); ^{13}C NMR (CD_3OD, 100 MHz): δ 145.3, 145.2, 142.6, 134.0, 128.8, 128.2, 126.6, 126.2, 120.9, 83.5, 68.0, 53.8, 49.6, 43.8, 32.4, 28.9, 22.9, MS (ESI+): m/z (intensity), 484.3 ([M+H]+, 100%).

Synthesis of 2-((2S,4S)-4-(((2R,4S,5S,6S)-4-(((allyloxy)carbonyl)amino)-5-hydroxy-6-methyltetrahydro-2H-pyran-2-yl)oxy)-2,5,12-trihydroxy-7-methoxy-6,11-dioxo-1,2,3,4,6,11-hexahydrotetracen-2-yl)-2-oxoethyl 3-(((S)-2,5-diamino-5-oxopentanamido)oxy)-2,2-dimethylpropanoate (Fmoc-Gln-NH-O-CH_2-C(Me)$_2$C(O)-14-*O*-(Alloc-Dox), 58b1)

Fmoc-Gln-NH-O-CH_2-C(Me)$_2$COOH (335 mg, 0.66 mmol) was converted to its sodium salt as previously described, added to a 10-mL acetone solution of 14-daunorubicin HCl (53 mg, 0.083 mmol) in the presence of 3Å molecular sieves, and the mixture stirred at room temperature for 48 h. After adding 10 mL of methanol, the mixture was centrifuged at 3000 rpm for 15 min. The supernatant was collected, dried *in vaccuo* and reconstituted in 4 mL of anhydrous ACN. Protection the aminoglycoside was carried out with the addition of Alloc-Osu (33 mg, 0.17 mmol) in the presence of 2 equivalents of $NaHCO_3$ (suspension) and stirring the mixture for 1 h at room tempertaure. Two-step FCC

purification from DCM/ACN; DCM/(20%MeOH/DCM) afforded the title compound in 40% yield (40 mg, greater than 90% pure by LC-UV). Fmoc-deprotection of Fmoc-Gln-NH-O-CH_2-C(Me)$_2$C(O)-14-*O*-(Alloc-Dox) was performed with 1% DBU in 1 mL of anhydrous DMF at room temperature in 10 min. Trituration with 10 mL of ice-cold ether followed by centrifugation at 3000 rpm afforded a dark orange solid wich was purified by HPLC (10 mM ammonium acetate/ACN) to afford 17 mg of crude H-Gln-NH-O-CH_2-C(Me)$_2$C(O)-14-*O*-(Alloc-Dox) (**58b**).

2-((2S,4S)-4-(((2R,4S,5S,6S)-4-(((allyloxy)carbonyl)amino)-5-hydroxy-6-methyltetrahydro-2H-pyran-2-yl)oxy)-2,5,12-trihydroxy-7-methoxy-6,11-dioxo-1,2,3,4,6,11-hexahydrotetracen-2-yl)-2-oxoethyl 3-(((S)-2,5-diamino-5-oxopentanamido)oxy)-2,2-dimethylpropanoate (58b1).

^{1}H NMR (DMSO-d6, 400 MHz): δ 11.32 (s, 2H), 7.90 (m, 2H), 7.69 (m, 2H), 7.41 (m, 2H), 7.30 (m, 3H), 5.61 (s, 1H), 5.24 (m, 3H), 4.94 (s, 1H), 4.54 (d, 2H, J = 5.4 Hz), 4.46 (m, 1H), 3.99 (s, 3H), 3.87 (s, 2H), 3.81 (m, 1H), 3.64 (m, 1H), 2.96 (d, 1H, J = 18.5 Hz), 2.10 (m, 8H), 1.27 (s, 6H), 1.11 (d, 3H, J = 2.9 Hz); ^{13}C NMR (DMSO-d6, 100 MHz): δ 210.0, 202.0, 174.5, 173.4, 172.7, 156.0, 154.5, 143.7, 140.6, 133.6, 127.6, 127.0, 125.3, 120.0, 116.8, 75.2, 66.7, 65.7, 64.1, 56.5, 46.6, 42.4, 40.1, 39.9, 39.7, 38.9, 31.2, 25.2, 22.1, 22.0, MS (ESI+): m/z (intensity), 1093.2 ([M+H]+, 100%).

Synthesis of prodrug 63 (GABA←mGly-Ala-Ser-Chg-Gln-NH-O-CH_2-C(Me)$_2$C(O)-14-*O*-Dox)

Fm-GABA←mGly-Ala-Ser-Chg-OH (7.6 mg, 0.011 mmol) and H-Gln-NH-O-CH_2-C(Me)$_2$C(O)-14-*O*-(Alloc-Dox) (5 mg, 0.0057 mmol) were dissolved in 300 μL of anhydrous DMF in the presence of DIEA (3 eq.) and the mixture allowed to stir under

nitrogen at 0 °C for 10 min. A solution of HATU (4.1 mg, 0.011 mmol, 200 μL in anhydrous DMF) was added dropwise, and the mixture stirred at 0 °C for 1 h to warm-up to room temperature in 1h. Trituration with 5 mL of ice-cold water, followed by centrifugation afforded a dark orange solid which was dissolved in 5 mL of methanol and dried over sodium sulfate. After removing methanol under reduced pressure, the residue was dissolved in 500 μL of anyhdrous THF in the presence of dimedone (11 mg, 0.08 mmol), and catalytic tetrakis(triphenylphosphine)palladium(0) added. The mixture was stirred at room temperature for 1 h to allow complete deprotection of the Alloc-protecting group. Addition of 5 mL of ice-cold ether followed by centrifugation at 10,000 rpm (repeated 3 three times) gave an orange solid which was re-dissolved in 500 μL of anyhdrous DMF. Fm-deprotection was performed with 2% DBU at room temperature in 10 min. The mixture was triturated with ice-cold ether as previously described, and the final peptide conjugate obtained in 18% yield (1.3 mg) after HLPC purification. GABA←mGly-Ala-Ser-Chg-Gln-NH-O-CH_2-C$(Me)_2$C(O**)**-14-*O*-Dox**;** HRMS (ESI+): *m/z* calc'd for $C_{58}H_{79}N_8O_{23}$: $[M+H]^+$= 1255.5258, found: 1255.5254.

Synthesis of 2-fluoro-4-nitrobenzyl alcohol (84)

EDC (2.3 g, 12 mmol) was added to a stirred 60-mL anhydrous THF solution of 2-fluoro-4-nitrobenzoic acid (2.0 g, 11 mmol) and HOBt (1.6 g, 12 mmol) under nitrogen. The reaction was conducted at room temperature for 1 h to generate the OBt ester. After removing EDU by filtration, the OBt ester solution was added to a 60-mL suspension of sodium borohydride in anhydrous THF drop-wise (over 30 min) and the mixture stirred at room temperature under nitrogen atmosphere for 1.5 h. The reaction was quenched with 20 mL of 1 N HCl, THF removed and the aqueous portion extracted with 40 ml ethyl

acetate. The combined organic phase was washed with 20 mL of water, brine and dried over sodium sulfate. Ethyl acetate was removed under reduced pressure, and the product obtained as an off-white solid in 86% yield (1.6 g).

2-Fluoro-4-nitrobenzyl alcohol (84). ^{1}H NMR (CD_3OD, 400 MHz): δ 8.00 (d, 1H, J_1 = 1.2 Hz, J_2 = 4.2 Hz), 7.87 (dd, 1H, J_1 = 1.2 Hz, J_2 = 5.0 Hz), 7.67 (t, 1H, J = 7.9 Hz), 4.66 (s, 2H); ^{13}C NMR (CD_3OD, 100 MHz): δ 162.0, 159.5, 137.8, 130.4, 120.4, 111.5, 58.3, MS (ESI+): m/z (intensity), 172.1 ([M+H]+, 100%).

Synthesis of 2-fluoro-4-aminobenzyl alcohol (85)

Reduction of 2-fluoro-4-nitrobenzyl alcohol (500 mg, 2.9 mmol) was accomplished by hydrogenation in the presence of 10% Pd-C in 10 mL de-aerated methanol at room temperature for 5 h. The mixture was filtered through a layer of celite and the product collected as an off-white solid in quasi-quantitative yield (410 mg, 99%).

2-Fluoro-4-aminobenzyl alcohol (85). ^{1}H NMR (CD_3OD, 400 MHz): δ 7.11 (t, 1H, J = 9.0 Hz), 6.48 (dd, 1H, J_1 = 1.2 Hz, J_2 = 4.0 Hz), 6.41 (dd, 1H, J_1 = 1.2 Hz, J_2 = 7.1 Hz), 4.51 (s, 2H); ^{13}C NMR (CD_3OD, 100 MHz): δ 162.0, 150.9, 131.9, 117.5, 111.7, 102.3, 58.9, MS (ESI+): m/z (intensity), 142.1 ([M+H]+, 100%).

Synthesis of 2-fluoro-4-azidobenzyl alcohol (86)

To a 40-mL suspension of 2-fluoro-4-aminobenzyl alcohol (1.1 g, 7.8 mmol) in 10% HCl was added 3 mL of a sodium nitrite (650 mg, 9.4 mmol) solution, and the mixture stirred at 0 °C for 30 min, after which 3 mL of a sodium azide (760 mg, 12 mmol) solution was added and the reaction carried out at 0 °C for 1 h. The product was extracted with 120 mL of ethyl acetate. The combined organic phase was washed with 20 mL of water, brine

and dried over sodium sulfate. Ethyl acetate was removed under reduced pressure, and the product obtained after FCC (hexane/ethyl acetate) in 63% yield (820 mg).

2-Fuoro-4-azidobenzyl alcohol (86). ^{1}H NMR (CD_3OD, 400 MHz): δ 7.49 (t, 1H, J = 8.1 Hz), 6.93 (d, 1H, J = 4.2 Hz), 6.83 (d, 1H, J = 6.1 Hz), 4.64 (s, 2H); ^{13}C NMR (CD_3OD, 100 MHz): δ 161.2, 142.4, 131.8, 126.4, 115.8, 107.2, 58., MS (ESI+): m/z (intensity), 168.1 ([M+H]+, 5%).

Synthesis of 2-fluoro-4-azidobenzyl phosphoramide mustard (87)

A 2 M solution of BuLi (2.7 mL in cyclohexane, 5.4 mmol) was added via syringe to 2-fluoro-4-azidobenzyl alcohol (830 mg, 5.0 mmol) in 20 mL anhydrous THF and the mixture stirred at -78 °C for 20 min. The mixture was cannulated into a pre-cooled 20 mL THF solution of bis (2-chloroethyl)phospharimidic dichloride and the reaction carried out at -78 °C for 2 h. The phoshoramidate dichloride ester solution was then bubbled with ammonia at -78 °C for 10 min to afford the desired product. After allowing the mixture to gradually warm up to room temperature in 1 h, solvents were removed under reduced pressure and the residue dissolved in 40 mL DCM. The DCM solution was washed with 10 mL water, brine and dried over sodium sulfate. The product was obtained as light-yellow solid following dry-loading on silica and FCC purification in 60% yield (1.1 g)

2-Fluoro-4-azidobenzyl phosphoramide mustard (87). ^{1}H NMR (CD_3OD, 400 MHz): δ 7.54 (t, 1H, J = 8.1 Hz), 6.96 (dd, 1H, J_1 = 1.4 Hz, J_2 = 3.7 Hz), 6.90 (dd, 1H, J_1 = 1.0 Hz, J2 = 4.9 Hz), 5.03 (d, 2H, J = 3.6 Hz), 3.66 (t, 4H, J = 6.5 Hz), 3.42 (m, 4H, J = 7.9 Hz); ^{13}C NMR (CD_3OD, 100 MHz): δ 161.5, 143.8, 132.8, 122.1, 116.0, 107.5, 61.7, 50.7, 43.1, MS (ESI+): m/z (intensity), 369.7 ([M+H]+, 100%).

Synthesis of TFA-Gln-OH (88)

To a 15 mL solution of H-Gln (2.0 g, 14 mmol) in 1 N NaOH was added 2.3 mL of S-ethyltrifluoroacetate (18 mmol) and the mixture stirred at room temperature for 24 h. The reaction mixture was acidified to pH 2 with 12 N HCl and extracted with 30 mL ethyl acetate (6x). The combined organic layer was washed with water, brine and dried over sodium sulfate. Ethyl acetate was removed under reduced pressure, and the product collected as a white solid in 80% yield (2.7 g).

TFA-Gln-OH (88). ^{1}H NMR (DMSO-d6, 400 MHz): δ 13.0 (s, 1H), 9.89 (d, 1H, J = 8.1 Hz), 7.43 (s, 1H), 6.91 (s, 1H), 4.32 (m, 1H), 2.23 (m, 2H), 2.14 (m, 1H), 1.94 (m, 1H); ^{13}C NMR (DMSO-d6, 100 MHz): δ 173.4, 171.7, 156.3, 117.2, 52.2, 31.0, 25.5, MS (ESI+): m/z (intensity), 243.1 ([M+H]+, 40%).

Synthesis of 2-fluoro-4-glutaminylaminobenzyl phosphoramide mustard (90)

TFA-Gln was coupled to 2-fluoro-4-azidobenzyl phosphoramide mustard linker using our previously described selenocarboxylate/azide amidation strategy.[194] The LiAlHSe reagent was freshly prepared (1.62 mmol in 10 mL of anhydrous THF at -15 °C under nitrogen atmosphere in 30 min) and added to a 10-mL solution of the mixed anhydride of TFA-Gln via cannula to generate the selenocarboxlate in situ at -15 °C under nitrogen atmosphere in 30 min. The mixed anhydride of TFA-Gln was obtained by adding isopropyl chloroformate (1.6 mL, 1.6 mmol) to a 10-mL solution of TFA-Gln (390 mg, 1.6 mmol) in the presence of N-methylpiperidine (200 μL, 1.6 mmol) and stirring the mixture at -15 °C under nitrogen atmosphere for 30 min. A solution of 2-fluoro-4-azidobenzyl phosphoramide mustard (0.81 mmol in 3 mL anhydrous THF) was subsequently added to the selenocarboxylate via cannula and the mixture stirred at room temperature for 20 h. After filtering out selenium and evaporating all solvents, the crude

mixture was dry-loaded on silica and purified by FCC. The product was obtained as an off-white solid in 54% yield (250 mg) and confirmed by NMR. TFA-protected 2-fluoro-4-glutaminylaminobenzyl phosphoramide mustard (960 mg, 1.7 mmol) was treated with 4 eq. of K_2CO_3 in ACN/water (3:1) at room temperature for 48 h. Solvents were removed and the residue re-suspended in 20 mL of a 25% MeOH/DCM solution containing 1% NH_4OH. The mixture was centrifuged at 3000 RPM for 15 min, and the supernatant collected and dried to afford 462 mg of crude 2-fluoro-4-glutaminylaminobenzyl phosphoramide mustard.

2-Fluoro-4-(*N*$^{\alpha}$-trifluoracetyl-*L*-glutaminyl)aminobenzyl phosphoramide mustard (TFA-NH-2-F-Bz-phosphoramide mustard, 89). ^{1}H NMR (CD_3OD, 400 MHz): δ 7.10 (t, 1H, J = 8.2 Hz), 6.74 (td, 1H, J_1 = 1.4 Hz, J_2 = 4.2 Hz), 3.83 (s, 1H), 3.35 (t, 2H, J = 7.6 Hz), 2.26 (t, 2H, J = 9.2 Hz), 1.94 (m, 2H); ^{13}C NMR (CD_3OD, 100 MHz): δ 177.7, 161.7, 154.0, 133.2, 126.8, 122.6, 115.9, 107.7, 50.8, 31.7, 29.8, 25.4, 18.7, MS (ESI+): m/z (intensity), 567.6 ([M+H]+, 100%).

Synthesis of prodrug 65 (Glutaryl-Ser-Ala-Ser-Chg-Gln-NH-2-F-Bz-phosphoramide mustard)

Fm-glutaryl-Ser-Ala-Ser-Chg-OH was prepared using out using standard automated peptide synthesis procedures. Fm-glutaryl-Ser-Ala-Ser-Chg-OH (40 mg, 0.058 mmol) and HBTU (22 mg, 0.058 mmol) were dissolved in the presence of 2.6 eq. DIEA in 250 μL of anhydrous DMF at 0 °C. 2-Fluoro-4-glutaminylaminobenzyl phosphoramide mustard (21 mg, 0.044 mmol) was added and the mixture stirred at 0 °C for 30 min, and allowed to warm up to room temperature in 30 min. The mixture was cooled to 0 °C and 4 mL of ice-cold water added drop-wise. After stirring the resulting suspension at 0 °C

for an additional 30 min, the precipitate was collected by centrifugation, washed with 2 mL ice-cold water (2x) and dried under reduced pressure. The crude solid was re-dissolved in 250 μL of anhydrous DMF and de-protected with 10% DEA. The mixture was triturated with ice-cold ether and the final peptide conjugate obtained in 26% yield (11 mg) after HLPC purification. Glutaryl-Ser-Ala-Ser-Chg-Gln-NH-2-F-Bz-phosphoramide mustard; HRMS (ESI+): *m/z* calc'd for $C_{38}H_{60}Cl_2FN_9O_{13}P$: $[M+H]^+$= 970.3409, found: 970.3417.

Synthesis of Fm-GABA←mGly-Ala-Ser-Chg-OH (55)

The Fm-GABA←mGly-OSu ester was freshly prepared as previously described and coupled to the amino end of H-Ala-Ser-Chg-OH. The tri-peptide was generated using standard automated peptide synthesis procedures. The OSu ester (410 mg, 0.87 mmol) was directly coupled (within 1 min) to H-Ala-Ser-Chg-OH (230 mg, 0.73 mmol) in 1 mL ACN/NMP (1:2) in the presence of 1 eq. DIEA. After FCC purification, the final peptide was obtained in 56% yield (270 mg).

Alternate Synthesis

Fm-GABA←mGly-OSu ester was freshly prepared as previously described from Fm-GABA←mGly (210 mg, 0.57 mmol), HOSu (66 mg, 0.57 mmol) and EDC (130 mg, 0.68 mmol) in 3 mL of anhydrous DCM at room temperature under a nitrogen atmosphere for 1 h. The reaction mixture was diluted to a 10-mL solution in DCM/DMF (9:1), added to the amino end of H-Ala-Ser-Chg-resin (0.5 g, 0.27 mmol) and the mixture stirred at room temperature under nitrogen atmosphere for 24 h; the resin-bound tri-peptide was generated on Wang resin using standard automated peptide synthesis procedures. The final peptide was cleaved off the resin with three 10-mL portions of 95%TFA/DCM. TFA

was azeotroped off with 30-mL portions (5x) and the final peptide (180 mg) was ready to be used for the next step without further purification.

Synthesis of prodrug 66 (GABA←mGly-Ala-Ser-Chg-Gln-NH-2-F-Bz-phosphoramide mustard)

Fm-GABA←mGly-Ala-Ser-Chg-OH (40 mg, 0.060 mmol) and HBTU (23 mg, 0.060 mmol) were dissolved in the presence of 2.6 eq. DIEA in 250 μL of anhydrous DMF at 0 °C. 2-Fluoro-4-glutaminylaminobenzyl phosphoramide mustard (16 mg, 0.055 mmol) was added and the mixture stirred at 0 °C for 30 min to warm-up to room temperature in 30 min. The mixture was cooled to 0 °C and 4 mL of ice-cold water added drop-wise. After stirring the resulting suspension at 0 °C for an additional 30 min, the precipitate was collected by centrifugation, washed with 2 mL of ice-cold water (2x) and dried under reduced pressure. The crude solid was re-dissolved in 250 μL of anhydrous DMF and de-protected with 10% DEA. The mixture was triturated with ice-cold ether and the final peptide conjugate obtained in 28% yield (10 mg) after HLPC purification. GABA←mGly-Ala-Ser-Chg-Gln-NH-2-F-Bz-phosphoramide mustard; HRMS (ESI+): *m/z* calc'd for $C_{37}H_{58}Cl_2FN_9O_{12}P$: $[M+H]^+$= 940.3304, found: 940.3311.

III. Biological Assays and Metabolism Studies

A. Measurement of Peptide Concentration and the PSA Enzyme Assay

1. AMC-conjugates

Peptide concentrations for AMC-conjugates were determined by measuring the UV absorbance at 324 nm of 20 μM solutions prepared (based on weight) in methanol from 10 mM DMSO stock solutions. Using the extinction coefficient of Boc-Gln-AMC at 324

nm (12,800 M-1.cm-1), peptide concentrations were calculated and adjusted accordingly to prepare 10 μM solutions in 50 mM Tris buffer, pH 8 containing 2 mM $CaCl_2$ and 0.1% Tween 20. Each peptide solution (4 μL) was added to 36 μL of Tris buffer (final concentration 1 μM) in triplicate wells of a white Costar 384-well plate (Corning, Inc., Corning, NY) and centrifuged at 3,000 RPM for 1 min. Reactions were initiated with the addition of 4 μL aliquots of a 1.1 μM solution of human PSA (final concentration 100 nM), and time points recorded over a period of 3 h. The stability of peptide conjugates in 50 mM Tris buffer was evaluated by measuring the fluorescence of 1 μM solutions throughout the course of the assay. Buffer fluorescence was measured by adding 40 μL aliquots of 50 mM Tris buffer to separate wells in triplicate. All wells were read using a 335 nm/460 nm (ex/em) filters on a Victor 3V 1420 Multilabel Counter (PerkinElmer Life and Analytical Sciences, Shelton, CT, USA). PSA cleavage rates were calculated by taking the slopes of the linear portions of fluorescence counts-time curves and using a fluorescence standard curve generated with known amounts of 7-AMC.

2. Prodrugs

For doxorubicin and phophoramide mustard conjugates, peptide solution concentrations were determined by measuring the UV absorbance at 484 and 254 nm (20 μM for doxorubicin and 50 μM for phosphoramide mustard conjugates, respectively) of solutions prepared (based on weight) in water from 10 mM DMSO stock solutions. Using the extinction coefficients of doxorubicin at 484 nm (10,800 M-1.cm-1) and 2-fluoro-4-glutaminylaminobenzyl phosphoramide mustard at 254 nm (20,800 M-1.cm-1), peptide concentrations were calculated and adjusted accordingly to prepare 100 μM solutions in 50 mM Tris buffer, pH 8 containing 2 mM $CaCl_2$ and 0.1% Tween 20. The stability of

peptide conjugates in 50 mM Tris buffer, pH 8 was determined from 48-h incubations in buffer (Fig. 23). Peptide solutions were prepared in Tris buffer pH 8 at a concentration of 1.11 μM from 1 mM DMSO stock solutions, and warmed up to 37 °C. Reactions were initiated at 37 °C with the addition of 5 μL aliquots of a 10 μM solution of human PSA to 45 μL aliquots of the 1.11 μM peptide solutions in eppendorf vials (total volume 50 μL, final PSA concentration 1 μM), and time points recorded over a period of 3 h. Reactions were terminated at 0, 10, 20, 30, 60, 120, 180 and 360 min by quenching 2 μL aliquots of incubates with 20 μL of chilled 50% ACN containing 0.1 μM internal standard (IS) and 0.1% formic acid (FA) pre-added to eppendorf vials. Samples were centrifuged at 3000 RPM for 15 min and the supernatants analyzed by LC-MS/MS in SRM mode as previously described. The fraction of prodrug remaining at each time point was calculated by dividing the prodrug/IS ratio by the 0-h prodrug/IS area ratio and half-life determined from prodrug disappearance rate.

B. Cell Culture

1. Carcinoma Cell Line Culture

Monolayer cultures of PSA-secreting LNCaP and non-PSA-secreting DU145 human prostate carcinoma cells were conducted in growth medium in a CO_2 incubator under a humidified atmosphere at 37 °C for 3 weeks prior to initiating cytotoxicity experiments. During cell growth, media were changed every 3 days and trypsinization carried out at 80% confluence with a 1:4 split for subsequent cultures. Cells were grown on 96-well plates for 48 h at initial concentrations of 5000 cells/well. At the end of the 48-h period, the growth medium was replaced by serum-free medium RPMI 1640 medium containing L-glutamine (2 mM), 2% TCM, penicillin G (100 units/mL) and streptomycin sulfate

(100 units/mL), and prodrugs added to wells at concentrations ranging from 0.07 to 100 μM. The plates were incubated at 37 °C for 72 h under a humidified CO_2 atmosphere, and cell viability determined using the MTT assay. Briefly, 10 μL aliquots of a 12 mM MTT solution were added to wells and the plates incubated in a CO_2 incubator under a humidified atmosphere at 37 °C for 4 h. Well contents were then solubilized with 1% SDS (100 μL/well) for 12 h, and OD_{570} values measured on a Dynatech MR5000 plate reader. Cell viability was computed as a percentage of control growth, and IC_{50} values determined as the concentration at which cell growth is inhibited by 50%.

2. Hepatocyte Cultures

Cryopreserved mouse or human hepatocytes (10-14 million cells) were thawed in 50 mL CHRM pre-warmed to 37 °C in a water bath. The cell suspensions were centrifuged at 800 RPM for 10 minutes and the pellet re-suspended in 5 mL CHPM by gentle mixing. Cell count and viability were determined using AOPI staining on a Nexcelcom Cellometer (Nexcelom Bioscience, Lawrence, MA). Cell suspensions with viability greater than 80% were diluted with CHPM to a concentration of 0.4 and 0.7 x 10 ^ 6 cells/mL, for mouse and human hepatocytes, respectively, and seeded at 2.5 mL per well on pre-coated collagen plates. Plates were incubated at 37 °C in a 95% humidified incubator at 5% CO_2 for 2-4 h to allow adequate cell attachment before replacing CHPM with the maintenance media spiked with prodrug.

C. Stability Assays

General Sample Treatment Procedures for Stability Studies

Blood samples were collected in sodium-heparin tubes from 15 male adult C57BL/6 mice; the use of EDTA as anticoagulant was avoided due to its anticipated inhibitory

effect on metalloproteases through ion metal chelation. Likewise, human blood was sampled from three adult male volunteers in heparinized collection tubes and stored on ice until use.

1. Stability of 7-AMC Conjugates

Non-specific hydrolysis of peptide conjugates was determined following a procedure similar to the PSA enzyme assay as described previously. Briefly, each peptide solution (4 μL) was added to 36 μL of phosphate buffer, human or mouse plasma (final peptide concentration 1 μM) in a white Costar 384-well plate (Corning, Inc., Corning, NY). The stability of peptide conjugates in 100 mM phosphate buffer, pH 7.4 was evaluated by measuring the fluorescence of 1 μM solutions throughout the course of the assay. Sample evaporation rate was also measured by adding mixtures of 36 μL of plasma and 4 μL of 100 mM phosphate to separate wells in triplicate, and recording fluorescence increase overtime. All wells were read using a 335 nm/460 nm (ex/em) filters on a Victor 3V 1420 Multilabel Counter (PerkinElmer Life and Analytical Sciences, Shelton, CT, USA) over a period of 24 h.

2. Prodrug Stability in Mouse and Human Blood

Stability to non-PSA-mediated hydrolysis was evaluated in heparinized mouse or human blood by incubating each prodrug at a concentration of 100 μM for a period of 24 h at 37 °C. Reactions were initiated by adding 10 μL of a 10 mM solution of each prodrug to 1 mL of mouse or human blood and allowing the mixture to shake at 37 °C in a 95% humidified incubator at 5% CO_2. Reactions were terminated at 0, 0.5, 1, 2, 4, 6 and 24 h by quenching 50 μL aliquots of incubates with 50 μL of chilled ACN containing 0.2 μM internal standard (IS) and 0.1% formic acid (FA) pre-added to 96-well plates. Precipitated

samples were centrifuged at 3000 RPM for 15 min and the supernatants analyzed by LC-MS/MS in SRM mode (Table 10). The fraction of prodrug remaining at each time point was calculated by dividing its prodrug/IS area ratio by the prodrug/IS area ratio at 0 h.

3. Prodrug Stability in Cultured Mouse and Human Hepatocytes

Prodrug incubations were initiated at a concentration of 100 μM by diluting 25 μL of 10 mM DMSO solutions in 2.5 mL of maintenance media added to 1.75 million cells per well. Reactions were carried out at 37 °C in a 95% humidified incubator at 5% CO_2. At 0, 0.5, 1, 2, 4, 8, 24 and 48 h, 50 μL aliquots of incubates were sampled and quenched 50 μL of chilled ACN containing 0.2 μM internal standard (IS) and 0.1% FA pre-added to 96-well plates. Precipitated samples were centrifuged at 3000 RPM for 15 min and the supernatants analyzed by LC-MS/MS in SRM mode. The fraction of prodrug remaining at each time point was calculated as previously described.

D. Prodrug Metabolism

1. Prodrug Metabolism in Blood and Cultured Hepatocytes

For each prodrug, 200 μL aliquots were drawn at 1, 2, 4, 8, and 24 h from blood and 1, 4, 8, 24 and 48 h from plated hepatocyte incubations, and quenched with 400 μL of chilled ACN containing 0.1% FA. Samples were centrifuged at 3000 RPM for 15 min, the supernatant removed and dried under a gentle stream of nitrogen. Residues were reconstituted in 100 μL of ACN:water (1:1) and analyzed by LC-MS system with accurate mass determination.

2. Prodrug Metabolism by Bacterial Thermolysin and Human Neprilysin

Each doxorubicin conjugate was incubated with human neprilysin (50 μg/ml) or thermolysin (300 μg/ml) at 100 μM by adding 5 μL of a 10 mM prodrug solution (in

DMSO) to 455 μL of 100 mM Tris/HCl buffer, pH 7.4 containing 3 mM $CaCl_2$ and shaking the mixture in a 37 °C water bath over the course of the reaction. Incubates (50 μL aliquots) were sampled at 10, 20, 30, and 60 min for thermolysin and 15, 30, 60 and 120 min for neprilysin. Reactions were terminated by adding 50 μL of chilled ACN, the mixtures centrifuged at 10000 rpm for 5 min and the supernatants were analyzed by LC-MS.

REFERENCES

(1) Brawley, O. W. Prostate cancer epidemiology in the United States. *World J. Urol.* **2012,** 30, 195-200.

(2) Siegel, R.; Ma, J.; Zou, Z.; Jemal, A. Cancer statistics, 2014. *CA-Cancer J. Clin.* **2014,** 64, 9-29.

(3) NCI Surveillance Epidemiology and End Results (SEER) Program. Cancer statistics review, 1975-2010, based on November 2012 SEER data submission, posted to the SEER web site, 2013. http://seer.cancer.gov/csr/1975_2010/

(4) O'Keefe, R. J.; Guise, T. A. Molecular Mechanisms of Bone Metastasis and Therapeutic Implications. *Clin. Orthop. Relat. Res.* **2003**, S100-S104.

(5) Roodman, G. D. Mechanisms of Bone Metastasis. *New Engl. J. Med.* **2004,** 350, 1655-1664+1698.

(6) Knudsen, B. S.; Vasioukhin, V. Mechanisms of prostate cancer initiation and progression. *Adv. Cancer Res.* **2010,** 109, 1-50.

(7) Robson, M.; Dawson, N. How is androgen-dependent metastatic prostate cancer best treated? *Hematol. Oncol. Clin. North. Am.* **1996,** 10, 727-747.

(8) Cai, C.; Chen, S.; Ng, P.; Bubley, G. J.; Nelson, P. S.; Mostaghel, E. A.; Marck, B.; Matsumoto, A. M.; Simon, N. I.; Wang, H.; Chen, S.; Balk, S. P. Intratumoral de novo steroid synthesis activates androgen receptor in castration-resistant prostate cancer and is upregulated by treatment with CYP17A1 inhibitors. *Cancer Res.* **2011,** 71, 6503-6513.

(9) de Bono, J. S.; Logothetis, C. J.; Molina, A.; Fizazi, K.; North, S.; Chu, L.; Chi, K. N.; Jones, R. J.; Goodman, O. B.; Saad, F.; Staffurth, J. N.; Mainwaring, P.; Harland, S.; Flaig, T. W.; Hutson, T. E.; Cheng, T.; Patterson, H.; Hainsworth, J. D.; Ryan, C. J.; Sternberg, C. N.; Ellard, S. L.; FlÃ©chon, A.; Saleh, M.; Scholz, M.; Efstathiou, E.; Zivi, A.; Bianchini, D.; Loriot, Y.; Chieffo, N.; Kheoh, T.; Haqq, C. M.; Scher, H. I. Abiraterone and increased survival in metastatic prostate cancer. *New Engl. J. Med.* **2011,** 364, 1995-2005.

(10) Efstathiou, E.; Titus, M.; Tsavachidou, D.; Tzelepi, V.; Wen, S.; Hoang, A.; Molina, A.; Chieffo, N.; Smith, L. A.; Karlou, M.; Troncoso, P.; Logothetis, C. J. Effects of abiraterone acetate on androgen signaling in castrate-resistant prostate cancer in bone. *J. Clin. Oncol.* **2012,** 30, 637-643.

(11) Knudsen, K. E.; Penning, T. M. Partners in crime: deregulation of AR activity and androgen synthesis in prostate cancer. *Trends Endocrinol. Metabol.* **2010,** 21, 315-324.

(12) Mizokami, A.; Koh, E.; Fujita, H.; Maeda, Y.; Egawa, M.; Koshida, K.; Honma, S.; Keller, E. T.; Namiki, M. The adrenal androgen androstenediol is present in prostate cancer tissue after androgen deprivation therapy and activates mutated androgen receptor. *Cancer Res.* **2004,** 64, 765-771.

(13) Shiota, M.; Yokomizo, A.; Naito, S. Increased androgen receptor transcription: a cause of castration-resistant prostate cancer and a possible therapeutic target. *J. Mol. Endocrinol.* **2011,** 47, R25-R41.

(14) Tindall, D.; Lonergan, P. Androgen receptor signaling in prostate cancer development and progression. *J. Carcinog.* **2011,** 10, 20.

(15) Akaza, H.; Hinotsu, S.; Usami, M.; Arai, Y.; Kanetake, H.; Naito, S.; Hirao, Y. Combined androgen blockade with bicalutamide for advanced prostate cancer. *Cancer* **2009,** 115, 3437-3445.

(16) Bennett, C. L.; Tosteson, T. D.; Schmitt, B.; Weinberg, P. D.; Ernstoff, M. S.; S.D., R. Maximum androgen-blockade with medical or surgical castration in advanced prostate cancer: a meta-analysis of nine published randomized controlled trials and 4128 patients using flutamide. *Prostate Cancer Prostatic. Dis.* **1999,** 2, 4-8.

(17) Dijkman, G. A.; Janknegt, R. A.; De Reijke, T. M.; Debruyne, F. M. J. Long-term efficacy and safety of nilutamide plus castration in advanced prostate cancer, and the significance of early prostate specific antigen normalization. *J. Urol.* **1997,** 158, 160-163.

(18) Scher, H. I.; Liebertz, C.; Kelly, W. K.; Mazumdar, M.; Brett, C.; Schwartz, L.; Kolvenbag, G.; Shapiro, L.; Schwartz, M. Bicalutamide for advanced prostate cancer: the natural versus treated history of disease. *J. Clin. Oncol.* **1997,** 15, 2928-38.

(19) Beardsley, E.; Hotte, S.; North, S.; Ellard, S.; Winquist, E.; Kollmannsberger, C.; Mukherjee, S.; Chi, K. A phase II study of sorafenib in combination with bicalutamide in patients with chemotherapy-naive castration resistant prostate cancer. *Invest. New Drugs* **2012,** 30, 1652-1659.

(20) Scher, H. I.; Beer, T. M.; Higano, C. S.; Anand, A.; Taplin, M.-E.; Efstathiou, E.; Rathkopf, D.; Shelkey, J.; Yu, E. Y.; Alumkal, J.; Hung, D.; Hirmand, M.; Seely, L.; Morris, M. J.; Danila, D. C.; Humm, J.; Larson, S.; Fleisher, M.; Sawyers, C. L. Antitumour activity of MDV3100 in castration-resistant prostate cancer: a phase 1-2 study. *Lancet* **2010,** 375, 1437-1446.

(21) Scher, H. I.; Fizazi, K.; Saad, F.; Taplin, M.-E.; Sternberg, C. N.; Miller, K.; Wit, R. D.; Mulders, P.; Hirmand, M.; Selby, B.; Bono, J. S. D. Effect of MDV3100, an androgen receptor signaling inhibitor (ARSI), on overall survival in patients with prostate cancer postdocetaxel: Results from the phase III AFFIRM study. *J. Clin. Oncol.* **2012,** 30, Suppl 5,abstr LBA1.

(22) Attard, G.; Reid, A. H. M.; A'Hern, R.; Parker, C.; Oommen, N. B.; Folkerd, E.; Messiou, C.; Molife, L. R.; Maier, G.; Thompson, E.; Olmos, D.; Sinha, R.; Lee, G.; Dowsett, M.; Kaye, S. B.; Dearnaley, D.; Kheoh, T.; Molina, A.; de Bono, J. S. Selective inhibition of CYP17 with abiraterone acetate is highly active in the treatment of castration-resistant prostate cancer. *J. Clin. Oncol.* **2009,** 27, 3742-3748.

(23) Attard, G.; Reid, A. H. M.; Yap, T. A.; Raynaud, F.; Dowsett, M.; Settatree, S.; Barrett, M.; Parker, C.; Martins, V.; Folkerd, E.; Clark, J.; Cooper, C. S.; Kaye, S. B.; Dearnaley, D.; Lee, G.; de Bono, J. S. Phase I clinical trial of a selective inhibitor of CYP17, abiraterone acetate, confirms that castration-resistant prostate cancer commonly remains hormone driven. *J. Clin. Oncol.* **2008,** 26, 4563-4571.

(24) Danila, D. C.; Morris, M. J.; de Bono, J. S.; Ryan, C. J.; Denmeade, S. R.; Smith, M. R.; Taplin, M.-E.; Bubley, G. J.; Kheoh, T.; Haqq, C.; Molina, A.; Anand, A.; Koscuiszka, M.; Larson, S. M.; Schwartz, L. H.; Fleisher, M.; Scher, H. I. Phase II multicenter study of abiraterone acetate plus prednisone therapy in patients with docetaxel-treated castration-resistant prostate cancer. *J. Clin. Oncol.* **2010,** 28, 1496-1501.

(25) Reid, A. H. M.; Attard, G.; Danila, D. C.; Oommen, N. B.; Olmos, D.; Fong, P. C.; Molife, L. R.; Hunt, J.; Messiou, C.; Parker, C.; Dearnaley, D.; Swennenhuis, J. F.; Terstappen, L. W. M. M.; Lee, G.; Kheoh, T.; Molina, A.; Ryan, C. J.; Small, E.; Scher, H. I.; de Bono, J. S. Significant and sustained antitumor activity in post-docetaxel, castration-resistant prostate cancer with the CYP17 inhibitor abiraterone acetate. *J. Clin. Oncol.* **2010,** 28, 1489-1495.

(26) Ryan, C. J.; Smith, M. R.; de Bono, J. S.; Molina, A.; Logothetis, C. J.; de Souza, P.; Fizazi, K.; Mainwaring, P.; Piulats, J. M.; Ng, S.; Carles, J.; Mulders, P. F. A.; Basch, E.; Small, E. J.; Saad, F.; Schrijvers, D.; Van Poppel, H.; Mukherjee, S. D.; Suttmann, H.; Gerritsen, W. R.; Flaig, T. W.; George, D. J.; Yu, E. Y.; Efstathiou, E.; Pantuck, A.; Winquist, E.; Higano, C. S.; Taplin, M.-E.; Park, Y.; Kheoh, T.; Griffin, T.; Scher, H. I.; Rathkopf, D. E. Abiraterone in metastatic prostate cancer without previous chemotherapy. *New Engl. J. Med.* **2013,** 368, 138-148.

(27) Trump, D. L.; Havlin, K. H.; Messing, E. M.; Cummings, K. B.; Lange, P. H.; Jordan, V. C. High dose ketoconazole in advanced hormone-refractory prostate cancer: endocrinologic and clinical effects. *J. Clin. Oncol.* **1989,** 7, 1093-1098.

(28) Taplin, M. E.; Regan, M. M.; Ko, Y. J.; Bubley, G. J.; Duggan, S. E.; Werner, L.; Beer, T. M.; Ryan, C. W.; Mathew, P.; Tu, S. M.; Denmeade, S. R.; Oh, W. K.; Sartor, O.; Mantzoros, C. S.; Rittmaster, R.; Kantoff, P. W.; Balk, S. P. Phase II study of androgen synthesis inhibition with ketoconazole, hydrocortisone, and dutasteride in asymptomatic castration-resistant prostate cancer. *Clin. Cancer Res.* **2009,** 15, 7099-7105.

(29) Figg, W. D.; Liu, Y.; Arlen, P.; Gulley, J.; Steinberg, S. M.; Liewehr, D. J.; Cox, M. C.; Zhai, S.; Cremers, S.; Parr, A.; Yang, X.; Chen, C. C.; Jones, E.; Dahut, W. L. A randomized, phase II trial of ketoconazole plus alendronate versus ketoconazole alone in patients with androgen independent prostate cancer and bone metastases. *J. Urol.* **2005,** 173, 790-796.

(30) Millikan, R.; Baez, L.; Banerjee, T.; Wade, J.; Edwards, K.; Winn, R.; Smith, T. L.; Logothetis, C. Randomized phase 2 trial of ketoconazole and ketoconazole/doxorubicin in androgen independent prostate cancer. *Urol. Oncol.* **2001,** 6, 111-115.

(31) Fizazi, K.; Carducci, M.; Smith, M.; DamiÃ£o, R.; Brown, J.; Karsh, L.; Milecki, P.; Shore, N.; Rader, M.; Wang, H.; Jiang, Q.; Tadros, S.; Dansey, R.; Goessl, C. Denosumab versus zoledronic acid for treatment of bone metastases in men with castration-resistant prostate cancer: A randomised, double-blind study. *Lancet* **2011,** 377, 813-822.

(32) Kantoff, P. W.; Schuetz, T. J.; Blumenstein, B. A.; Michael Glode, L.; Bilhartz, D. L.; Wyand, M.; Manson, K.; Panicali, D. L.; Laus, R.; Schlom, J.; Dahut, W. L.; Arlen, P. M.; Gulley, J. L.; Godfrey, W. R. Overall survival analysis of a phase II randomized controlled trial of a poxviral-based PSA-targeted immunotherapy in metastatic castration-resistant prostate cancer. *J. Clin. Oncol.* **2010,** 28, 1099-1105.

(33) Daly, M. E.; Makris, A.; Reed, M.; Lewis, C. E. Hemostatic regulators of tumor angiogenesis: A source of antiangiogenic agents for cancer treatment? *J. Natl. Cancer Inst.* **2003,** 95, 1660-1673.

(34) Yu, E. M.; Jain, M.; Aragon-Ching, J. B. Angiogenesis inhibitors in prostate cancer therapy. *Discov. Med.* **2010,** 10, 521-530.

(35) Ning, Y. M.; Gulley, J. L.; Arlen, P. M.; Woo, S.; Steinberg, S. M.; Wright, J. J.; Parnes, H. L.; Trepel, J. B.; Lee, M. J.; Kim, Y. S.; Sun, H.; Madan, R. A.; Latham, L.; Jones, E.; Chen, C. C.; Figg, W. D.; Dahut, W. L. Phase II trial of bevacizumab, thalidomide, docetaxel, and prednisone in patients with metastatic castration-resistant prostate cancer. *J. Clin. Oncol.* **2010,** 28, 2070-2076.

(36) Gohji, K.; Kitazawa, S.; Tamada, H.; Katsuoka, Y.; Nakajima, M. Expression of endothelin receptor A associated with prostate cancer progression. *J. Urol.* **2001,** 165, 1033-1036.

(37) Nelson, J. B.; Fizazi, K.; Miller, K.; Higano, C.; Moul, J. W.; Akaza, H.; Morris, T.; McIntosh, S.; Pemberton, K.; Gleave, M. Phase 3, randomized, placebo-controlled study of zibotentan (ZD4054) in patients with castration-resistant prostate cancer metastatic to bone. *Cancer* **2012,** 118, 5709-5718.

(38) Lewington, V. J.; McEwan, A. J.; Ackery, D. M.; Bayly, R. J.; Keeling, D. H.; Macleod, P. M.; Porter, A. T.; Zivanovic, M. A. A prospective, randomised

double-blind crossover study to examine the efficacy of strontium-89 in pain palliation in patients with advanced prostate cancer metastatic to bone. *Eur. J. Cancer Clin. Oncol.* **1991,** 27, 954-958.

(39) Oosterhof, G. O. N.; Roberts, J. T.; de Reijke, T. M.; Engelholm, S. A.; Horenblas, S.; von der Maase, H.; Neymark, N.; Debois, M.; Collette, L. Strontium(89) chloride versus palliative local field radiotherapy in patients with hormonal escaped prostate cancer: a phase III study of the European Organisation for Research and Treatment of Cancer, Genitourinary Group. *Eur. Urol.* **2003,** 44, 519-526.

(40) Sartor, O.; Reid, R. H.; Hoskin, P. J.; Quick, D. P.; Ell, P. J.; Coleman, R. E.; Kotler, J. A.; Freeman, L. M.; Olivier, P. Samarium-153-Lexidronam complex for treatment of painful bone metastases in hormone-refractory prostate cancer. *Urology* **2004,** 63, 940-945.

(41) Tu, S. M.; Millikan, R. E.; Mengistu, B.; Delpassand, E. S.; Amato, R. J.; Pagliaro, L. C.; Daliani, D.; Papandreou, C. N.; Smith, T. L.; Kim, J.; Podoloff, D. A.; Logothetis, C. J. Bone-targeted therapy for advanced androgen-independent carcinoma of the prostate: A randomised phase II trial. *Lancet* **2001,** 357, 336-341.

(42) Gravis, G.; Fizazi, K.; Joly Lobbedez, F.; Oudard, S.; Priou, F.; Latorzeff, I.; Delva, R.; Krakowski, I.; Laguerre, B.; Rolland, F.; Zanetta, S. Survival analysis of a randomized phase III trial comparing androgen deprivation therapy (ADT) plus docetaxel versus ADT alone in hormone-sensitive metastatic prostate cancer (GETUG-AFU 15/0403). *Ann. Oncol.* **2012,** 23, Suppl 9,abstr. 8930.

(43) Berthold, D. R.; Pond, G. R.; Soban, F.; De Wit, R.; Eisenberger, M.; Tannock, I. F. Docetaxel plus prednisone or mitoxantrone plus prednisone for advanced prostate cancer: Updated survival in the TAX 327 study. *J. Clin. Oncol.* **2008,** 26, 242-245.

(44) Tannock, I. F.; De Wit, R.; Berry, W. R.; Horti, J.; Pluzanska, A.; Chi, K. N.; Oudard, S.; ThÃ©odore, C.; James, N. D.; Turesson, I.; Rosenthal, M. A.; Eisenberger, M. A. Docetaxel plus prednisone or mitoxantrone plus prednisone for advanced prostate cancer. *New Engl. J. Med.* **2004,** 351, 1502-1512.

(45) Regan, M. M.; O'Donnell, E. K.; Kelly, W. K.; Halabi, S.; Berry, W.; Urakami, S.; Kikuno, N.; Oh, W. K. Efficacy of carboplatin-taxane combinations in the management of castration-resistant prostate cancer: A pooled analysis of seven prospective clinical trials. *Ann. Oncol.* **2010,** 21, 312-318.

(46) Amato, R. J.; Sarao, H. A phase I study of paclitaxel/doxorubicin/ thalidomide in patients with androgen- independent prostate cancer. *Clin. Genitourin Cancer* **2006,** 4, 281-286.

(47) Petrylak, D. P. The treatment of hormone-refractory prostate cancer: docetaxel and beyond. *Rev. Urol.* **2006,** 8, S48-S55.

(48) Tannock, I. F., Osoba, D., Stockler, M.R., Ernst, D.S., Neville, A.J., Moore, M.J., Armitage, G.R., Wilson, J.J., Venner, P.M., Coppin, C.M., Murphy, K.C. Chemotherapy with mitoxantrone plus prednisone or prednisone alone for symptomatic hormone-resistant prostate cancer: a Canadian randomized trial with palliative end points. *J. Clin. Oncol.* **1996,** 14, 1756-1764.

(49) Lowenthal, R. M.; Eaton, K. Toxicity of chemotherapy. *Hematol. Oncol. Clin. North. Am.* **1996,** 10, 967-990.

(50) Nielsen, D.; Maare, C.; Skovsgaard, T. Cellular resistance to anthracyclines. *Gen. Pharmacol.* **1996,** 27, 251-255.

(51) Stavrovskaya, A. A. Cellular mechanisms of multidrug resistance of tumor cells. *Biochemistry (Mosc)* **2000,** 65, 95-106.

(52) Rautio, J.; Laine, K.; Gynther, M.; Savolainen, J. Prodrug approaches for CNS delivery. *AAPS J.* **2008,** 10, 92-102.

(53) Bignami, G. S.; Senter, P. D.; Grothaus, P. G.; Fischer, K. J.; Humphreys, T.; Wallace, P. M. *N*-(4'-hydroxyphenylacetyl)palytoxin: a palytoxin prodrug that can be activated by a monoclonal antibody-penicillin G amidase conjugate. *Cancer Res.* **1992,** 52, 5759-5764.

(54) Vrudhula, V. M.; Senter, P. D.; Fischer, K. J.; Wallace, P. M. Prodrugs of doxorubicin and melphalan and their activation by a monoclonal antibody-penicillin-G amidase conjugate *J. Med. Chem.* **1993,** 36, 919-923.

(55) Kerr, D. E.; Senter, P. D.; Burnett, W. V.; Hirschberg, D. L.; Hellstrom, I.; Hellstrom, K. E. Antibody-penicillin-V-amidase conjugates kill antigen-positive tumor cells when combined with doxorubicin phenoxyacetamide. *Cancer Immunol. Immunother.* **1990,** 31, 202-206.

(56) Pedone, E.; Searle, F.; Brocchini, S. Diethylstilbestrol glutamate as a potential substrate for ADEPT. *J. Drug Target.* **2006,** 14, 437-443.

(57) Hao, X. K.; Liu, J. Y.; Yue, Q. H.; Wu, G. J.; Bai, Y. J.; Yin, Y. In vitro and in vivo prodrug therapy of prostate cancer using anti-γ-Sm-scFv/hCPA fusion protein. *Prostate* **2006,** 66, 858-866.

(58) Alaoui, A. E.; Saha, N.; Schmidt, F.; Monneret, C.; Florent, J. C. New Taxol® (paclitaxel) prodrugs designed for ADEPT and PMT strategies in cancer chemotherapy. *Bioorg. Med. Chem.* **2006,** 14, 5012-5019.

(59) Sahin, U.; Hartmann, F.; Senter, P.; Pohl, C.; Engert, A.; Diehl, V.; Pfreundschuh, M. Specific activation of the prodrug mitomycin phosphate by a bispecific anti-

CD30/anti-alkaline phosphatase monoclonal antibody. *Cancer Res.* **1990,** 50, 6944-6948.

(60) Vrudhula, V. M.; Svensson, H. P.; Senter, P. D. Immunologically specific activation of a cephalosporin derivative mitomycin C by monoclonal antibody Î²-lactamase conjugates. *J. Med. Chem.* **1997,** 40, 2788-2792.

(61) Atwell, G. J.; Boyd, M.; Palmer, B. D.; Anderson, R. F.; Pullen, S. M.; Wilson, W. R.; Denny, W. A. Synthesis and evaluation of 4-substituted analogues of 5-[N,N-bis(2-chloroethyl)amino]-2-nitrobenzamide as bioreductively activated prodrugs using an Escherichia coli nitroreductase. *Anti-Cancer Drug Des.* **1996,** 11, 553-567.

(62) Senter, P. D.; Springer, C. J. Selective activation of anticancer prodrugs by monoclonal antibody-enzyme conjugates. *Adv. Drug Del. Rev.* **2001,** 53, 247-264.

(63) Sharma, S. K.; Bagshawe, K. D.; Begent, R. H. J. Advances in antibody-directed enzyme prodrug therapy. *Curr. Opin. Investig. Drugs* **2005,** 6, 611-615.

(64) Miyamoto, H.; Messing, E. M.; Chang, C. Androgen deprivation therapy for prostate cancer: Current status and future prospects. *Prostate* **2004,** 61, 332-353.

(65) Sayed, Y.; Taxel, P. The use of estrogen therapy in men. *Curr. Opin. Pharmacol.* **2003,** 3, 650-654.

(66) Scherr, D.; Pitts Jr, W. R.; Vaughan Jr, E. D. Diethylstilbesterol revisited: Androgen deprivation, osteoporosis and prostate cancer. *J. Urol.* **2002,** 167, 535-538.

(67) Francis, R. J.; Sharma, S. K.; Springer, C.; Green, A. J.; Hope-Stone, L. D.; Sena, L.; Martin, J.; Adamson, K. L.; Robbins, A.; Gumbrell, L.; O'Malley, D.; Tsiompanou, E.; Shahbakhti, H.; Webley, S.; Hochhauser, D.; Hilson, A. J.; Blakey, D.; Begent, R. H. J. A phase I trial of antibody directed enzyme prodrug therapy (ADEPT) in patients with advanced colorectal carcinoma or other CEA producing tumours. *Br. J. Cancer* **2002,** 87, 600-607.

(68) Napier, M. P.; Sharma, S. K.; Springer, C. J.; Bagshawe, K. D.; Green, A. J.; Martin, J.; Stribbling, S. M.; Cushen, N.; O'Malley, D.; Begent, R. H. J. Antibody-directed enzyme prodrug therapy: Efficacy and mechanism of action in colorectal carcinoma. *Clin. Cancer Res.* **2000,** 6, 765-772.

(69) Aghi, M.; Hochberg, F.; Breakefield, X. O. Prodrug activation enzymes in cancer gene therapy. *J. Gene Med.* **2000,** 2, 148-164.

(70) Deonarain, M. P.; R.A., S.; Epenetos, A. A. Genetic delivery of enzymes for cancer therapy. *Gene Ther.* **1995,** 2, 235-244.

(71) Greco, O.; Dachs, G. U. Gene directed enzyme/prodrug therapy of cancer: Historical appraisal and future prospectives. *J. Cell. Physiol.* **2001,** 187, 22-36.

(72) Singhal, S.; Kaiser, L. R. Cancer chemotherapy using suicide genes. *Surg. Oncol. Clin. North Am.* **1998,** 7, 505-536.

(73) Smythe, W. R. Prodrug/drug sensitivity gene therapy: current status. *Curr. Oncol. Rep.* **2000,** 2, 17-22.

(74) Russell, P. J.; Kathri, A. Novel gene-directed enzyme prodrug therapies against prostate cancer. *Exp. Opin. Invest. Drugs* **2006,** 15, 947-961.

(75) Vajda, A.; Marignol, L.; Foley, R.; Lynch, T. H.; Lawler, M.; Hollywood, D. Clinical potential of gene-directed enzyme prodrug therapy to improve radiation therapy in prostate cancer patients. *Cancer Treat. Rev.* **2011,** 37, 643-654.

(76) Green, N. K., Youngs, D.J., Neoptolemos, J.P., Friedlos, F., Knox, R.J., Springer, C.J., Anlezark, G.M., Michael, N.P., Melton, R.G., Ford, M.J., Young, L.S., Kerr, D.J., Searle, P.F. Sensitization of colorectal and pancreatic cancer cell lines to the prodrug 5-(aziridin-1-yl)-2,4-dinitrobenzamide (CB1954) by retroviral transduction and expression of the E. coli nitroreductase gene. *Cancer Gene Ther.* **1997,** 4, 229-238.

(77) Knox, R. J.; Friedlos, F.; Jarman, M.; Roberts, J. J. A new cytotoxic, DNA interstrand crosslinking agent, 5-(aziridin-1-yl)-4-hydroxylamino-2-nitrobenzamide, is formed from 5-(aziridin-1-yl)-2,4-dinitrobenzamide (CB 1954) by a nitroreductase enzyme in walker carcinoma cells. *Biochem. Pharmacol.* **1988,** 37, 4661-4669.

(78) Race, P. R., Lovering, A.L., White, S.A., Grove, J.I., Searle, P.F., Wrighton, C.W., Hyde, E.I. . Kinetic and structural characterisation of Escherichia coli nitroreductase mutants showing improved efficacy for the prodrug substrate CB1954. *J. Mol. Biol.* **2007,** 368, 481-492.

(79) Palmer, D. H., Milner, A.E., Kerr, D.J., Young, L.S. . Mechanism of cell death induced by the novel enzyme-prodrug combination, nitroreductase/CB1954, and identification of synergism with 5-fluorouracil. *Br. J. Cancer.* **2003,** 89, 944-950.

(80) Palmer, D. H., Mautner, V., Mirza, D., Oliff, S., Gerritsen, W., van der Sijp, J.R., Hubscher. S., Reynolds, G., Bonney, S., Rajaratnam, R., Hull, D., Horne, M., Ellis, J., Mountain, A., Hill, S., Harris, P.A., Searle, P.F., Young, L.S., James, N.D., Kerr, D.J. . Virus-directed enzyme prodrug therapy: intratumoral administration of a replication-deficient adenovirus encoding nitroreductase to patients with resectable liver cancer *J. Clin. Oncol.* **2004,** 22, 1546-1552.

(81) Djeha, A. H., Hulme, A., Dexter, M.T., Mountain, A., Young, L.S., Searle, P.F., Kerr, D.J., Wrighton, C.J. . Expression of Escherichia coli B nitroreductase in established human tumor xenografts in mice results in potent antitumoral and

bystander effects upon systemic administration of the prodrug CB1954. *Cancer Gene Ther.* **2000,** 7, 721-731.

(82) Weedon, S. J., Green, N.K., McNeish, I.A., Gilligan, M.G., Mautner, V., Wrighton, C.J., Mountain, A., Young, L.S., Kerr, D.J., Searle, P.F. . Sensitisation of human carcinoma cells to the prodrug CB1954 by adenovirus vector-mediated expression of E. coli nitroreductase. *Int. J. Cancer* **2000,** 86, 848-854.

(83) Helsby, N. A., Ferry, D.M., Patterson, A.V., Pullen, S.M., Wilson, W.R. . 2-Amino metabolites are key mediators of CB 1954 and SN 23862 bystander effects in nitroreductase GDEPT. *Br. J. Cancer* **2004,** 90, 1084-1092.

(84) Patel, P.; Young, J. G.; Mautner, V.; Ashdown, D.; Bonney, S.; Pineda, R. G.; Collins, S. I.; Searle, P. F.; Hull, D.; Peers, E.; Chester, J.; Wallace, D. M.; Doherty, A.; Leung, H.; Young, L. S.; James, N. D. A phase I/II clinical trial in localized prostate cancer of an adenovirus expressing nitroreductase with CB1984. *Mol. Ther.* **2009,** 17, 1292-1299.

(85) Wang, X. Y.; Martiniello-Wilks, R.; Shaw, J. M.; Ho, T.; Coulston, N.; Cooke-Yarborough, C.; Molloy, P. L.; Cameron, F.; Moghaddam, M.; Lockett, T. J.; Webster, L. K.; Smith, I. K.; Both, G. W.; Russel, P. J. Preclinical evaluation of a prostate-targeted gene-directed enzyme prodrug therapy delivered by ovine atadenovirus. *Gene Ther.* **2004,** 11, 1559-1567.

(86) Martiniello-Wilks, R.; Wang, X. Y.; Voeks, D. J.; Dane, A.; Shaw, J. M.; Mortensen, E.; Both, G. W.; Russell, P. J. Purine nucleoside phosphorylase and fludarabine phosphate gene-directed enzyme prodrug therapy suppresses primary tumour growth and pseudo-metastases in a mouse model of prostate cancer. *J. Gene Med.* **2004,** 6, 1343-1357.

(87) Yoshimura, I.; Ikegami, S.; Suzuki, S.; Tadakuma, T.; Hayakawa, M. Adenovirus Mediated Prostate Specific Enzyme Prodrug Gene Therapy Using Prostate Specific Antigen Promoter Enhanced by the Cre-loxP System. *J. Urol.* **2002,** 168, 2659-2664.

(88) Yoshimura, I.; Suzuki, S.; Tadakuma, T.; Hayakawa, M. Suicide gene therapy on LNCaP human prostate cancer cells. *Int. J. Urol.* **2001,** 8, S5-S8.

(89) Singh, P. P.; Joshi, S.; Russell, P. J.; Verma, N. D.; Wang, X.; Khatri, A. Molecular chemotherapy and chemotherapy: A new front against late-stage hormone-refractory prostate cancer. *Clin. Cancer Res.* **2011,** 17, 4006-4018.

(90) Biotech Equity Partners Pty Ltd. A phase I gene therapy study of FP253/Fludarabine for prostate cancer (FP253-GDEPT). http://www.clinicaltrials.gov/ct2/show/NCT00625430

(91) Yue, Q. H.; Hu, X. B.; Yin, Y.; Su, M. Q.; Cheng, X. D.; Yang, L.; Zhou, T. C.; Hao, X. Inhibition of prostate cancer by suicide gene targeting the FCY1 and HSV-TK genes. *Oncol. Rep.* **2009,** 22, 1341-1347.

(92) Advantagene Inc. Phase 3 study of ProstAtak™ with standard radiation therapy for localized prostate cancer (PrTK03). http://www.clinicaltrials.gov/ct2/show/NCT01436968

(93) Shalev, M.; Kadmon, D. O. V.; Teh, B. S.; Butler, E. B.; Aguilar-Cordova, E.; Thompson, T. C.; Herman, J. R.; Adler, H. L.; Scardino, P. T.; Miles, B. J. Suicide gene threrapy toxicity after multiple and repeat injections in patients with localized prostate cancer. *J. Urol.* **2000,** 163, 1747-1750.

(94) Ayala, G.; Satoh, T.; Li, R.; Shalev, M.; Gdor, Y.; Aguilar-Cordova, E.; Frolov, A.; Wheeler, T. M.; Miles, B. J.; Rauen, K.; Teh, B. S.; Butler, E. B.; Thompson, T. C.; Kadmon, D. Biological Response Determinants in HSV-tk + Ganciclovir Gene Therapy for Prostate Cancer. *Mol. Ther.* **2006,** 13, 716-728.

(95) Fujita, T.; Teh, B. S.; Timme, T. L.; Mai, W.-Y.; Satoh, T.; Kusaka, N.; Naruishi, K.; Fattah, E. A.; Aguilar-Cordova, E.; Butler, E. B.; Thompson, T. C. Sustained long-term immune responses after in situ gene therapy combined with radiotherapy and hormonal therapy in prostate cancer patients. *Int. J. Radiat. Oncol. Biol. Phys.* **2006,** 65, 84-90.

(96) Dubowchik, G. M.; Walker, M. A. Receptor-mediated and enzyme-dependent targeting of cytotoxic anticancer drugs. *Pharmacol. Ther.* **1999,** 83, 67-123.

(97) Afshar, S.; Asai, T.; Morrison, S. L. Humanized ADEPT comprised of an engineered human purine nucleoside phosphorylase and a tumor targeting peptide for treatment of cancer. *Mol. Cancer Ther.* **2009,** 8, 185-193.

(98) Yang, Y.; Aloysius, H.; Inoyama, D.; Chen, Y.; Hu, L. Enzyme-mediated hydrolytic activation of prodrugs. *Acta Pharm. Sin. B* **2011,** 1, 143-159.

(99) Chang, S. S.; Reuter, V. E.; Heston, W. D. W.; Bander, N. H.; Grauer, L. S.; Gaudin, P. B. Five different anti-prostate-specific membrane antigen (PSMA) antibodies confirm PSMA expression in tumor-associated neovasculature. *Cancer Res.* **1999,** 59, 3192-3198.

(100) Pinto, J. T.; Heston, W. D. W. Prostate specific membrane antigen, a unique glutamate carboxypeptidase: A review of recent findings. *Prostate J.* **1999,** 1, 15-26.

(101) Pinto, J. T.; Suffoletto, B. P.; Berzin, T. M.; Qiao, C. H.; Lin, S.; Tong, W. P.; May, F.; Mukherjee, B.; Heston, W. D. W. Prostate-specific Membrane Antigen: A Novel Folate Hydrolase in Human Prostatic Carcinoma Cells. *Clin. Cancer Res.* **1996,** 2, 1445-1451.

(102) Gregorakis, A. K.; Holmes, E. H.; Murphy, G. P. Prostate-specific membrane antigen: Current and future utility. *Semin. Urol. Oncol.* **1998,** 16, 2-12.

(103) Warren, P.; Li, L.; Song, W.; Holle, E.; Wei, Y.; Wagner, T.; Yu, X. In vitro targeted killing of prostate tumor cells by a synthetic amoebapore helix 3 peptide modified with two γ-linked glutamate residues at the COOH terminus. *Cancer Res.* **2001,** 61, 6783-6787.

(104) Uchida, A.; O'Keefe, D. S.; Bacich, D. J.; Molloy, P. L.; Heston, W. D. W. In vivo suicide gene therapy model using a newly discovered prostate-specific membrane antigen promoter/enhancer: A potential alternative approach to androgen deprivation therapy. *Urology* **2001,** 58, 132-139.

(105) Leippe, M.; Andrä, J.; Müller-Eberhard, H. J. Cytolytic and antibacterial activity of synthetic peptides derived from amoebapore, the pore-forming peptide of Entamoeba histolytica. *Proc. Natl. Acad. Sci. U. S. A.* **1994,** 91, 2602-2606.

(106) Holle, L.; Song, W.; Holle, E.; Nilsson, J.; Wei, Y.; Li, J.; Wagner, T.; Yu, X. In vivo targeted killing of prostate tumor cells by a synthetic amoebapore helix 3 peptide modified with two γ-linked glutamate residues at the COOH terminus. *Mol. Med. Rep.* **2009,** 2, 399-403.

(107) Mhaka, A.; Gady, A. M.; Rosen, D. M.; Lo, K. M.; Gillies, S. D.; Denmeade, S. R. Use of methotrexate-based peptide substrates to characterize the substrate specificity of Prostate-Specific Membrane Antigen (PSMA). *Cancer Biol. Ther.* **2004,** 3, 551-558.

(108) Yagoda, A.; Petrylak, D. Cytotoxic chemotherapy for advanced hormone-resistant prostate cancer. *Cancer* **1993,** 71, 1098-1109.

(109) Davidson, G. A.; Varhol, R. J. Kinetics of thapsigargin-Ca2+-ATPase (sarcoplasmic reticulum) interaction reveals a two-step binding mechanism and picomolar inhibition. *J. Biol. Chem.* **1995,** 270, 11731-11734.

(110) Furuya, Y.; Lundmo, P.; Short, A. D.; Gill, D. L.; Isaacs, J. T. The role of calcium, pH, and cell proliferation in the programmed (apoptotic) death of androgen-independent prostatic cancer cells induced by thapsigarin. *Cancer Res.* **1994,** 54, 6167-6175.

(111) Lin, X. S.; Denmeade, S. R.; Cisek, L.; Isaacs, J. T. Mechanism and role of growth arrest in programmed (apoptotic) death of prostatic cancer cells induced by thapsigargin. *Prostate* **1997,** 33, 201-207.

(112) Denmeade, S. R.; Mhaka, A. M.; Rosen, D. M.; Brennen, W. N.; Dalrymple, S.; Dach, I.; Olesen, C.; Gurel, B.; DeMarzo, A. M.; Wilding, G.; Carducci, M. A.; Dionne, C. A.; Møller, J. V.; Nissen, P.; Christensen, S. B.; Isaacs, J. T. Engineering a prostate-specific membrane antigen-activated tumor endothelial cell prodrug for cancer therapy *Sci. Transl. Med.* **2012,** 4, 1-21.

(113) Chang, S. S.; O'Keefe, D. S.; Bacich, D. J.; Reuter, V. E.; Heston, W. D. W.; Gaudin, P. B. Prostate-specific membrane antigen is produced in tumor-associated neovasculature. *Clin. Cancer Res.* **1999,** 5, 2674-2681.

(114) Israeli, R. S.; Powell, C. T.; Corr, J. G.; Fair, W. R.; Heston, W. D. W. Expression of the prostate-specific membrane antigen. *Cancer Res.* **1994,** 54, 1807-1811.

(115) Silver, D. A.; Pellicer, I.; Fair, W. R.; Heston, W. D. W.; Cordon-Cardo, C. Prostate-specific membrane antigen expression in normal and malignant human tissues. *Clin. Cancer Res.* **1997,** 3, 81-85.

(116) GenSpera Inc. Study of G-202 as second-line therapy following Sorafenib in hepatocellular carcinoma (G-202-003). http://clinicaltrials.gov/show/NCT01777594

(117) GenSpera Inc. Efficacy, safety and CNS exposure of G-202 in patients with recurrent or progressive glioblastoma. http://clinicaltrials.gov/show/NCT02067156

(118) Mahalingam, D.; Wilding, G.; Denmeade, S.; Sarantopoulas, J.; Cosgrove, D.; Cetnar, J.; Azad, N.; Bruce, J.; Kurman, M.; Carducci, M. 601 A first-in-human, Phase 1 clinical study of the safety, tolerability and pharmacokinetics (PK) of G-202, a Thapsigargin-based PSMA-activated prodrug, in patients with advanced solid tumors. *Eur. J. Cancer* **2012,** 48, Suppl 6,184-185.

(119) GenSpera Inc. Phase 2 study of G-202 in patients with chemotherapy-naïve metastatic castrate-resistant prostate cancer. http://www.clinicaltrials.gov/ct2/show/NCT01734681

(120) Herschman, J. D.; Smith, D. S.; Catalona, W. J. Effect of ejaculation on serum total and free prostate-specific antigen concentrations. *Urology* **1997,** 50, 239-243.

(121) Nadler, R. B.; Humphrey, P. A.; Smith, D. S.; Catalona, W. J.; Ratliff, T. L. Effect of inflammation and benign prostatic hyperplasia on elevated serum prostate specific antigen levels. *J. Urol.* **1995,** 154, 407-413.

(122) Balk, S. P.; Ko, Y.-J.; Bubley, G. J. Biology of prostate-specific antigen. *J. Clin. Oncol.* **2003,** 21, 383-391.

(123) Catalona, W. J., Smith, D.S., Ratliff, T.L., Dodds, K. M., Coplen, D.E., Yuan, J. J., Petros, J.A., Andriole, G.L. . Measurement of prostrate-specific antigen in serum as a screening test for prostrate cancer. *New Engl. J. Med.* **1991,** 324, 1156-1161.

(124) Diamandis, E. New diagnostic applications and physiological functions of prostate specific antigen. *Scand. J. Clin. Lab. Invest* **1995,** 55, 105-112.

(125) Williams, S. A.; Singh, P.; Isaacs, J. T.; Denmeade, S. R. Does PSA play a role as a promoting agent during the initiation and/or progression of prostate cancer? *Prostate* **2007,** 67, 312-329.

(126) Culig, Z.; Hobisch, A.; Cronauer, M. V.; Radmayr, C.; Trapman, J.; Hittmair, A.; Bartsch, G.; Klocker, H. Androgen receptor activation in prostatic tumor cell lines by insulin-like growth factor-1, keratinocyte growth factor and epidermal growth factor. *Eur. Urol.* **1995,** 27, 45-47.

(127) Iwamura, M.; Sluss, P. M.; Casamento, J. B.; Cockett, A. T. K. Insulin-Like growth factor I: action and receptor characterization in human prostate cancer cell lines. *Prostate* **1993,** 22, 243-252.

(128) Cramer, S. D.; Chen, Z.; Peehl, D. M. Prostate specific antigen cleaves parathyroid hormone-related protein in the PTH-like domain: Inactivation of PTHrP-stimulated cAMP accumulation in mouse osteoblasts. *J. Urol.* **1996,** 156, 526-531.

(129) Dallas, S. L.; Zhao, S.; Cramer, S. D.; Chen, Z.; Peehl, D. M.; Bonewald, L. F. Preferential production of latent transforming growth factor Î²-2 by primary prostatic epithelial cells and its activation by prostate-specific antigen. *J. Cell. Physiol.* **2005,** 202, 361-370.

(130) Iwamura, M.; Hellman, J.; Cockett, A. T. K.; Lilja, H.; Gershagen, S. Alteration of the hormonal bioactivity of parathyroid hormone-related protein (PTHrP) as a result of limited proteolysis by prostate-specific antigen. *Urology* **1996,** 48, 317-325.

(131) Lilja, H. A kallikrein-like serine protease in prostatic fluid cleaves the predominant seminal vesicle protein. *J. Clin. Investig.* **1985,** 76, 1899-1903.

(132) Malm, J.; Hellman, J.; Hogg, P.; Lilja, H. Enzymatic action of prostate-specific antigen (PSA or hK3): Substrate specificity and regulation by Zn2+, a tight-binding inhibitor. *Prostate* **2000,** 45, 132-139.

(133) Ménez, R., Michel, S., Muller, B.H., Bossus, M., Ducancel, F., Jolivet-Reynaud, C., Stura, E.A. Crystal structure of a ternary complex between human prostate-specific antigen, its substrate acyl intermediate and an activating antibody. *J. Mol. Biol.* **2008,** 376, 1021-1033.

(134) Michel, S.; Collomb-Clerc, E.; Geourjon, C.; Charrier, J. P.; Passagot, J.; Courty, Y.; Deleage, G.; Jolivet-Reynaud, C. Selective recognition of enzymatically active prostate-specific antigen (PSA) by anti-PSA monoclonal antibodies. *J. Mol. Recognit.* **2005,** 18, 225-235.

(135) Denmeade, S. R.; Sokoll, L. J.; Chan, D. W.; Khan, S. R.; Isaacs, J. T. Rapid communication: Concentration of enzymatically active prostate-specific antigen

(PSA) in the extracellular fluid of primary human prostate cancers and human prostate cancer xenograft models. *Prostate* **2001,** 48, 1-6.

(136) Leinonen, J., Zhang. W., Stenman, U. Complex formation between PSA isoenzymesand protease inhibitors. *J. Urol.* **1996,** 155, 1099-1103.

(137) Otto, A., Bar, J., Birkenmeier, G. Prostate specific antigen forms complexes with human α2-macroglobulin and binds to the α2-macroglobulin receptor/ldl receptor-related protein. *J. Urol.* **1998,** 159, 297-303.

(138) Denmeade, S. R.; Lou, W.; Lovgren, J.; Malm, J.; Lilja, H.; Isaacs, J. T. Specific and efficient peptide substrates for assaying the proteolytic activity of prostate-specific antigen. *Cancer Res.* **1997,** 57, 4924-4930.

(139) Garsky, V. M., Lumma, P.K., Feng, D.M., Wai, J., Ramjit, H.G., Sardana, M.K., Oliff, A., Jones, R.E., DeFeo-Jones, D., Freidinger, R.M. The synthesis of a prodrug of doxorubicin designed to provide reduced systemic toxicity and greater target efficacy. *J. Med. Chem.* **2001,** 44, 4216-4224.

(140) DeFeo-Jones, D., Garsky, V.M., Wong, B.K., Feng, D.M., Bolyar, T., Haskell, K., Kiefer DM, Leander K, McAvoy E, Lumma P, Wai J, Senderak ET, Motzel SL, Keenan, K., Van Zwieten, M., Lin, J.H., Freidinger, R., Huff, J., Oliff, A., Jones, R.E. . A peptide-doxorubicin prodrug activated by prostate-specific antigen selectively kills prostate tumor cells positive for prostate-specific antigen in vivo. *Nat. Med.* **2000,** 6, 1248-1252.

(141) Denmeade, S. R., Nagy, A., Gao, J., Lilja, H., Schally, A.V., Isaacs, J.T. . Enzymatic activation of a doxorubicin-peptide prodrug by prostate-specific antigen. *Cancer Res.* **1998,** 58, 2537-2540.

(142) Denmeade, S. R.; Jakobsen, C. M.; Janssen, S.; Khan, S. R.; Garrett, E. S.; Lilja, H.; Christensen, S. B.; Isaacs, J. T. Prostate-specific antigen-activated thapsigargin prodrug as targeted therapy for prostate cancer. *J. Natl. Cancer Inst.* **2003,** 95, 990-1000.

(143) Kumar, S. K.; Williams, S. A.; Isaacs, J. T.; Denmeade, S. R.; Khan, S. R. Modulating paclitaxel bioavailability for targeting prostate cancer. *Bioorg. Med. Chem.* **2007,** 15, 4973-4984.

(144) Jakobsen, C. M.; Denmeade, S. R.; Isaacs, J. T.; Gady, A.; Olsen, C. E.; Christensen, S. B. Design, synthesis, and pharmacological evaluation of thapsigargin analogues for targeting apoptosis to prostatic cancer cells. *J. Med. Chem.* **2001,** 44, 4696-4703.

(145) Tang, X.; Xian, M.; Trikha, M.; Honn, K. V.; Wang, P. G. Synthesis of peptide-diazeniumdiolate conjugates: Towards enzyme activated antitumor agents. *Tetrahedron Lett.* **2001,** 42, 2625-2629.

(146) Williams, S. A.; Merchant, R. F.; Garrett-Mayer, E.; Isaacs, J. T.; Buckley, T. J.; Denmeade, S. R. A prostate-specific antigen-activated channel-forming toxin as therapy for prostatic disease. *J. Natl. Cancer Inst.* **2007,** 99, 376-385.

(147) Mhaka, A.; Denmeade, S. R.; Yao, W.; Isaacs, J. T.; Khan, S. R. A 5-fluorodeoxyuridine prodrug as targeted therapy for prostate cancer. *Bioorg. Med. Chem. Lett.* **2002,** 12, 2459-2461.

(148) Jiang, Y.; DiPaola, R. S.; Hu, L. Synthesis and stereochemical preference of peptide 4-aminocyclophosphamide conjugates as potential prodrugs of phosphoramide mustard for activation by prostate-specific antigen (PSA). *Bioorg. Med. Chem. Lett.* **2009,** 19, 2587-2590.

(149) Jiang, Y., Hu, L. . Phenylalanyl-aminocyclophosphamides as model prodrugs for proteolytic activation: synthesis, stability, and stereochemical requirements for enzymatic cleavage. *Bioorg. Med. Chem. Lett.* **2007,** 17, 517-521.

(150) Jones, G. B.; Mitchell, M. O.; Weinberg, J. S.; D'Amico, A. V.; Bubley, G. J. Towards enzyme activated antiprostatic agents. *Bioorg. Med. Chem. Lett.* **2000,** 10, 1987-1989.

(151) Hu, L.; Wu, X. Chemotherapeutic conjugates and methods of use. US20100075927 A1, 2007.

(152) Brady, S. F.; Pawluczyk, J. M.; Lumma, P. K.; Feng, D. M.; Wai, J. M.; Jones, R.; DeFeo-Jones, D.; Wong, B. K.; Miller-Stein, C.; Lin, J. H.; Oliff, A.; Freidinger, R. M.; Garsky, V. M. Design and synthesis of a pro-drug of vinblastine targeted at treatment of prostate cancer with enhanced efficacy and reduced systemic toxicity. *J. Med. Chem.* **2002,** 45, 4706-4715.

(153) DeFeo-Jones, D.; Brady, S. F.; Feng, D. M.; Wong, B. K.; Bolyar, T.; Haskell, K.; Kiefer, D. M.; Leander, K.; McAvoy, E.; Lumma, P.; Pawluczyk, J. M.; Wai, J.; Motzel, S. L.; Keenan, K.; Van Zwieten, M.; Lin, J. H.; Garsky, V. M.; Freidinger, R.; Oliff, A.; Jones, R. E. A prostate-specific antigen (PSA)-activated vinblastine prodrug selectively kills PSA-secreting cells in vivo. *Mol. Cancer Ther.* **2002,** 1, 451-459.

(154) DiPaola, R. S., Rinehart, J., Nemunaitis, J., Ebbinghaus, S., Rubin, E., Capanna, T., Ciardella, M., Doyle-Lindrud, S., Goodwin, S., Fontaine, M., Adams, N., Williams, A., Schwartz, M., Winchell, G., Wickersham, K., Deutsch, P., Yao, S.L. Characterization of a novel prostate-specific antigen-activated peptide-doxorubicin conjugate in patients with prostate cancer. *J. Clin. Oncol.* **2002,** 20, 1874-1879.

(155) Atkinson, J. M.; Siller, C. S.; Gill, G. H. Tumour endoproteases: the cutting edge of cancer drug delivery? . *Br. J. Pharmacol.* **2008,** 153, 1344-1352.

(156) Spencer, C. M.; Faulds, D. Paclitaxel: A review of its pharmacodynamic and pharmacokinetic properties and therapeutic potential in the treatment of cancer. *Drugs* **1994,** 48, 794-847.

(157) Stein, C. A. Mechanisms of action of taxanes in prostate cancer. *Semin. Oncol.* **1999,** 26, 3-7.

(158) Wani, M. C.; Taylor, H. L.; Wall, M. E.; Coggon, P.; McPhail, A. T. Plant antitumor agents. VI. The isolation and structure of taxol, a novel antileukemic and antitumor agent from Taxus brevifolia. *J. Am. Chem. Soc.* **1971,** 93, 2325-2327.

(159) Hitt, R.; Paz-Ares, L.; BrandÃ¡riz, A.; Castellano, D.; PeÃ±a, C.; MillÃ¡n, J. M.; Calvo, F.; Ortiz de Urbina, D.; LÃ³pez, E.; Ã lvarez-Vicent, J. J.; CortÃ©s-Funes, H. Induction chemotherapy with paclitaxel, cisplatin and 5-fluorouracil for squamous cell carcinoma of the head and neck: long-term results of a phase II trial. *Ann. Oncol.* **2002,** 13, 1665-1673.

(160) Perez, E. A. Paclitaxel in Breast Cancer. *Oncologist* **1998,** 3, 373-389.

(161) Cattaneo-Pangrazzi, R. M. C.; Schott, H.; Schwendener, R. A. In vivo activity of a PSA-activated doxorubicin prodrug against PSA-producing human prostate cancer xenografts. *Prostate* **2000,** 45, 80-83.

(162) Christensen, S. B.; Andersen, A.; Kromann, H.; Treiman, M.; Tombal, B.; Denmeade, S.; Isaacs, J. T. Thapsigargin analogues for targeting programmed death of androgen-independent prostate cancer cells. *Bioorg. Med. Chem.* **1999,** 7, 1273-1280.

(163) Garthwaite, J.; Charles, S. L.; Chess-Williams, R. Endothelium-derived relaxing factor release on activation of NMDA receptors suggests role as intercellular messenger in the brain. *Nature* **1988,** 336, 385-388.

(164) Gillespie, J. S.; Liu, X.; Martin, W. The effects of L-arginine and N(G)-monomethyl L-arginine on the response of the rat anococcygeus muscle to NANC nerve stimulation. *Br. J. Pharmacol.* **1989,** 98, 1080-1082.

(165) Hibbs Jr, J. B.; Taintor, R. R.; Vavrin, Z. Macrophage cytotoxicity: Role for L-arginine deiminase and imino nitrogen oxidation to nitrite. *Science* **1987,** 235, 473-476.

(166) Nathan, C. F.; Hibbs Jr, J. B. Role of nitric oxide synthesis in macrophage antimicrobial activity. *Curr. Opin. Immunol.* **1991,** 3, 65-70.

(167) Wink, D. A.; Vodovotz, Y.; Laval, J.; Laval, F.; Dewhirst, M. W.; Mitchell, J. B. The multifaceted roles of nitric oxide in cancer. *Carcinogenesis* **1998,** 19, 711-721.

(168) Fitzhugh, A. L.; Keefer, L. K. Diazeniumdiolates: Pro- and antioxidant applications of the 'NONOates'. *Free Radic. Biol. Med.* **2000,** 28, 1463-1469.

(169) Keefer, L. K. Nitric oxide-releasing compounds: From basic research to promising drugs. *Chem. Tech.* **1998,** 28, 30-35.

(170) Coombs, G. S.; Bergstrom, R. C.; Pellequer, J. L.; Baker, S. I.; Navre, M.; Smith, M. M.; Tainer, J. A.; Madison, E. L.; Corey, D. R. Substrate specificity of prostate-specific antigen (PSA). *Chem. Biol.* **1998,** 5, 475-488.

(171) Jiang, Y.; Hu, L. Peptide conjugates of 4-aminocyclophosphamide as prodrugs of phosphoramide mustard for selective activation by prostate-specific antigen (PSA). *Bioorg. Med. Chem.* **2013,** 21, 7507-7514.

(172) Abrami, L.; Fivaz, M.; Van Der Goot, F. G. Adventures of a pore-forming toxin at the target cell surface. *Trends Microbiol.* **2000,** 8, 168-172.

(173) Rossjohn, J.; Feil, S. C.; McKinstry, W. J.; Tsernoglou, D.; Van Der Goot, G.; Buckley, J. T.; Parker, M. W. Aerolysin - A paradigm for membrane insertion of beta-sheet protein toxins? *J. Struct. Biol.* **1998,** 121, 92-100.

(174) Singh, R.; Browning, J. L.; Abi-Habib, R.; Wong, K.; Williams, S. A.; Merchant, R.; Denmeade, S. R.; Buckley, T. J.; Frankel, A. E. Recombinant prostate-specific antigen proaerolysin shows selective protease sensitivity and cell cytotoxicity. *Anti-Cancer Drugs* **2007,** 18, 809-816.

(175) Denmeade, S. R.; Egerdie, B.; Steinhoff, G.; Merchant, R.; Abi-Habib, R.; Pommerville, P. Phase 1 and 2 studies demonstrate the safety and efficacy of intraprostatic injection of PRX302 for the targeted treatment of lower urinary tract symptoms secondary to benign prostatic hyperplasia. *Eur. Urol.* **2011,** 59, 747-754.

(176) Sophiris Bio Corp. An open-label, multi-center, phase IIa trial of PRX302 treatment of patients with locally recurrent prostate cancer after primary radiation therapy. http://www.clinicaltrials.gov/ct2/show/NCT00686088

(177) Elhilali, M. M.; Pommerville, P.; Yocum, R. C.; Merchant, R.; Roehrborn, C. G.; Denmeade, S. R. Prospective, randomized, double-blind, vehicle controlled, multicenter phase IIb clinical trial of the pore forming protein PRX302 for targeted treatment of symptomatic benign prostatic hyperplasia. *J. Urol.* **2012,** 189, 1421-1426.

(178) Sophiris Bio Corp. Randomized, double-blind, vehicle-controlled, multicenter safety and efficacy study of intraprostatic PRX302 for LUTS BPH (PLUS-1). http://www.clinicaltrials.gov/ct2/show/NCT01966614

(179) Santi, D. V.; McHenry, C. S.; Raines, R. T.; Ivanetich, K. M. Kinetics and thermodynamics of the interaction of 5-fluoro-2′-deoxyuridylate with Thymidylate Synthase. *Biochemistry* **1987,** 26, 8606-8613.

(180) Hu, L.; Wu, X.; Han, J.; Chen, L.; Vass, S. O.; Browne, P.; Hall, B. S.; Bot, C.; Gobalakrishnapillai, V.; Searle, P. F.; Knox, R. J.; Wilkinson, S. R. Synthesis and structure-activity relationships of nitrobenzyl phosphoramide mustards as nitroreductase-activated prodrugs. *Bioorg. Med. Chem. Lett.* **2011,** 21, 3986-3991.

(181) Shanafelt, T. D., Lin, T., Geyer, S.M., Zent, C.S., Leung, N., Kabat, B., Bowen, D., Grever, M.R., Byrd, J.C., Kay, N.E. Pentostatin, cyclophosphamide, and rituximab regimen in older patients with chronic lymphocytic leukemia. *Cancer J.* **2007,** 109, 2291-2298.

(182) Korkmaz, A.; Topal, T.; Oter, S. Pathophysiological aspects of cyclophosphamide and ifosfamide induced hemorrhagic cystitis; implication of reactive oxygen and nitrogen species as well as PARP activation. *Cell Biol. Toxicol.* **2007,** 23, 303-312.

(183) Brock, N. The history of the oxazaphosphorine cytostatics. *Cancer J.* **1996,** 78, 542-547.

(184) Wu, X.; Hu, L. Efficient amidation from carboxylic acids and azides via selenatriazoline: application to the coupling of amino acids and peptides with azides. *J. Org. Chem.* **2007,** 72, 765-774.

(185) Wu, X.; H, L. Amide bond formation from selenocarboxylates and aromatic azides. *Tetrahedron Lett.* **2005,** 46, 8401-8405.

(186) Hortobagyi, G. N., Willey, J., Rahman, Z., Holmes, F.A., Theriault, R.L., Buzdar, A.U. Prospective assessment of cardiac toxicity during a randomized phase II trial of doxorubicin and paclitaxel in metastatic breast cancer. *Semin. Oncol.* **1997,** 24, S17-65-S17-68.

(187) Weiss, R. B. The anthracyclines: will we ever find a better doxorubicin? *Semin. Oncol.* **1992,** 19, 670-686.

(188) Xu, X., Persson, H.L., Richardson, D.R. . Molecular Pharmacology of the interaction of anthracyclines with iron. *Mol. Pharmacol.* **2005,** 68, 261-271.

(189) DiPaola, R. S.; Plante, M.; Kaufman, H.; Petrylak, D. P.; Israeli, R.; Lattime, E.; Manson, K.; Schuetz, T. A phase I trial of Pox PSA vaccines (PROSTVAC®-VF) with B7-1, ICAM-1, and LFA-3 co-stimulatory molecules (TRICOM™) in Patients with Prostate Cancer. *J. Transl. Med.* **2006,** 4, 1-5.

(190) Desai, R. B.; Schwartz, M. S.; Matuszewski, B. K. The identification of three human metabolites of a peptide-doxorubicin conjugate using HPLC-MS-MS in positive and negative ionization modes. *J. Chromatogr. Sci.* **2004,** 42, 317-322.

(191) Johnson, I. S. Historical background of Vinca alkaloid research and areas of future interest. *Cancer Chemother. Rep. Pt. 1* **1968,** 52, 455-461.

(192) Wong, B. K., DeFeo-Jones, D., Jones, R.E., Garsky, V.M., Feng, D.M., Oliff, A., Chiba, M,, Ellis, J.D., Lin, J.H. PSA-specific and non-PSA-specific conversion of a PSA-targeted peptide conjugate of doxorubicin to its active metabolites. *Drug Metab. Dispos.* **2001,** 29, 313-318.

(193) Shelkov, R.; Nahmany, M.; Melman, A. Acylation through ketene intermediates. *J. Org. Chem.* **2002,** 67, 8975-8982.

(194) Wu, X., Chen, Y., Aloysius, H., Hu, L. A novel high-yield synthesis of aminoacyl p-nitroanilines and aminoacyl 7-amino-4-methylcoumarins: important synthons for the synthesis of chromogenic/fluorogenic protease substrates. *Beilstein J. Org. Chem.* **2011,** 7, 1030-1035.

(195) Ge, Y.; Wu, X.; Zhang, D.; Hu, L. 3-Aminoxypropionate-based linker system for cyclization activation in prodrug design. *Bioorg. Med. Chem. Lett.* **2009,** 19, 941–944.

(196) Kres, W. Current chemotherapy and future directions in research for the treatment of advanced hormone-refractory prostate cancer. *Cancer Invest.* **1995,** 13, 296-312.

(197) Cotterill, I. C.; Rich, J. O. Chemoenzymatic synthesis of N-trifluoroacetyl doxorubicin-14-valerate (Valrubicin). *Org. Process Res. Dev.* **2005,** 9, 818-821.

(198) Cotterill, I. C.; Rich, J. O.; Scholten, M. D.; Mozhaeva, L.; Michels, P. C. Reversible derivatization to enhance enzymatic synthesis: Chemoenzymatic synthesis of doxorubicin-14-fl-esters. *Biotechnol. Bioeng.* **2008,** 101, 435-440.

(199) Rho, Y. S.; Kim, G.; Kim, W.-J.; Park, S.; Yoo, D. J.; Kang, H. S.; Chung, S.-R. Synthesis of new anthracycline derivatives containing acetylsalicylic or palmitic acid moiety. *Bull. Korean Chem. Soc.* **2001,** 22, 587-592.

(200) Rho, Y. S.; Ko, H. K.; Kim, W.-J.; Yoo, D. J.; Wing, H. S. Total synthesis of a new 7-deoxyidarubicinone derivative through the functionalization of an A-ring side chain. *Bull. Korean Chem. Soc.* **2000,** 21, 774-778.

(201) Rho, Y. S.; Park, S.; Kim, W.-J.; Kim, G.; Yoo, D. J.; Kang, H.-S.; Chung, S.-R. Synthesis of new anthracyline derivatives contaning pyruvic, aspartic, or N-acetylaspartic acid molecule. *Synth. Commun.* **2002,** 32, 1961-1975.

(202) van Hensbergen, Y.; Broxterman, H. J.; Elderkamp, Y. W.; Lankelma, J.; Beers, J. C. C.; Heijn, M.; Boven, E.; Hoekman, K.; Pinedo, H. M. A doxorubicin-CNGRC-peptide conjugate with prodrug properties. *Biochem. Pharmacol.* **2002,** 63, 897-908.

(203) Hayashi, R.; Cook, G. R. Bi(OTf)3-catalyzed 5-exo-trig cyclization via halide activation. *Tetrahedron Lett.* **2008,** 49, 3888-3890.

(204) Keizer, H. G.; Pinedo, H. M.; Schuurhuis, G. J.; Joenje, H. Doxorubicin (adriamycin): A critical review of free radical-dependent mechanisms of cytotoxicity. *Pharmacol. Ther.* **1990,** 47, 219-231.

(205) Frank, N. Y.; Margaryan, A.; Huang, Y.; Schatton, T.; Waaga-Gasser, A. M.; Gasser, M.; Sayegh, M. H.; Sadee, W.; Frank, M. H. ABCB5-Mediated Doxorubicin Transport and Chemoresistance in Human Malignant Melanoma. In 2005; Vol. 65, pp 4320-4333.

(206) Shen, F.; Chu, S.; Bence, A. K.; Bailey, B.; Xue, X.; Erickson, P. A.; Montrose, M. H.; Beck, W. T.; Erickson, L. C. Quantitation of doxorubicin uptake, efflux, and modulation of multidrug resistance (MDR) in MDR human cancer cells. *J. Pharm. Exp. Ther.* **2008,** 324, 95-102.

(207) Singhal, S.; Singhal, J.; Nair, M.; Lacko, A.; Awasthi, Y.; Awasthi, S. Doxorubicin transport by RALBP1 and ABCG2 in lung and breast cancer. *Int. J. Oncol.* **2007,** 30, 717-725.

(208) Murphy, L. J.; Corder, R.; Mallet, A. I.; Turner, A. J. Generation by the phosphoramidon-sensitive peptidases, endopeptidase-24.11 and thermolysin, of endothelin-1 and C-terminal fragment from big endothelin-1. *Br. J. Pharmacol.* **1994,** 113, 137-142.

(209) Rawlings, N. D.; Barrett, A. J. Evolutionary families of metallopeptidases. *Methods Enzymol.* **1995,** 248, 183-228.

(210) Roques, B. P.; Noble, F.; Dauge, V.; Fournie-Zaluski, M. C.; Beaumont, A. Neutral endopeptidase 24.11: Structure, inhibition, and experimental and clinical pharmacology. *Pharmacol. Rev.* **1993,** 45, 87-146.

(211) Benchetrit, T.; Bissery, V.; Mornon, J. P.; Devault, A.; Crine, P.; Roques, B. P. Primary structure homologies between two zinc metallopeptidases, the neutral endopeptidase 24.11 ("enkephalinase") and thermolysin, through clustering analysis. *Biochemistry* **1988,** 27, 592-596.

(212) Schulz, H.; Dale, G. E.; Karimi-Nejad, Y.; Oefner, C. Structure of human endothelin-converting enzyme I complexed with phosphoramidon. *J. Mol. Biol.* **2009,** 385, 178-187.

(213) Oefner, C.; Roques, B. P.; Fournie-Zaluski, M.-C.; Dale, G. E. Structural analysis of neprilysin with various specific and potent inhibitors. *Acta Crystallogr. Section D* **2004,** 60, 392-396.

(214) Tronrud, D. E.; Monzingo, A. F.; Matthews, B. W. Crystallographic structural analysis of phosphoramidates as inhibitors and transition-state analogs of thermolysin. *Eur. J. Biochem.* **1986,** 157, 261-268.

(215) Sahli, S.; Stump, B.; Welti, T.; Schweizer, W. B.; Diederich, F.; Blum-Kaelin, D.; Aebi, J. D.; Böhm, H.-J. A new class of inhibitors for the metalloprotease neprilysin based on a central imidazole scaffold. *Helv. Chim. Acta* **2005,** 88, 707-730.

(216) Velazquez, E. F.; Yancovitz, M.; Pavlick, A.; Berman, R.; Shapiro, R.; Bogunovic, D.; O'Neill, D.; Yu, Y. L.; Spira, J.; Christos, P. J.; Zhou, X. K.; Mazumdar, M.; Nanus, D. M.; Liebes, L.; Bhardwaj, N.; Polsky, D.; Osman, I. Clinical relevance of Neutral Endopeptidase (NEP/CD10) in melanoma. *J. Transl. Med.* **2007,** 5.

(217) Thong, A.; Müller, D.; Feuerstacke, C.; Mietens, A.; Stammler, A.; Middendorff, R. Neutral endopeptidase (CD10) is abundantly expressed in the epididymis and localized to a distinct population of epithelial cells-Its relevance for CNP degradation. *Mol. Cell. Endocrinol.* **2014,** 382, 234-243.

(218) Kalled, S. L.; Siva, N.; Stein, H.; Reinherz, E. L. The distribution of CD10 (NEP 24.11, CALLA) in humans and mice is similar in non-lymphoid organs but differs within the hematopoietic system: absence on murine T and B lymphoid progenitors. *Eur. J. Immunol.* **1995,** 25, 677-687.

(219) Klayman, D. L., Griffin, T. S. Reaction of selenium with sodium borohydride in protic solvents. A Facile Method for the introduction of selenium into organic molecules. *J. Am. Chem. Soc.* **1973,** 95, 197-199.